

**Assessment of the influence of
chromatin elements on stability of
recombinant protein production in
amplified CHO cells**

A thesis submitted to the University of Manchester for the
degree of Doctor of Philosophy in
The Faculty of Life Sciences

2012

Zeynep Betts

TABLE OF CONTENTS

LIST OF FIGURE	6
LIST OF TABLES	10
ABSTRACT	11
DECLARATION	10
COPYRIGHT STATEMENT	10
ACKNOWLEDGEMENTS	13
ABBREVIATIONS	14
CHAPTER 1: Introduction	16
1.1 Biopharmaceuticals in Biotechnology.....	17
1.2 Expression Systems.....	20
1.2.1 Bacteria	21
1.2.2 Yeast	22
1.2.3 Mammalian Cells.....	23
1.2.3.1 NS0 Cells	23
1.2.3.2 CHO Cells.....	24
1.2.3.2.1 CHO Cell Chromosomes	25
1.2.3.2.1 MTX-mediated Gene Amplification in CHO Cells	27
1.2.4 Summary	31
1.3 Stability of Recombinant Gene Expression.....	31
1.4 Gene Silencing	34
1.4.1 Transcriptional Gene Silencing	34
1.4.1.1 Chromatin Structure and Position Effect.....	34
1.4.1.2 Histone Modifications	38
1.4.1.3 DNA Methylation.....	40
1.4.2 Post-Transcriptional Gene Silencing (PTGS)	42
1.4.3 Summary	44
1.5 Nuclear Organization and Regulatory Elements.....	44
1.5.1 Nuclear Organization	44
1.5.2 DNA Regulatory Elements and Their Potential Use in Recombinant Gene Expression.....	47
1.5.2.1 LCRs.....	48
1.5.2.2 S/MARs	50
1.5.2.3 UCOEs.....	52
1.6 Summary and Objectives.....	56
CHAPTER 2: Materials and Methods	59
2.1 Materials and Equipment.....	60

2.1.1 Sources of Chemicals, Reagents and Special Equipment	60
2.1.2 Preparation and Sterilisation of Solutions.....	60
2.1.3 pH measurements.....	60
2.2 Generation and Purification of Plasmids in Bacterial Cells	60
2.2.1. Bacterial Growth Medium.....	60
2.2.2. Midi-Preparation of Plasmid DNA	61
2.2.3. Estimation of Nucleic Acid Concentration	61
2.3. Preparation of Mammalian Expression Vectors for Transfection into CHO cells	61
2.3.1 Phenol Extraction and Ethanol Precipitation of DNA	62
2.4. Mammalian Cell Culture	62
2.4.1. Cell Harvesting and Maintenance.....	62
2.4.2 Measurement of Cell Number and Viability	63
2.4.3 Cryopreservation of Mammalian Cells	63
2.4.4 Cell Revival.....	64
2.4.5 Transfection of CHO Cells.....	64
2.4.6 Limiting Dilution Cloning.....	64
2.4.7 MTX-mediated gene Amplification.....	65
2.4.8 Long Term Culture	66
2.4.9 Batch Culture Analysis	66
2.5. Analysis of Protein Expression.....	68
2.5.1. Protein Extraction	68
2.5.2. Protein Quantitation by Bradford Assay	68
2.5.3. SDS-PAGE	69
2.5.4. Protein Transfer and Western Blotting	69
2.5.5. Densitometric Analysis	70
2.5.6. Membrane Stripping	70
2.5.7. Detection of GFP fluorescence by Flow Cytometry.....	70
2.5.8. Detection of EPO by Enzyme-Linked Immunosorbent Assay.....	71
2.5.8.1. Preparation of Standard Curve and Samples for EPO ELISA.....	72
2.6 Analysis mRNA Expression by Quantitative-Reverse Transcription PCR (q-RT PCR	72
2.6.1. Extraction and Isolation of RNA.....	72
2.6.2. DNase I treatment of RNA.....	73
2.6.3. cDNA Synthesis from RNA	73
2.6.4. Preparation of Samples and “Standard” sample.....	74
2.6.5. q-PCR Reaction	74
2.6.6. Analysis of q-PCR Results	74
2.7. DNA Analysis	76
2.7.1. Isolation of Genomic DNA	76

2.7.2 Plasmid Copy-Number Analysis by q-PCR	76
2.7.2.1 Preparation of Standard Curve and DNA samples	76
2.8. Fluorescent In Situ Hybridisation	77
2.8.1. Preparation of Metaphase Spreads.....	77
2.8.2. Preparation of Probe	77
2.8.3. Agarose Gel Electrophoresis	78
2.8.4. Hybridisation Protocol	78
2.8.5. Antibody Detection.....	79
2.9. Chromosome Painting	79
2.9.1. Labeling DOP-PCR Product	80
2.9.2. Preparation of Probe	80
2.9.3. Hybridisation Protocol	80
2.9.4. Antibody Detection.....	81
2.9.5. Image Acquisition.....	81
2.10. Statistical Methods	81
2.11. Calculations.....	82
CHAPTER 3: Results 1	84
3.1. Characterization of Initial Cell Lines	85
3.1.1 Analysis of Growth During Long-Term Continuous Culture In Initial CHO-GFP Cell Lines.....	86
3.1.2 Analysis of eGFP Expression During Long-Term Culture In Initial CHO-GFP Cell Lines.....	86
3.2. Amplification of CHO-GFP cell lines.....	93
3.2.1 Analysis of Batch Culture Growth Of Amplified CHO-GFP Cell Lines ..93	
3.2.2 Effect of Long-Term Culture on Recombinant eGFP and DHFR Expression	97
3.2.2.1. Analysis of eGFP Fluorescence in Amplified Cell Lines Over Long-Term Culture By Flow Cytometry	97
3.2.2.2. Analysis of GFP and DHFR Protein Expression Over Long Term Culture By Western Blot	104
3.2.3 Copy Number Analysis Over Long-Term Culture By qPCR	113
3.2.4 Analysis of mRNA expression Over Long-Term Culture in Amplified CHO-GFP Cell Lines.....	121
3.2.5 Effect of Sodium Butyrate (NaB) on eGFP expression	132
3.3. Discussion.....	136
3.3.1 Summary	142
CHAPTER 4: Results 2	143
4.1 Establishment of CHO-EPO Initial Cell Lines	144

4.1.1 Analysis of Growth Characteristics and Productivity of Initial CHO-EPO Cell Lines During Long-Term Culture	147
4.2 Establishment of Amplified CHO-EPO Cell Lines	153
4.2.1 Long-Term Culture in Amplified CHO-EPO cell lines	155
4.2.1.1 Analysis of Batch Growth of Amplified CHO-EPO cell lines	155
4.2.1.2 Effect of Amplification on Recombinant EPO Production During Long-Term Culture	161
4.2.1.3 Copy Number Analysis Over Long-Term Culture in Amplified CHO-EPO cell lines.....	166
4.2.1.4 Analysis of EPO mRNA Over Long-Term Culture in Amplified CHO-EPO cell lines.....	171
4.3. Discussion.....	179
4.3.1 Summary	183
CHAPTER 5: Results 3	184
5.1 Effect of Amplification and Long-Term Culture on Chromosome Number ...	185
5.2 Analysing Plasmid Localization Using Dual Colour FISH.....	186
5.3 Effect of Long-Term Culture on Plasmid Localization.....	200
5.4. Discussion.....	219
5.4.1 Summary	224
CHAPTER 6: Concluding Remarks and Future Work	225
6.1 Concluding Remarks	226
6.2 Future Work.....	233
REFERENCES	236
APPENDICIES.....	255
APPENDIX 1 Materials, Chemicals and Special Equipment	255
APPENDIX 2 p1010-, p-901-eGFP Plasmid Construct	261
APPENDIX 3 p1010-, p901-EPO Plasmid Construct	262

Word Count: 63944

LIST OF FIGURES

Figure 1.1: Percentage of approved biopharmaceuticals in different production systems by January 2009	20
Figure 1.2: Derivation of CHO Subclones	25
Figure 1.3: Breakage fusion bridge (B-F-B) cycle mechanism.....	29
Figure 1.4: Epigenetic regulation of gene expression in mammalian cells.....	36
Figure 1.5: The major post-translational histone modifications and their effect on transcriptional states	40
Figure 1.6: Common mechanisms of DNAmethylation and cross-talk between DNA methylation and histone modifications	43
Figure 2.1: Establishment of CHO-GFP and CHO-EPO cell lines	67
Figure 3.1: Analysis of batch culture growth and cumulative cell time in initial CHO- GFP cell lines	89
Figure 3.2: Effect of long-term culture on eGFP fluorescence and the degree of variation in initial cell lines	90
Figure 3.3: Western Blot determination of eGFP expression over long-term continuous culture	92
Figure 3.4: Analysis of batch culture growth of amplified CHO-GFP cell lines	95
Figure 3.5: Effect of long-term culture on cumulative cell time in amplified CHO-GFP cell lines	96
Figure 3.6: eGFP fluorescence in amplified cell lines over long term culture, in the presence and absence of MTX selection.....	100
Figure 3.7: Flow cytometry histograms of amplified UCOE cell lines over long-term culture	101
Figure 3.8: Flow cytometry histograms of amplified non-UCOE cell lines over long term culture	102
Figure 3.9: Effect of long term culture on the degree of variation in eGFP fluorescence in amplified cell lines.....	103
Figure 3.10: Western blot assessment of eGFP expression in amplified cell lines over long-term culture in amplified clones, in the presence of MTX selection.....	105
Figure 3.11: Western blot assessment of eGFP expression in amplified cell lines over long-term culture in amplified clones, without MTX selection	106
Figure 3.12: Comparison of eGFP expression detected by flow cytometry against by western blotting	107
Figure 3.13: Western blot assessment of DHFR expression in amplified cell lines over long term culture in the presence of MTX selection	109
Figure 3.14: Western blot assessment of DHFR expression in amplified cell lines over long-term culture without MTX selection	110
Figure 3.15: Comparison of eGFP against DHFR protein expression	112

Figure 3.16: eGFP and DHFR gene copy numbers in amplified cell lines during long-term culture in the presence of MTX selection	115
Figure 3.17: eGFP and DHFR gene copy numbers in amplified cell lines during long-term culture in the absence of MTX selection	116
Figure 3.18: Comparison of protein expression against plasmid copy number	119
Figure 3.19: Comparison of eGFP and DHFR gene copy numbers	120
Figure 3.20: Analysis of eGFP mRNA expression over long-term culture in amplified cell lines	123
Figure 3.21: Changes to the molecular characteristics of a recombinant gene system during long-term culture in the absence of MTX selection	127
Figure 3.22: Analysis of DHFR mRNA expression over long-term culture in amplified cell lines	129
Figure 3.23: Comparison of protein production against mRNA expression.....	131
Figure 3.24: Effect of Sodium Butyrate on growth, eGFP fluorescence and mRNA ..	135
Figure 4.1: EPO production in initial CHO-EPO cell lines	146
Figure 4.2: Analysis of growth characteristics of initial CHO-EPO cell lines during batch growth	150
Figure 4.3: Analysis of total EPO production and specific productivity in initial CHO-EPO cell lines over long-term culture.....	152
Figure 4.4: EPO production in amplified CHO-EPO cell lines	154
Figure 4.5: Analysis of batch culture growth and cumulative cell time in amplified CHO-EPO cell lines	159
Figure 4.6: Growth kinetics of amplified CHO-EPO cell lines over long-term culture	160
Figure 4.7: Production of recombinant EPO during long-term culture in amplified CHO-EPO cell lines	163
Figure 4.8: Effect of amplification and long-term culture on specific productivity in CHO-EPO cell lines	164
Figure 4.9: Comparison of growth rate and volumetric EPO production against the specific productivity	165
Figure 4.10: Analysis of EPO gene copy number over long-term culture in amplified CHO-EPO cell lines	168
Figure 4.11: Analysis of EPO mRNA expression over long-term culture in amplified CHO-EPO cell lines	172
Figure 4.12: Comparison of specific productivity and EPO gene copy number against mRNA expression.....	174
Figure 4.13: Changes to the molecular characteristics during long-term culture in amplified CHO-EPO cell lines.....	178
Figure 5.1: Investigating chromosome number distribution over long-term culture in amplified CHO-GFP cell lines	187
Figure 5.2: Karyotype of CHO-DG44 parental cell line.....	188

Figure 5.3: Plasmid localization in amplified CHO-GFP cell lines	191
Figure 5.4: Plasmid localization and chromosome 4 hybridization observed for N2 cell line	192
Figure 5.5: Plasmid localization and chromosome 4 hybridization observed for U2 cell line	193
Figure 5.6: Plasmid localization and chromosome 6 hybridization observed for N2 cell line	194
Figure 5.7: Plasmid localization and chromosome 6 hybridization observed for U2 cell line	195
Figure 5.8: Plasmid localization and chromosome 7 hybridization observed for N2 cell line	196
Figure 5.9: Plasmid localization and chromosome 7 hybridization observed for U2 5cell line	197
Figure 5.10: Plasmid localization and chromosome X and Y hybridization observed for N2 cell line	198
Figure 5.11: Plasmid localization and chromosome X and Y hybridization observed for U2 cell line	199
Figure 5.12: Different plasmid integration patterns observed in amplified CHO-GFP cell lines	204
Figure 5.13: Plasmid integration patterns observed in non-UCOE cell lines at the start of long-term culture in the presence of MTX.....	205
Figure 5.14: Plasmid integration patterns observed in UCOE cell lines at the start of long-term culture in the presence of MTX.....	206
Figure 5.15: Frequency of occurrence of plasmid integration patterns in non-UCOE cell lines at the start of long-term culture in the presence of MTX	207
Figure 5.16: Frequency of occurrence of plasmid integration patterns in UCOE cell lines at the start of long-term culture in the presence of MTX	208
Figure 5.17: Plasmid integration patterns observed in non-UCOE cell lines at the end of long-term culture in the presence of MTX.....	209
Figure 5.18: Plasmid integration patterns observed in UCOE cell lines at the end of long-term culture in the presence of MTX	210
Figure 5.19: Frequency of occurrence of plasmid integration patterns in non-UCOE cell lines at the end of long-term culture in the presence of MTX	211
Figure 5.20: Frequency of occurrence of plasmid integration patterns in UCOE cell lines at the end of long-term culture in the presence of MTX	212
Figure 5.21: Plasmid integration patterns observed in non-UCOE cell lines at the end of long-term culture in the absence of MTX.....	213
Figure 5.22: Plasmid integration patterns observed in UCOE cell lines at the end of long-term culture in the absence of MTX.....	214

Figure 5.23: Frequency of occurrence of plasmid integration patterns in non-UCOE cell lines at the end of long-term culture in the absence of MTX.....215

Figure 5.24: Frequency of occurrence of plasmid integration patterns in UCOE cell lines at the end of long-term culture in the absence of MTX.....216

LIST OF TABLES

Table 1.1: The top selling biopharmaceutical products	18
Table 2.1: Primers used for q-PCR.....	75
Table 3.1: Effect of long-term culture on eGFP gene copy number and protein expression	118
Table 4.1: Effect of amplification and long-term culture on EPO gene copy number and specific productivity	170
Table 4.2: Summary of EPO gene copy number per cell and relative amount of EPO mRNA	173
Table 5.1: Summary of genomic parameters and plasmid integration patterns for eGFP expression.....	218

ABSTRACT

Therapeutic proteins require proper folding and post-translational modifications (PTMs) to be effective and biologically active. Chinese hamster ovary (CHO) cells are the most frequently used host for commercial production of therapeutic proteins and DHFR-mediated gene amplification is extensively applied to generate cell lines with increased protein production. However, decreased protein productivity is observed unpredictably during the time required for scale-up with consequences for yield, time, finance and regulatory approval. Ubiquitous Chromatin Opening Elements (UCOEs) are DNA elements naturally found upstream of specific housekeeping genes, which are proposed to maintain open chromatin structure, supporting stable and high-level transgene expression by prevention of transgene silencing. In this study we have examined the interaction between UCOE and DHFR-linked amplification in relation to cell expression stability.

CHO-DG44 cell lines were engineered to express erythropoietin (EPO) or a green fluorescent protein (GFP) from constructs with or without the inclusion of a UCOE. Cell lines were amplified in the presence of 250 nM metotrexate (MTX) and were then grown continuously for over 70 days in the presence and absence of MTX. Growth characteristics, protein expression, plasmid copy numbers, mRNA expression, karyotype and recombinant gene localisation (by fluorescent in situ hybridisation – FISH) were assessed for cells at stages throughout the period of long-term culture. In summary the inclusion of UCOE elements generated cells that;

- achieved higher cell densities and exhibited increased production of recombinant mRNA/cell and protein yield
- allowed isolation of greater numbers of high producing clones
- resulted in greater mRNA recovery/recombinant gene copy
- retained stable mRNA and protein expression after amplification provided MTX was present (but not in the absence of MTX when instability was observed)
- exhibited a more consistent karyotype and no abnormal chromosomal rearrangements.

It was concluded that the inclusion of UCOEs within expression constructs offer significant advantages for certainty of cell line generation (and the number of recovered clones for more detailed characterisation/optimisation) and that UCOEs are compatible with DHFR amplification protocols. The data suggested that enhanced cell line recovery by transcriptional enhancement of selection markers, such as DHFR.

DECLARATION

No portion of this work referred to in the thesis has been submitted in support of an application for another degree or qualification of this or any other university or other institute of learning.

COPYRIGHT

Copyright in text of this thesis rests with the author. Copies (by any process) either in full, or of extracts, may be made only in accordance with instructions given by the author and lodged in the John Rylands University of Manchester. Details may be obtained from the librarian. This page must form part of any such copies made. Further copies (by any process) of copies made in accordance with such instructions may not be made without the permission (in writing) of the author.

The ownership of any intellectual property rights which may be described in this thesis is vested in the University of Manchester, subject to any prior agreement to the contrary, and may not be made available for use by third parties without the written permission of the University, which will prescribe the terms and conditions of any such agreement.

Further information on the conditions under which disclosures and exploitation may take place is available from the Director of Graduate Education, School of Biological Sciences.

ACKNOWLEDGEMENTS

I would like to express my deepest gratitude to my supervisor Alan Dickson for his guidance, advice, insight, encouragement and valuable supervision. I would also like to thank my advisor Catherine Millar for her comments and criticism.

I would like to thank all the members of the Dickson Lab. for providing an enjoyable work environment and their supports. I would like to specially thank Dr Alexandra Croxford for the cells and kindly sharing her experience.

I would like to gratefully acknowledge Republic of Turkey Ministry of National Education for funding.

This thesis is dedicated to my family in Turkey and the UK, especially my mother who offered me unconditional love and support throughout this PhD. It is also dedicated to my husband, Richard, who taught me even the largest task can be accomplished if it is done one step at a time.

ABBREVIATIONS

A260nm	- absorbance at 260nm
A280nm	- absorbance at 280nm
bp	- base pair
BSA	- Bovine serum albumin
CBX	- chromobox homolog 3
cDNA	- complementary DNA
ChIP	- chromatin immunoprecipitation
CHO	- Chinese hamster ovary
CV	- coefficient of variation
DEPC	- diethylpyrocarbonate
DHFR	- dihydrofolate reductase
ddH ₂ O	- double distilled water
DMSO	- dimethyl sulfoxide
DNA	- deoxyribonucleic acid
ECACC	- European Collection of Animal Cell Cultures
<i>E. coli</i>	- <i>Escherichia coli</i>
EDTA	- ethylenediaminetetra acetic acid
EPO	- erythropoietin
FBS	- foetal bovine serum
FISH	- fluorescent in situ hybridisation
h	- hour
HAT	- histone acetyltransferase
hCMV	-human cytomegalovirus promoter
HDAC	- histone deacetylase
hnRPA2B1	- heterogeneous nuclear ribonucleoprotein A2/B1
IFN- β	- Interferon- β
Ig	- immunoglobulin
IRES	- internal ribosome entry site
kb	- kilobase pair

LB	- Luria Bertani
LCR	- Locus control region
M	- Molar
min	- minute
MTX	- Methotrexate
OD	- optical density
qRTPCR	-quantitative reverse transcription PCR
qPCR	- quantitative PCR
pA	- polyadenosine tail
PBS	- phosphate buffered saline
PCR	- polymerase chain reaction
PDCD2	- programmed cell death 2
PSMB1	- proteasomal subunit C5
RNA	- ribonucleic acid
RNAi	- RNA interference
rRNA	- ribosomal RNA
RT	- reverse transcription
s	- seconds
<i>S. cerevisiae</i>	- <i>Saccharomyces cerevisiae</i>
SD	- standard deviation
SEM	- standard error of mean
siRNA	- small interfering RNA
S/MAR	- Scaffold/Matrix Attachment Region
SSC	- standard saline citrate
SV40	- simian virus 40 promoter
TBE	- tris, borate, EDTA
TBP	- tata binding protein
TE	- tris, EDTA
TMB	- 3, 3', 5, 5'-tetramethylethylenediamine
tRNA	- transfer RNA
UCOE	- ubiquitous chromatin opening element

CHAPTER 1:

Introduction

1.1. Biopharmaceuticals in Biotechnology

The term biopharmaceuticals refers to proteins used as therapeutics, some of which may be genetically engineered. These therapeutic proteins include hormones, therapeutic enzymes, monoclonal antibodies, growth factors, blood factors and vaccines. 30 years ago, the first biopharmaceutical, “humulin” a recombinant human insulin, has been approved for medical use and since then the pharmaceutical biotechnology industry has developed rapidly. There are over 200 biopharmaceutical products that have been approved in today’s market (Walsh, 2010a). The global biopharmaceutical market value reached \$99 billion in 2009 (R&D-Pipeline-News, 2011) and it is predicted to grow at between 7% and 15% annually over the next several years (Walsh, 2010a, Hiller, 2009). The top 10 biotechnology drugs by global sales are shown in Table 1.1.

The majority of therapeutic proteins display one or more post-translational modifications (PTMs) and the functions of these biopharmaceuticals are dependent on particular PTMs. The main PTMs associated with therapeutic proteins are glycosylation, carboxylation, hydroxylation, amidation, sulfation, disulfide bond formation and proteolytic processing (Walsh, 2010b). Among all, glycosylation is one of the most widespread and complex PTM process. More than 50% of all proteins are glycosylated in their natural forms (Wong, 2005, Solá and Griebenow, 2009).

Glycosylation may affect different properties of proteins such as biological activity, function, clearance from circulation, and crucially antigenicity (Walsh and Jefferis, 2006). Well-defined examples include erythropoietin (EPO) where it has been shown that, removal of any of the N-linked sugar chains significantly reduced the biological activity *in vivo* (Delorme et al., 1992). Other studies have shown that the presence of carbohydrates can be critical for antibody function as carbohydrate-deficient antibodies lose their ability to activate complement and to induce antibody-dependent cellular cytotoxicity (ADCC) (Wright and Morrison, 1997). Another example is Interferon- β (IFN- β) which can be produced in both Chinese hamster ovary (CHO) cells (Avonex) and *Eschericia coli* (Betaseron). The systems produce glycosylated and unglycosylated variants, respectively.

A detailed study of the effect of glycosylation on functional activity of human IFN- β showed that the specific activity is 10-fold higher for the glycosylated form *in vitro* (Karpusas et al., 1998, Runkel et al., 1998).

Table.1.1: The top selling biopharmaceutical products. Source: R&D Pipeline News (2011) and Walsh (2010a)

Biopharmaceutical	Tradename (Company)	2009 sales (US \$ billion)	Expression System
Tumor Necrosis Factor (TNF) Blocker Monoclonal Antibody (mAb)	Enbrel (Amgen, Wyeth)	6.58	CHO
TNF blocker mAb	Remicade (Centocor, Schering-Plough)	5.93	Confidential
Humanized mAb	Avastin (Genentech)	5.77	CHO
Chimeric mAb	Rituxan/MabThera (Genentech)	5.65	CHO
Human TNF Antibody	Humira (Abbott, Eisai)	5.48	CHO
Erythropoietin (EPO)	Epogen/Procrit/Eporex/ESPO	5.03	CHO
Humanized mAb	Herceptin (Genentech)	4.89	CHO
Insulin	Lantus (Sanofi-Aventis)	4.18	<i>E. coli</i>
Granulocyte colony stimulating factor	Neulusta (Amgen)	3.35	<i>E. coli</i>
EPO	Aranesp/Nespo (Amgen)	2.65	CHO

In addition to glycosylation, product stability and biological activity of specific proteins can be influenced by several additional PTMs (Walsh, 2010b). Many of the modern recombinant insulins are synthesized as proinsulin and purified followed by proteolytic processing (Walsh, 2005). Failure of protein folding and disulfide-bond formation

processes can cause degradation (Arolas et al., 2006). The functional activity of salmon calcitonin (Forcaltonin; Unigene, Fairfield, NJ, USA) is dependent on amidation (Ray et al., 1993), and that of several blood factors is depend on γ -carboxylation and β -hydroxylation (Kaufman, 1998). It has also been shown that tyrosine sulfation is required for full procoagulant activity of factor VIII (Michnick et al., 1994). These PTMs are structurally well-defined and have limited and often predictable effects upon the therapeutic proteins (Walsh and Jefferis, 2006).

It has been shown so far that the differences of the PTMs in a recombinant protein relative to the natural product might influence the therapeutic profile. Therefore, it is important to select a suitable expression system when considering production of a potential biopharmaceutical (see Section 1.2). The ability to perform specific forms of PTM is dependent on expression of the relevant enzymatic pathways and not all systems are equally capable of performing the same range of PTMs. Although relatively simple proteins, such as insulin and bovine growth hormone, can be successfully produced in *E. coli* (see Section 1.2.1) (Swartz, 2001) or *Saccharomyces cerevisiae* (*S. cerevisiae*) (see Section 1.2.2) (Hard et al., 1989) more complex biomolecules, such as monoclonal antibodies or highly glycosylated proteins, require the post-translational metabolic machinery only available in mammalian cells (see Section 1.2.3) (Butler, 2005).

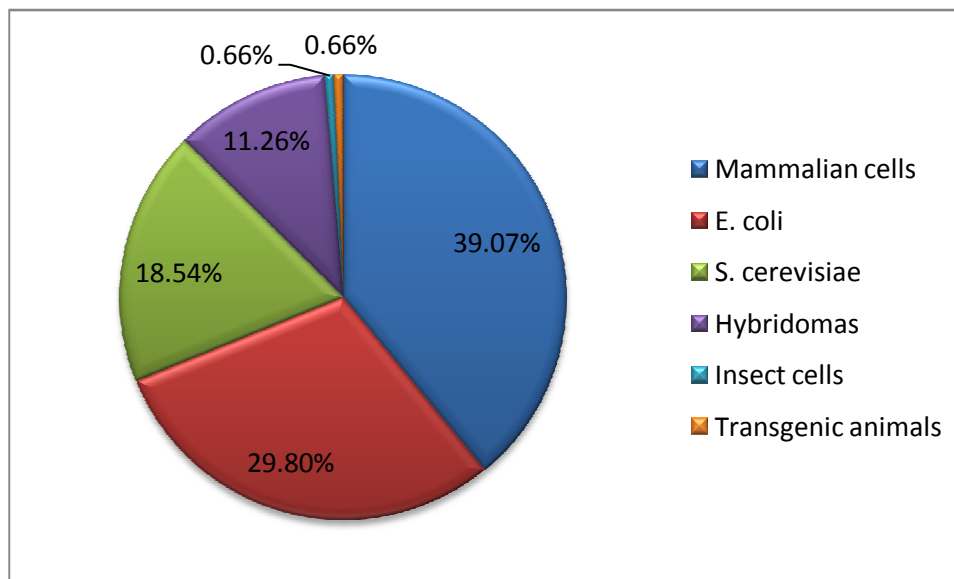
There have been recent advances in the biopharma industry related to engineering PTMs, glycosylation in particular, for the improvement of the therapeutic product (Beck et al., 2010, Jefferis, 2009). One of the glycoengineering approaches is introduction of additional carbohydrates onto the target protein and creates hyperglycosylated variants. An example to this is EPO glycosylation analogue, which contains two additional N-linked glycosylation sites in contrast to the native molecule. Glycoengineered version of this product displayed an increased *in vivo* activity and substantially extended half-life (Elliott et al., 2003, Sinclair and Elliott, 2005). A more recent approach for the glycoengineering focuses upon the producer cell line. Notable advances have been recorded in terms of engineering yeast (Hamilton and Gerngross, 2007) and plant-based systems (Karg and Kallio, 2009) for the production of glycosylated therapeutic proteins. However, there are

some other factors that need to be taken into account when choosing an expression system for production, including cost-effectiveness and safety requirements.

1.2. Expression Systems

Choosing which expression system to use is one of the most important decisions for a drug developer to make in the context of therapeutic protein production. Several expression systems have been developed including transgenic animals (Louis-Marie, 2009) and plants (Karg and Kallio, 2009), insect cell lines (Altmann et al., 1999, Marchal et al., 2001) and fungal systems (Nevalainen et al., 2005). However, the majority of the approved therapeutics is produced in bacterial, yeast and mammalian cell lines (Durocher and Butler, 2009, Walsh, 2010a, Walsh, 2010b).

Figure 1.1: Percentage of approved biopharmaceuticals in different production systems by January 2009. Adapted from Ferrer-Miralles et al. (2009).



In 2009, among all the recombinant protein-based pharmaceuticals approved by the FDA and EMEA, about 39% of them produced using mammalian cells; the remaining portion was produced using *E. coli* (~30%), *S. cerevisiae* (~19%), hybridomas (~11%), insect cells

(~0.7%) and transgenic animals (0.7%, Figure 1.1) (Ferrer-Miralles et al., 2009, Walsh, 2010a). In this section, the advantages and disadvantages of therapeutic protein production in bacterial (Section 1.2.1), yeast (Section 1.2.2) and mammalian cells (Section 1.2.3) will be discussed.

1.2.1. Bacteria

Due to ease of genetic manipulation, rapid growth and relatively low cost *E. coli* is one of the earliest and most widely utilized system for the expression of cloned genes (Demain and Vaishnav, 2009). The main drawback is that *E. coli* cannot perform glycosylation and have limited capacity to perform other PTMs that are often required for the functional characteristics of the protein of interest (see Section 1.1) (Demain and Vaishnav, 2009, Yin et al., 2007). Another drawback is that proteins synthesized in *E. coli* often retain an extra methionine residue at the N-terminus, which remarkably affects protein stability and may produce immunogenicity (Chaudhuri et al., 1999). New strategies have been employed to overcome these problems one of which is secretion of proteins into periplasmic space or medium. Advantages of this includes avoidance of N-terminal methionine extension, facilitating correct disulfide bond formation enabled by the enzymes in the periplasm of *E. coli* and production of soluble and biologically active proteins (Choi and Lee, 2004, Mergulhao et al., 2005, Georgiou and Segatori, 2005). Furthermore, a recent study reported generation of N-linked glycoproteins from *E. coli*, which is promising for the future improvements (Guarino and DeLisa, 2011). Due to their low cost and convenience, the expression of heterologous secreted proteins in *E. coli* is widely employed for laboratory and preparative purposes (Georgiou and Segatori, 2005) and also expression of non-glycosylated therapeutic proteins (Yin et al., 2007).

Other bacterial expression systems that have potential include the Gram-Positive bacilli. They are genetically well characterized, easily manipulated, generally regarded as safe (GRAS status) and can secrete homologous and potentially heterologous proteins directly into the medium (Westers et al., 2004, Demain and Vaishnav, 2009). *Bacillus* is preferred for the production of commercially available enzymes such as proteases and amylases. The

major limitations for using *Bacillus* have been occurrence of misfolded proteins, instability of plasmid, and production of proteases (Westers et al., 2004). Most attempts have focused on construction of bacterial strains with reduced protease activity by the deletion of extracellular proteases which allowed production of proteins that are sensitive to degradation (Gupta et al., 2002) and greatly improved the production yield (Wong et al., 1994, Wu et al., 1991). However, optimization of host strains which facilitates correct folding is still a challenge in bacilli (Westers et al., 2004).

1.2.2. Yeast

Yeasts share several molecular, genetic and biochemical characteristics with higher eukaryotes and are suitable for large-scale production. Compared to mammalian cells yeast can grow relatively rapidly with low cost (Yin et al., 2007). In contrast to *E. coli*, yeast can secrete proteins into the extracellular environment, and potentially produce soluble, correctly-folded proteins. Yeasts are known to be able to perform many PTMs such as glycosylation, disulfide bond formation and proteolytic processing (see Section 1.1) (Porro et al., 2011, Hamilton et al., 2003). There are several yeast species used for production of recombinant proteins including *S. cerevisiae*, *Pichia pastoris* and *Schizosaccharomyces pombe* (Porro et al., 2011). *S. cerevisiae* was first engineered to express heterologous genes in 1981 (Hitzeman et al., 1981). Until recently, the main limitation of yeast expression system has been the differences of N-linked glycosylation from those of mammalian cells and humans. In this respect, advances have been made in glycoengineering of yeast strains enabling them to express human-like glycosylated proteins (Hamilton and Gerngross, 2007). To achieve this, four genes have been knocked out to prevent hyper-mannosylation and fourteen additional glycosylation genes have been introduced to the *P. pastoris* strain. Engineered *P. pastoris* strains, branded as GlycoFi (Merck), are capable of producing complex terminally sialylated uniform N-glycans (Hamilton et al., 2003, Hamilton et al., 2006, Hamilton and Gerngross, 2007). This system has been used for production of full length antibodies (Potgieter et al., 2009).

1.2.3. Mammalian Cells

When compared to the bacterial and yeast systems discussed above, mammalian cells require expensive and complex media. Product yields from mammalian cells have significantly increased in the past 30 years, however generation of recombinant cell lines remains tedious and time-consuming process. Moreover, recombinant protein expression can be unstable with time (Wurm, 2004). Despite this, mammalian cells are still predominant systems for production of biopharmaceuticals (Table 1.1) due to their ability to carry out correct complex PTMs (see Section 1.2) and secrete these proteins (Andersen and Krummen, 2002, Yin et al., 2007).

Among mammalian cells, Mouse myeloma (NS0) and Chinese hamster ovary (CHO) cells are the predominant systems for mammalian expression because of the well-characterised platform technologies that allow for transfection, amplification and selection of high-producer clones (Butler, 2005, Andersen and Krummen, 2002). Over the past two decades CHO cells have been successfully used for therapeutic protein production and extensive testing and safety data has been amassed during this period (Jayapal et al., 2007). This accumulated knowledge of CHO cell platform ultimately eases the regulatory approval process which ensures that CHO cells are likely to retain as the major workhorse for the production of therapeutic protein in the near future. CHO cell lines has been used in my project as the host cell type and therefore the next section will be focussed on CHO cells after a brief history of both NS0 myeloma and CHO cells.

1.2.3.1. NS0 Cells

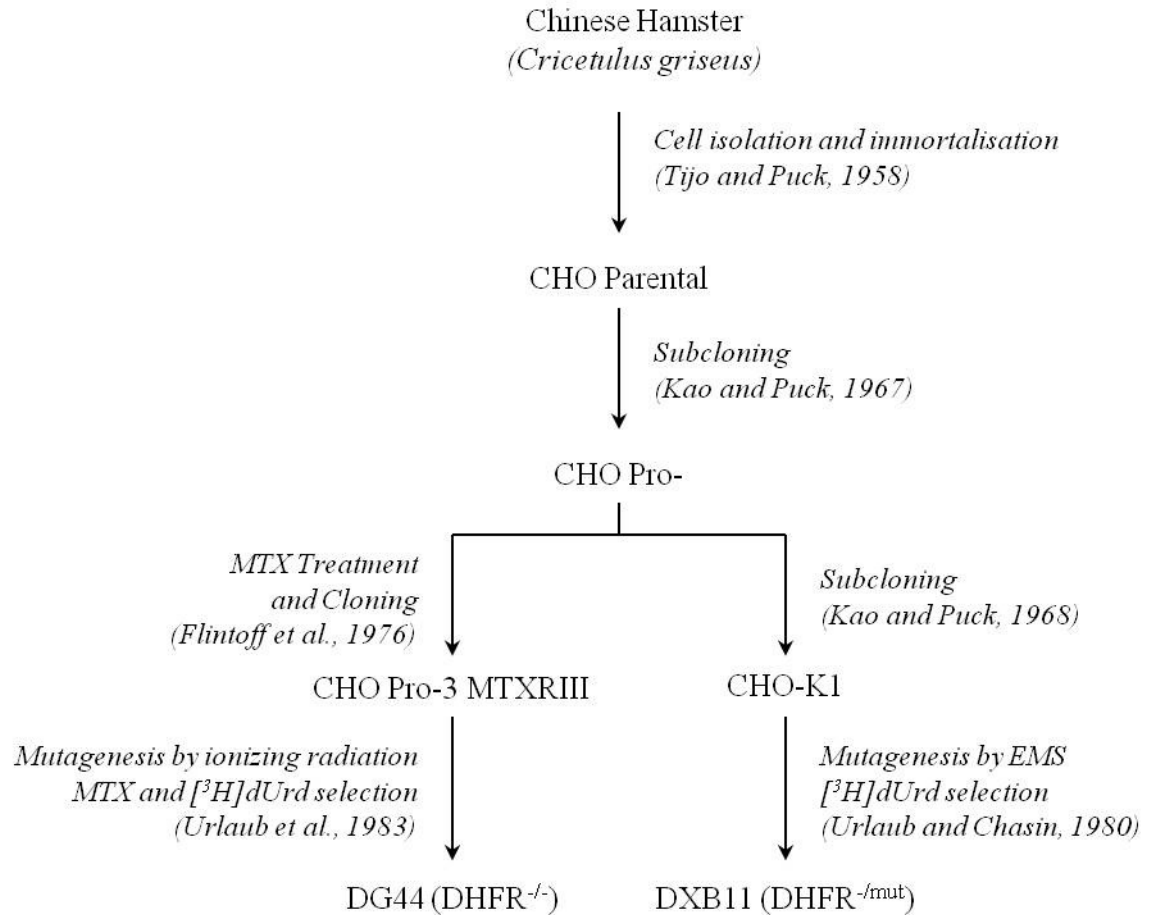
The NS0 myeloma cell line originated from mouse plasmacytoma cells (Barnes et al., 2000). The expression of low levels of Glutamine synthetase (GS) enzyme in NS0 cells gives it advantages for the GS system which works as a dominant selectable marker (Bebbington et al., 1992). GS enzyme catalyzes the formation of glutamine from glutamate and ammonia. GS inhibition and gene amplification can be mediated by methionine sulphoximine (MSX). Concentrations of 10-100 μ M MSX are required to provide clones

that have amplified the transgene complex containing the GS gene and the gene of interest (Butler, 2005, Wurm, 2004). Despite the low copy number of genes per cell (4-10 genes/cell) in GS system, the expression is as high as Dihydrofolate reductase (DHFR) system, which characterised by 10-100 fold the number of gene copies. Based on this, another advantage of GS system is that the GS-high producer clones can be produced in around 3 months, whereas in DHFR system it may take at least 6 months (Butler, 2005).

1.2.3.2. CHO Cells

Before the isolation of CHO cells, Chinese hamsters (*Cricetulus griseus*) had been used as an experimental laboratory species for a significant time. They were particularly useful in radiation cytogenetics and tissue culture studies due to their low chromosome number ($2n=22$). The first CHO cells were isolated by Dr. Theodore T. Puck in 1957 (Tjio and Puck, 1958). It soon became obvious that these cells had relatively fast doubling times *in vitro*. CHO cells have thereafter been used extensively in numerous biomedical researches. After several years of study, sub-clones of CHO cells were isolated which were found to require proline for growth, which were later named CHO-K1 (Figure 1.2) (Kao and Puck, 1967, Kao and Puck, 1968). These cells have been extensively used in industry and several sub-clones have been isolated from initial cell lines. Chasin et al. isolated double DHFR deficient mutants DXB11 and DG44, which are widely used today as host cell lines for recombinant protein expression (Flintoff et al., 1976, Urlaub and Chasin, 1980, Urlaub et al., 1983). These cells do not contain DHFR therefore heterologous genes can be co-transfected into cells with DHFR gene as a selectable amplifiable marker (Section 1.2.3.2.2).

Figure 1.2: Derivation of CHO Subclones.



The isolation of different subclones are shown in the chart. Abbreviations: CHO, Chinese hamster ovary; DHFR, dihydrofolate reductase; [³H]dUrd, tritiated deoxyuridine; EMS, Ethyl methanesulfonate.

1.2.3.2.1. CHO Cell Chromosomes

There has been a substantial accumulation of genetic heterogeneity in CHO cell lines during their growth, expansion and sub-cloning since the first CHO cells were isolated from Chinese hamster in 1956 (Figure 1.2). Karyologic studies have shown a high degree of aneuploidy in CHO cell lines. Early characterisation of the CHO-Pro- cell line karyotype indicated a modal chromosome number of 21 as compared to 22 chromosomes found in Chinese hamster cells (Kao and Puck, 1969). Trypsin-giemsa banding

karyotyping technique revealed that only 8 of the CHO chromosomes including chromosomes 1, 2, 6, 8, 9, 10 and X appeared to be normal compared to Chinese hamster chromosomes (Deaven and Petersen, 1973). The remaining chromosomes contained deletions, translocations and/or additions, which have been termed “Z” group chromosomes. Moreover, cells within a clonal population also displayed chromosomal heterogeneity that 24% of the cells contained 19, 20, 22 or 44 chromosomes. Karyotype of the CHO-K1 subclone was found to be similar to the parental CHO, although one small chromosome was missing therefore containing only 20 chromosomes (Kao and Puck, 1970). More recently a karyotype of the DG44 cell line showed that it possesses a modal chromosome number of 20. Only 7 of the DG44 chromosomes were found to be normal compared to Chinese hamster chromosomes, including two copies of chromosome 1, and one copy of each chromosomes 2, 4 5, 8 and 9. The remaining chromosomes were 4 Z-group chromosomes, 7 derivative chromosomes, which were generated by rearrangements within the chromosomes, and 2 marker chromosomes, which contained no recognizable landmarks corresponding to the parental cell chromosomes (Derouazi et al., 2006). Moreover, recombinant CHO-DG44 cell lines harboured further chromosomal rearrangements resulting in an altered karyotype compared to the parental DG44 cell lines (Derouazi et al., 2006).

CHO cells have shown to display some unusual chromosome structures including the location of telomeric sequences. Telomeric DNA sequences are composed of tandem arrays of duplex 5'-TTAGGG-3' repeats, which are located at the end of eukaryotic chromosomes in many eukaryotic organisms. Telomeric DNA maintains the stability and integrity of the chromosomes (Bolzan, 2011). However, it was reported that telomeric signals were not located at the ends of most of the CHO cell chromosomes. Instead the telomeric repeats are located near centromeric regions of the chromosomes (so-called interstitial telomeric repeat sequences [ITSs]) (Balajee et al., 1994, Jun et al., 2006). ITSs are probably originated from inversions and fusions that occurred during the establishment of these cell lines. It was shown that some ITSs might undergo a variety of chromosomal aberrations including dicentrics, extended chromosomes, terminal translocation (Balajee et al., 1994, Lin and Yan, 2008). Therefore, this tendency of CHO cells to display

chromosomal rearrangements may have implications on the stability of both endogenous and integrated exogenous DNA within CHO cell chromosomes (Jun et al., 2006).

Recently, sequence information of an amplified CHO cell line engineered to express human secreted alkaline phosphatase (SEAP) has been reported (Hammond et al., 2011). Initial sequencing of this cell line using reference-guided alignment yielded 2.72Gb of genomic sequence. Moreover, the draft genomic sequence of the CHO-K1 cell line was published, showing ~24,000 predicted genes and ~29,000 transcripts in the 2.45Gb assembly (Xu et al., 2011). This is a huge step forward for the development of genome-scale tools and technologies for further in-depth studies of the CHO cells. Although the different CHO cell lines display a large genomic diversity, the CHO-K1 genome can serve as a reference for the sequencing analysis of other CHO cell lines.

1.2.3.2.2. MTX-mediated Gene Amplification in CHO Cells

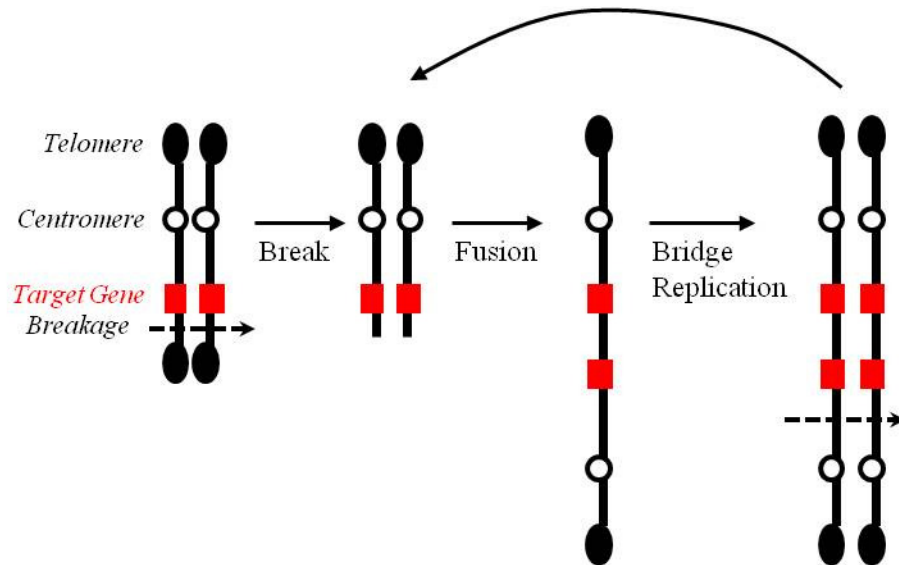
The isolation of DHFR-deficient CHO cells made it possible to use the DHFR gene as a selectable and amplifiable marker. DHFR is involved in nucleotide biosynthesis and it converts dihydrofolate to tetrahydrofolate. Selective pressure is applied to the cell culture with an inhibitor of DHFR (Butler, 2005, Kaufman and Schimke, 1981). Methotrexate (MTX) is a folic acid analog that inhibits DHFR activity. Exposure of the cells to gradually increased amounts of MTX promotes amplification of DHFR gene copies and co-transfected gene of interest. After several rounds of increasing concentration of MTX, the surviving cells frequently contain several hundred to a few thousand copies of the recombinant gene (Kaufman and Goeddel, 1990, Wurm, 2004).

CHO cells can achieve MTX resistance by other mechanisms aside from DHFR amplification including a reduced affinity of DHFR enzyme to MTX (Flintoff and Essani, 1980, Haber and Schimke, 1981) and impairment of MTX transport (Assaraf and Schimke, 1987, Cavalcanti et al., 1992, Saikawa et al., 1993). To overcome acquiring alternative resistance, MTX amplification is generally obtained by gradual increase of MTX concentration rather than single step high concentration of MTX.

The cytogenic studies in various MTX-amplified cells have revealed two types of abnormal chromosome structure, including 'homologous staining regions (HSRs)' and 'double minute chromosomes (DMs)' (Omasa, 2002). DMs are described as acentromeric, circular chromosome bodies. Due to the unequal distribution of DMs at mitosis, the amount of amplified DNA decreases in subsequent generations in the absence of selective pressure. Therefore, amplified DNA localized on DMs is considered unstable (Kaufman et al., 1979). HSRs are expanded chromosomal regions which fail to exhibit any banding patterns when stained by the trypsin-Giemsa method. In CHO cells, gene amplification is usually associated with the formation of HSRs (Kaufman et al., 1983, Wurm et al., 1996, Kim and Lee, 1999). HSRs normally exist in host cell chromosome and, consequently, recombinant DNA in HSRs is replicated in early S phase along with the host cell DNA and is inherited equally into the daughter cells. Therefore, by contrast, HSRs are often associated with stable amplified DNA (Nunberg et al., 1978, Kaufman et al., 1983). However, several studies have reported loss of integrated plasmid DNA during long-term culture in the absence of selective pressure (Fann et al., 2000, Hammill et al., 2000, Kim et al., 1998b). In addition, although very high producer cell lines were isolated with MTX amplification, the main problem is that MTX amplification is a very long and tedious process usually isolation and screening for high producing cell lines may take more than 6 months.

Several mechanisms have been proposed to be responsible for gene amplification, and for CHO cell lines the most frequently proposed mechanisms is the Break-Fusion-Bridge cycle model (B-F-B, Figure 1.3) (Kaufman et al., 1979, Kaufman et al., 1983, Kim and Lee, 1999). This model explains the possibility of the chromosomal aberrations associated with gene amplification including dicentric chromosomes, extended arrays of amplified DNA and elongated chromosomes (Kaufman et al., 1983, Kim and Lee, 1999, Wurm et al., 1996).

Figure 1.3: Breakage fusion bridge (B-F-B) cycle mechanism



Suggested mechanism for MTX-induced amplification is depicted above. Adapted from Omasa (2002).

In the B-F-B model, genomic rearrangements starts with chromosomal breakage from a site that depends on the chromosomal structure (Ma et al., 1993, Ruiz and Wahl, 1990). These breaks might occur naturally in the cell, but are almost always repaired by DNA repair mechanisms in a normal cell. This indicates that cells that contain unrepaired DNA regions probably have mutated DNA repair mechanisms. It has been shown previously that in malignant human cells the tumour suppressor gene p53 is mutated (Livingstone et al., 1992). p53 acts as a cell-cycle checkpoint protein, activates the DNA repair mechanisms when DNA is damaged and induces growth arrest by holding the cell cycle at G1/S phase until the damage is repaired (Goodsell, 1999). Studies with MTX resistant CHO cell lines carrying amplified DHFR genes showed sequestration of p53 within the cytoplasm as opposed to nuclear localisation in parental cells, resulting in lack of p53 function. This atypical localisation was found to be dependent on the presence of gene amplification, suggesting that mutant p53 cells have a tendency for gene amplification events (Ottaggio et al., 2000, Ottaggio et al., 2006).

These mutations occur spontaneously in all cells in culture, which can be considered Darwinian in nature (Wurm et al., 2003), i.e. only cells that do not repair damaged DNA and amplified DHFR gene are selected by increasing MTX concentrations. However, it should also be noted that MTX is known to be a clastogenic drug and causes chromosomal damage and gene mutations (Li and Kaminskas, 1984). Such clastogenic activity was reported to be associated with the initiation of gene amplification (Coquelle et al., 1997). Blocking DHFR with MTX leads to starvation of cells for DNA precursors, consequently this can result in mis-incorporation of uracil into DNA. This can induce the single-strand excising activity of repair enzyme and might be responsible for increased recombigenic activity (Goulian et al., 1980). Therefore, when added to the cells, MTX could contribute to the DNA amplification by increasing the rate of mutations and recombigenic events as well as selecting the cells with high DHFR-activity.

It is of particular interest in mammalian cells to examine the role of integration site in amplification and genomic stability. Wahl et al. (1984) reported that the chromosomal position affects the amplification frequency and the size and the stability of the amplified sequence in CHO cells. Gajduskova et al. (2007) have studied human cell lines and found a unique site associated with enhanced propensity to amplify and recurrent amplicon boundaries. This presumably implicates the expression of a rare folate-sensitive fragile site that initiates the amplification process. It was also reported in colorectal cancer cells that a small number of regions are associated with an enhanced rate of amplification and genomic instability (Bartos et al., 2007). Recently, BAC libraries were used to investigate the chromosomal region adjacent to the transgene vector in amplified CHO cell lines (Omasa et al., 2009). It has been suggested that endogenous repetitive structures of the amplified region on a specific CHO chromosome may promote the gene amplification and increase the stability of the inserted gene (Park et al., 2010).

A number of studies reported that expression of recombinant gene was variable between different clones from the same transfection following amplification (Jiang et al., 2006, Lattenmayer et al., 2007b, Kim et al., 1998a). One reason could be the different response of the primary cells to MTX amplification, resulting in variation in copy numbers of

integrated plasmid (Wurm and Petropoulos, 1994). Another reason for the differences in expression might be the effect of integration locus. Therefore, a high-level of DHFR production could be as a result of high expression level from a few plasmid DNAs which probably integrated into a locus that favours high transcription rate, or greater level of amplification of DHFR plasmids that individually express at low levels (Wurm et al., 2003).

1.2.4. Summary

It has been shown so far that there are a number of different expression systems that can be used for therapeutic protein production. Despite the recent improvements in bacteria and yeast cell platforms, mammalian cells, in particular CHO cells remain to be the most widely used host cell platform for production of therapeutic proteins that require complex post-translational modifications. To increase the productivity of these cell lines gene amplification methods, in particular MTX-mediated amplification, are extensively applied. One of the problems often encountered, however, is that these cell lines are highly unpredictable and display variable levels of recombinant protein. In addition, it is often observed that a cell lines display a decrease in recombinant protein production during long periods of culture. As a result a large number of clones need to be screened to achieve clones with desirable properties, which may take several months to develop cell lines with high and stable recombinant production. The stability of recombinant gene expression and phenotypic variability is discussed in the following section.

1.3. Stability of recombinant gene expression

An important consideration in CHO cell line development for commercial production is the potential instability of clonal cell lines over long-term culture (Wurm, 2004). It is important for commercial production to obtain cell lines that maintain stability of production over the long-term culture (i.e. the period to scale-up to manufacture), because the loss of productivity may jeopardize the regulatory approval of product (Barnes et al., 2003).

A number of reports have indicated instability for the DHFR-CHO expression system during long term culture in the absence of selective agent. Examples of these are instability of production of *c-myc* (Pallavicini et al., 1990), tissue plasminogen activator (Fann et al., 2000, Weidle et al., 1988), antibodies (Strutzenberger et al., 1999, Kim et al., 1998b, Chusainow et al., 2009, Dorai et al., 2011), and DHFR (Kaufman and Schimke, 1981). In some cases instability has also occurred in the presence of MTX but not as profoundly as when the selective pressure was absent (Chusainow et al., 2009, Fann et al., 2000, Kim et al., 1998a). It has been shown that decrease in productivity in this system during the long term culture was often related to loss of gene copy number for individual clones (Hammill et al., 2000, Fann et al., 2000, Pallavicini et al., 1990, Kim et al., 1998b, Kim et al., 2011). The location of integrated plasmid DNA into the CHO cell chromosome is suspected to play a role in stability (Section 1.2.3.2.2) (Kim and Lee, 1999). In the absence of selective pressure, amplified genes localized on extrachromosomal double minutes are usually lost during mitosis (Kaufman et al., 1983). However, amplified genes incorporated into the genome are not always stable, because CHO cells express a very unstable karyotype due to genomic rearrangements and such events may disrupts the integrity of endogenous genes (Section 1.2.3.2.2) (Kaufman and Schimke, 1981, Kim and Lee, 1999, Ruiz and Wahl, 1990, Weidle et al., 1988). Yoshikawa et al. (2000a) suggested that amplified genes located near the telomeric regions of chromosomes are more likely to be stable than those integrated in other regions. Furthermore, it has been reported that localization of the (TTAGGG)_n sequences around the telomeric ends of amplified arrays may be important for the stable maintenance of amplified genes (Section 1.2.3.2.1) (Kim and Lee, 1999). Recent studies have reported that recombinant CHO-derived cell lines lost their productivity during prolonged culture through transcriptional silencing by methylation in the absence of MTX (Chusainow et al., 2009, Kim et al., 2011, Yang et al., 2010b). Furthermore, another group reported that loss of monoclonal antibody productivity may occur as a result of genetic re-arrangement of transgenes (Heller-Harrison et al., 2009). They observed a loss of HC-DHFR bi-cistronic transcript with the appearance of a smaller transcript over time. Sequencing of this smaller transcript showed a lack of HC sequence but it contained an intact DHFR gene. Therefore, they suggested that despite producing

DHFR protein this cell line was no longer expressing HC protein or intact antibody partly due to uncoupling of HC-DHFR bi-cistronic transcription unit (Heller-Harrison et al., 2009). They also reported a gradual loss of antibody production by epigenetic gene silencing via methylation of DNA (Heller-Harrison et al., 2009).

Another major aspect that may have relevance to instability for specific cell lines is clonal variability (Barnes et al., 2001). This has traditionally been thought to be an aspect of genetic heterogeneity in the transfectant pools. However, recent studies have shown that in addition to genetic heterogeneity this variation may be due to phenotypic differences between cells in each clone (Barnes et al., 2006, Pilbrough et al., 2009). Barnes et al. (2006) found that even after three rounds of limiting dilution cloning of the parental NS0 cells the resulting clones showed a range of growth properties, suggesting that the high degree of variation in recombinant cell lines is not only due to added pressure of producing a foreign protein. Emerging research in mammalian cells has revealed that genetically-identical cells can show considerable variation in gene expression even in a common environment (Neildez-Nguyen et al., 2008, Raj et al., 2006, Sigal et al., 2006, Raj and van Oudenaarden, 2008, Liu et al., 2006). Protein expression is a stochastic process and leads to variation in mRNA and protein levels among cells (Raj and van Oudenaarden, 2008). Such expression noise can occur in transgenes as well as a wide range of endogenous genes, which may also have an indirect effect on transgene expression (Kaufmann and van Oudenaarden, 2007). This stochasticity was found to be originated from transcriptional bursting, which was visualized in CHO cells using a method similar to fluorescent in situ hybridization (Raj et al., 2006). Stochastic events of chromatin remodeling has been suggested as a possible mechanism to mediate such regulation by causing genes to switch between active and inactive transcriptional states (Becskei et al., 2005, Raj et al., 2006). Furthermore, it has been shown that genes coding for essential proteins display lower levels of expression noise (switching) than that of genes coding for non-essential proteins (Fraser et al., 2004). Recently, Pilbrough et al. (2009) have investigated the degree of variation within a recombinant CHO cell clone and suggested that intraclonal expression noise could account for the observed clonal variation and the apparent instability of expression over time.

In summary, mammalian cell lines display a considerable variation and unpredictable stability of expression, which remains as major issues in establishing high-producer cell lines for large-scale production of recombinant protein. The causes for this substantial variation and instability of protein production are discussed in the following section.

1.4. Gene silencing

As discussed in previous Section 1.3, in addition to the loss of transgene copies, instability of protein production from recombinant genes in engineered cell lines may arise without any loss in recombinant gene copy number due to silencing of the transgene as a result of epigenetic gene regulation (Barnes et al., 2001, Bestor, 2000, Kwaks and Otte, 2006, Heller-Harrison et al., 2009, Kim et al., 2011, Yang et al., 2010b). The term "epigenetic" has been defined as 'the study of heritable changes in gene expression that do not require, or do not generally involve, changes in genomic deoxyribonucleic acid (DNA) sequence' (Wolffe and Matzke, 1999). Epigenetic mechanisms determine phenotype, therefore, function and characteristics of cells during differentiation and are necessary in normal cell development.

The first part of this Section will include an overview of transcriptional silencing mechanisms associated with chromatin structure, modification of DNA and Histone proteins. The second part will look at post-transcriptional silencing that involves RNA-mediated mechanisms. The summary of gene silencing mechanisms can be seen in Figure 1.4.

1.4.1. Transcriptional gene silencing

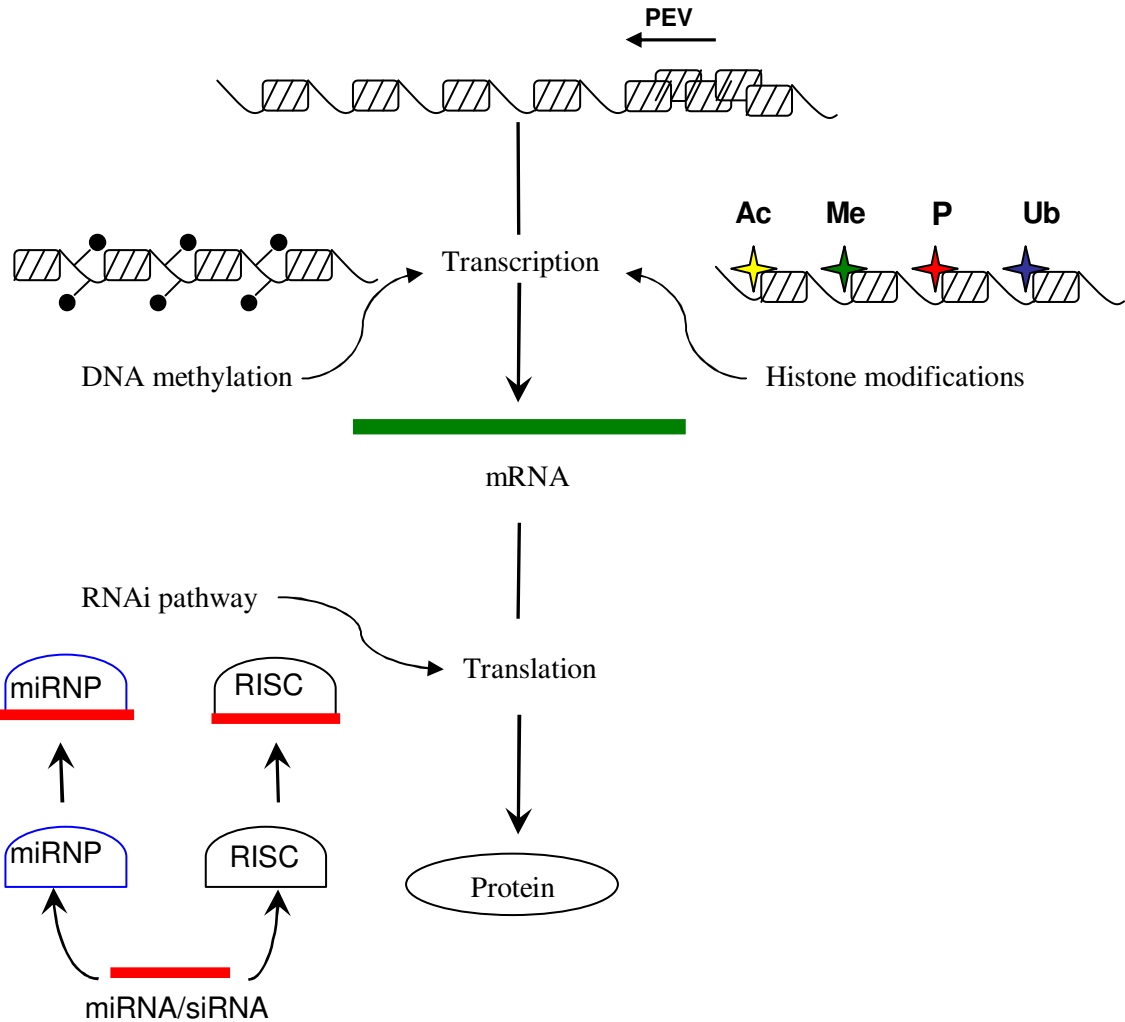
1.4.1.1. Chromatin Structure and position effect

In all eukaryotic cells, the DNA double helix is compacted to form a nucleoprotein complex (chromatin) in the nucleus (Wolffe, 1998). The fundamental unit of the chromatin

is called the nucleosome in which DNA is wrapped around an octamer of core histones (composed of two subunits of the histones H2A, H2B, H3 and H4). Core histones are characterized by having a histone fold domain which mediates histone-histone and histone-DNA interactions. Each histone also contains an N-terminal tail region that is rich in basic amino acids. N-terminal tails are subjected to PTMs and combinations of these modifications have an influence on gene expression (Section 1.1). In addition histone modifications mediate the folding of nucleosomal arrays into higher-order structures and have an essential role in inter-nucleosomal histone-histone interactions (Quina et al., 2006). Electron microscopy studies revealed that, at low ionic strengths, these nucleosome arrays appear as beads on a string.

Chromatin has a dynamic nature and the structure of chromatin can be altered with chromatin modification and remodelling enzymes. The first group of enzymes are the histone modifying enzymes, which are responsible for addition or removal of PTMs to various histone proteins. The second group of enzymes include ATP-dependent chromatin remodelling enzymes, which facilitates the weakening of the interaction between DNA and histones and repositioning of the nucleosome in an energy-dependent manner (Smith and Peterson, 2004). These enzymes consist of at least three subfamilies, including the SWI/SNF family, ISWI complexes and Mi-2 complexes. SWI/SNF complexes are associated with transcriptional activation by disrupting nucleosome structures and increasing DNA accessibility. They have also shown to promote transcriptional repression (Harikrishnan et al., 2005). The ISWI complexes are involved in chromatin assembly by moving the nucleosome on linear DNA. The Mi-2 complexes are found to be associated with transcriptional repression (Smith and Peterson, 2004).

Figure 1.4: Epigenetic regulation of gene expression in mammalian cells



PEV: Position effect variegation, miRNA: micro RNA, miRNP: miRNA ribonucleoprotein complex, siRNA: Small interfering RNA, RISC: RNA-Induced silencing complex, RNAi: RNA interference. ✨ Various histone modifications. Adapted from Croxford (2008).

Electron microscopy studies showed that chromatin isolated at higher ionic strength displayed further condensation to form a higher level of organization called 30nm fibres that are stabilized by binding of a linker Histone H1 (Hansen et al., 1989). The arrangement of nucleosomes and linker DNA into 30nm fibres remains unresolved (Woodcock and Ghosh, 2010). Most available data to date suggests a zigzag arrangement, with contacts between nucleosomes 1 and 3 and between 2 and 4, with the linker criss-crosses between each stack of nucleosomes (Schalch et al., 2005). Chromatin architecture beyond the 30 nm fibres is still not well understood but there is no doubt that it is further condensed into higher level of organization, particularly during the formation of metaphase chromosomes (Woodcock and Ghosh, 2010).

Chromatin is organized into two general "functional" forms, euchromatin and heterochromatin. Euchromatin corresponds to regions that are generally transcriptionally active and less condensed while heterochromatin refers to the transcriptionally inactive and highly condensed regions (Vermaak et al., 2003). Over the recent years heterochromatin and euchromatin have been further associated with different covalent modifications that are present within histones and DNA. These modifications are detailed in the following section.

The recombinant mammalian cell lines are generated by transfection of the cells with a vector containing the gene of interest and a selectable marker that confers the recipient cells a selective advantage (e.g. DHFR, Section 1.2.3.2.2). The integration of transgene into host cell chromosomes is generally a random process, and therefore transgenes may be inserted into euchromatin or heterochromatin. When transgene is integrated within heterochromatin the chromosomal condensation spreads into the integrated transgene, by the phenomenon known as position-effect variegation (PEV), and result in silencing of integrated DNA (Figure 1.4) (Dobie et al., 1996). PEV is correlated with histone hypoacetylation (Section 1.4.1.2) and DNA methylation (Section 1.4.1.3), and as a consequence, cell lines containing similar numbers of plasmid copies show variable levels of protein expression.

1.4.1.2. Histone Modifications

DNA is compacted into a higher order nucleoprotein complex termed chromatin, in which the fundamental structural unit is nucleosome (Section 1.4.1.1). Therefore, considerable interest has focused on how the genes within chromatin are made accessible to the transcriptional machinery and expressed in an organized program. It is thought that the covalent modifications of chromatin facilitate the change of its organization and enable access of transcriptional factors (Henikoff, 2008). Nucleosome stabilization is associated with heterochromatin resulting in transcriptional repression, whereas in euchromatin nucleosomes are destabilised and as a result chromatin is in an accessible state. Therefore, histone modifications that are related to nucleosome stabilization or destabilisation promote the formation of heterochromatin or euchromatin respectively.

N-terminal tails of histone proteins are located outside of the chromatin fibre and targets for a variety of post-translational modifications (Figure 1.4, Figure 1.5). These covalent modifications function either by disrupting the contact between nucleosome or by recruiting non-histone proteins (Kouzarides, 2007). The disruption of chromatin contacts occurs via modifications that affect the histone-histone or histone-DNA interactions. For example acetylation of the histones structurally alters the chromatin architecture by neutralizing the positive charge of the lysine residues (Lee et al., 1993). A number of proteins bind to modified histones via specific domains and affects the overall chromatin structure indirectly (Gelato and Fischle, 2008). One example is heterochromatin protein 1 (HP1), a non-histone chromosomal protein, which specifically binds to methylated H3K9 (Fanti and Pimpinelli, 2008). HP1 correlates the communication between histone methyltransferase (HMT) and DNA methyltransferase (Dnmt1) and subsequent formation of heterochromatin and transcriptional silencing (Smallwood et al., 2007).

For the purposes of coordination of the regulation of gene expression, histone modifications can be divided into two categories: those that are associated with activation of transcription and those that correlate with repression of transcription (Figure 1.5). The major post-translational modifications, which play essential roles in gene expression, are

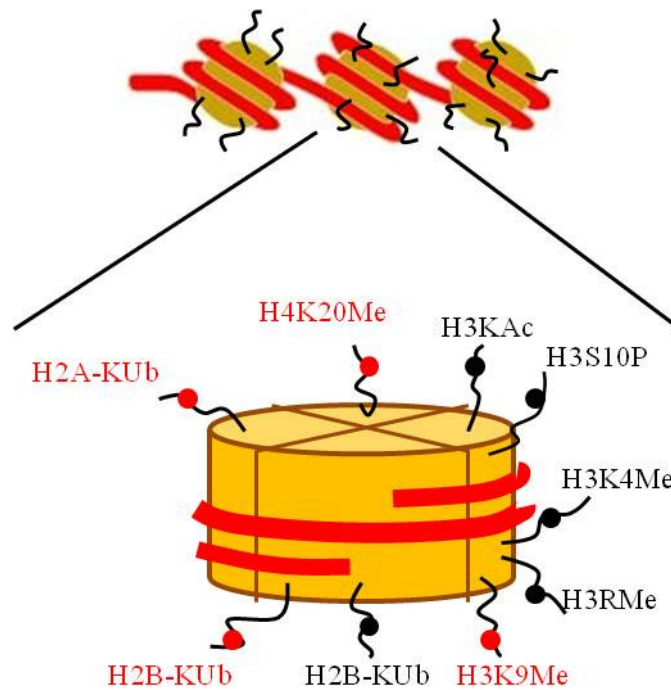
acetylation, phosphorylation, methylation and ubiquitination and are discussed briefly below.

Histone acetylation is a reversible modification controlled by histone acetyltransferase (HAT) and histone deacetylases (HDAC). It is generally accepted that a high degree of histone lysine acetylation leads to activated genomic regions, whereas deacetylation mainly results in repression and silencing (Figure 1.5). Histone acetylation can modulate gene expression at different levels. Acetylation of the core histone lysine residues directly inhibits heterochromatin formation and facilitates accessibility of the transcriptional machinery to DNA templates. Secondly, histone acetylation has an influence on the interaction of transcription-regulatory proteins with DNA in chromatin and can serve as a signal for the binding of these trans-acting factors (Bulger, 2005).

Phosphorylation of histone H3 serine residues is known to be related to chromosome condensation during mitosis (Hendzel et al., 1997) and has also been shown to correlate with transcriptional activation of immediate-early genes (Figure 1.5) (Thomson et al., 1999). The finding that the same modification may be involved in opposing physical changes in chromatin structure suggested that they act may as binding surfaces rather than direct alteration of chromatin (Nowak and Corces, 2004).

Histone proteins can be methylated either at arginine or lysine residues, and methylation of histones appears to have multiple effects on chromatin function (Figure 1.5). Methylation of H3 on Lysine 4 (K4) (Strahl et al., 1999) and some of the arginine residues in H3 and H4 (Chen et al., 1999), for instance, induce transcriptional activation. In contrast, methylation of H3 on Lysine 9 (K9) is mostly associated with stable silencing and repression of genes as mentioned above. Methylation of H3 on Lysine 27 (K27) and H4 on Lysine 20 (K20) are also found to be connected to transcriptional repression (Kouzarides, 2007).

Figure 1.5: The major post-translational histone modifications and their effect on transcriptional states.



Ac: Acetylation, P, Phosphorylation, Me: Methylation, Ub: Ubiquitylation. Red circles indicate transcriptional repression, whereas black circles display transcriptional activation.

Ubiquitylation of histone H2A and H2B plays important roles in modulating many processes within the nucleus such as transcription initiation, elongation, silencing and DNA repair. From a transcriptional point of view, H2A ubiquitylation is considered to be involved in repression, whereas H2B ubiquitylation has roles in both transcriptional activation and silencing (Figure 1.5) (Weake and Workman, 2008).

1.4.1.3. DNA Methylation

There is considerable evidence that suggests a strong correlation between DNA methylation and gene silencing. For example, early in mammalian development one of the X chromosome is randomly inactivated (Panning and Jaenisch, 1998). This inactivated X

chromosome is heavily methylated and this observation implicates a role of methylation in gene silencing. Moreover, treatment of cells with 5-azacytidine, which is an inhibitor of DNA-methylation, has shown demethylation and reactivation of expression of previously methylated genes (Jones et al., 1983). DNA methylation is often associated with silencing of sequence duplications in most cases. This normally serves as a defence mechanism against invasive DNA pathogens (Garrick et al., 1998, Selker, 1997). However, this complicates the gene therapy applications and production of therapeutic proteins from recombinant mammalian cells (Bestor, 2000).

DNA methylation usually occurs on carbon 5 of cytosine, to generate 5-methylcytosine (5mC), and in higher vertebrates this modification generally takes place in 5'-CpG-3' dinucleotides (Nakao, 2001). DNA methylation in mammalian cells is classified as either maintenance or de novo methylation. It is considered that maintenance methylation is controlled by DNA methyltransferase (DNMT1), also known as maintenance methylase, and de novo methylases (DNMT3a, DNMT3b) are responsible for de novo methylation (Okano et al., 1999, Pradhan et al., 1999). Maintenance methylases recognize and modify hemi-methylated DNA produced during replication of DNA, therefore preserving the methylation pattern of the newly synthesized daughter strands. Moreover, it has been reported that DNMT1 works together with HDAC to repress transcription (Figure 1.6c) (Kimura and Shiota, 2003). In addition this enzyme also associates with the HP1 protein and methylates the DNA that contain methylated H3K9 residues (Figure 1.6d) (Smallwood et al., 2007). On the other hand, de novo methylases add methyl groups to unmethylated-DNA to create new hemi-methylated DNA, which may explain how the methylation pattern can be changed (Okano et al., 1999).

Similar to histone modifications, DNA methylation can have downstream influences on transcription and chromatin structure. DNA methylation may directly hinder binding of the methylation-sensitive transcription factors to DNA (Figure 1.6a, 1.6b), or indirectly, it may recruit adaptor proteins, containing methyl binding domains (MBD), which promotes transcriptional silencing (Miranda and Jones, 2007). One of the members of the MBD protein family is methylated DNA complex 2 (MeCP2), which promotes the formation of

repressed chromatin via interaction with HDAC and an adaptor protein Sin3 (Figure 1.6c) (Nan et al., 1998).

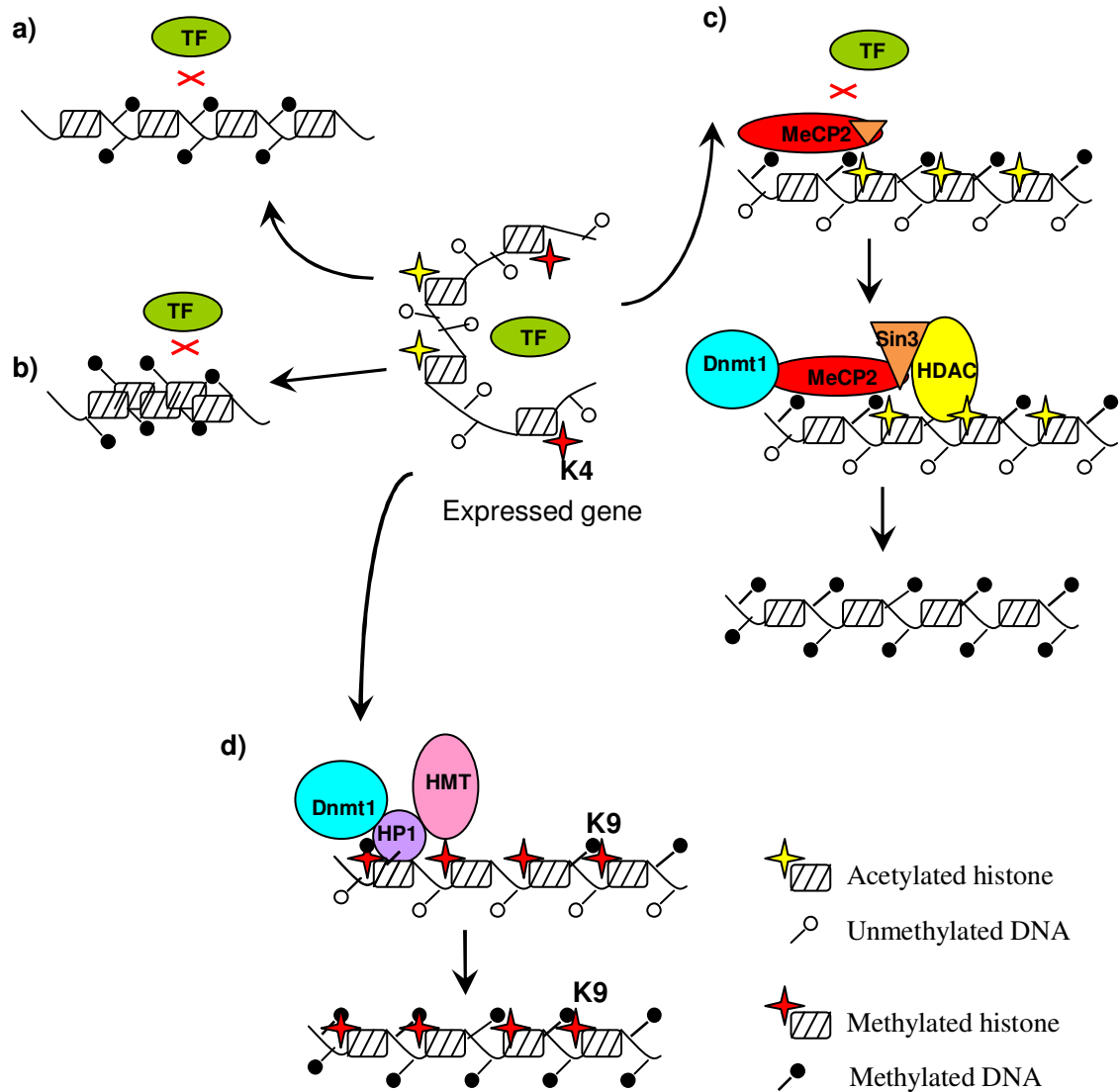
Nearly 60-90% of all CpG sequences are methylated in the vertebrate genome, whereas unmethylated CpGs are mainly located in CpG islands. CpG islands are often part of functional promoters and other regulatory elements (Antequera and Bird, 1993), and it has been shown that transcription is repressed when such elements become hypermethylated (Bird and Wolffe, 1999).

1.4.2. Post-Transcriptional Gene Silencing (PTGS)

Although transcription is the initial process in protein expression, it is now clear that post-transcriptional events also have an important role in final level of protein product in which silencing of genes can occur at post-transcriptional level (Figure 1.4). Post-transcriptional gene silencing (PTGS) has been found to occur naturally in a number of organisms from nematodes to plants to humans (Cogoni and Macino, 2000), and the mechanism has been called RNA interference (RNAi).

The initiating factor in RNAi pathways is either long double-stranded RNA (dsRNA, which may be viral RNAs or artificially introduced into the cell) or micro RNAs (miRNA, which can occur naturally) (Wightman et al., 1993, Tuschl et al., 1999). RNAi pathways are based on two steps. In first step, the trigger RNA (either dsRNA or miRNA primary transcript) is processed into short dsRNAs (small interfering RNA [siRNA] or miRNA) by the RNaseIII-type enzyme Dicer. Afterwards, siRNA/miRNAs are incorporated into the effector complex, RNA-induced Silencing Complex (RISC) or miRNA ribonucleoprotein complex (miRNP). RISC mediates the cleavage of target mRNA, whereas miRNP guides to translational repression in animals (Hammond et al., 2000, Meister and Tuschl, 2004).

Figure 1.6.: Common mechanisms of DNAmethylation and cross-talk between DNA methylation and histone modifications



a) Direct inhibition of transcription by blocking the transcription factor (TF) binding. b) Assembling of heterochromatin associated with methylated DNA and deacetylated histones may block the TF binding. c) Binding of MBD proteins to methylated DNA and subsequent recruitment of HDAC promotes the formation of repressed chromatin. d) Binding of HP1 to the methylated H3K9 residues and subsequent association of DNMT1 promotes the methylation of the DNA and mediates the formation of repressed chromatin. Adapted from Vaissiere et al. (2008).

Furthermore, an association of PTGS with DNA methylation has been shown in plant studies (Section 1.4.1.3). These data suggested that interactions between RNA and the promoter region leads to methylation of DNA which in turn results in transcriptional silencing (Jones et al., 1999). Likewise, deletion of several genes which encode part of the machinery responsible for RNAi in yeast, resulted in transcriptional de-repression of previously silenced transgenes accompanied by overall loss in methylation H3K9 (Volpe et al., 2002). These data indicate that dsRNA can induce transcriptional level repression of gene expression as well as PTGS, and these two silencing mechanisms may act in concert.

1.4.3. Summary

This Section has described the epigenetic gene regulation in various organisms. It has been demonstrated that chromatin structure, DNA methylation and histone modifications are connected in mammalian cells leading up to gene silencing. Interaction between DNA methylation and chromatin may result transcriptional silencing, and heterochromatic region are usually have high levels of CpG methylation, while unmethylated CpG island is enriched in hyperacetylated histones. Additionally, genes can be silenced post-transcriptionally through an RNAi pathway. These mechanisms are summarized in Figure 1.4. It was also demonstrated that inactivation of a gene can occur through spreading neighbouring heterochromatin (Dobie et al., 1996). In the next section, the elements that may prevent the spread of heterochromatin are discussed.

1.5. Nuclear Organization and DNA Regulatory Elements

1.5.1. Nuclear Organization

The previous sections demonstrated the effect of covalent modification of DNA and histones on the transcriptional activity of associated genes, through chromatin condensation. Recent studies have indicated the possibility that gene expression may also be regulated by the spatial organization of the genome in the cell nucleus and interactions between DNA and nuclear sub-structures (Schneider and Grosschedl, 2007). The view that

chromatin was arranged into discrete nucleosomal domains, separating heterochromatin from euchromatin, was first put forward by Heitz in 1929 (Section 1.4.1.1). This theory is now seen as potentially implying further mechanisms in the maintenance of transcriptional regulation of gene expression. For example, heterochromatin sub-compartments may be associated with chromatin remodelling complexes that maintain condensed chromatin structure, whereas euchromatin compartments are associated with enzymes and proteins that decondense the chromatin.

Over the past decade, the evidence accumulated has supported the notion that nuclear architecture may have a functional impact on epigenetic gene regulation. Current models of nuclear architecture of mammals acknowledge that individual chromosomes occupy distinct regions, termed chromosome territories, which are non-randomly organized in the cell nucleus (Cremer et al., 2006). The impact of nuclear position on the regulation of gene expression has been examined in recent studies, which have considered whether the transcriptional activity of a gene may be associated with its radial position (Küpper et al., 2007), or may correlate with its position with respect to other genes/chromosomes (Noordermeer et al., 2008), and/or relative to its nuclear neighbourhood (Pavan et al., 2007).

The emerging idea, with the help of recent technological advancements, is that genes tend to be taken to different nuclear environments, which are often shared by other genes (Fraser and Bickmore, 2007, Sutherland and Bickmore, 2009). Chromosome territories do not have rigid boundaries, therefore genes sometimes relocate outside of their expected territories. This relocation can occur as a result of a self-organizing process as seen in the domain of constitutively high gene expression (Brown et al., 2006) or, in some cases as a consequence of the induction of gene expression (Chambeyron and Bickmore, 2004). For example, the looping out of genes in Hoxb locus was observed by using the 4C method. It was shown that the relocation of the Hoxb gene cluster occurred in synchrony with the activation of the gene expression (Chambeyron and Bickmore, 2004). Moreover, the repositioning of an interphase chromosome site was visualised by live-cell imaging which

revealed that the interphase chromosome migrated to the nuclear interior site after a transcriptional activator was targeted against it (Chuang et al., 2006).

Furthermore, increasing evidence indicates that the nucleus is highly organised into distinct structural and functional domains. One example is that microscopic analysis of actively transcribed regions in HeLa cell nuclei revealed that the active forms of RNA polymerase units are clustered in their own dedicated transcription sites. These sites have subsequently been identified as ‘transcription factories’ (Pombo et al., 1999). The standard view of gene transcription was that the active genes recruit RNA polymerase and the peripheral transcriptional machinery in order to be transcribed. However, recent experimental evidence has provided new insights into the organization of the transcriptional machinery and suggested that most genes are dynamically relocated and recruited to transcription factories (Osborne et al., 2004). Moreover, it was shown that multiple active genes and gene clusters tend to be localized together and therefore share the same factory. FISH studies have shown that temporarily quiescent alleles of active genes are located away from factories, suggesting that genes can move in and out of these active transcription sites resulting in activation or repression of their transcription (Osborne et al., 2004).

A new area of study concerns the interactions within the nucleus between regulatory elements (Fraser and Bickmore, 2007). These elements are co-localized, probably not because they are recruited to a particular nuclear compartment but rather, due to direct protein–protein interactions between the loci. These interactions promote or inhibit the movement of the genes within other nuclear environments necessary for their activation or repression or their ability to directly alter the chromatin structure of the interacting alleles. The DNA regulatory elements that are associated with such transcriptional factories are discussed further in the following section.

1.5.2. DNA Regulatory Elements and their potential use in recombinant gene expression

Our current understanding of the chromatin structure of mammals indicates that genes are arranged into discrete chromatin domains, which may exist in either a state which is active and decondensed or inactive and condensed. There are a number of regulatory elements within these gene domains that play a role in the regulation of gene expression (Cockerill, 2011). These elements include enhancers and Locus Control Regions (LCRs), which tend to have a positive effect on transcription.

Enhancers are discrete cis-acting DNA sequences that increase transcription by interacting with DNA-binding proteins and the promoter region of the genes (Blackwood and Kadonaga, 1998). LCRs are defined as DNA fragments that are able to enhance the expression of the genes which are linked in *cis*, in an integration-site-independent manner (Section 1.5.2.1) (Dean, 2006). Boundary and insulator elements are neutral DNA elements that demarcate the range over which other regulatory influences act. These elements have either an enhancer-blocking activity or they inhibit the spread of heterochromatin (Valenzuela and Kamakaka, 2006). Boundary elements tend to be nuclear scaffold/matrix attachment regions (S/MAR), which attach DNA to the nuclear matrix in 30-100bp loops (Section 1.5.2.2).

As one of the functions of these regulatory elements involve maintaining genes in a transcriptionally active state, they may be linked to the transgene with the aim of preventing recombinant protein instability due to PEV and gene silencing (Section 1.4). This section will discuss the use of LCRs, S/MARs and Ubiquitous Chromatin Opening Elements (UCOE) in recombinant protein production.

1.5.2.1. LCRs

In an attempt to locate the regulatory elements that are important in controlling the differentially expressed β -like-globin genes, Tuan et al. mapped the DNase I-hypersensitive (HS) sites located upstream of the transcribed human globin genes (Tuan et al., 1985). They found five HS sites which were only present in erythroid cell types, suggesting that their sensitivity to nuclease was tissue-specific. Their sequencing data revealed that this region, now known as the LCR, contained two or three enhancer core-like sequences.

Studies performed on transgenic mice showed that placing the LCR in front of a β -globin transgene led to an increased expression that was independent of the chromosomal integration site (Grosveld et al., 1987). Moreover, the increase in the expression of recombinant β -globin was correlated with the copy-number. Festenstein et al. generated transgenic mouse lines carrying human CD2 transgene either with or without the additional 3'LCR sequence (Festenstein et al., 1996). They demonstrated that the transgene expression was consistently high no matter even when the transgene was inserted into heterochromatin in mice carrying the additional LCR sequence. The LCRs were found to be associated with chromatin enriched with acetylation of H3 and H4 and di-methylation of H3K4 histone modifications (Kim et al., 2007, Litt et al., 2001), which are hallmarks of an active chromatin region (Section 1.4.1.2). In addition to the β -globin LCR, other LCRs have been identified, including the growth hormone locus, the T_H2 cytokine locus and the major histocompatibility locus (Dean, 2006).

The HS sites within β -globin LCR contain binding sites for transcription factors, including NF-E2, EKLF and GATA-1, which are important for recruitment of histone acetyltransferases HAT to the LCR. Carter et al. investigated the spatial organization of the β -globin locus by using a modified version of RNA-FISH to tag and they recovered the proteins associated with elongating mRNA (Carter et al., 2002). They found that the HS sites of LCRs were in close proximity with the actively transcribed β -globin genes, demonstrating that two distant cis-regulatory elements, LCR and promoter, were in close

proximity in expressing cells. This suggested that they directly interacted by forming chromatin loops. Subsequent investigations have demonstrated that the β -globin locus can cluster and form a structure called a chromatin hub, via associations with HS sites (Palstra et al., 2003). In erythroid progenitors, prior to β -globin gene expression, a "poised" chromatin hub exists where the β -globin genes are in loops that are not in association with each other. Upon erythroid differentiation, the remaining HS sites interact and form a fully functional chromatin hub which contains all the regulatory elements and the β -globin gene that will be actively expressed. The role of transcription factors in active chromatin hub formation was investigated in a number of studies and it was shown that erythroid-specific transcription factors were required for the formation of the three-dimensional organization of the β -globin locus (Drissen et al., 2004, Vakoc et al., 2005). The presence of active chromatin hubs supports the theory of gene recruitment to the nuclear regions containing transcription factories described in Section 1.5.1.

Since LCRs are shown to confer a position-independent expression of linked transgenes, these elements have been used to construct vectors to improve transgene expression particularly for the gene therapy applications (Lisowski and Sadelain, 2008). PEV and gene silencing can potentially hamper the effectiveness of the gene therapy strategy (Section 1.4). May et al. addressed this problem in their study and constructed recombinant lentiviruses containing β -globin gene and LCR elements to successfully treat β -thalassemic heterozygous mice (May et al., 2000). They showed that lentivirus carrying the β -globin gene and LCR yielded higher and stable levels of transgene expression which was in the therapeutic range.

In addition to its use in gene therapy, LCR based expression systems have been used for recombinant protein production on a few occasions. Examples of these include pre-erythroid mouse erythroleukemia (MEL) C88 cells which displayed higher levels of recombinant hMCP-1 and human calcitonin receptor production when linked with LCR (Needham et al., 1996, Needham et al., 1995). However the tissue-specificity of the β -globin LCR limits its applicability to MEL cells only. Ortiz et al. reported an LCR within the T-cell receptor locus which demonstrated a non-tissue specific expression of a linked

transgene (Ortiz et al., 1997). Although this LCR is promising, the expression level was variable between different tissue types. Subsequently, this LCR was used in CHO cells with the aim of improving the expression. The increase was only 2-4 fold, whereas use of the chicken lysozyme MAR provided a 20-fold increase which is discussed in Section 1.5.2.2 (Zahn-Zabal et al., 2001).

The tissue-specificity and relatively large size of LCRs has limited their usefulness and applicability in mammalian cell lines. Smaller elements of the LCR have been successfully used in viral gene therapy vectors (Ren et al., 2006). However, only modest improvements in transgene expression have been observed in CHO cells when these elements were linked to the transgene (Izumi and Gilbert, 2000, Otte et al., 2007).

1.5.2.2. S/MARs

S/MARs are genomic DNA sequences in which the chromatin is attached to the nuclear matrix/scaffold (Mirkovitch et al., 1984). In a manner analogous to LCRs, S/MARs have been shown to be necessary for the formation of chromatin loops where the S/MARs function as anchors (Heng et al., 2004). Furthermore, it was shown that the looping of the β -globin locus is mediated by a nuclear matrix association, which therefore suggests that S/MARs may anchor the active chromatin hub to the nuclear matrix (Ostermeier et al., 2003). S/MARs do not usually affect the transient expression of transgenes suggesting that they do not display any enhancer-like activity (Bode et al., 2000). However, it was reported that a specific MAR element also increased transient expression from some expression vectors in CHO cells, which related to the presence or absence of elements on the vector backbone (Harraghy et al., 2011).

It has been reported that S/MARs bind transcription factors including the special AT-rich binding protein 1 (SATB1) and CTCF (Yasui et al., 2002, Yusufzai and Felsenfeld, 2004). SATB1 has been shown to recruit the HDAC and ISWI in interleukin-2-receptor α (IL-1R α) suggesting that SATB1 functions as a landing platform for several chromatin remodelling complexes (Section 1.4.1.1). Therefore, these data suggest that S/MARs affect

the local chromatin structure and nucleosome positioning by recruiting chromatin remodelling enzymes and mediating chromatin loop formation.

Numerous studies have reported the use of different S/MARs-containing expression vectors to improve high and stable levels of recombinant gene expression in mammalian systems. These include the chicken lysozyme S/MAR (Girod et al., 2005, Zahn-Zabal et al., 2001), the human β -globin S/MAR (Kim et al., 2004, Wang et al., 2008) and the human interferon β S/MAR (Kim et al., 2005). Recently, several new SMARs were identified from the human genome using a bioinformatic approach (Harraghy et al., 2011, Girod et al., 2007). Some of these new S/MARs were found to be more potent than the previously known chicken lysozyme S/MAR, opening the prospect for the identification of even more potent elements that can improve transgene expression. The performance of several human origin S/MAR elements was evaluated in order to increase production of self-inactivating (SIN) retroviral vectors (Buceta et al., 2011). They found that one of the S/MAR elements was capable of increasing the viral RNA expression using various types of transgenes and packaging cells.

In all these studies, incorporating S/MAR elements into the expression vector increased the level of protein production and the proportion of cells or cell lines producing recombinant protein following transfection. Moreover, S/MAR incorporation into the vector was shown to decrease the clonal heterogeneity and reduce the time for scale-up by reducing the number of clones that needed to be screened (Girod et al., 2007, Girod et al., 2005). A recent study reported that one of these newly identified S/MARs provided persistent expression of the transgene and reduced the expression noise by increasing the probability of switching the genes to a transcriptionally active state (Galbete et al., 2009). Stable transgene expression was maintained in S/MAR-driven expression after 26 weeks of culture in the absence of neomycin selection.

Zahn-Zabal et al. (2001) compared the ability to improve stable transgene expression in different chromosomal elements (e.g. LCRs, insulators and S/MARs). They reported that,

the chicken lysozyme S/MAR was the most effective and increased the transgene expression by 20-fold.

S/MAR-containing vector constructs have also been used in combination with MTX-mediated gene amplification (Kim et al., 2005, Kim et al., 2004). It was shown that the S/MAR element enhanced the recombinant protein expression. Moreover, CHO cells transfected with the S/MAR containing expression vector displayed a higher frequency of colonies that expressed a detectable level of recombinant protein than those transfected with the control vector (Kim et al., 2004). It was also reported that cells with the S/MAR expression vector demonstrated enhanced growth characteristics in the presence of MTX selection compared to control vectors. These characteristics were exploited to improve the mammalian cell expression system by shortening the time required for the MTX gene amplification process (Section 1.2.3). It was shown that high producer cell lines with uniform growth properties could be generated by a simple two step MTX treatment, rather than multi-step treatments of MTX (Kim et al., 2004). However, these studies did not report the stability of recombinant protein production following MTX amplification over prolonged culture in the presence or absence of MTX selection.

1.5.2.3. UCOEs

Functional studies were undertaken with a 44kb cosmid clone containing the TATA binding protein (TBP) locus to gain insight into the genetic elements responsible for the transcriptionally competent structure of housekeeping genes (Harland et al., 2002). The TBP locus consists of three functionally distinct genes including TBP, proteosomal C5 subunit (PSMB1) and programmed cell death-2 (PDCD2) within a 50 kb interval. It has been reported that murine fibroblast L-cells transfected with a 44-kb genomic region containing the entire TBP gene and extending 12 kb 5' into the PSMB1 gene maintained a constant TBP expression for up to 60 days, even in the absence of drug selective pressure (Harland et al., 2002). This led to the suggestion that this 44kb genomic region may possess regulatory elements which negate chromatin-mediated gene silencing.

These initial studies were extended by additional analysis of the TBP-PSMB1 region and the organizationally similar heterogeneous nuclear ribonucleoprotein A2/B1-chromobox homolog 3 (HNRPA2/B1-CBX3) locus (Antoniou et al., 2003). Both TBP-PSMB1 and HNRPA2/B1-CBX3 regions consist of three closely spaced, ubiquitously expressed genes. A structural feature these two regions have in common is that they contain a methylation-free CpG island extending over two closely spaced, divergently transcribed promoters. It was shown that murine fibroblast L cells transfected with transgenes containing TBP-PSMB1 and HNRPA2/B1-CBX3 exhibited stable protein production and were resistant to silencing even when integrated into the centromeric heterochromatin region. Furthermore, these properties of dual-promoter regions do not appear to be associated with either LCR or insulator function since analysis of these genomic regions failed to reveal clusters of DNase I hypersensitive sites characteristic of LCR-type elements. These results suggested that expression vectors based on dual-promoter CpG island regions may have significant value in biotechnological applications and such CpG island regions have been termed Ubiquitous Chromatin Opening Elements (UCOEs) (Antoniou and Crombie, 2000).

UCOEs are defined as being comprised of an extended methylation-free CpG-island, and, normally, bi-directional promoters that are divergently transcribed. It has been claimed that UCOEs open chromatin or maintain chromatin in an open state in order to facilitate reproducible expression of an operably-linked gene in cells of at least two different tissue types (Antoniou and Crombie, 2000).

The transgene expression level from vectors with or without inclusion of an 8kb UCOE have been analysed in CHO-S cells. It has been shown that vectors containing the UCOE element upstream of the GFP transgene provided a higher proportion of positive clones with much higher levels of transgene expression following stable transfection and cloning (Benton et al., 2002). In the same study, the UCOE vectors were also used for recombinant antibody production. The inclusion of UCOE in the expression construct resulted in a dramatic increase in production of the recombinant antibody and also allowed for screening of a small number of subclones to obtain high-producer suitable candidates for scale-up. In another study, vectors combining the 8kb HNRPA2B1-UCOE fragment with

the human cytomegalovirus (hCMV) promoter were used for the expression of transgene in CHO K1 cells (Williams et al., 2005). It has been shown that UCOE-containing vectors provided a substantial increase in the level of recombinant EPO expression and maintained the stability of protein expression over 100 generations of continuous culture in transfectant pools. They also evaluated a smaller 1.5kb fragment of the HNRPA2B1-UCOE which conferred improvements in the level of eGFP expression and proportions of expressing cells compared to the control vectors (Williams et al., 2005). The effects of the UCOE on eGFP expression and stability were further studied in clonal cell lines which showed that a large proportion of the clones generated with 8kb UCOE construct displayed detectable eGFP expression and that, overall, the UCOE improved the level of transgene expression. Also, no decrease was observed in the percentage of high-producer cells after 38 generations in the absence of drug selection in clones containing UCOE vector (Williams et al., 2005). Nair et al. (2011) reported the comparison of use of the 1.5kb UCOE and the 3.2kb mouse ribosomal protein S3 (RPS3) gene locus UCOE in expression of B-domain deleted factor VIII (BDD-FVIII) using different promoters including hCMV in BHK21 cells. They found that the 1.5kb UCOE performed better than the 3.2kb mouse RPS3 UCOE in expressing transgene in all promoter combinations.

A comparative study used a cHS4 insulator, a 2.6kb UCOE, an anti-repressor and a S/MAR element and tested their effects on protein expression levels (Otte et al., 2007). Contradictory to the previous studies, they reported that incorporation of 2.6kb UCOE did not result in improved transgene expression levels compared to the control. They found that vector constructs containing S/MAR and anti-repressor elements resulted in a marked increase in reporter gene expression level than control vectors.

A truncated (2.2kb) HNRPA2B1-UCOE (A2UCOE) element has been used by Zhang et al. in the construction of lentiviral vectors, for possible gene therapy applications (Zhang et al., 2007). It was shown that transgenes regulated by A2UCOE produced high, consistent and homogeneous populations of cells both *in vitro* and *in vivo* in transgenic mouse models. Moreover, transgene expression was observed to be copy-number dependent. In contrast, Katsantoni et al. stated that the transgene expression linked with 8kb UCOE

element was not copy-number dependent in transgenic mice (Katsantoni et al., 2007). They showed that the 8kb UCOE was capable of driving expression of a linked transgene in all tissues analysed. However, the transgene expression was not related to copy number, suggesting that the transgenes were prone to chromosomal position effects *in vivo*.

So far, little is known about the molecular mechanisms of UCOE as to how the linked transgene expression is improved. It was reported that UCOEs have no effect on the transient expression of linked transgenes suggesting that UCOEs do not have enhancer-like activity (de Poorter et al., 2007, Zhang et al., 2007). The observations that transgene expression is copy number dependent when linked with UCOE, and that protein expression is stable even when integrated within centromeric heterochromatin, also indicates that UCOEs may provide and maintain an open chromatin environment. The DNA methylation and histone modification patterns across the entire HNRPA2B1-CBX3 locus were studied to gain some insight into the molecular mechanism of the UCOE elements (Allen and Antoniou, 2007). It was found that the CpG island spanning between HNRPA2B1 and CBX3 genes was fully unmethylated and the methylation-free DNA extends beyond this region to within the central areas of both genes, making a total of ~5kb in length. Moreover, it was shown that, although actively transcribed, the DNA of the 3' half of both HNRPA2B1 and CBX3 genes was methylated and this methylated DNA was also associated with transcriptionally-permissive hyperacetylated histone H4 and methylated histone H3K4, showing that these two functionally opposite epigenetic marks may co-exist. Therefore, the dominant chromatin opening function of UCOE may be attributed to the large region of methylation-free DNA, which may allow transcription factors to bind and promote efficient bi-directional transcription. Moreover, transcriptionally active histones H3, H4 acetylation and H3K4 methylation modifications were found to be distributed across HNRPA2B1 and CBX3 regions. Overall, this study suggested that the UCOE function was connected to an extended region of unmethylated DNA in combination with a distinct pattern of active histone modification marks.

Furthermore, the expression and DNA methylation status of the 2.2kb truncated A2UCOE were investigated within the lentiviral vector system in mouse embryonic carcinoma P19

cells *in vitro* and in transgenic mice *in vivo* (Zhang et al., 2010). These study demonstrated that the promoter region of the A2UCOE-eGFP vector displayed very low level and widely scattered DNA methylation in P19 cells, suggesting that the stability of the transgene expression from A2UCOE vector was associated with resistance to DNA methylation. Similar results were obtained from the *in vivo* assessment of DNA methylation where A2UCOE displayed little or no methylated CpG residues in all mice analysed. These observations demonstrated that the molecular basis for the stability of transgene expression regulated by UCOE was partly due to its resistance to DNA methylation.

The evidence available to date indicates that UCOEs can potentially reduce the time required for the production of stable cell line and consequently may be valuable in the biopharmaceutical production of recombinant proteins.

1.6. Summary and Objectives

Recombinant proteins have great importance for therapeutic applications. Due to the requirement for glycosylation and other post-translational modifications for the biologic activity of therapeutic protein, mammalian cells are currently the preferred system for expression. Although there are different mammalian cell types available, CHO cells, especially DHFR-deficient DG44 lines are the most frequently used cell lines for the market-scale production of therapeutic protein (Section 1.2.3.2). However, clonal heterogeneity, instability and loss of gene expression remain as major obstacles to predictability with the CHO expression system. This may be due to changes in the regulation of transgene expression. Such unpredictability means that a large number of clones are screened to isolate stable high producing clones, a process that is tedious and time consuming. Therefore, there is a requirement for greater understanding of recombinant gene transcriptional events in mammalian cells with the aim of decreasing the need for the cumbersome evaluation of large number of clones. In this regard, chromosomal elements including LCR, S/MARs and more recently UCOEs have been utilised to overcome problems related to gene silencing mechanisms (Section 1.5.2).

Although it is widely believed that UCOEs promote an open chromatin configuration, thereby improving expression of linked transgene (Section 1.5.2.3), I hypothesize that there may be profoundly different regulation when UCOE containing vector cassettes are exposed to DHFR-mediated amplification, which is associated with potentially significant changes to chromatin structure and organization.

The overall aim of my project is to assess the effect of UCOE on the long term expression of recombinant genes in amplified and non-amplified CHO cells in relation to stability studies. Improved understanding in this area will provide an enhancement of the efficiency of the overall process in recombinant protein production.

Therefore the main specific objectives of my project are to:

1. Determine whether recombinant protein production is more stable over long term culture when UCOE is present in the expression construct.
2. Determine if incorporation of UCOE in vector constructs improves the frequency of cell lines that produce high levels of an industrially relevant recombinant protein following MTX amplification.
3. Determine if recombinant protein production is maintained during long-term culture in UCOE-containing cell lines which have undergone MTX amplification.
4. Investigate the genetic parameters and their effect on the recombinant protein production.
5. Investigate the site(s) of integration of transgene following MTX amplification using specific chromosome paints and FISH.
6. Determine how the transgene integration changed over time as one indicator of protein productivity and stability by using FISH.

The objectives 1, 3 and 4 listed above will be addressed by use of a reporter gene, green fluorescent protein (GFP). (It should be noted here that the GFP engineered cell lines had been created and amplified in our lab by Dr Alexandra Croxford). Considering the

potential limitations of use of an intracellular protein such as GFP I extended the studies to use of a recombinant EPO transgene. EPO is an ideal candidate as an industrially relevant protein as it requires complex post-translational modifications for biological activity and therefore is most suitably produced in a mammalian cell host. Therefore, objectives 2, 3 and 4 will also be addressed by using EPO-engineered cells. To address the last two objectives (i.e. Transgene localization experiments) I used selected GFP-expressing CHO cell lines. The results presented in this thesis fall into three discrete chapters. Chapter 3 details the effect of UCOE on stability of protein production in amplified GFP-CHO cell lines whereas Chapter 4 examines the development and amplification of EPO-CHO cell lines and the stability of protein production over long term culture. Finally Chapter 5 investigates the effect of transgene localization on stability of production. An overall summary and discussion is presented in Chapter 6.

CHAPTER 2:

Materials and Methods

2.1. Materials and Equipment

2.1.1. Sources of Chemicals, Reagents and Special Equipment

All chemicals and reagents were of the highest grade and obtained from standard sources. A full list of the materials used, and their suppliers, is to be found in Appendix 1.

2.1.2. Preparation and Sterilisation of Solutions

All solutions were prepared in miliQ water (ddH₂O) unless otherwise stated. All solutions used in the processing of RNA were made in 0.05% (v/v) diethylpyrocarbonate (DEPC)-treated ddH₂O. Solutions were sterilised by autoclaving in a LTE Scientific Series 250 autoclave or by filtration through a 0.2µm filter where autoclaving was not appropriate. Solutions were stored at room temperature, unless otherwise stated.

2.1.3. pH measurements

pH was measured by using a digital Corning pH meter 120 with a glass electrode. The pH was adjusted using hydrochloric acid or sodium hydroxide as appropriate, unless otherwise stated.

2.2. Generation and Purification of Plasmids in Bacterial Cells

2.2.1. Bacterial Growth Medium

Luria bertani (LB) broth was used as the bacterial growth medium, unless otherwise stated, which consisted of 1% (w/v) tryptone, 0.5% (w/v) yeast extract and 0.5% (w/v) sodium chloride and ampicillin at 50µg/ml, where appropriate. The solid medium contained the above constituents with the addition of 1.5% (w/v) agar. Ampicillin was added to the LB agar once it was below a temperature of 55°C.

2.2.2. Midi-preparation of Plasmid DNA

Midi-preparation was used when relatively large quantities of pure plasmid were required for transfection of cells or for further plasmid manipulation. Plasmid was prepared from a 200ml bacterial culture using the Qiagen[®] Plasmid Midi Kit (see Appendix 1). The protocol for low-copy number plasmids was followed from the Qiagen Plasmid purification handbook.

2.2.3. Estimation of Nucleic Acid Concentration

DNA and RNA concentration was estimated using the NanoDrop1000 UV/Vis spectrophotometer, according to the manufacturer's instructions. The purity was assessed by using the $A_{260\text{nm}}/A_{280\text{nm}}$ ratio, where a ratio of 1.6-2.0 was considered pure.

2.2.4. Restriction Enzyme Digestion

DNA was digested in a final volume of 15 μ l (unless otherwise stated) using the following reagents: Required amount of DNA, 10U of each appropriate enzyme and 1 \times final concentration of appropriate restriction buffer. The digestion mixture was incubated at 37°C routinely for 2 hours, unless otherwise stated.

2.3. Preparation of Mammalian Expression Vectors for Transfection into CHO Cells

Linearised p1010-EPO was produced for transfection into CHO cells, by restriction digestion of 100 μ g of vector for 16h at 37°C with 30U of restriction enzyme *Pme* I in 1 \times concentration of restriction buffer, in a final volume of 100 μ l. Linearised p901-EPO was produced by digesting 37 μ g (equimolar to 100 μ g of p1010-EPO) of vector with *Ssp*I as described above. Linearised DNA was purified by phenol:chloroform:isoamyl alcohol extraction (Section 2.3.1), and resuspended in a final volume of 100 μ l in ddH₂O.

2.3.1. Phenol Extraction and Ethanol Precipitation of DNA

The DNA to be purified from solution was mixed with an equal volume of phenol/chloroform/isoamyl alcohol (25:24:1) for 5 minutes. The mixture was centrifuged at 13,000g for 10 minutes at room temperature and the upper aqueous phase removed into a fresh tube. The phenol/chloroform/isoamyl extraction was repeated on the aqueous phase. 4 volumes of ddH₂O and 0.5 volumes of 3M sodium acetate (pH5.2) were added to the final aqueous phase. DNA was precipitated by addition of 3 volumes of 100% ethanol, the solution was mixed by inversion and the mixture was centrifuged at 13,000g for 10 minutes. The supernatant was removed and discarded. The pellet was washed with 70% ethanol and re-centrifuged as above. The final DNA pellet was air-dried for 5-10 minutes and resuspended in 300µl of ddH₂O.

2.4. Mammalian Cell Culture

All cell culture media and additives were either sterilised by the manufacturers prior to purchase or by filtration through 0.2µm syringe filters. All cell culture procedures were performed within sterile laminar flow cabinets. The parental CHO-DG44 cells were originally supplied by British Biotech. All transfected cell lines were grown in RPMI medium supplemented with L-Glutamine (4mM final) and 10% (v/v) Foetal Bovine Serum (FBS) (growth medium) either with or without MTX selection. When MTX selection was required MTX was added to a final concentration of 250 nM. 1 x Hypoxanthine & Thymidine (HT) solution was added to growth medium for DHFR-deficient non-transfected parental CHO-DG44 cells.

2.4.1. Cell Harvesting and Maintenance

The anchorage-dependent CHO cells used in this work were cultured routinely in T-75 flasks at 37° C and 5% CO₂. Cells were sub-cultured every 48 to 72 hours. Volumes stated below were used for a fully confluent T-75 flask, containing approximately 1-2 x 10⁷ cells.

Medium was removed from the cells to be sub-cultured and the cell layers were washed with 5ml PBS. 3 ml of trypsin (1 x EDTA in HBSS w/o Calcium or Magnesium) was added to the cell layer and agitated by hand, until the cells were detached (approximately 3-5 minutes). Trypsinisation was stopped by addition of an equal amount of growth medium (i.e. containing FBS) and the cells were transferred to a 50ml tube and centrifuged at 100g for 5 minutes. The supernatant was discarded and the cell pellet was resuspended in 10ml of fresh growth medium and a 0.5ml sample of cells was taken for counting and viability measurements (Section 2.4.2). An appropriate volume of cells was diluted in fresh growth medium to give a cell density of 1×10^5 viable cells/ml.

2.4.2. Measurement of Cell Number and Viability

The cell suspension (Section 2.4.1) was diluted 1:1 with 0.5% (w/v) trypan blue (prepared in PBS) and a portion of this mixture was placed into an Improved Neubauer hemacytometer and observed under a light microscope. Viable cells excluded the blue dye as they had an intact membrane. Dead cells, having decreased membrane integrity, took up the dye and thus appeared blue. Both the total number and number of viable cells were counted in 4 fields of view of 0.1 mm^3 .

The number of cells was calculated by:

Number of cells/ml = (n x Dilution Factor) x Correction Factor

Where n is the mean number of cells/ 0.1 mm^3

2.4.3. Cryopreservation of Mammalian Cells

Approximately 1×10^7 cells were harvested (Section 2.4.1) and resuspended in 1ml of freezing medium (10% [v/v] DMSO in FBS), and then aliquoted into Corning cryovials. The vials were frozen slowly, within a polystyrene box, at -80°C for approximately 24 hours before transfer to liquid nitrogen.

2.4.4. Cell Revival

Vials of frozen cells were removed from liquid nitrogen and thawed quickly by hand. Cells were immediately transferred to a T-75 flask containing 19ml of appropriate growth medium, pre-warmed to 37° C.

2.4.5. Transfection of CHO Cells

CHO cells were transfected with the appropriate linearised plasmids (See Section 2.3). For each reaction approximately 1×10^7 cells were harvested (Section 2.4.1) and washed in 50ml of cold PBS. The cells were re-centrifuged, the supernatant removed and the cell pellet was resuspended in 950 μ l of PBS. For any transfection protocol three electroporation cuvettes were prepared, two containing 100 μ l of each type of plasmid and one with 100 μ l of sterile water as a control. A 950 μ l cell-PBS suspension was added to each cuvette and the mixtures were incubated on ice for 5 minutes. Transfection was achieved by electroporation, using the BIORAD pulse controller/gene pulser. Two consecutive pulses (1500volts, 3 μ fd) were applied to each DNA/cell mixture. After that treatment, cuvettes containing cells were placed on ice for 5 minutes and then limiting dilution cloning was performed (Section 2.4.6)

2.4.6. Limiting Dilution Cloning

Following transfection (Section 2.4.5), cells were diluted as below in non-selective medium (growth medium with HT supplement):

I 1ml of transfected cells plus 29 ml of medium (3.3×10^5 cells/ml)

II 10ml of dilution I plus 30 ml of medium (8.25×10^4 cells/ml)

III 10 ml of dilution II plus 40 ml of medium (1.65×10^4 cells/ml)

5 \times 96 well plates of each dilution were prepared by the addition of 50 μ l of the relevant cell suspension per well. The plates were wrapped in foil to minimise evaporation of the medium and incubated at 37°C and 5% CO₂. Approximately 24 hours later 150 μ l of growth medium was added to each well containing transfected cells. Plates were wrapped again in

foil and incubated at 37°C and 5% CO₂ for about 14 days. The plates were then screened by light microscopy to identify wells with single colonies. Selected wells were fed by replacing the existing medium with 200µl of fresh growth medium. Cells were monitored for growth by light microscopy and transferred to 24-well plates when confluence was reached. Once in 24-well plates, cells were fed with growth medium in a final volume of 1ml and when confluence was reached the cells were transferred to 6-well plates. Cells were monitored by light microscopy until confluent and then transferred to T-25 flasks in a final volume of 5ml and once confluent again were then transferred to T-75 flasks for maintenance (Section 2.4.1). Frozen stocks of obtained clones were created (Section 2.4.3).

2.4.7. MTX-mediated gene Amplification

The strategy for MTX amplification is outlined in Figure 2.1. Initial cell lines were created by transfection of DG44 cells (Section 2.4.5) and limiting dilution cloning was performed (Section 2.4.6) until cell lines were in 6-well plates. Cell lines were maintained in 6-well plates (Section 2.4.1) and EPO production was analysed by ELISA (Section 2.5.8). The top ten EPO producing cell lines were scaled up into T-75 flasks and frozen stocks were made (Section 2.4.3). Equal number of cells from each cell line were pooled and made up to a volume of 50ml with RPMI plus 10% (v/v) FBS to give a final concentration of 1.5×10^5 cells/ml. Pooled cells were then diluted in growth medium containing 250nM MTX as follows:

- I Pooled cells in 50 ml medium (1.5×10^5 cells/ml)
- II 10 ml of dilution I plus 40 ml of medium (3×10^4 cells/ml)
- III 10 ml of dilution II plus 40 ml of medium (6×10^3 cells/ml)

Limiting dilution cloning was then continued as described in Section 2.4.6 until cell lines were in 6-well plates. EPO production was assessed by ELISA (Section 2.5.8) and the top three cell lines, in terms of EPO production, were scaled up into T-75 flasks and frozen stocks were made (Section 2.4.3).

2.4.8. Long-term Continuous Culture

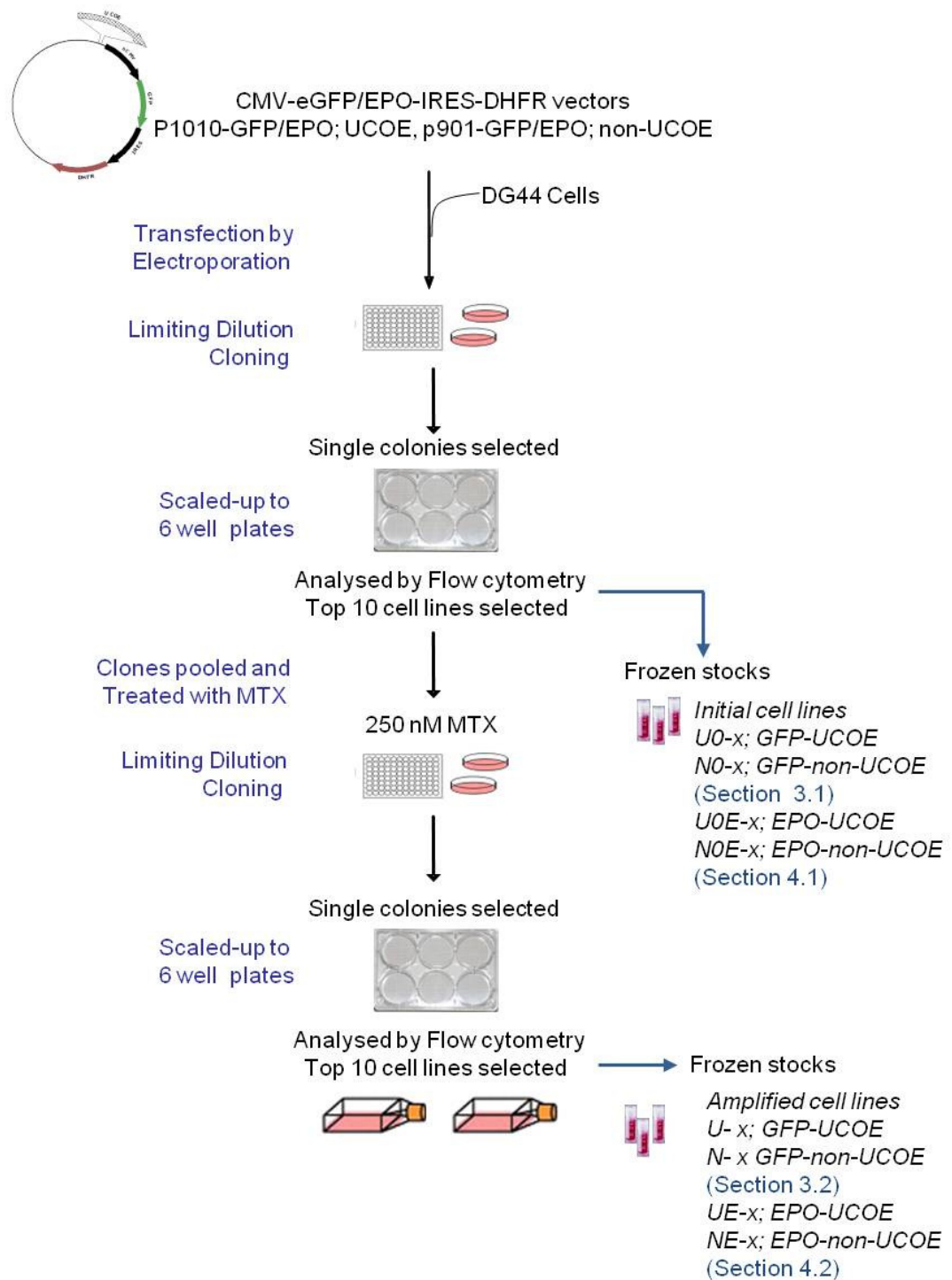
Cells were sub-cultured continuously every 48–72 hours as described in Section 2.4.1 for up to 80 days in growth medium with or without MTX. Samples for further experimental work were taken on days 10 and 80 of long-term culture in CHO-GFP cell lines and days 0 and 77 of long-term culture in CHO-EPO cell lines.

2.4.9. Batch Culture Analysis

Cells were maintained in T-75 flasks as described in Section 2.4.1. For batch growth analysis cells were harvested (Section 2.4.1) in early (days 0-10) and late (day 80) generations of long-term culture (Section 2.4.8) and inoculated into 6-well plates. Cell number and viability counts were made every 24-48 hours. The cell layer was washed with PBS and trypsinized until cells were detached (Section 2.4.1). The medium previously removed from the same cell culture was added to deactivate the trypsin solution and 0.5ml of that mixture was taken for counting and viability measurement (Section 2.4.2).

For CHO-EPO cell lines, samples of culture medium supernatant were also taken to allow determination of recombinant protein production. Samples were stored at -80°C until required for Enzyme-Linked Immunosorbent Assay (ELISA, Section 2.5.8).

Figure 2.1: Establishment of CHO-GFP and CHO-EPO cell lines.



The strategy of establishment of cell lines is summarised above. CHO-DG44-GFP cell lines were created in our laboratory by Dr Alexandra Croxford.

2.5. Analysis of Protein Expression

2.5.1. Protein Extraction

Cells on day 3 of culture were harvested as described in Section 2.4.1 at the beginning and end of long-term culture (Section 2.4.8). Harvested cells were centrifuged at 100g for 5 minutes at room temperature. The cell pellet was washed with 5ml of $1 \times$ PBS and centrifuged at 100g for 5 minutes. The pellet was resuspended in RIPA buffer (0.5% [w/v] Sodium deoxycholate, 0.2% [w/v] SDS, 1.0% [v/v] Triton X-100, 125mM Sodium chloride, 10mM Sodium fluoride, 10mM Sodium orthovanadate, 10mM Sodium pyrophosphate, 25mM HEPES, pH 7.5) using 300 μ l for every 1×10^7 viable cells. Protease inhibitors, PMSF (10mg/ml stock), Aprotinin (1mg/ml stock) and Leupeptin (1mg/ml stock) were added (10 μ l of each for every 1ml of RIPA buffer used per sample). The extracts underwent sheering, by passage through a syringe and 21g needle. Then 3.5 μ l PMSF (10mg/ml stock) was added per 1×10^7 cells and cell lysates were incubated on ice for 30 minutes and then centrifuged at 11000g at 4° C for 30 minutes. Supernatant were transferred to fresh tubes and aliquoted into 100 μ l portions before storage at -80° C.

2.5.2. Protein Quantitation by Bradford Assay

Standard BSA solution was prepared (100 μ g/ml) and cell lysates were diluted to an appropriate degree for assessment against the standard. For generation of standard curves, BSA standard and water were added to the wells in the range of 5 to 60 μ l up to a total volume of 60 μ l in each well. 1 μ l of diluted cell lysates and 59 μ l water were added to the other wells. Cell lysates and standards were assayed in duplicate. Biorad reagent, diluted in 1:3, was added to all wells and the absorbance was measured at 570nm in a plate reader after 10-15 minutes. The protein amount in cell lysates was calculated by comparison to the standard curve generated with BSA.

2.5.3. SDS-PAGE

The Bio-Rad mini gel II lab system was used for SDS-PAGE. The system consisted of a 12.5% (w/v) separating gel overlaid by a 4% (w/v) stacking gel. The separating gel was prepared by mixing 6.2ml Protogel solution (30% [w/v] Acrylamide), 3.75ml separating buffer (1.5M Tris, 14mM SDS, pH 8.8) and 5.05ml ddH₂O. Stacking gel was prepared by mixing 1.6ml Protogel solution, 2.5ml stacking buffer (0.5M Tris, 14mM SDS, pH 6.8) and 6ml ddH₂O. Polymerisation was initiated by the addition of 0.2 µg/ml final concentration of ammonium persulphate and 0.2% (v/v) TEMED.

20µg protein samples (cell lysates, Section 2.5.1) were mixed 1:1 with sample buffer (20% [v/v] glycerol, 7mM SDS, 0.025% (w/v) bromophenol blue). β-mercaptoethanol was added at a final concentration of 1.75% (v/v) to the sample buffer just before use. Samples were then boiled at 100° C for 5 minutes and centrifuged briefly. Electrophoresis was performed in an electrode buffer (10mM Tris, 80mM glycine, 1.4mM SDS) and the samples, together with protein markers (see Appendix 1), were loaded onto the wells. Electrophoresis was performed at 60V until the bromophenol blue dye had reached the separating gel and then at 200V until the dye had reached the bottom of the gel.

2.5.4. Protein Transfer and Western Blotting

Separated proteins from SDS-PAGE were transferred onto nitrocellulose membranes. Gels, together with thick filter paper and nitrocellulose membrane, were soaked in blotting buffer (25mM Tris, 190mM glycine, 20% [v/v] methanol) for 10 minutes prior to use. The transfer was performed on a Bio-Rad Semi-Dry electroblotter at 15V for 45-60 minutes. To assess whether proteins were transferred successfully, the membrane was stained with Ponceau Stain (0.5% [w/v] in 1% [v/v] glacial acetic acid). The membrane was blocked in 3% (w/v) milk in PBS overnight at 4° C with shaking. The primary antibodies were diluted in the blocking buffer, the GFP antibody at 1:20000, the DHFR antibody at 1:1000 and the ERK antibody at 1:2000 (antibodies are listed in Appendix 1). Membranes were incubated with a primary antibody for either 30 minutes at room temperature or overnight at 4° C for

the GFP and DHFR, respectively, with shaking. After incubation, membranes were washed twice with PBS twice with 3% (v/v) Tween-20 in PBS and twice with PBS for 5 minutes. Membranes were incubated for 30-60 minutes in a secondary antibody with dilutions of 1:5000, 1:1000 and 1:5000 for GFP, DHFR and ERK, respectively, at room temperature with shaking (antibodies are listed in Appendix 1). Washing steps were repeated as mentioned before. Once the last wash had been drained from the membrane, protein bands were detected with an enhanced chemiluminescence (ECL) system according to the manufacturer's instructions. The membranes were exposed to Kodak X-ray film and band densities were assessed by densitometric analysis.

2.5.5. Densitometric Analysis

The density of bands on X-ray film was determined using ImageJ software.

2.5.6. Membrane Stripping

Membranes were stripped to allow sequential blotting with different primary antibodies. Stripping was performed in a mild stripping buffer (0.1M glycine, pH 2.5) for 30 minutes at room temperature with agitation. After stripping, membranes were briefly washed with PBS, blocked and incubated with another primary antibody as described in Section 2.5.4. ECL detection, exposure (Section 2.5.4) and densitometric analysis (Section 2.5.5) were performed, as before.

2.5.7. Detection of GFP fluorescence by Flow Cytometry

Cells on day 3 of batch culture were harvested (Section 2.4.1) at the beginning and the end of long-term culture (Section 2.4.8) and resuspended in 1 ml of PBS. The intensity of GFP fluorescence was assessed using a CYAN ADP flow cytometer, using the 488nm excitation laser, according to the manufacturer's instructions. Fluorescence was measured with a photomultiplier (PMT) input of 235V. Fluorescent data was acquired using a 530/40 nm bandpass filter and analysed using Summit v.4.3 software. Live cells were gated by

eye, using a forward scatter versus side scatter log plot and single cells were gated using a forward scatter versus pulse width plot.

2.5.8. Detection of EPO by Enzyme-linked Immunosorbent Assay

Monoclonal mouse anti-human EPO antibody was diluted in sterile PBS at a final concentration of 2µg/ml and then used to coat Nunc 96-well immunoassay plates (100µl per well). Plates were incubated at 4°C for 16 hours. The coating antibody was discarded the following day and plates were washed three times by forcefully filling each well with 250µl wash buffer (0.05% [v/v] Tween-20, 0.05% [v/v] phenol red solution [from a 1% w/v stock], in sterile PBS) and wells were then flick-blotted dry. Plates were blocked by incubating for one hour at room temperature after the addition of 220µl blocking solution per well (25% [w/v] BSA, 0.4% [w/v] sodium azide in sterile PBS). Blocking solution was discarded and 100µl diluted standards and samples (Section 2.5.8.1) were added to each well. These additives were incubated at 37 °C for 2 hours. Standards/samples were removed and the wells were washed three times with wash buffer and blotted dry. 100µl polyclonal rabbit anti-human EPO antibody, diluted to a final concentration of 400ng/ml in dilution buffer (1% [w/v] BSA in sterile PBS), was added to each well as a detection antibody. Plates were incubated at room temperature for 2 hours. After the incubation, wells were washed three times with wash buffer and blotted dry. Goat anti-rabbit IgG antibody-peroxidase conjugate was diluted as 1:2000 with the dilution buffer and used as a secondary antibody. 100µl of secondary antibody was added to each well and plates were incubated at room temperature for 90 minutes. Wells were subsequently washed with wash buffer and blotted dry. The development solution was prepared immediately before use by dissolving two TMB (3,3',5,5' Tetramethyl Benzidine Chromogen) tablets and 5µl 30% (v/v) hydrogen peroxide in 12 ml TMB substrate solution (10mM sodium acetate and 10mM sodium citrate, pH5.5). 100µl development solution was added per well and incubated for 20-30 minutes at room temperature. The reaction was stopped by adding 100µl 0.2M sulphuric acid to each well. The OD of each well was measured at 450nm.

2.5.8.1. Preparation of Standard Curve and Samples for EPO ELISA

Serial dilution of recombinant human EPO produced in CHO cells (Appendix 1) was used as the EPO standard. Dilutions were made with dilution buffer to give a final concentration of 0-8000pg/ml. The recombinant human EPO standard curve was used to calculate the amount of recombinant EPO secreted by CHO cells. Initially ELISAs were performed on samples diluted to a range of dilutions, between 1:1000 to 1:50000 in the dilution buffer. This was done to assess the dilution that would fall within the range of the standard curve. Once suitable sample dilutions were established, diluted samples and standards were loaded in duplicate and mean values taken to quantify EPO content of each sample.

2.6. Analysis mRNA Expression by Quantitative-Reverse Transcription PCR (q-RT PCR)

2.6.1. Extraction and Isolation of RNA

RNA was isolated from cells 24 to 48 hours after sub-culture during the exponential phase of growth at the start and end of long-term cultures (Section 2.4.8). Medium was removed from culture and cells were lysed by addition of 1ml of TRIzol[®] Reagent per 10 cm². Cell lysates were passed through a pipette tip several times. After this treatment, TRIzol extracts were aliquoted as 1ml portions and stored at -80° C until purification. For purification, samples were thawed samples and then incubated for 5 minutes at room temperature. 0.2ml of chloroform was added for each 1ml of TRIzol[®] cell extract in 1.5ml microcentrifuge tubes and the tubes were shaken vigorously for 15 seconds. After incubation for 2-3 minutes at room temperature, tubes were centrifuged at 12000g for 15 minutes at 4° C. The upper aqueous phase was transferred to a fresh tube and the RNA in that supernatant was precipitated by addition of 0.5ml isopropanol, mixing and subsequent incubation at room temperature for 10 minutes. Tubes were centrifuged at 12000g for 10 minutes at 4° C and the resultant (RNA) pellets were washed with 75% (v/v) ethanol by vortexing. After washing, the tubes were centrifuged at 7500g for 5 minutes at 4° C, the

resultant pellets were air-dried for 5-10 minutes and dissolved by addition of 30 μ l DEPC-treated ddH₂O. These RNA samples were stored at -80° C until use.

2.6.2. DNase I treatment of RNA

The concentration of RNA in cell extracts (Section 2.6.1) was quantified using a NanoDrop[®] ND-1000 UV-Vis Spectrophotometer. Extracts was then treated with DNase I to remove any trace contamination of genomic DNA, using the DNaseI kit from Sigma-Aldrich (see Appendix 1). All reagents were supplied with the kit. The following reagents were prepared in a 0.5ml microcentrifuge tube:

- 1 μ g of RNA in 8 μ l DEPC-treated ddH₂O.
- 1 μ l of 10 x Reaction buffer
- 1 μ l of DNase enzyme

The reaction was incubated at room temperature for 15 minutes, 1 μ l of stop solution was added after incubation and then the solution was heated at 70° C for 10 minutes and chilled on ice.

2.6.3. cDNA Synthesis from RNA

cDNA was prepared from DNase I-treated RNA extracts (Section 2.6.2) using the cDNA synthesis kit from Bioline (see Appendix 1). All reagents were supplied by the manufacturer unless otherwise stated. 1 μ l of Oligo (dT)₁₈ and 1 μ l of 10mM dNTP were added to DNaseI-treated samples and incubated at 65° C for 10 minutes. The following reagents were added per reaction:

- 4 μ l of 5 \times RT buffer
- 1 μ l of RNase inhibitor
- 0.25 μ l of Reverse Transcriptase (200u/ μ l)
- Up to 10 μ l DEPC-treated ddH₂O.

The reaction was mixed and incubated at 42° C for an hour and terminated by heating to 70° C for 15 minutes. Reactions were stored at -20° C until needed.

2.6.4. Preparation of Samples and “Standard” sample for q-PCR reactions

One cell RNA extract sample was dedicated as the ‘standard’ sample and was assessed in all q-PCR reaction plates to allow “internal control” comparison of the mRNA content of samples. The cDNA reaction from the standard sample was diluted 1:5 in ddH₂O, to give the 100% standard. Serial dilutions were prepared from the 100% standard in ddH₂O to give 10% and 1% final concentrations. All other samples were diluted at a ratio of 1:7 with ddH₂O.

2.6.5. q-PCR Reaction

The following reagents were added to each well of the MJ-White 96 well plate:

- 5µl of appropriately diluted cDNA (Section 2.6.3)
- 2.5µl of forward primer (10 µM) (Table 2.1)
- 2.5µl of reverse primer (10 µM) (Table 2.1)
- 10µl of 2 x SYBR[®] Green qPCR master mix.

Plates were sealed with clear plastic caps and centrifuged at 900g. Primers were designed using the Primer 3 website (<http://Frodo.wi.mit.edu>) and are shown in Table 2.1. Samples and standards were analysed in triplicate. Additionally, triplicate wells containing 5µl ddH₂O and non-reverse transcriptase treated sample were prepared as negative controls.

The PCR reaction was performed using a Chromo 4 thermal cycler with the following settings: 95° C for 10 minutes, followed by 35 cycles of denaturation at 95° C for 10 seconds, annealing at 57° C for 10 seconds, elongation at 72° C for 20 seconds and denaturation of primer dimers at 76° C for 1 second. A final elongation step at 72° C for 10 minutes was performed.

2.6.6. Analysis of q-PCR Results

Data was quantified using an Opticon Monitor analysis software. Blanks and baseline fluorescence were subtracted from fluorescence plots. The threshold was raised to 0.05

(within exponential phase) and the cycle at which samples reached this fluorescence was obtained. A standard curve was generated using standard values by plotting log [cDNA] versus Ct. The relative concentration of cDNA was achieved by extrapolating from the standard curve using the Ct values. Total mRNA content was normalised using a β -actin q-PCR reaction. The melting curve was assessed to check the quality of the amplified product where a single peak at between 80° C and 90° C indicated a pure product.

Table 2.1: Primers used for q-PCR

Primer Name	Forward (5'-3')	Reverse (5'-3')	Annealing Temp(°C)
β-Actin (mRNA)	TGTGACGTTGAC ATCCGTA AAA	GCAATGATCTT GATCTTCATG	57
β-Actin (DNA)	ACTGCTCTGGCT CCTAGCAC	CATCGTACTCC TGCTTGCTG	57
GFP (mRNA)	CAGGTACCCAG ACCACATGA	TCACCCTCGAA TTTGACCTC	57
GFP (DNA)	CGTGTACGGTGG GAGGTCTA	AACAGCTCTTC CCCTTTCT	57
DHFR	CAGGAAGCCAT GAATCAACC	AGAGAGGACGC CTGGGTA TT	57
EPO (mRNA)	TGGGAGCCCAG AAGGAAG	CTCCCCTGTGT ACAGCTTCAG	57
EPO (DNA)	GTAACA ACTCCG CCCCATT	ACAGCCAGGC AGGACATTC	57

2.7. DNA Analysis

2.7.1. Isolation of Genomic DNA

An adapted version of the protocol detailed by Blin & Stafford (1976) was used to extract genomic DNA from CHO cells. Cells on day 3 of culture were harvested as described in Section 2.4.1 at the beginning and end of long-term culture (Section 2.4.8). Approximately 2×10^7 cells were harvested by centrifugation at 100g for 10 minutes at room temperature. The cell pellet obtained was washed three times in 1×PBS with centrifugation between each wash as above. The final pellet was then resuspended in 100µl of 1×PBS and 3ml of EDTA-Sarcosine solution (0.1M EDTA, pH8.0, containing 0.5% [w/v] N-Lauroyl-Sarcosine) was then added to the pellet in a dropwise fashion with continuous gentle mixing. 60µl of Proteinase K (10mg/ml) and 10µl of RNase A (10mg/ml) were then added. The mixture was incubated at 55°C for 2 hours and mixed by inversion every 15 minutes. The sample was purified by three rounds of phenol extraction and ethanol precipitation (Section 2.3.1). DNA was quantified as described in Section 2.2.3.

2.7.2. Plasmid Copy-Number Analysis by q-PCR

q-PCR reactions and analysis were performed as described in Sections 2.6.5 and 2.6.6, although samples and standards were prepared as described in Section 2.7.2.1.

2.7.2.1. Preparation of Standard curve and DNA Samples

The p1010-EPO/GFP vectors were diluted to a final concentration of 1,000,000 – 457 copies per 5µl reaction, in a background (10ng/µl) of genomic DNA isolated from non-transfected CHO-DG44 cells (Section 2.7.1). Background DNA was used to ensure the efficiency of the PCR reaction was the same for all samples. Stock dilutions were made, aliquoted and stored at -80°C, for use for future assays.

One sample was dedicated as the 'check' sample that was run on all plates and used to normalise the total DNA content in each well. The 'check' sample was diluted to final concentrations of 20, 10 and 5ng/ μ l, using ddH₂O, and aliquots of these dilutions were made and stored at -80°C, to be used for future assays. All other samples were diluted to a final concentration of 10ng/ μ l in ddH₂O.

2.8. Fluorescent *In Situ* Hybridisation (FISH)

2.8.1. Preparation of Metaphase Spreads

Cells were grown until they were approximately 50% confluent and then treated with colcemid solution at a final concentration of 130ng/ml (w/v) for 16 to 20 hours, at 37°C with 5% CO₂. Cells were harvested (Section 2.4.1) by centrifugation at 100g for 5 minutes. Cell pellets were resuspended in approximately 100 μ l of fresh growth medium. 10 ml of hypotonic solution (0.04M potassium chloride, 0.025M tri-sodium citrate) was added dropwise, with gentle mixing, to the resuspended cells. Cells in the hypotonic solution were incubated at room temperature for 10 minutes and then centrifuged at 220g for 5 minutes. Supernatant was removed and the cell pellet was resuspended in, approximately, 100 μ l of fresh hypotonic solution. 5ml of ice cold methanol:acetic acid (3:1) was added to the resuspended cells. Cells were centrifuged at 220g for 5 minutes and the supernatant was removed. This process was performed three times in total. After this, cells were resuspended in a 100 μ l of ice cold methanol:acetic acid (3:1) for fixation. Fixed metaphase nuclei preparations were store at -20°C until required. Approximately 10 μ l of this solution was pipetted onto each of several precleaned (acetic acid wiped and allowed to evaporate) glass slides. Spreads were left to age (overnight at the least and up to 4 weeks) at room temperature before examination.

2.8.2. Preparation of Probes for FISH analyses

FISH probes were prepared with p1010-GFP plasmid through incorporation of modified dUTPs via nick translation. For each reaction, 1 μ g of plasmid DNA was resuspended in

16µl ddH₂O. 4µl digoxigenin (DIG)-nick translation mix (see Appendix 1) was added to the reaction mixture and the whole mixture was then incubated at 15°C for approximately 3 hours. The nick translation reaction was halted by transferring the reaction tube on ice. 5µl of the reaction product was separated on a 2% agarose gel (Section 2.8.3) to confirm that the plasmid DNA has been reduced to under 300bp in size. If plasmid size is above 300bp, reaction is resumed by incubating the reaction mix at 15°C until plasmid is the optimal size. Nick translated probes were stored at -20°C until needed.

2.8.3. Agarose Gel Electrophoresis

Agarose gels were prepared by dissolving 2% (w/v) agarose in TBE buffer (0.09M tris, 0.09M orthoboric acid and 0.2mM EDTA, pH8.0), by boiling in a microwave. Once the gel had cooled to less than 55°C ethidium bromide was added to a final concentration of 0.25µg/ml. Gels were set and run in horizontal electrophoresis tanks with TBE as running buffer. Samples were mixed at a 5:1 ratio with loading buffer (1mM EDTA, 50% [w/v] glycerol, 4% [w/v] bromophenol blue and 20% [w/v] Ficoll), and loaded into wells. 5µl of DNA Hyperladder I was also loaded as a reference. The DNA fragments were separated by electrophoresis at 70V for 45 minutes – 1 hour, and visualised by UV light.

2.8.4. Hybridisation Protocol

Metaphase spreads on glass slides, prepared as described in Section 2.8.1, were dehydrated through sequential incubation in increasing concentrations of ethanol solution (70%, 90%, 100% [v/v]) for three times, three minutes each. Slides were air-dried and then incubated in 0.005% (w/v) pepsin in 0.01M HCl solution at 37°C for 20 minutes. Slides were subsequently immersed in 10% FBS/PBS (v/v) solution to quench pepsin digestion and then dehydrated again as described above.

For each hybridisation reaction, 25µl of nick translated probe was mixed with 5µl herring sperm DNA and precipitated with ethanol (Section 2.3.1). The resultant DNA pellet was then washed with 70% ethanol (v/v) and resuspended in 30µl FISH probe hybridisation

buffer (10% dextran sulfate (v/v), 50% formamide (v/v), 2×SSC [0.3M NaCl, pH7.0, 0.03M tri-sodium citrate]). 15µl of this hybridisation solution was applied onto each slide, and the area of application was then covered with a 22mm×22mm coverslip and the edges of the coverslip were sealed with nail varnish. Slides were incubated on a heat block at 70°C for 2 minutes for denaturation, followed by incubation in a humidified chamber at 37°C for 16 hours. After hybridisation, coverslips were removed and slides were washed three times for three minutes each in 50% formamide/2×SSC (v/v) at 37°C. Slides were then washed with 2×SSC three times for three minutes each and allowed to dry at room temperature.

2.8.5. Antibody Detection

The remainder of this procedure was performed in the dark. Samples probed with DIG labelled DNA fragments (Section 2.8.2, 2.8.4) were detected with rhodamine conjugated Fab fragments diluted 1:10 in 1% (v/v) FBS/PBS. 25µl of the diluted antibody was applied to each slide, which was then covered with a coverslip and incubated in humidified chamber at 37°C for 30 minutes. Slides were washed three times in 2×SSC for three minutes each at 37°C. Slides were then quickly dipped in ddH₂O and allowed to air-dry in the dark. Slides were fixed with Prolong anti-fade Gold Dapi (Invitrogen, see Appendix 1) according to the manufacturer's instructions and then covered with a 22mm×22mm coverslip. After overnight incubation at room temperature, slides were sealed with nail varnish. Images were acquired as described in Section 2.9.5.

2.9. Chromosome Painting

Metaphase spreads were prepared as described in Section 2.8.1. Chromosome-specific DNAs were supplied by Cambridge Resource Centre for Comparative Genomics and used as templates for degenerate oligonucleotide-primed PCR amplification (DOP-PCR product) and labelled with biotin-16-dUTP.

2.9.1. Labeling DOP-PCR Product

Biotin-16-dUTP was incorporated into the DOP-PCR product by including the following per 25µl reaction:

- 12.5µl of sterile ddH₂O
- 2.5 µl of 10×NH₄ buffer
- 2.5µl of 6MW (20µM primer)
- 2.5µl of ½T dNTP mix
- 2.5µl of Biotin-16-dUTP (50nM)
- 1.25µl of MgCl₂ (50mM)
- 0.25µl of Taq polymerase
- 1µl of DNA (DOP- product)

The PCR reaction settings were as follows: 94°C for 5 minutes followed by 30 cycles of denaturation at 94° C for 90 seconds, annealing at 57° C for 90 seconds, elongation at 72° C for 3 minutes. A final elongation step at 72°C for 8 minutes was performed.

2.9.2. Preparation of Probe

4µl of chromosome paint reaction mix was mixed with 12µl of H₂O and 4µl of biotin-nick translation mix (see Appendix 1) and incubated as described in Section 2.8.2.

2.9.3. Hybridisation Protocol

Hybridisation of chromosome paint probes were as described in Section 2.8.3. For the slides that were hybridised with both FISH and chromosome paint probes 15µl of each probe was mixed and the mixture was applied onto the slide.

2.9.4. Antibody Detection

FITC conjugated avidin antibody was diluted 1:100 in 1% (v/v) FBS/PBS and used for the chromosome paint samples as described in Section 2.8.5. Sequential incubation was performed for the slides that had been hybridised with both FISH and chromosome paint probes.

2.9.5. Image Acquisition

FISH (Section 2.8) and chromosome paint (Section 2.9) slides were observed under an Olympus inverted microscope at 100× magnification. Images were taken with Coolsnap ES camera through MetaVue Software.

2.10. Statistical Methods

All data presented is represented as a mean ± standard error of mean (SEM); or mean ± range, where mean is taken from two observations only, unless otherwise stated.

- Standard Deviation (SD) = $(\sqrt{[\sum\{x-m\}^2]/\{n-1\}})$
x: observed value
m: mean of n observations
n-1: degrees of freedom
- SEM= (SD/\sqrt{n})
n: number of independent observations
- Coefficient of Variance (CV) = $(SD/m) \times 100$
- The correlation coefficient (r value) was calculated for standard curves produced in EPO ELISAs (Section 2.5.1) and q-PCR assays (Section 2.6.6), using Microsoft

Excel. Any assays performed, where the standard curve had a correlation coefficient ≤ 0.98 , were disregarded.

- An independent samples t-test was used to determine whether the difference between the mean of two independent samples (i.e. comparison of mean for UCOE and non-UCOE cell lines) was statistically significant, unless otherwise stated. The independent samples t-test was performed using SPSS (v16.0.1) software. Data was considered significant if $p < 0.05$.
- A paired samples t-test was used to determine whether the difference between the mean of two related samples (i.e. comparison of mean in time 1 and time 2) was statistically significant, using SPSS (v16.0.1) software. Data was considered significant if $p < 0.05$.
- Bivariate correlation analysis was performed to determine the association between two variables, using SPSS (v16.0.1) software. Correlation was considered significantly different if $p < 0.05$.

2.11. Calculations

- Cumulative cell times (CCT) were calculated as follows.

$$\text{CCT} = [(X + X_0)/2] \times (T - T_0)$$

X_0 = Viable cell density ($\times 10^6$ cells/ml) by first point of analysis

X = Viable cell density ($\times 10^6$ cells/ml) at time (T)

T_0 = time at the beginning (days)

T = time at the end (days)

- The cell specific growth rate (μ) was calculated as follows.

$$\mu = (\ln X_0 - \ln X) / T$$

T = Time in culture (hours)

- The cell specific productivity was calculated between two points during batch growth culture (typically exponential growth), using the following formula:

$$\text{Specific productivity (pg/cell/day)} = \frac{\left(\frac{P_1 - P_0}{\left\{ \frac{X_1 + X_0}{2} \right\}} \right)}{T_1 - T_0}$$

Where

P_0	= productivity ($\mu\text{g/ml}$) by first point of analysis
P_1	= productivity ($\mu\text{g/ml}$) by second point of analysis
X_0	= Viable cell density ($\times 10^6$ cells/ml) by first point of analysis
X_1	= Viable cell density ($\times 10^6$ cells/ml) by second point of analysis
T_0	= day of first point of analysis
T_1	= day of second point of analysis

CHAPTER 3:

Results-1

In this section, the results obtained during the long-term culture of CHO-GFP cell lines will be analysed. Cell lines used in this study were provided by Dr Alexandra Croxford. The strategy of cell line establishment was explained in Figure 2.1. In short, parental CHO-DG44 cells were transfected with either the p1010-eGFP vector (UCOE) (Appendix 2) or the p901-eGFP vector (non-UCOE) (Appendix 2). Cells expressing the DHFR transgene were obtained by the exclusion of hypoxanthine and thymine from the medium. Limiting dilution cloning was performed after transfection and single colonies were selected and then scaled up into 6-well plates. eGFP fluorescence was measured by flow cytometry and the top-ten eGFP producing initial cell lines were scaled-up into T-75 flasks from both the UCOE and non-UCOE group and cryopreserved for further studies (Section 3.1). For each group, the selected high producing initial cell lines were pooled and then treated with 250 nM MTX. Limiting dilution cloning was carried out immediately after resuspension in a MTX-containing medium. Single colonies were scaled-up into 6-well plates and eGFP fluorescence was measured by flow cytometry. The top ten eGFP producing cell lines from both groups were selected and scaled up. Frozen stocks were prepared for subsequent studies (Section 3.2).

3.1. Characterization of initial cell lines

This section describes the characterization of initial UCOE and non-UCOE cell lines (hereafter called U0-x and N0-x respectively where x is a number from 1 to 5). Frozen stocks of randomly chosen 5 UCOE and 5 non-UCOE cell lines were revived (Section 2.4.4) and grown in adherent culture in T-75 flasks. Cells were sub-cultured every 2-3 days continuously for up to 80 days. Viable cell densities (Section 3.1.1) and eGFP expression (Section 3.1.2) were analysed 10 days after revival and at the end of long-term cultivation (day 80).

3.1.1. Analysis of growth during long-term continuous culture in initial CHO-GFP cell lines

At the beginning and the end of long-term culture, cells were used to create a batch growth culture at an initial seeding density of 2×10^5 cells/ml (Section 2.4.9). Samples were taken throughout batch culture for cell number measurements. Figure 3.1 shows the average viable cell densities (Figure 3.1A) and cumulative cell time (CCT) (Figure 3.1B) for each group during batch growth culture. There was no difference in viable cell densities between the UCOE and non-UCOE cell lines in early and late generation. Although patterns of growth changed, with cells transfected with either vector, as long-term culture progressed, there was no significant change in viable cell densities and CCT between cultures created at late generation compared to at early generation (Figure 3.1).

3.1.2. Analysis of eGFP expression during long-term culture in initial CHO-GFP cell lines

eGFP protein expression for the cell lines was examined over long-term culture (Figures 3.2 and 3.3) by flow cytometry (Section 2.5.7) and Western blotting (Section 2.5.4) in cultures at day 10 (early generation) and day 80 (late generation). Samples for analyses were taken on day 3 of batch culture.

The eGFP fluorescence (Figure 3.2A) (and the coefficient of variation [CV] of fluorescence measurement) (Figure 3.2B) were analysed by flow cytometry (Section 2.5.7) on day 10 and day 80 of long-term culture (Section 2.4.8). The mean fluorescence intensity indicates the level of fluorescence of the cell population, whereas the CV is a measure of fluorescence distribution within the cell population. CV represents the ratio of the standard deviation to the mean and therefore allows comparison of populations with different means (Section 2.10).

Results are presented as individual cell lines and the overall mean fluorescence of each group is shown (Figure 3.2A). UCOE cell lines showed consistent and significantly higher

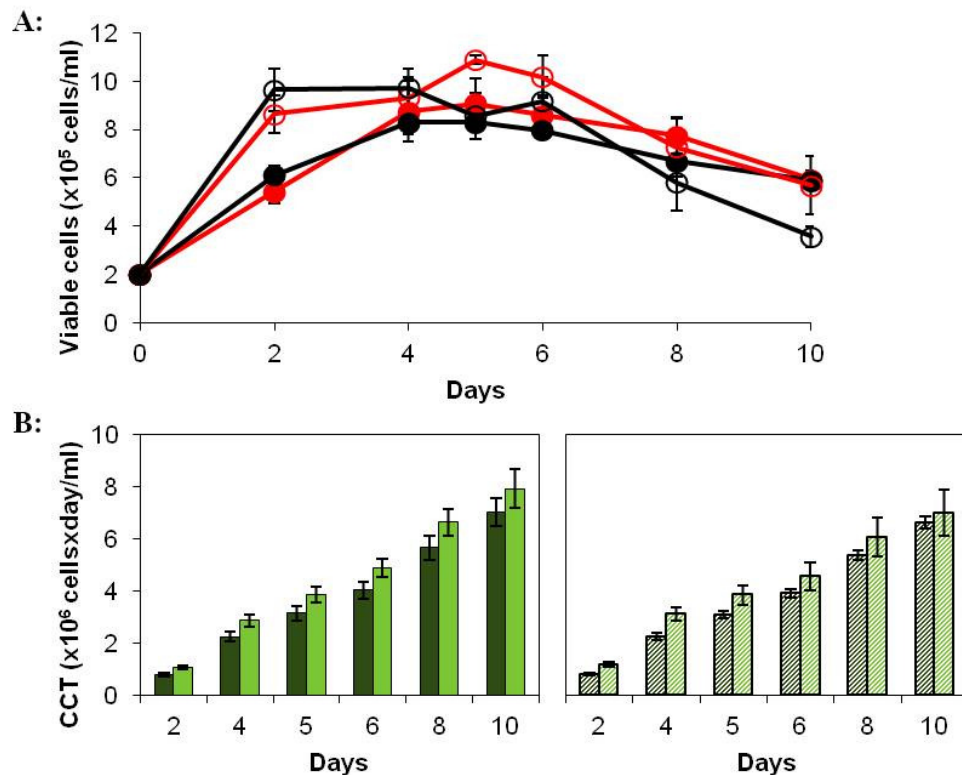
extent of eGFP fluorescence than non-UCOE cell lines. An increase in eGFP fluorescence was observed to occur after long-term culture in some of the non-UCOE cell lines, which is also reflected by the mean fluorescence of the non-UCOE group (Figure 3.2A). UCOE cell lines had significantly lower CV compared to non-UCOE cell lines at the beginning of long term culture (Figure 3.2B). However, over 80 days of continuous culture, 4 out of 5 UCOE cell lines showed an increase in CV, which was reflected in the mean CV of UCOE cell lines. In contrast, 3 of the non-UCOE cell lines displayed a decrease in CV over long-term culture and this was again reflected by the mean CV, although the difference was not significant (Figure 3.2B).

Flow cytometry is a useful tool for determining the number of positive cells in a population and also for providing information on a number of statistical parameters that are useful for understanding the population's cell characteristics within a cell line. Western Blot analysis can provide additional information such as detection and relative quantification of individual proteins in samples, in order to assess changes in protein expression level from a population of cells. Therefore, in parallel to the assessment of the eGFP fluorescence by flow cytometry eGFP production was also analysed using Western blotting (Figure 3.3). ERK was used as a loading control. The band intensity corresponding to the eGFP confirmed the conclusions reached from the flow cytometry analysis, where UCOE cell lines showed significantly higher eGFP production compared to the non-UCOE group. All the UCOE cell lines displayed stable and high amounts of recombinant eGFP production over long-term culture, whereas a significant increase was observed at the later stage of long term culture for three out of five non-UCOE cell lines. This was also reflected in group mean values (Figure 3.3A). Although some of the non-UCOE cell lines showed an increase in eGFP production throughout the culture, the mean values of eGFP production were higher in the UCOE cell lines, as compared to the non-UCOE group in early and late generations, where the difference was observed as 3 and 1.6 fold respectively.

Despite the fact that a significant positive correlation was observed between the results of eGFP expression assessed by western analysis and flow cytometry (Figure 3.3C), the increase in eGFP expression was greater than the increase in eGFP fluorescence detected

by flow cytometry in the N0-1 and N0-2 cell lines. Moreover, the N0-3 cell line showed an increase in eGFP expression but no change in eGFP fluorescence. One possible reason for the difference between these results may be explained by the requirement for GFP to assume a functional 3-D structure in order to exhibit fluorescence (Tsien, 1998). If the intact protein fails to fold correctly fluorescence may not be detectable, whereas eGFP can still be detected by western blotting.

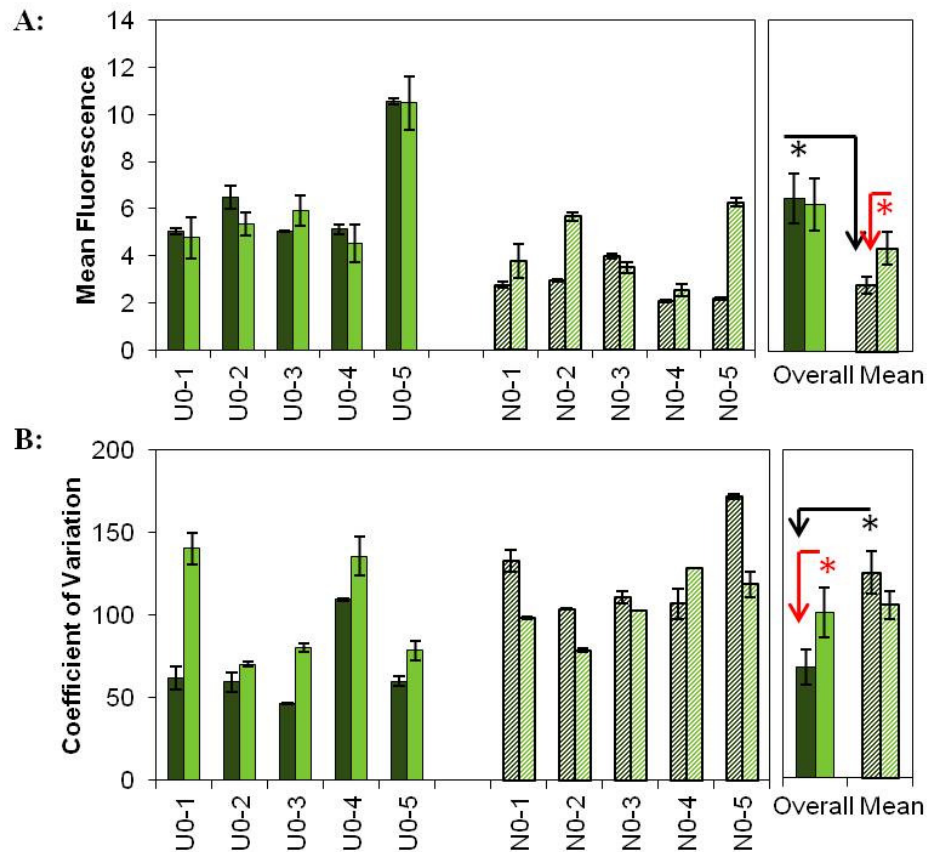
Figure 3.1: Analysis of batch culture growth and cumulative cell time in initial CHO-GFP cell lines.



CHO-DG44 cell lines, transfected with either *p1010-eGFP-DHFR* (UCOE) or *p901-eGFP-DHFR* (non-UCOE) (Section 2.4.5), were cultured in T-75 flasks using RPMI medium plus 4mM L-Glutamine and 10% FBS. Cells were cultured every 2-3 days up to 80 days (Section 2.4.1). Batch growth cultures were created at an initial density of 2×10^5 cells/ml in T-25 flasks, at early (day 10), and late (day 80) generations. Samples were taken throughout batch culture for determining cell number. (A) Viable cell numbers were measured using light microscopy and trypan blue exclusion (Section 2.4.2). All batch cultures were performed in duplicate flasks. (B) Cumulative cell time (CCT) was calculated during batch growth culture created in early and late generations (Section 2.11) Values are presented as average of each group \pm SEM ($n=5$) (Section 2.10). An independent samples *t*-test performed to compare cultures created at early and late generations and also UCOE vs non-UCOE cell lines (on the same day of batch culture), $p > 0.05$ (Section 2.10).

—●—■ UCOE cell lines early generation; —○—□ UCOE cell lines late generation;
 —●—■ non-UCOE cell lines early generation; —○—□ non-UCOE cell lines late generation.

Figure 3.2: Effect of long-term culture on eGFP fluorescence and the degree of variation in initial cell lines.



Cell lines were cultured as described in Figure 3.1 (Section 2.4.1). eGFP fluorescence was measured on day 10 and day 80. A fully confluent T-75 flask was sub-cultured at an initial density of 0.2×10^6 cells/ml and cells were grown for 3 days. Fluorescence was then measured by flow cytometry with a PMT input of 235V (Section 2.5.7). (A) eGFP fluorescence for individual cell lines are shown and group mean values are shown. (B) CVs for individual cell lines are calculated as described in Section 2.10. Values are quoted \pm SD ($n=3$) Overall mean values are quoted \pm SEM ($n=5$) (Section 2.10).

■ = UCOE day 10, ■ = UCOE day 80, ▨ = non-UCOE day 10, ▨ = non-UCOE day 80. * indicates $p < 0.05$, using independent samples *t*-test to compare UCOE and non-UCOE cell lines (at the same time of long-term culture). * indicates $p < 0.05$, using paired samples *t*-test to compare early and late generation cultures (for the same group of cell lines) (Section 2.10)

Cell lines were cultured for 80 days as described in Figure 3.1 (Section 2.4.1) Cells were sub-cultured every 2-3 days and eGFP expressions were measured on day 10 and day 80 by western blot analysis (Section 2.5.4). ERK is used as a loading control. Prefix U0- indicates UCOE cell lines; N0- indicates non-UCOE cell lines.

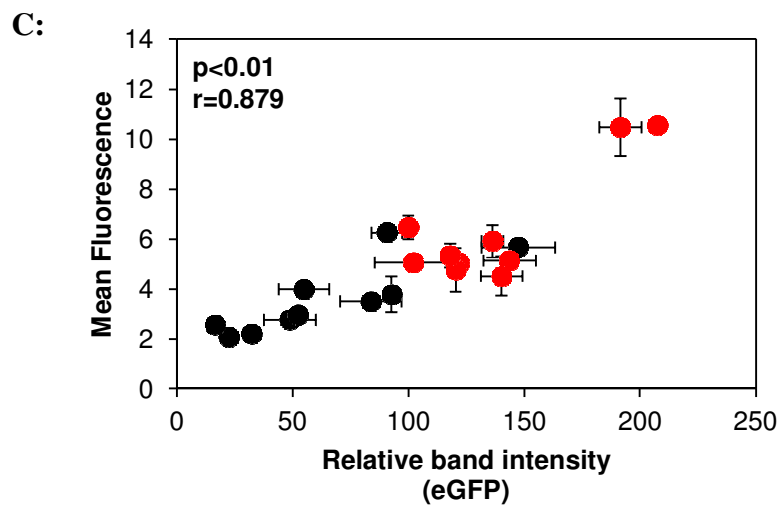
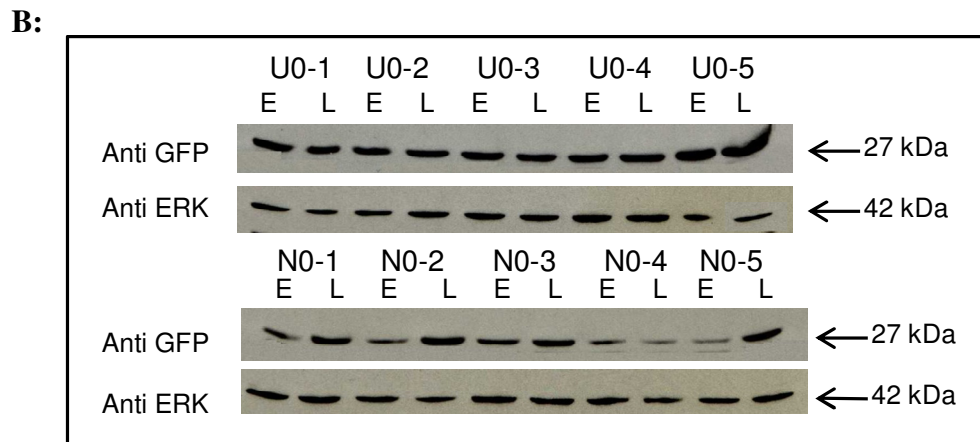
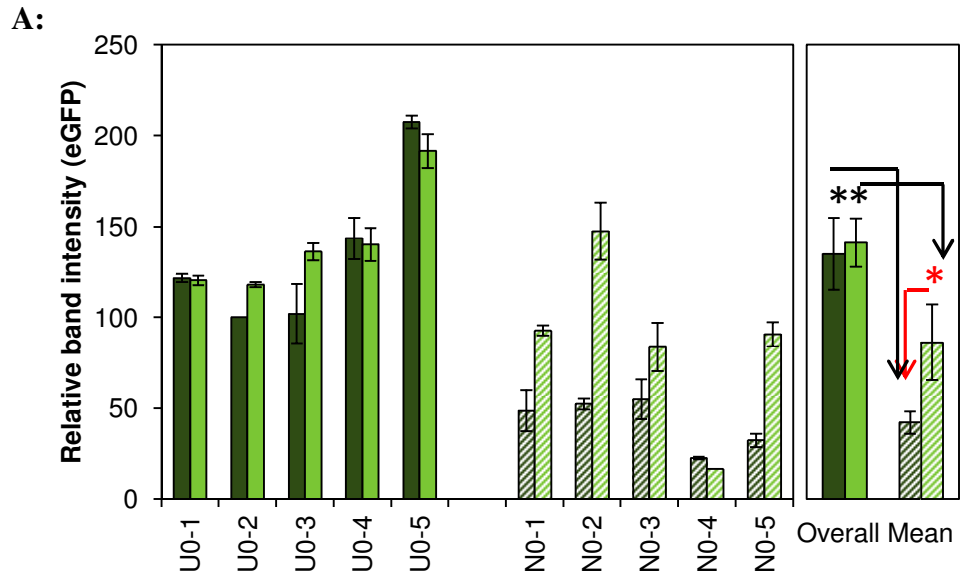
(A) Relative intensity of eGFP band, as determined by densitometric analysis normalized to ERK. Values are quoted \pm range ($n=2$), overall mean values are quoted \pm SEM ($n=5$). * indicates $p<0.05$, using independent samples t -test to compare UCOE and non-UCOE cell lines (at the same time of long-term culture).

* indicates $p<0.05$, using paired samples t -test to compare early and late generation cultures (for the same group of cell lines) (Section 2.10).

■ = UCOE day 10, ■ = UCOE day 80, ▨ = non-UCOE day 10, ▩ = non-UCOE day 80. (B) eGFP expression for individual cell lines is shown: Lane E=Early generation (day 10), Lane L= Late generation (day 80). (C) Results obtained from Western analysis are plotted against those of flow cytometry. ● = UCOE, ● = non-UCOE

Correlation coefficient and statistical significance are indicated in the top left of the scatter plot.

Figure 3.3: Western Blot determination of eGFP expression over long-term continuous culture.



3.2 Amplification of CHO-GFP cell lines

The strategy for creating amplified CHO-GFP cell lines was explained in the beginning of this Chapter and in Figure 2.1. From the frozen stocks of amplified cell lines, 5 from each group were revived and recultivated in T-75 flasks. Cells were subcultured every 2-3 days, either with or without MTX in the medium, continuously for up to 80 days. Growth (Section 3.2.1) and protein production (Section 3.2.2) were analysed at the beginning and end of long-term culture. In order to have a better understanding of the effect of amplification, plasmid copy number and mRNA expression were analysed over long-term culture in Section 3.2.3 and 3.2.4 respectively. Finally, chromatin environment surrounding the inserted plasmid was investigated using sodium butyrate (Section 3.2.5).

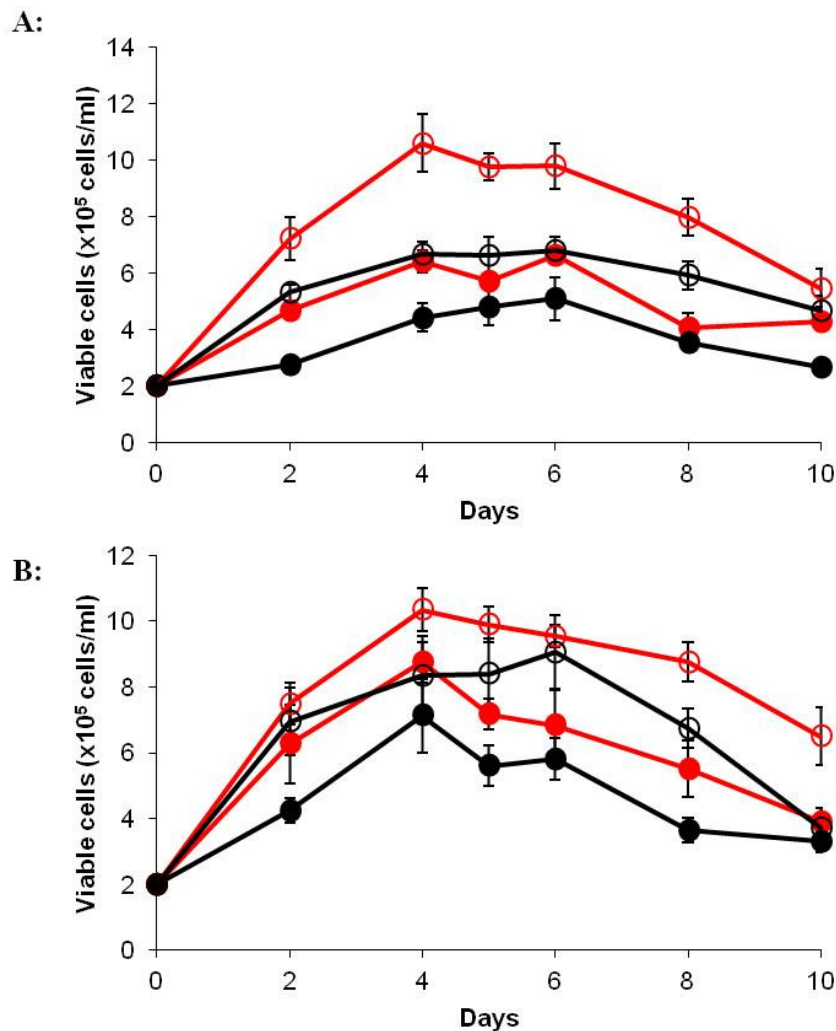
3.2.1. Analysis of batch culture growth of amplified CHO-GFP cell lines.

The growth of batch cultures was analysed in early (day 10) and late (day 80) generation cell lines as described in Section 3.1.1. The average viable cell densities and CCTs of each group of cell lines are shown in Figures 3.4 and 3.5. The patterns of growth were similar to the initial cell lines at early generation (Figure 3.1). However, both the amplified UCOE and non-UCOE cell lines at early generation showed significantly lower cell densities and CCTs compared to the initial cell lines ($p < 0.05$, using independent t-test to compare the amplified and non-amplified cell lines on the same day of batch culture for the same generations [Section 2.10]). The amplified UCOE cell lines achieved similar cell densities and CCTs at late generation in the presence and absence of MTX selection compared to the initial cell lines. However, viable cell numbers in amplified non-UCOE cell lines at late generation in the presence of MTX were still significantly lower than the initial cell lines ($p < 0.05$, using independent samples t-test test to compare the amplified and non-amplified cell lines on the same day of batch culture for the same generations [Section 2.10]).

The data for amplified cell lines showed that UCOE cell lines achieved higher maximum cell densities both in the presence and absence of MTX, compared to non-UCOE cell lines. Furthermore, batch cultures created by early generations had lower cell densities than late

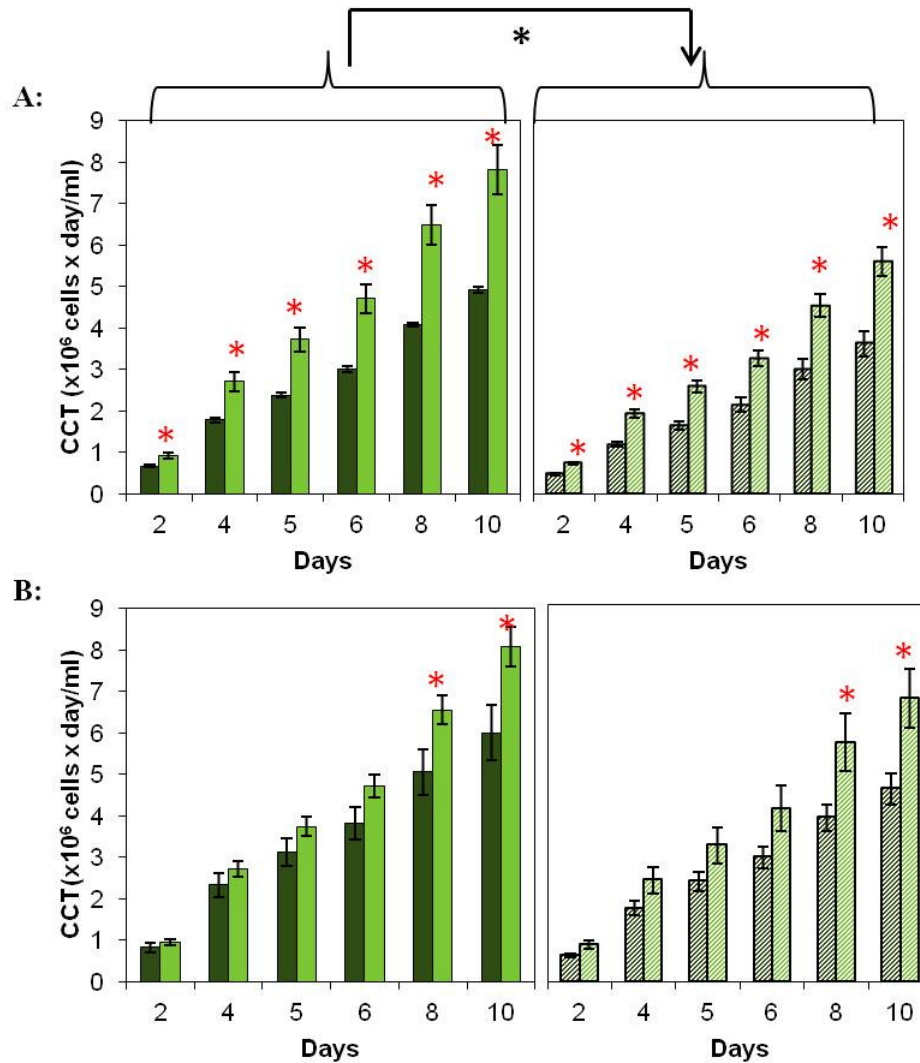
generation cultures. Changes in viable cell densities can also be seen in CCT (Figure 3.5). CCT values were significantly higher on all days of batch cultures created at late generations than early generations in the presence of MTX selection for both UCOE and non-UCOE cell lines. However, the difference in CCT was observed on days 8 and 10 of batch cultures in the absence of MTX selection. Moreover, CCT values of UCOE cell lines were significantly higher than non-UCOE cell lines at all data points in the presence of MTX. These results differed from those obtained with the non-amplified initial cell lines where no difference between the UCOE and non-UCOE group of cell lines was observed (Figure 3.1). Therefore, results indicate that UCOE cell lines show better growth characteristics than non-UCOE cell lines in the presence of MTX.

Figure 3.4: Analysis of batch culture growth of amplified CHO-GFP cell lines.



The top ten highest producing initial cell lines were pooled and treated with 250 nM MTX (Section 2.4.7). Cell lines were cultured every 2-3 days up to 80 days in T-75 flasks using RPMI medium plus 4mM L-Glutamine and 10% FBS either with or without MTX selection (Section 2.4.1). Batch growth cultures were created as described in Figure 3.1. (Section 2.4.9). The viable cell numbers are presented as mean values \pm SEM ($n=5$) (Section 2.10). (A) Viable cell numbers with MTX selection, (B) Viable cell numbers without MTX selection: ● UCOE cell lines early generation, ○ UCOE cell lines late generation; ● non-UCOE cell lines early generation, ○ non-UCOE cell lines late generation;

Figure 3.5: Effect of long-term culture on cumulative cell time in amplified CHO-GFP cell lines.



CCTs are calculated during batch growth culture created in early and late generations (Figure 3.4, Section 2.11) and are presented as mean values \pm SEM ($n=5$). (A) CCT for cell lines with MTX selection, (B) CCT for cell lines without MTX selection. ■ =UCOE cell lines early generation, ■ =UCOE cell lines late generation; ▨ =non-UCOE cell lines early generation, ▨ =non-UCOE cell lines late generation. * indicates $p < 0.05$, using independent samples t -test to compare UCOE and non-UCOE cell lines (on the same day of batch culture). * indicates $p < 0.05$, using paired samples t -test to compare early and late generation cultures (for the same group of cell lines on the same day of batch culture) (Section 2.10).

3.2.2. Effect of long-term culture on recombinant eGFP and DHFR expression

Amplified UCOE and non-UCOE cell lines were grown in the presence and absence of MTX selection over 80 days. Cells were grown in adherent culture in T75 flasks and subcultured every 2-3 days (Section 2.4.1). eGFP expression was assessed by flow cytometry (Section 2.5.7) and Western Blot analysis (Section 2.5.4). In addition to this, DHFR protein production in amplified cell lines was also analysed by Western Blotting (Section 2.5.4).

3.2.2.1. Analysis of eGFP fluorescence in amplified cell lines over long-term culture by flow cytometry

As mentioned in Section 3.1.2, for each cell line eGFP fluorescence (Figures 3.6-8) and the CV (Figure 3.9, Section 2.10) were analysed by flow cytometry (Section 2.5.7) on days 10 and 80 of long-term culture.

In contrast to the results of the non-amplified cell lines (Figure 3.2), the mean fluorescence in the amplified UCOE cell lines was significantly less than the mean fluorescence in the amplified non-UCOE cell lines over long-term culture (Figure 3.6). Furthermore, there was no difference between the mean CV values of each group during prolonged culture (Figure 3.9), where the initial UCOE cell lines showed significantly lower CVs compared to the non-UCOE cell lines (Figure 3.2B).

In the presence of MTX, eGFP fluorescence remained relatively constant in 3 out of 5 UCOE cell lines, whereas a decrease was observed in the late generation of U2 cell line and U4 cell line (Figure 3.6A). 3 non-UCOE cell lines showed a decrease in eGFP fluorescence after 80 days. Moreover, GFP fluorescence increased in the N1 cell line after 80 days and was stable in the N2 cell line throughout long-term culture (Figure 3.6A). The overall mean fluorescence for each group displayed no significant difference in the level of eGFP between the start of the culture and after 80 days of long-term culture, for both UCOE and non-UCOE cell lines when MTX was present (Figure 3.6A). However, in the

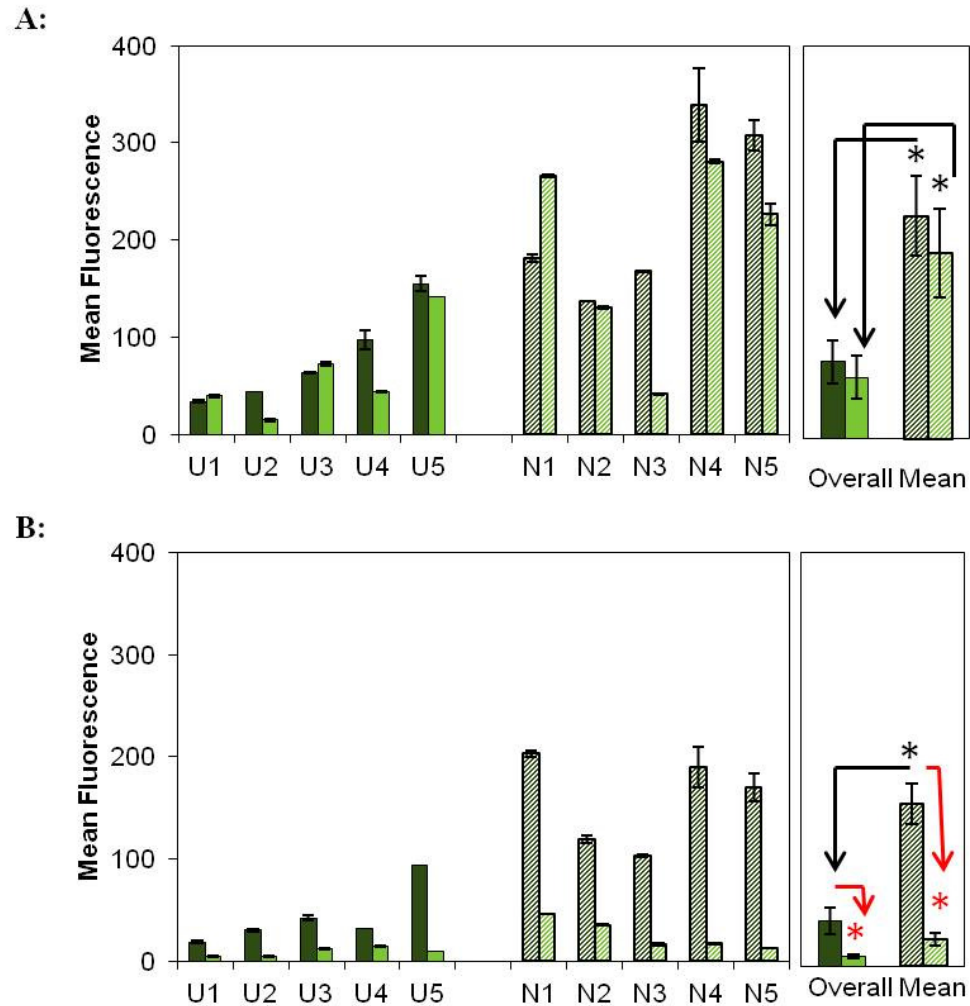
absence of MTX all cell lines tested showed a progressive loss of eGFP fluorescence throughout long-term culture (Figure 3.6B). This was also reflected in the overall mean fluorescence of each group. Values for the % decrease were calculated by comparing the results obtained from cell lines 10 and 80 days after MTX removal to the results of early generation (day 10) cell lines with MTX selection. The results showed a 44% loss of eGFP fluorescence in the early generation UCOE cell lines without MTX selection and only less than 12% of initial fluorescence remained at the end of long-term culture. The overall mean fluorescence of the early generation non-UCOE cell lines declined by 30% in the absence of MTX. The loss of fluorescence was >88% after 80 days without MTX (Figure 3.6B). The results achieved by flow cytometry indicate that eGFP expression (as determined by fluorescence) is unstable in non-UCOE and UCOE cell lines in the absence of MTX, whereas, for both cell line backgrounds, a relative stability of expression in the presence of MTX.

Histograms obtained from each cell line over long-term culture are compared in Figures 3.7 and 3.8 to show how eGFP expression changed within populations of cells. Cell lines U1, U2, U3 and U5 displayed a more spread eGFP fluorescence profile over time after removal of MTX. This suggests a more heterogeneous population at the end of long-term culture, which is reflected by a higher CV in the late generation without MTX selection (Figures 3.7 and 3.9). This may indicate that in these cell lines, all cells within the population lost eGFP fluorescence but at a different rate. The U4 cell line lost eGFP expression but showed no change in CV, which resulting in a histogram shifted to the left, suggesting that all cells displayed a decrease in eGFP fluorescence at an equal rate (Figures 3.7 and 3.9). In addition to the spreading (N1, N4 and N5) and shift (N2) patterns, the N3 cell line showed a more pronounced peak in the cell population at late generation with a decrease in variance over long-term culture in the absence of MTX (Figure 3.8 and 3.9). This suggests that the population of cells are moving from varied eGFP expression to one where cells do not express eGFP.

The effect of long-term culture on CV values for each cell line is shown in Figure 3.9. Although the mean CV of each group shows no difference between the start and end of

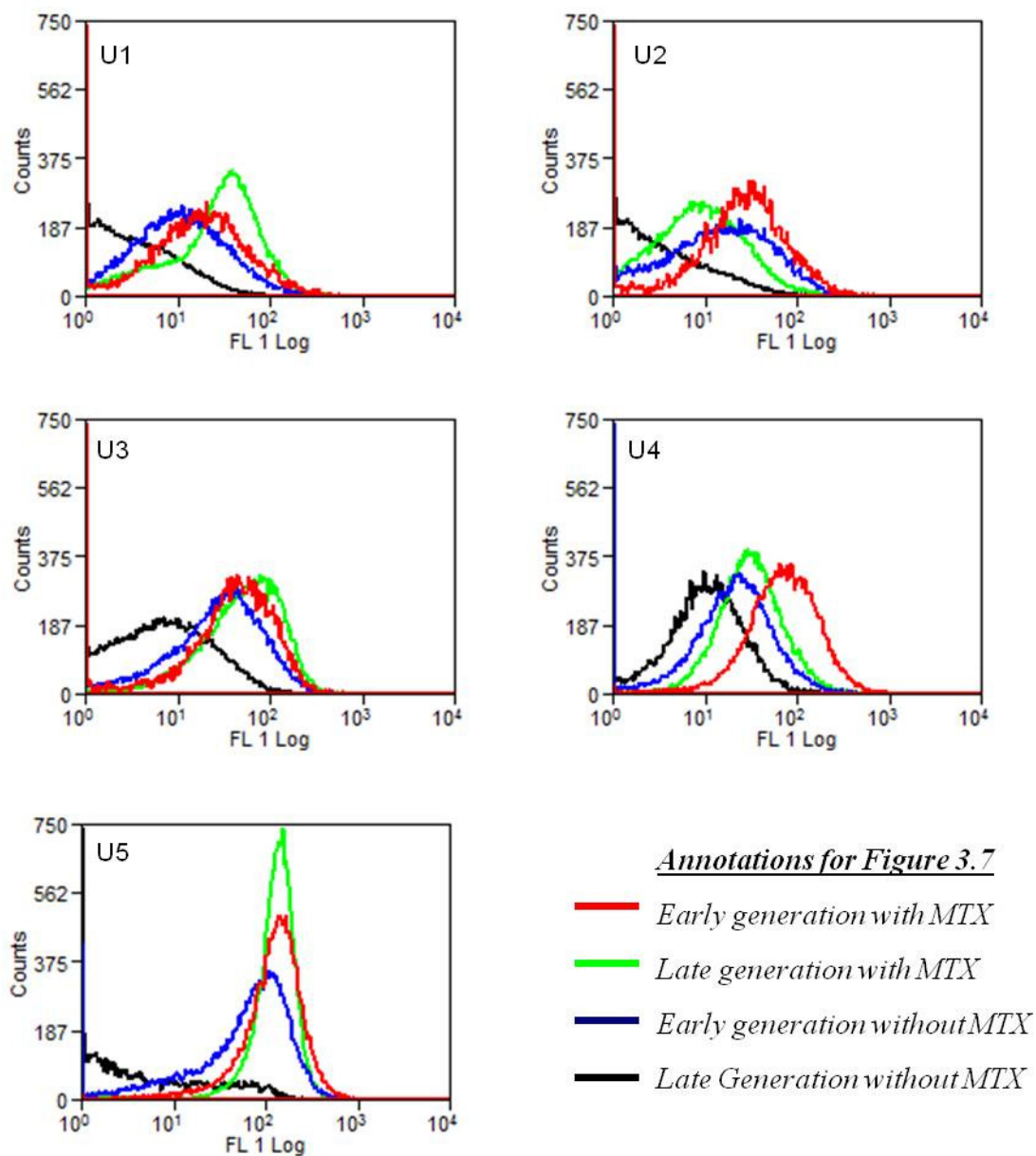
prolonged culture in the presence of MTX, CVs are affected by long-term culture as some cell lines responded differently. Among UCOE cell lines, the U2 cell line showed a change in CV over time, whereas CV was stable in the U4 cell line. The remaining UCOE cell lines displayed a decrease in CV over long-term culture, which was the same for the non-UCOE cell lines as it was only the N3 cell line that experienced an increase over time in CV. The remaining non-UCOE cell lines showed a decrease over time, which was similar to the UCOE cell lines. After MTX removal, a significant increase in mean CV was observed in both the UCOE and non-UCOE group. However, there were some exceptions such as the U4 and N2 cell line in which CV remained stable over time. Similarly, the N3 cell line showed a decrease over 80 days without MTX selection.

Figure 3.6: eGFP fluorescence in amplified cell lines over long term culture, in the presence and absence of MTX selection.



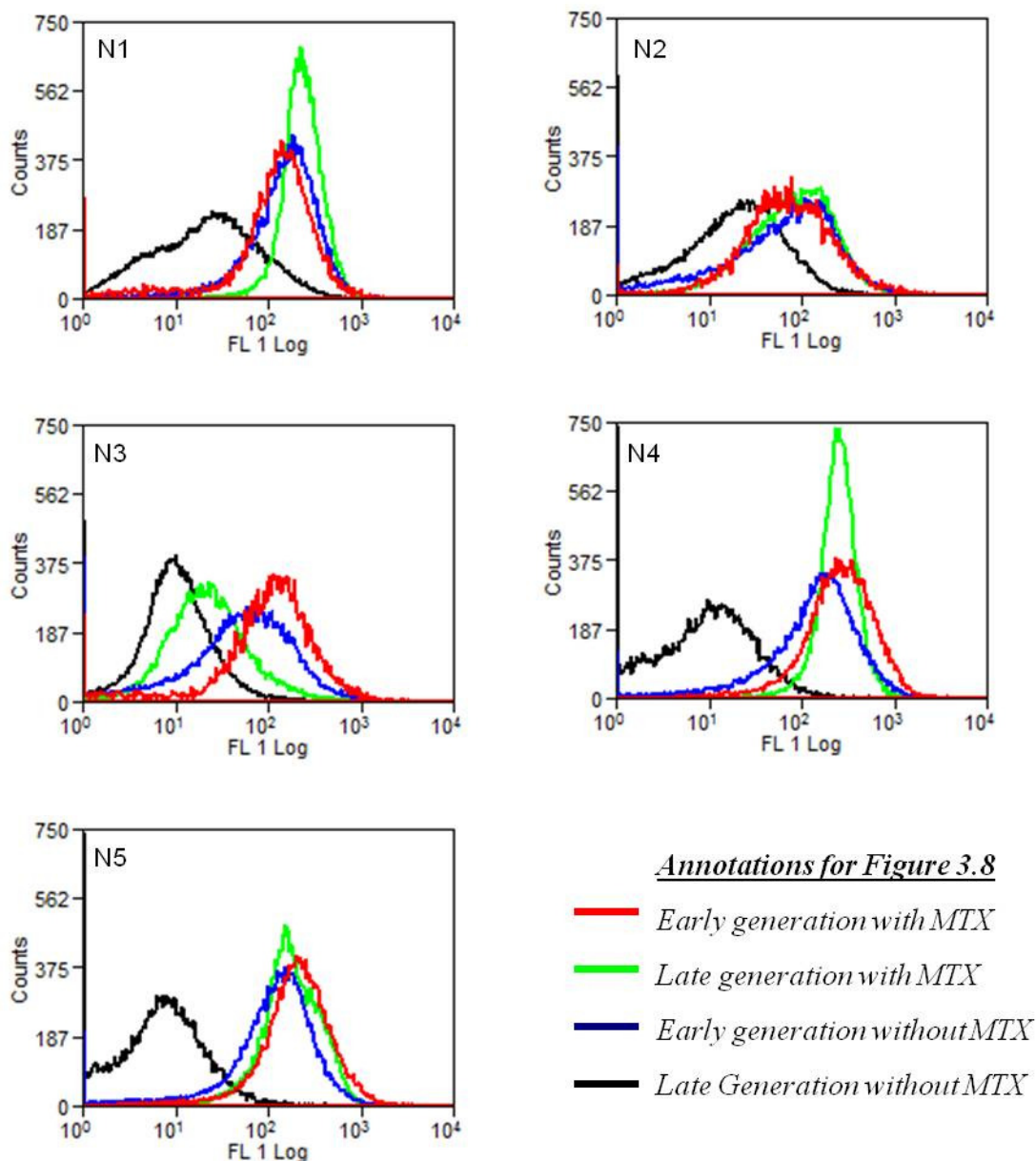
GFP fluorescence were measured in day 10 and day 80 as described in Figure 3.2. Cells were grown either with or without MTX selection. (A) GFP fluorescence for individual cell lines in the presence of MTX. (B) GFP fluorescence for individual cell lines without MTX selection. ■ = UCOE day 10, ■ = UCOE day 80, ▨ = non-UCOE day 10, ▨ = non-UCOE day 80. Values are quoted \pm SD ($n=3$). Overall mean values are quoted \pm SEM ($n=5$). * indicates $p < 0.05$, using independent samples t -test to compare UCOE and non-UCOE cell lines (at the same time of long-term culture). * indicates $p < 0.05$, using paired samples t -test to compare early and late generation cultures (for the same group of cell lines) (Section 2.10).

Figure 3.7: Flow cytometry histograms of amplified UCOE cell lines over long-term culture.



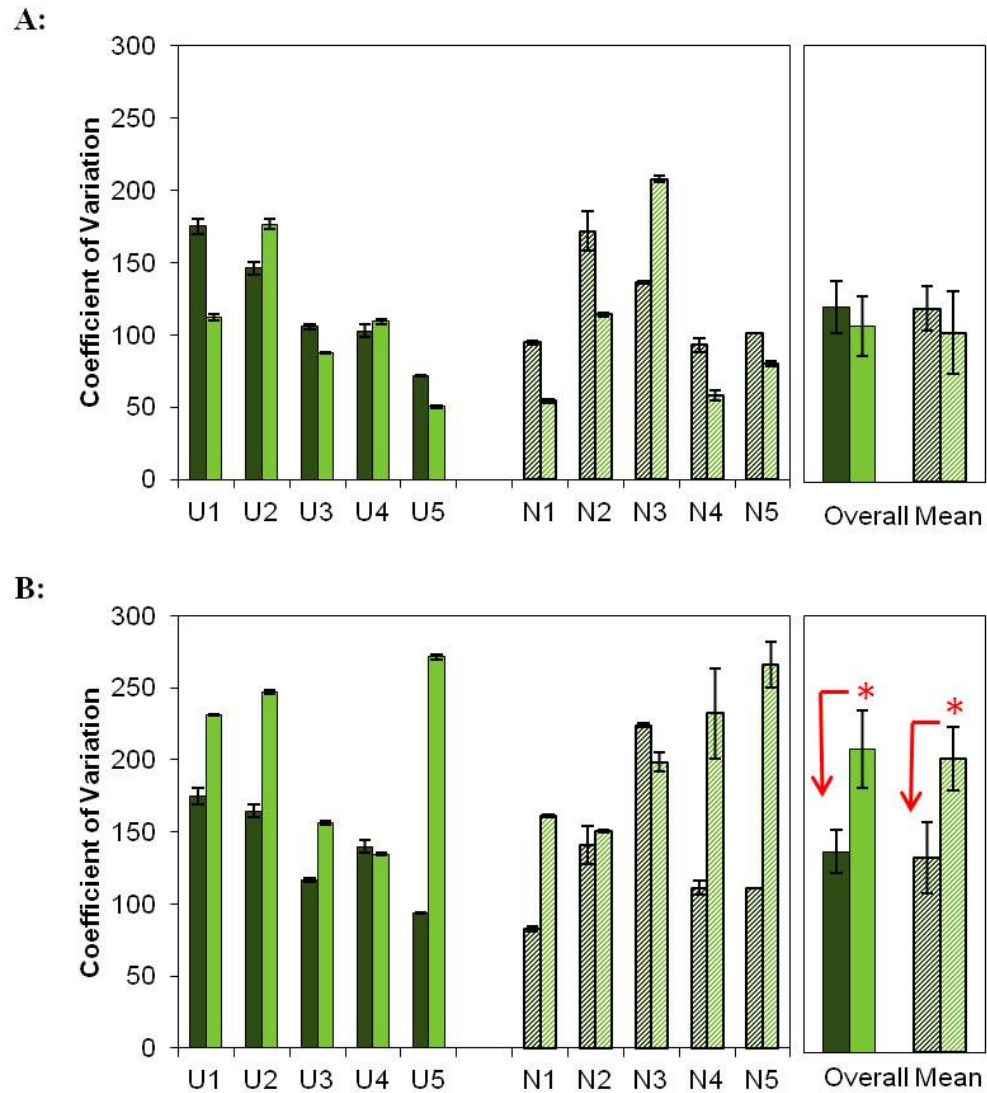
Experimental details are described in the legend to Figure 3.2. Histograms obtained from the UCOE cell lines over long term culture study.

Figure 3.8: Flow cytometry histograms of amplified non-UCOE cell lines over long term culture.



Experimental details are described in the legend to Figure 3.2. Histograms obtained from the non-UCOE cell lines over long-term culture study.

Figure 3.9: Effect of long term culture on the degree of variation in eGFP fluorescence in amplified cell lines.



Experimental details are described in Figure 3.2. Cells were grown either with or without MTX selection. CVs are calculated as described in Section 2.10. (A) CVs for individual cell lines in the presence of MTX. (B) CVs for individual cell lines cultured without MTX selection ■ = UCOE day 10, ■ = UCOE day 80, ▨ = non-UCOE day 10, ▩ = non-UCOE day 80. Values are quoted \pm SD ($n=3$) Overall mean values are quoted \pm SEM ($n=5$),

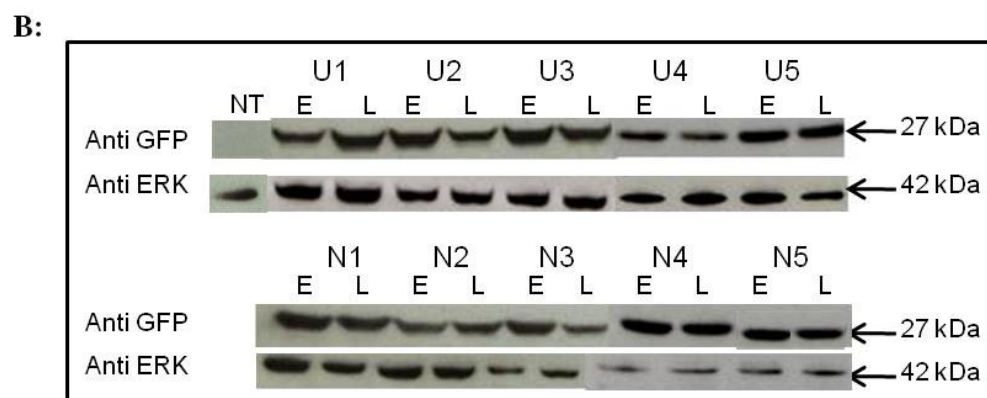
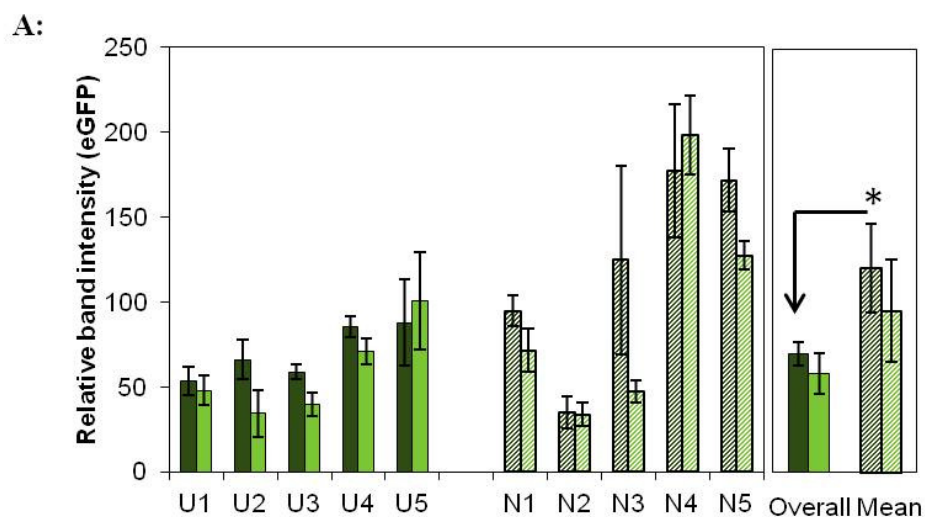
* indicates $p < 0.05$, using paired samples t -test to compare early and late generation cultures (for the same group of cell lines) (Section 2.10).

3.2.2.2. Analysis of GFP and DHFR protein expression over long term culture by Western Blot

In parallel to the assessment of eGFP fluorescence by flow cytometry, recombinant eGFP (Figures 3.10-12) and DHFR protein production (Figures 3.13 and 3.14) were assessed by Western blotting (Section 2.5.4).

The band intensities for individual cell lines showed that the eGFP production was stable over 80 days in U1, U4 and U5 cell lines, whereas a slight decrease was observed in U2 and U3 cell lines. 3 of the non-UCOE cell lines also demonstrated constant eGFP production throughout long-term culture, while the N3 and N5 cell lines experienced a loss of eGFP production at the end of prolonged culture (Figure 3.10A and B). The overall mean of eGFP production was similar at the start and end of long-term culture for both UCOE and non-UCOE cell lines. Furthermore, in agreement with the flow cytometry analysis, the mean eGFP expression determined by western blotting was significantly higher in non-UCOE cell lines compared to UCOE cell lines at the beginning of long-term culture. Although the overall eGFP expression was also higher at the end of prolonged culture, this difference was not statistically significant (Figure 3.10A). In accordance with the results obtained from flow cytometry analysis, all cell lines showed a loss of eGFP production over long-term culture in the absence of MTX (Figure 3.11). The loss of eGFP expression was reflected in the overall mean of each group, where a decrease of 44% was observed in the UCOE cell lines 10 days after MTX removal, which decreased further by approximately 85% at the end of long-term culture when compared to early generation cell lines in the presence of MTX. Similar to this, non-UCOE cell lines also showed an initial 29% loss of eGFP production and continued to decline by over 82% by the end of prolonged culture (values for % decrease were calculated by comparing the results obtained from cell lines 10 and 80 days after MTX removal to the results of early generation (day 10) cell lines with MTX selection.). Mean fluorescence is plotted against the results obtained from Western blot analysis, which showed a positive correlation (Figure 3.12).

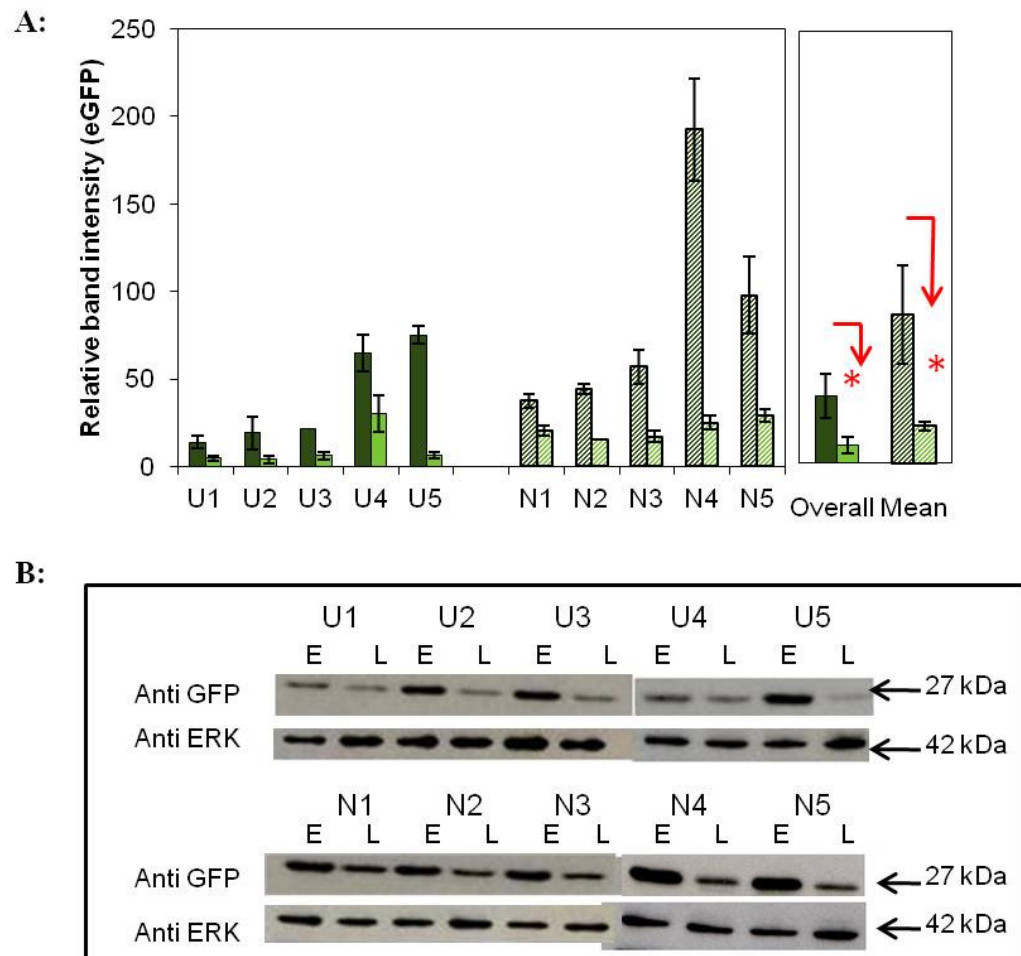
Figure 3.10: Western blot assessment of eGFP expression in amplified cell lines over long-term culture in amplified clones, in the presence of MTX selection.



Cell lines were cultured for 80 days as described in Figure 3.3 (Section 2.4.1) Cells were sub-cultured every 2-3 days in the presence of MTX and eGFP expressions were measured on day 10 and day 80 by western blot analysis (Section 2.5.4). ERK is used as a loading control. (A) Relative intensity of eGFP bands, as determined by densitometric analysis normalized to ERK. ■ = UCOE day 10, ■ = UCOE day 80, ▨ = non-UCOE day 10, ▨ = non-UCOE day 80. Values are quoted \pm range ($n=2$), overall mean values are quoted \pm SEM ($n=5$). (B) eGFP expression for individual cell lines is shown: Lane E=Early generation (day 10), Lane L= Late generation (day 80), NT= non transfected CHO-DG44.

* indicates $p < 0.05$, using independent samples t-test to compare UCOE and non-UCOE cell lines (at the same time of long-term culture). (Section 2.10).

Figure 3.11: Western blot assessment of eGFP expression in amplified cell lines over long-term culture in amplified clones, without MTX selection.



Experimental details explained in Figure 3.10 but with cell lines cultured without MTX selection. (A) Relative intensity of eGFP bands, as determined by densitometric analysis normalized to ERK.

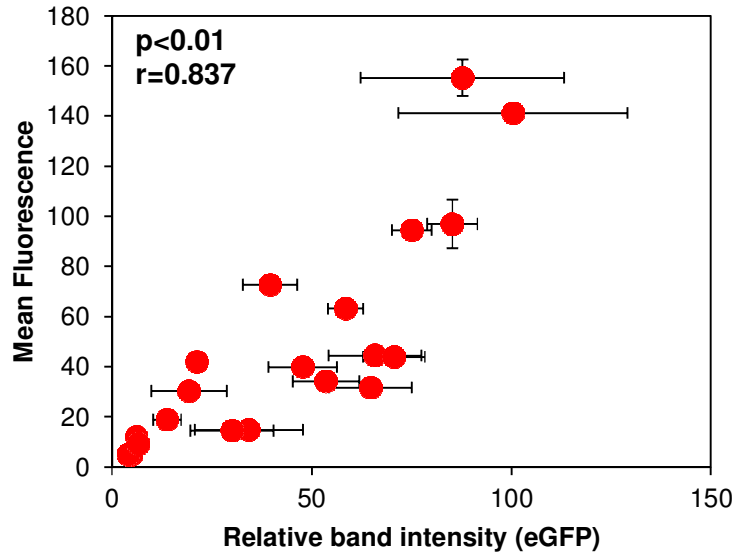
■ = UCOE day 10, □ = UCOE day 80, ▨ = non-UCOE day 10, ▩ = non-UCOE day 80. Values are quoted \pm range ($n=2$), overall mean values are quoted \pm SEM ($n=5$).

(B) GFP expression for individual cell lines is shown: Lane E=Early generation (day 10), Lane L=Late generation (day 80).

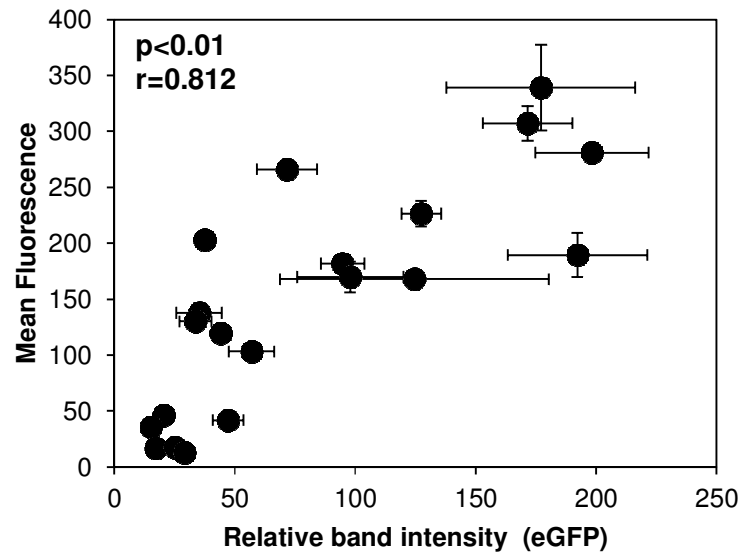
* indicates $p < 0.05$, using paired samples *t*-test to compare early and late generation cultures (for the same group of cell lines) (Section 2.10).

Figure 3.12: Comparison of eGFP expression detected by flow cytometry against by western blotting.

A:



B:



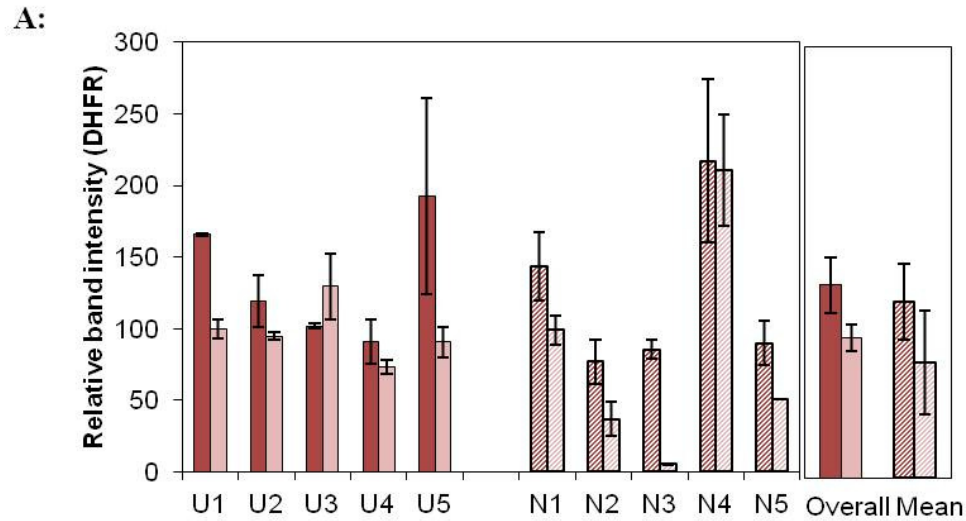
eGFP expression was determined by flow cytometry (Section 2.5.7, Figure 3.6, 3.10-11) and western blotting (Section 2.5.4). *eGFP* fluorescence is plotted against densitometer values for individual cell lines. (A) ● UCOE, (B) ● non-UCOE cell lines. Correlation coefficients and statistical significance are indicated in the top left of the scatter plots.

As growth analysis showed that the peak cell densities were higher in UCOE cell lines compared to non-UCOE cell lines in the presence of MTX, Western blotting was performed for DHFR protein production to examine whether this was as a result of the difference in DHFR expression (Figures 3.13-14).

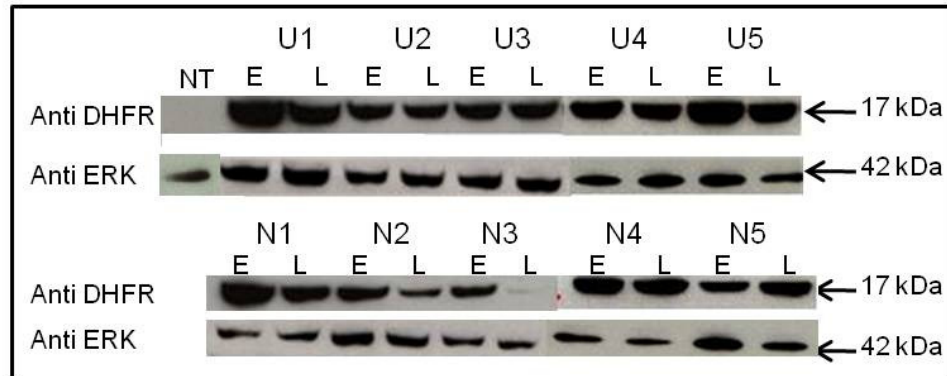
DHFR expression decreased over long-term culture in U1 and U5 cell lines in the presence of MTX selection whereas it was relatively constant in the other 3 UCOE cell lines (Figure 3.13). The mean values of DHFR expression in UCOE cell lines showed a decrease over long-term culture but it was not statistically significant. Moreover, DHFR expression was similar in all UCOE cell lines. In contrast, a variable DHFR expression was observed in non-UCOE cell lines. Furthermore, a decrease in DHFR expression was observed for all non-UCOE cell lines with the exception of N4 cell line in the presence of MTX, which was reflected in the mean values. However, the difference in the means was not statistically significant (Figure 3.13).

A decrease in the intensity of the bands corresponding to DHFR for both UCOE and non-UCOE cell lines maintained in the absence of MTX was clearly visible from Western blot analysis (Figure 3.14B). All cell lines tested showed a loss of DHFR expression after MTX removal (Figure 3.14A and B). The results of the early and late generation cell lines in the absence of MTX were compared with the results from the early generation cell lines maintained with MTX (Mean [M]=134 ±19.5). UCOE cell lines lost 69% of their DHFR expression on day 10 in the absence of MTX (M=40.7 ±13) whereas the decrease was up to 92% after 80 days (M=10.5 ±3). The decrease was more dramatic in non-UCOE cell lines where cell lines lost 77% of DHFR expression within 10 days without MTX selection (M=28.5 ±12.9) with a 97% decrease after 80 days (M=3.6 ±0.7, Figure 3.14).

Figure 3.13: Western blot assessment of DHFR expression in amplified cell lines over long term culture in the presence of MTX selection.



B:

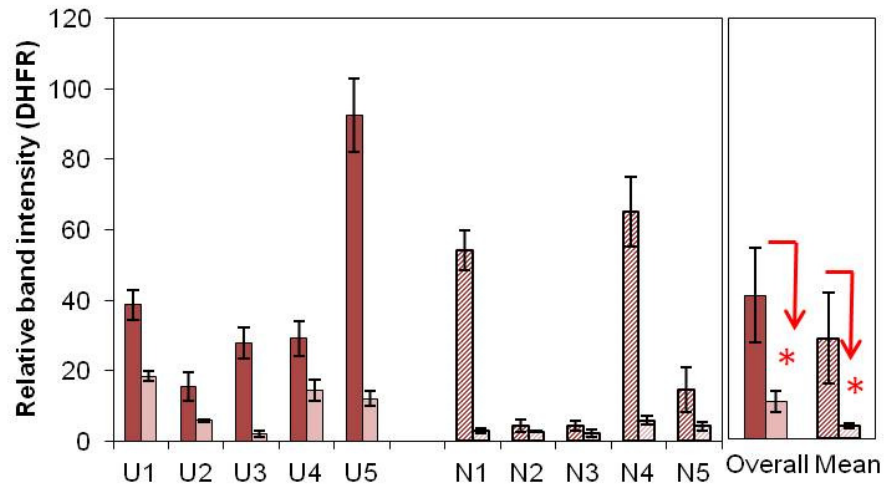


Experimental details explained in the legend to Figure 3.10. ERK is used as a loading control. (A) Relative band intensities of DHFR protein were quantitated and normalized to ERK.

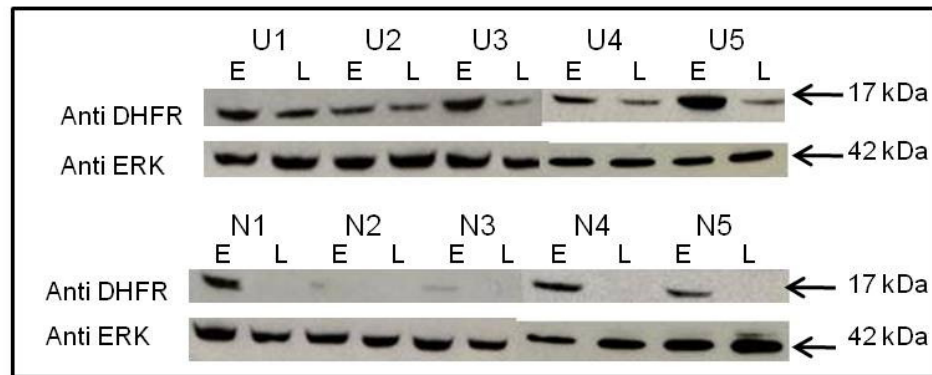
■ = UCOE day 10, ▨ = UCOE day 80, ▩ = non-UCOE day 10, ▪ = non-UCOE day 80. Values are quoted \pm range ($n=2$), overall mean values are quoted \pm SEM ($n=5$) (Section 2.10). (B) DHFR expression for individual cell lines is shown: Lane E=Early generation (day 10), Lane L= Late generation (day 80), NT= non-transfected CHO-DG44.

Figure 3.14: Western blot assessment of DHFR expression in amplified cell lines over long-term culture without MTX selection.

A:



B:



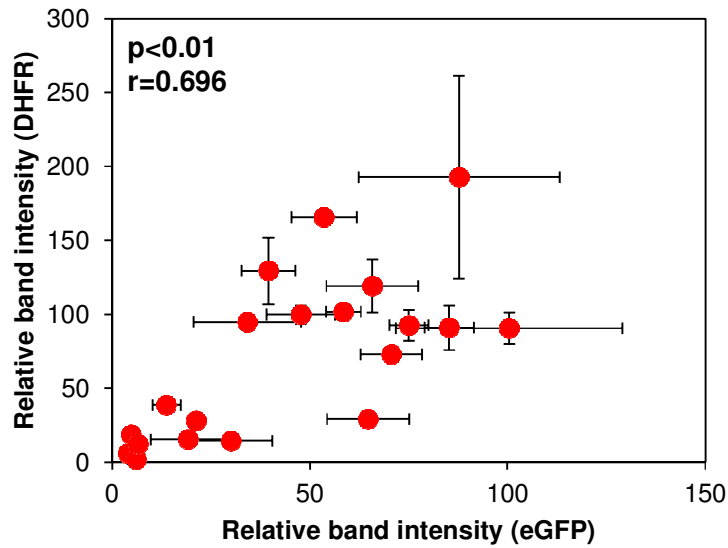
Experimental details explained in the legend to Figure 3.10 but with cell lines cultured without MTX selection ERK is used as a loading control. (A) Relative band intensities of DHFR protein were quantified and normalized to ERK. ■ = UCOE day 10, □ = UCOE day 80, ▨ = non-UCOE day 10, ▩ = non-UCOE day 80. Values are quoted \pm range ($n=2$), overall mean values are quoted \pm SEM ($n=5$). (B) DHFR expression for individual cell lines is shown: Lane E=Early generation (day 10), Lane L=Late generation (day 80).

* indicates $p < 0.05$, using paired samples t -test to compare early and late generation cultures (for the same group of cell lines) (Section 2.10).

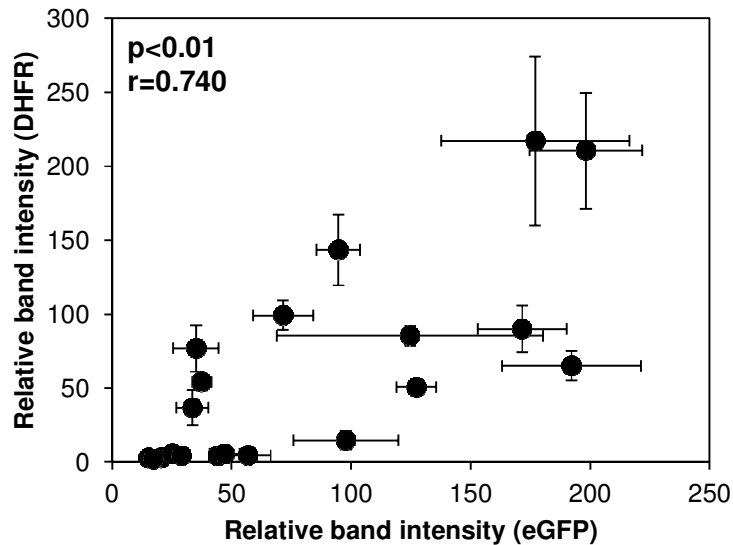
Since CHO cells were transfected with the bi-cistronic expression vectors coding for eGFP and DHFR proteins in a single transcription unit (Appendix 2), it was expected that DHFR protein and eGFP protein would show a coupled and, hence, parallel pattern of expression. A moderate positive correlation was found between the expressions of these two proteins (Figure 3.15). However, the pattern of expression was different. For example, although eGFP expression was significantly higher in the non-UCOE cell lines compared with the UCOE cell lines (Figures 3.6 and 3.10), DHFR protein expression was similar (Figures 3.13 and 3.14). One possible explanation for the different levels of eGFP and DHFR protein expression is that translation process of DHFR is facilitated by an Internal Ribosomal Entry Site (IRES) and eGFP expression by cap-dependent translation. It has been shown that IRES mediated translation is frequently used during stress conditions (Spriggs et al., 2010). Although UCOE and non-UCOE cell lines may have the same amount of DHFR protein, it was shown in Section 3.2.1 that UCOE cell lines exhibit higher viable cell numbers in the presence of MTX, and this suggested that UCOE cell lines may have higher tolerance to MTX than non-UCOE cell lines.

Figure 3.15: Comparison of eGFP against DHFR protein expression.

A:



B:



GFP and DHFR protein expression were determined by Western blotting (Section 2.5.4, Figure 3.10-14)). Densitometer values of eGFP and DHFR for individual cell lines are plotted against each other.

(A) ● UCOE, (B) ● non-UCOE cell lines.

Correlation coefficients and statistical significance are indicated in the top left of the scatter plots.

3.2.3. Copy number analysis over long-term culture by qPCR

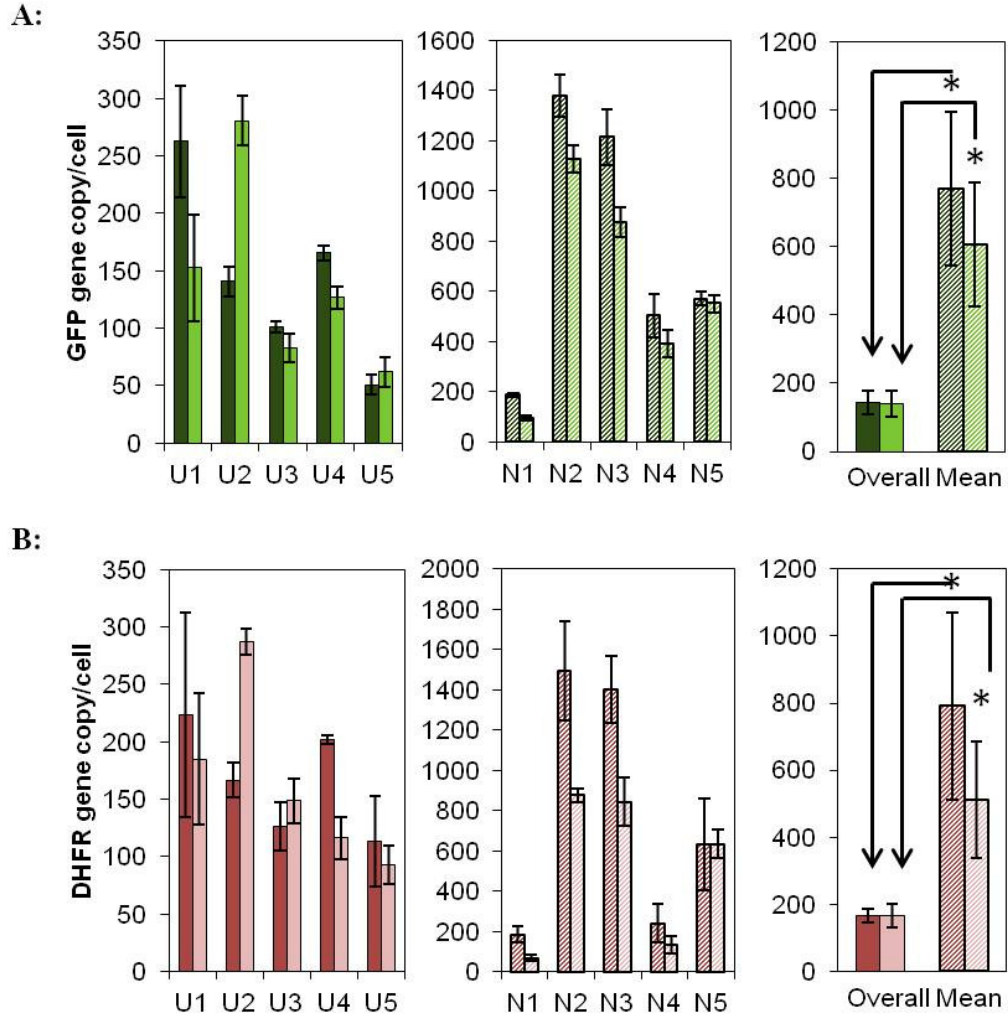
It has been shown so far that all cell lines displayed loss of eGFP and DHFR expression over long-term culture when MTX selection was removed (Figures 3.7, 3.12, 3.15). To further investigate the reason for the instability observed during long-term culture, plasmid copy numbers were analysed for individual cell lines. Samples were taken at the beginning (day 10) and at the end of long term culture (day 80) from cell lines growing either with or without MTX selection. qPCR experiments were performed for plasmid copy number determination (Section 2.7.2).

Using a stepwise MTX amplification strategy, a number of cell lines that contained up to 1000 transfected plasmid copies were produced in previous studies (Pallavicini et al., 1990, Wurm et al., 1986, Kim et al., 1998a). Non-UCOE cell lines used in this study had between 185 and 1400 copies of the eGFP and DHFR genes/cell, whereas the UCOE cell lines contained 50 to 260 plasmid copies per cell. Therefore, gene copy numbers in non-UCOE cell lines were significantly higher than the UCOE cell lines in all conditions (Figure 3.16 and 3.17), which suggests that the higher eGFP expressions observed in the non-UCOE cell lines may be due to higher gene copy numbers.

An increase in plasmid copy numbers was observed in the U2 cell line in the presence of MTX, which was not reflected in protein production (Figure 3.16A and B). Furthermore the U4, N1, N2 and N3 cell lines growing with MTX selection showed a decrease in plasmid copy numbers over time (Figure 3.16A and B). Among these, only the U4 and N3 cell line lost their eGFP expression in accordance with their gene copy number. The U1 cell line also displayed a decrease in eGFP gene copy number but this was not statistically significant (Figure 3.16A). The U3, U5, N4 and N5 cell lines were stable in terms of eGFP and DHFR gene copy numbers over long-term culture in the presence of MTX (Figures 3.16A and B). The group mean values of plasmid copy numbers for eGFP and DHFR in the UCOE cell lines showed no difference over long-term culture in the presence of MTX, whereas a decrease was observed in the non-UCOE cell lines. However, this was not statistically significant (Figure 3.16). The gene copy numbers for eGFP and DHFR were

stable in the U5, N4 and N5 cell lines over long-term culture after MTX removal (Figures 3.17A and B). The remaining cell lines lost some of their eGFP and DHFR genes within 10 days in response to MTX removal when compared to the early generation cell lines in the presence of MTX. A further loss of gene copies was observed in the U1, U3 and N2 cell lines at the end of long-term culture in the absence of MTX (Figures 3.17A and B). There was no significant difference in the group mean values of eGFP and DHFR gene copy numbers over long-term culture in the absence of MTX ($p > 0.05$, using independent samples t-test to compare early and late generation cell lines [Section 2.10]).

Figure 3.16: eGFP and DHFR gene copy numbers in amplified cell lines during long-term culture in the presence of MTX selection.



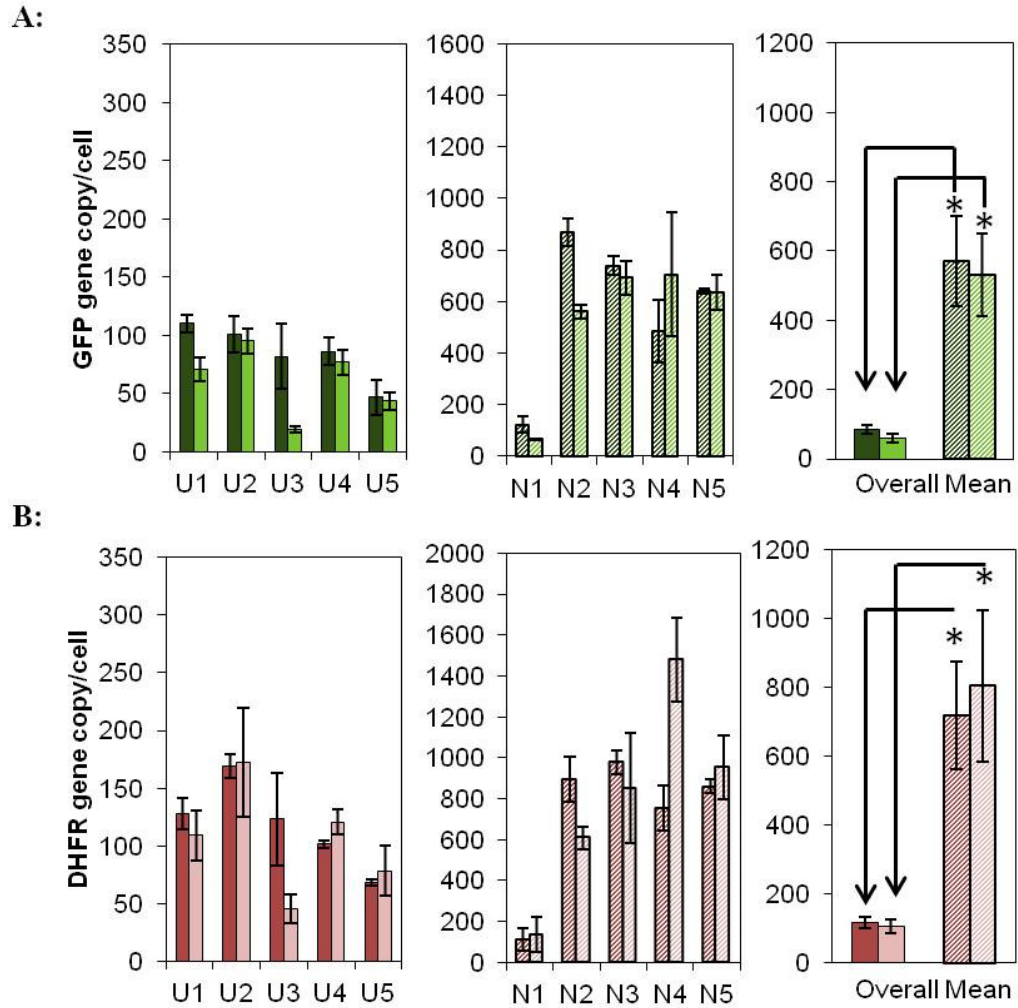
Genomic DNA were extracted at early and late generations for each clone (Section 2.7.1) and plasmid copy number was determined by qPCR (Section 2.7.2). (A) GFP gene copy numbers per cell are compared between UCOE and non-UCOE cell lines.

■ = UCOE day 10, ■ = UCOE day 80, ▨ = non-UCOE day 10, ▨ = non-UCOE day 80. (B) DHFR gene copy numbers per cell.

■ = UCOE day 10, ■ = UCOE day 80, ▨ = non-UCOE day 10, ▨ = non-UCOE day 80. Values are quoted \pm range ($n=2$), overall mean values are quoted \pm SEM ($n=5$).

* indicates $p < 0.05$, using independent samples t -test to compare UCOE and non-UCOE cell lines (at the same time of long-term culture). (Section 2.10).

Figure 3.17: eGFP and DHFR gene copy numbers in amplified cell lines during long-term culture in the absence of MTX selection.



Experimental details explained in the legend to, Figure 3.16 but with cell lines cultured without MTX selection.

(A) GFP gene copy numbers per cell are compared between UCOE and non-UCOE cell lines. ■ = UCOE day 10, ■ = UCOE day 80, ▨ = non-UCOE day 10, ▨ = non-UCOE day 80. (B) DHFR gene copy numbers per cell are shown.

■ = UCOE day 10, ■ = UCOE day 80, ▨ = non-UCOE day 10, ▨ = non-UCOE day 80. Values are quoted \pm range ($n=2$), overall mean values are quoted \pm SEM ($n=5$).

* indicates $p < 0.05$, using independent samples t -test to compare UCOE and non-UCOE cell lines (at the same time of long-term culture). (Section 2.10).

Table 3.1 shows the summary of eGFP gene copy number and protein expression in individual cell lines. The results obtained from cell lines in early generation with MTX selection were compared to the results after 10 and 80 days of MTX removal. According to these results, the declining eGFP expression observed for the U3 cell line following MTX removal was accompanied by a decrease in gene copy number. For the remaining UCOE cell lines, eGFP production decreased >40% within 10 days of MTX removal, which was comparable to the loss of the gene copy number. However, although these cell lines continued losing their eGFP expression (approximately 85% loss) after 80 days of MTX removal (Figures 3.6, 3.11, Table 3.1), eGFP gene copy numbers declined only 54% within 80 days after they were transferred to MTX-free medium (Figure 3.17A). Therefore, the loss of eGFP expression observed in these cell lines may indicate a decreased transcription via preferential loss of transcriptionally active DNA or that some gene silencing might be occurring in these cell lines.

Some of the non-UCOE cell lines showed no change in eGFP gene copy numbers although they lost >80% of their eGFP expression (i.e. N4 and N5), which strongly suggests that these cell lines are experiencing gene silencing. Despite displaying 64% and 43% loss of eGFP gene copy numbers after 80 days of MTX removal, protein production declined 78% and 86% in N1 and N3 cell lines respectively, which also may indicate that some gene silencing is taking place in these cell lines following MTX removal. Loss of eGFP production was associated with loss of the gene copy numbers in N2 cell line in the absence of MTX (Table 3.1, Figures 3.6, 3.11 and 3.17A). Therefore, no direct correlation was observed between the gene copy number and protein production in cell lines with or without UCOE in their expression constructs (Figure 3.18).

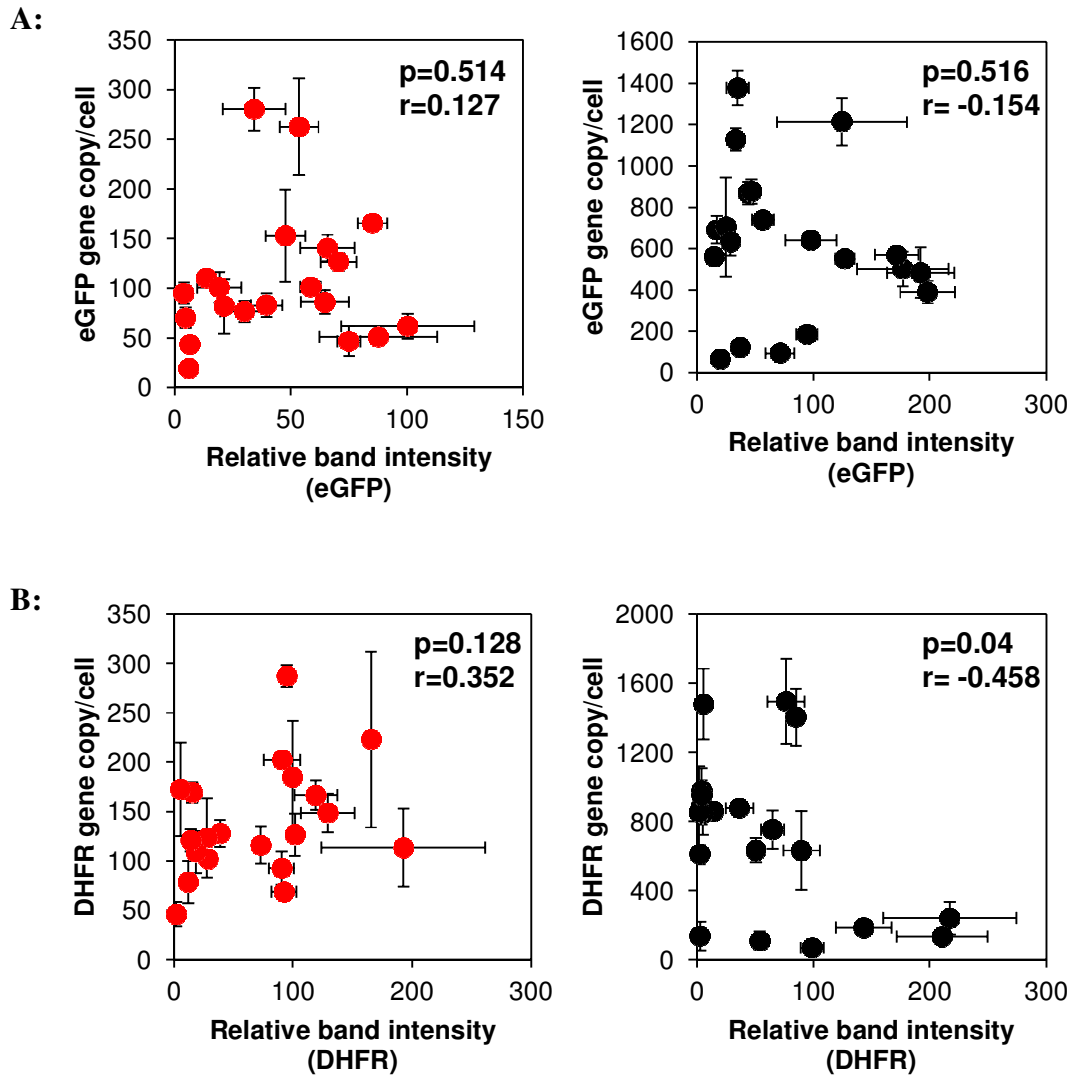
eGFP gene copy numbers were compared to DHFR gene copy numbers and the results are shown in Figure 3.19. Although eGFP and DHFR genes were in the same plasmid, not all cell lines displayed equal numbers of eGFP and DHFR gene copies after MTX amplification (Figure 3.19). However, the difference was not statistically significant ($p > 0.05$, using independent samples t-test to compare eGFP and DHFR gene copy numbers [Section 2.10]).

Table 3.1: Effect of long-term culture on eGFP gene copy number and protein expression.

	eGFP Gene Copy Number			eGFP Expression	
	Days after MTX removal	% decrease	Mean values \pm range (day 10+MTX, 10/80 -MTX)	% decrease	Mean values \pm range (day 10+MTX, 10/80 -MTX)
U1	10	58	262 \pm 49, 110 \pm 8	74.3	54 \pm 8, 14 \pm 3
	80	73.2	262 \pm 49, 70 \pm 10	91.1	54 \pm 8, 5 \pm 1.5
U2	10	28.2	141 \pm 13, 101 \pm 15	70.7	66 \pm 12, 19 \pm 9
	80	32.4	141 \pm 13, 95 \pm 11	93.9	66 \pm 12, 4 \pm 1.9
U3	10	19	101 \pm 5, 82 \pm 27	63.6	59 \pm 4, 21 \pm 0.03
	80	81	101 \pm 5, 19 \pm 2.6	89.5	59 \pm 4, 6 \pm 2.1
U4	10	47.9	165 \pm 6, 86 \pm 12	24	85 \pm 6, 65 \pm 10
	80	53.7	165 \pm 6, 77 \pm 11	64.7	85 \pm 6, 30 \pm 10
U5	10	8.3	51 \pm 8, 47 \pm 15	14.5	88 \pm 25, 75 \pm 5
	80	14.7	51 \pm 8, 43 \pm 8	92.4	88 \pm 25, 7 \pm 1.8
N1	10	33.5	185 \pm 6, 123 \pm 31	60.3	95 \pm 9, 38 \pm 4
	80	64.8	185 \pm 6, 65 \pm 1.5	78.4	95 \pm 9, 20 \pm 3
N2	10	36.9	1377 \pm 85, 868 \pm 54	-25	35 \pm 9, 44 \pm 3
	80	59.3	1377 \pm 85, 560 \pm 28	56.6	35 \pm 9, 15 \pm 0.1
N3	10	39.1	1213 \pm 113, 739 \pm 36	54.3	125 \pm 55, 57 \pm 10
	80	43	1213 \pm 113, 691 \pm 67	86.2	125 \pm 55, 17 \pm 3
N4	10	3.5	501 \pm 85, 483 \pm 122	-8	177 \pm 39, 192 \pm 29
	80	-40	501 \pm 85, 704 \pm 240	85.8	177 \pm 39, 25 \pm 4
N5	10	-12	569 \pm 27, 640 \pm 10	42.9	171 \pm 19, 99 \pm 22
	80	-11	569 \pm 27, 633 \pm 68	83.1	171 \pm 19, 29 \pm 3

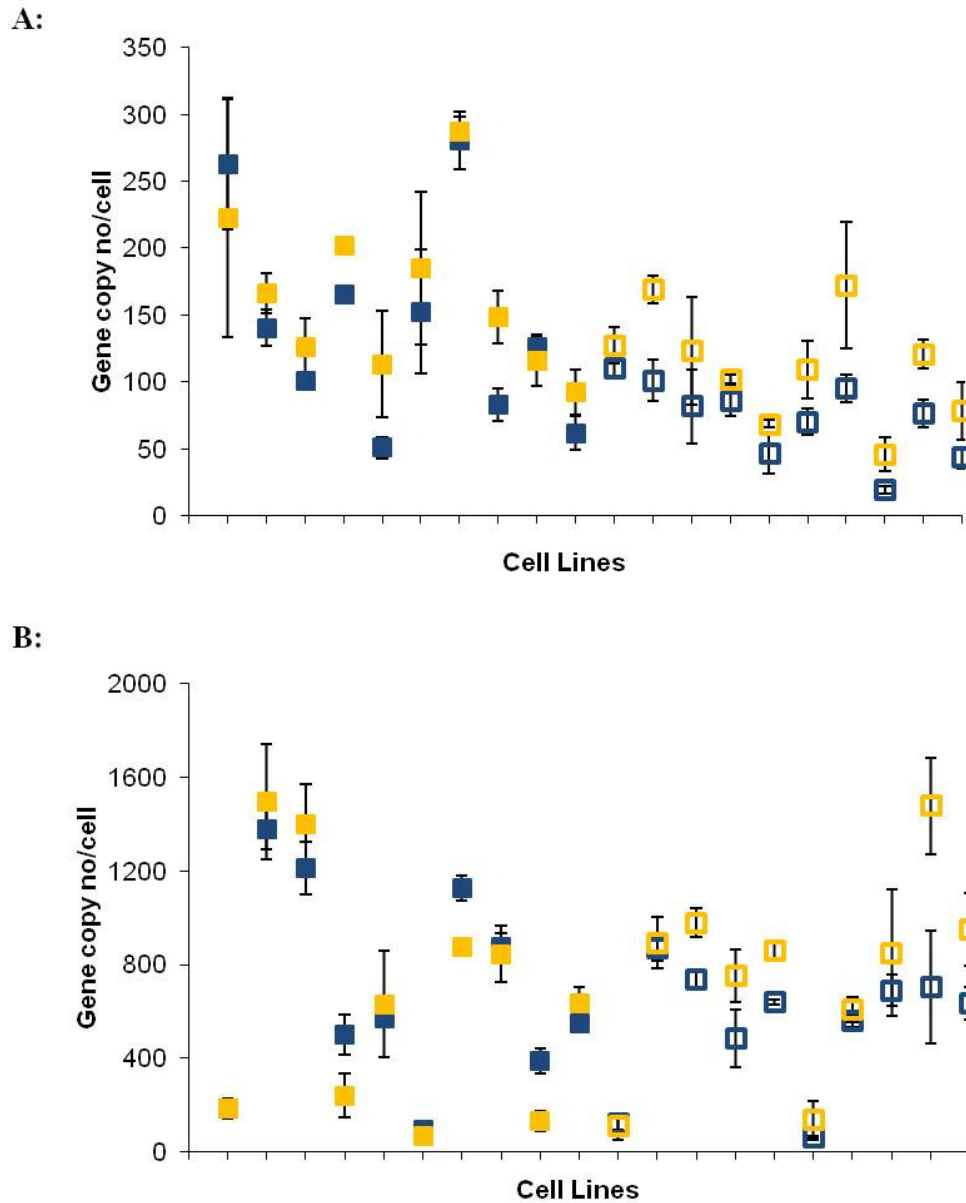
Summary of eGFP gene copy number and protein expression detected by western blotting during long-term culture for individual cell lines are shown (Figures 3.10, 3.11, 3.16 and 3.17). Values for % decrease were calculated by comparing the results obtained from cell lines 10 and 80 days after MTX removal to the results of early generation (day 10) cell lines with MTX selection.

Figure 3.18: Comparison of protein expression against plasmid copy number.



Plasmid copy numbers were determined as described in Section 2.7.2 (Figure 3.16-17), Western Blot analysis was performed to determine GFP & DHFR production (Section 2.5.4, Figure 3.10-14). Protein expression is plotted against gene copy numbers for individual cell lines. (A) GFP gene copy number vs GFP production, (B) DHFR gene copy number vs DHFR protein production. ● =UCOE, ● =non-UCOE cell lines. Correlation coefficients and statistical significance are indicated in the top right of the scatter plots.

Figure 3.19: Comparison of eGFP and DHFR gene copy numbers.



Plasmid copy numbers were determined as described in Section 2.7.2 (Figure 3.16-17) eGFP gene copy numbers are plotted against DHFR gene copy numbers for individual cell lines in all conditions. (A) eGFP vs DHFR gene copy numbers in UCOE cell lines, (B) eGFP vs DHFR gene copy numbers in non-UCOE cell lines. Filled shapes represent cell lines in the presence of MTX, empty shapes indicates cell lines without MTX selection. ■ □ =eGFP gene copy numbers, ■ □ =DHFR gene copy numbers.

3.2.4. Analysis of mRNA expression over long-term culture in amplified CHO-GFP cell lines

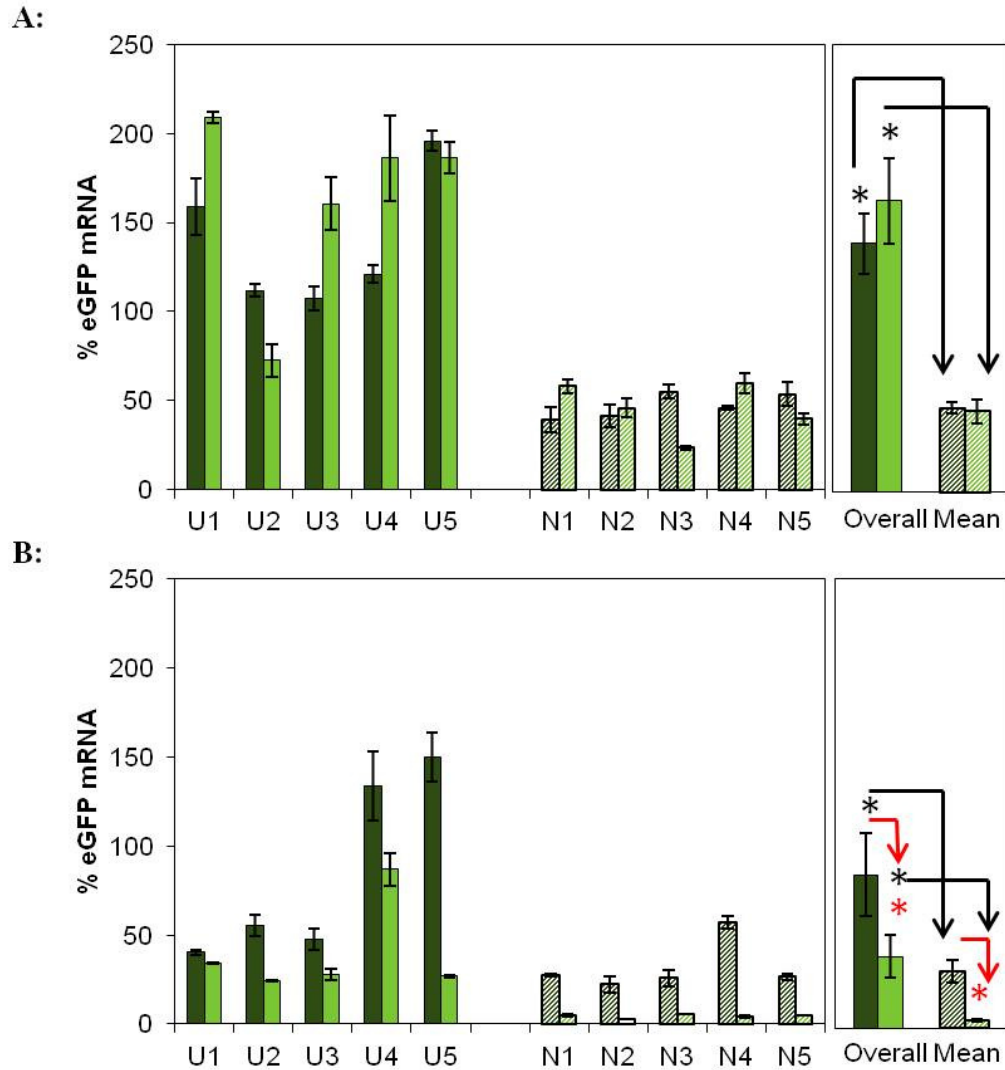
All cell lines showed a continuous decrease in recombinant eGFP and DHFR protein production in the absence of MTX and although some cells showed a decline in gene copy numbers, the decrease in gene copy number was not proportional to the protein expression. Therefore, it was necessary to confirm the effect of long-term culture and removal of MTX on expression of eGFP and DHFR at mRNA level. Consequently, RNA samples were taken at the beginning and at the end of long-term culture and analysed by q-RT PCR (Section 2.6.5).

Although the non-UCOE cell lines had a significantly higher numbers of eGFP gene copies/cell when compared to the UCOE cell lines (Figures 3.16 and 3.17), this was not reflected in the eGFP mRNA expression. The amount of eGFP mRNA was found to be significantly higher in the UCOE cell lines than non-UCOE cell lines both in the presence and absence of MTX (Figure 3.20). These findings suggest that UCOE provides a higher transcriptional activity for the eGFP gene. However, the low level of eGFP production in the UCOE cell lines may indicate that the high level of eGFP mRNA causes saturation of the translational capacity.

An increase in eGFP mRNA was observed in the U1, U3 and U4 cell lines in the presence of MTX but this was not reflected in the eGFP expression. The U2 cell line displayed a decrease in eGFP mRNA whereas eGFP mRNA was constant in the U5 cell line over long-term culture in the presence of MTX (Figure 3.20A). The non-UCOE cell lines showed relatively stable eGFP mRNA expression in the presence of MTX throughout prolonged culture with the exception of the N3 cell line, which lost its mRNA copies over time (Figure 3.20A). In the absence of MTX, all cell lines showed a decrease in eGFP mRNA expression over the course of the culture, which was reflected by the mean values of each group (Figure 3.20B). The differing amounts of eGFP mRNA expression were similar to the differences in eGFP protein expression detected during prolonged culture. To calculate the % decrease for individual cell lines, early and late generations in the absence of MTX

selection were compared to the cell lines at early generation with MTX. Despite the eGFP gene copy number remaining relatively constant in the N4 and N5 cell lines and up to a 40% loss in the N1, N2, N3 cell lines, all early generation non-UCOE cell lines lost >30% of their eGFP mRNA expression in the absence of MTX compared to the cell lines with MTX selection. This loss of eGFP mRNA was approximately 90% at the end of long-term culture in the absence of MTX. Therefore, the very low amount of eGFP production by the end of long term culture could not solely be as a result of gene copy loss, suggesting some gene silencing is occurring in these cell lines.

Figure 3.20: Analysis of eGFP mRNA expression over long-term culture in amplified cell lines.



*eGFP mRNA expression was measured on day 10 and day 80 by q-PCR (Section 2.6). (A) Relative eGFP mRNA expression in the presence of MTX. (B) Relative eGFP mRNA expression in the absence of MTX. ■ = UCOE day 10, ■ = UCOE day 80, ▨ = non-UCOE day 10, ▨ = non-UCOE day 80. Values are quoted \pm SD ($n=3$), overall mean values are quoted \pm SEM ($n=5$). * indicates $p < 0.05$, using independent samples *t*-test to compare UCOE and non-UCOE cell lines (at the same time of long-term culture), * indicates $p < 0.05$, using paired samples *t*-test to compare early and late generation cultures (for the same group of cell lines) (Section 2.10).*

Figure 3.21 summarizes the results of eGFP gene copy number, mRNA expression and protein production in the non-UCOE and UCOE cell lines. The results show the cell lines at early generation with MTX selection compared to the cell lines after removal of MTX. The transcriptional activity was higher in the beginning of long-term culture in the N1 cell line. However, eGFP expression after 10 days of culture in MTX-free medium was 61% less than early generation cells in the presence of MTX. The difference in eGFP gene copy and mRNA content was less pronounced than protein expression (34%, 28%, respectively, suggesting that some of the remaining genes were not active after MTX removal. The difference in eGFP expression was 79% after 80 days in the absence of MTX compared to the early generation N1 cell lines with MTX selection, whereas 65% and 44% difference in eGFP gene copy and mRNA content, respectively, was observed. These data suggest that the loss of eGFP expression was partly as a result of gene copy loss in the N1 cell line. However, a less pronounced decline observed in mRNA content may indicate problems related to translation of recombinant protein (Figure 3.21A). The N2 cell line displayed the highest eGFP gene copy per cell. However, this was not reflected in eGFP expression or mRNA content suggesting a very low transcriptional activity per gene copy or that not all the genes are actively transcribed. Moreover, it was observed that the decline in eGFP expression over long-term culture was mainly due to gene copy loss in the absence of MTX selection. The N3 cell line showed a decrease in eGFP gene copies in within first 10 days after removal of MTX and this remained constant up to 80 days in the absence of MTX. However, the N3 cell line continued losing eGFP protein and mRNA expression during 80 days culture without MTX, suggesting that not all the remaining genes are transcriptionally active at the end of long term culture. For the N4 and N5 cell lines eGFP gene copies per cell were similar and remained relatively constant at all times, whereas these two cell lines showed different levels of mRNA and protein expression in the absence of MTX. For example, eGFP mRNA and protein expression did not change in the N4 cell line 10 days after removal of MTX. In contrast, the N5 cell line experienced a loss of protein and mRNA expression after 10 days of culture in the absence of MTX. Despite there being no change in gene copy number, both the N4 and N5 cell lines displayed a very low level of eGFP mRNA and protein at the end of long-term culture in the absence of

MTX, suggesting that the genes might be in a place that is susceptible to epigenetic control.

According to the results summarised in Figure 3.21B, the decrease in eGFP production in U1 cell line is mainly due to loss of eGFP gene copies. Despite having a relatively stable eGFP gene copy number, the U3 cell line showed a loss of protein production accompanied by a decrease in mRNA expression within 10 days after removal of MTX and after 80 days it lost >80% of its eGFP gene copies together with its protein production. This might indicate that the U3 cell line experienced a decrease in transcriptional activity in the first 10 days of MTX-free culture followed by a loss of gene copies within 80 days in the absence of MTX. The U2 and U4 cell lines showed similar numbers of eGFP gene copies at all points tested. However, the response of the U2 and U4 cell lines to MTX removal was different. For example, the U2 cell line displayed a gradual decrease in eGFP production along with mRNA expression suggesting that some of the remaining eGFP genes may not be transcriptionally active. Whereas the U4 cell line lost its eGFP gene copies within the first 10 days of MTX removal accompanied by a loss of protein production. After 10 days, the gene copy number remained constant for up to 80 days in the absence of MTX. However, cells continued losing their eGFP production and mRNA expression suggesting that some of the genes might be silenced over the course of culture. Although the U5 cell line had the lowest eGFP gene copy per cell displayed relatively high level of eGFP production and mRNA expression in the beginning of long-term culture. In addition, the eGFP gene copies were not changed over long-term culture in the absence of MTX. However, this cell line experienced >92% loss of eGFP along with 86% loss of eGFP mRNA within 80 days after they were transferred to MTX-free medium.

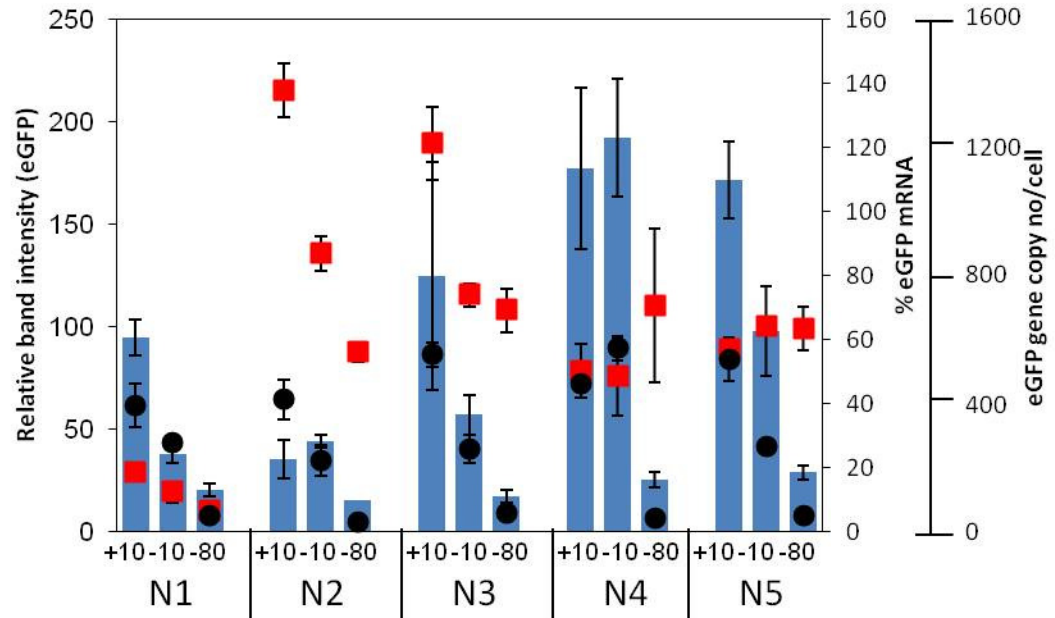
eGFP expression was detected by western blotting (Figures 3.10 and 3.11, Section 2.5.4). Plasmid copy number (Figures 3.16 and 3.17) and mRNA expression (Figure 3.20) were determined as described in Sections 2.7 and 2.6 respectively. *eGFP* expression is plotted against relative *eGFP* mRNA expression, and *eGFP* gene copy number. Results obtained from cell lines at day 10 growing with MTX (+10), day 10 (-10) and day 80 (-80) in the absence of MTX compared to each other.

(A) non-UCOE cell lines, (B) UCOE cell lines

■ =Protein, ● = mRNA, ■ =Gene copy number

Figure 3.21: Changes to the molecular characteristics of a recombinant gene system during long-term culture in the absence of MTX selection.

A:



B:

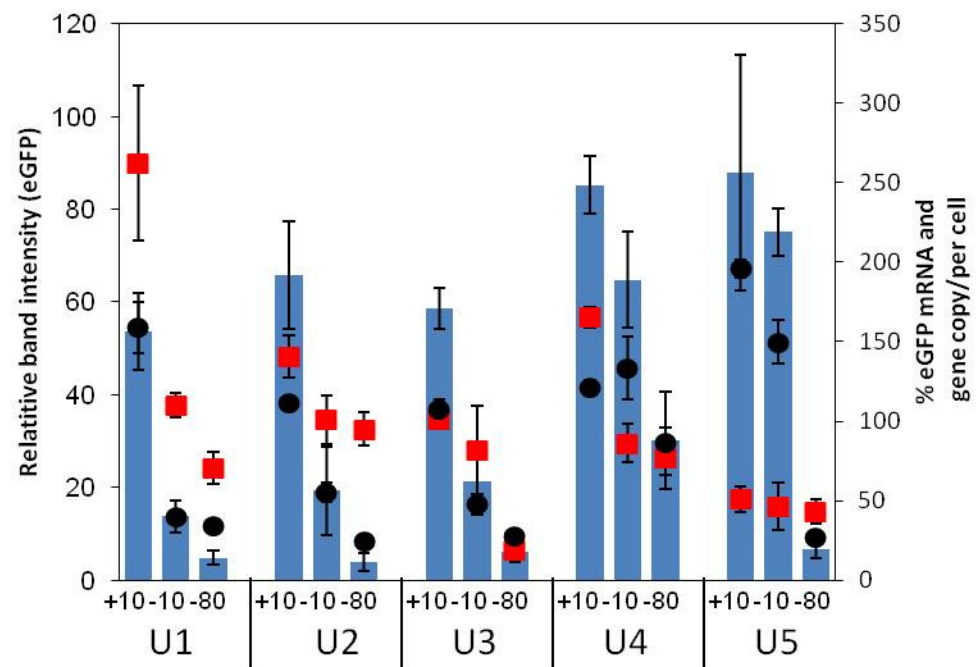
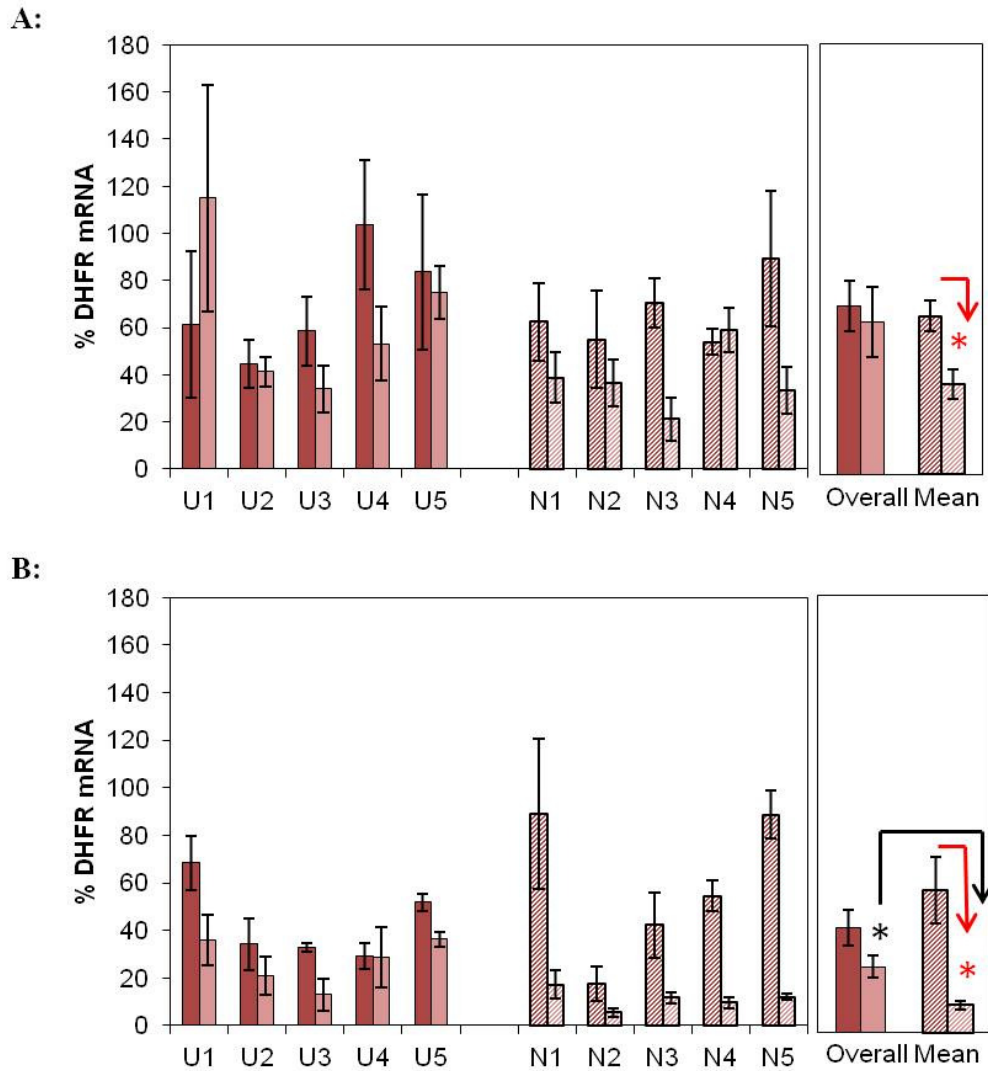


Figure 3.22 shows DHFR mRNA expression over-long term culture in the presence and absence of MTX selection. Overall UCOE and non-UCOE cell lines showed similar amounts of DHFR mRNA at the start of long-term culture. Although DHFR mRNA was stable throughout continuous culture in the presence of MTX, a decrease was observed after the removal of MTX in UCOE cell lines. A loss of DHFR mRNA was observed in non-UCOE cell lines both in the presence and absence of MTX selection (Figures 3.22A and 3.22B).

The scatter plots summarize the results of mRNA and protein levels (Figure 3.23). Overall, there was a fairly strong positive correlation between eGFP mRNA copies and protein production (Figures 3.23 and 3.23B). However, no correlation was found between DHFR mRNA and DHFR protein production (Figure 3.23C).

Figure 3.22: Analysis of DHFR mRNA expression over long-term culture in amplified cell lines.



DHFR mRNA expression was measured on day 10 and day 80 by q-PCR (Section 2.6). (A) Relative eDHFR mRNA expression in the presence of MTX. (B) Relative DHFR mRNA expression in the absence of MTX.

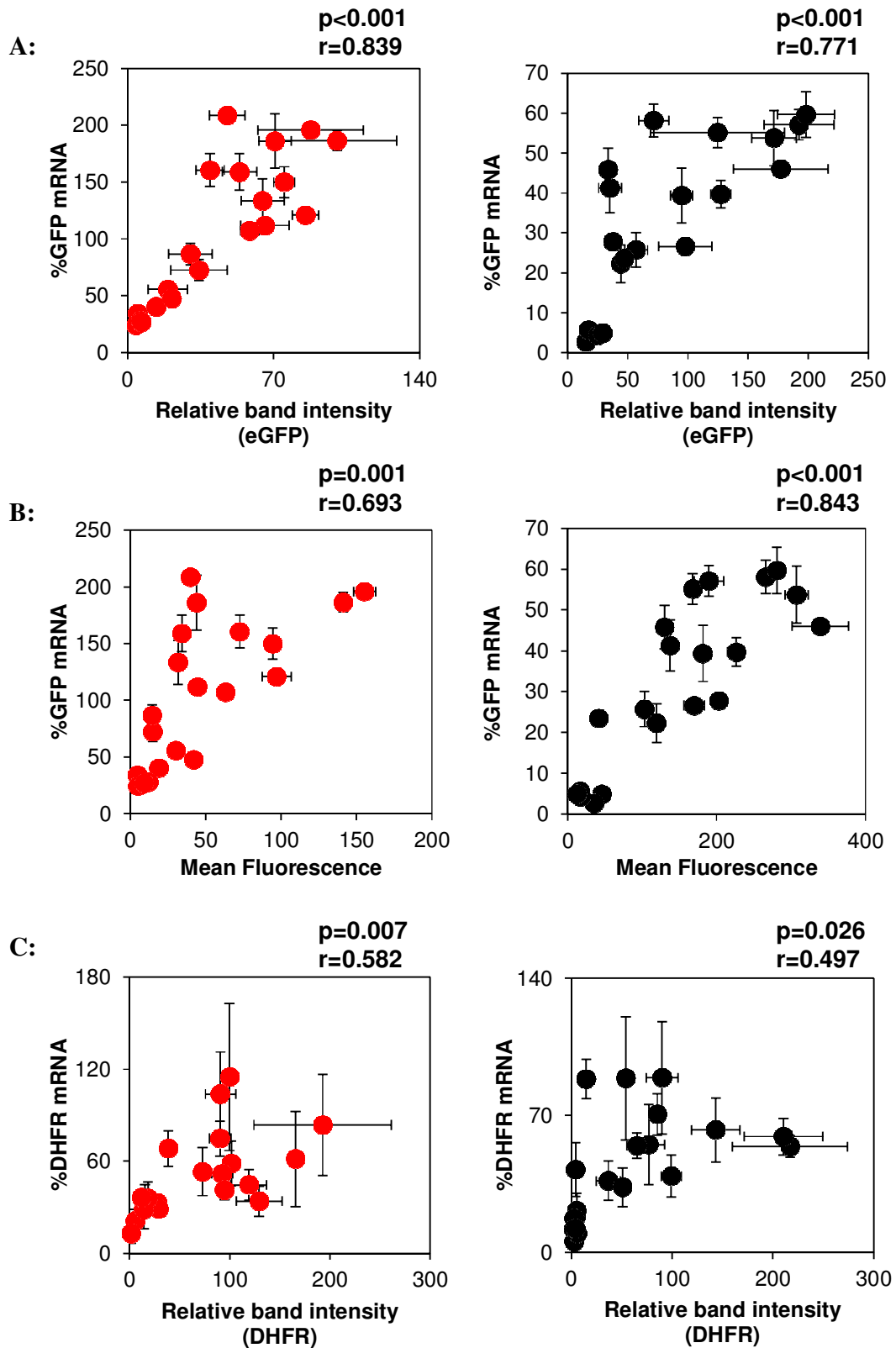
■ = UCOE day 10, □ = UCOE day 80, ▨ = non-UCOE day 10, □ = non-UCOE day 80. Values are quoted \pm SD ($n=3$), overall mean values are quoted \pm SEM ($n=5$). * indicates $p<0.05$, using independent samples t-test to compare UCOE and non-UCOE cell lines (at the same time of long-term culture), * indicates $p<0.05$, using paired samples t-test to compare early and late generation cultures (for the same group of cell lines) (Section 2.10).

mRNA and protein expression were determined as described in Sections 2.6, 2.5.4 and 2.5.7. Protein expression is plotted against relative mRNA expression. (A) eGFP mRNA expression vs eGFP expression measured by Western analysis, (B) eGFP mRNA expression vs eGFP fluorescence measured by flow cytometry, (C) DHFR mRNA expression vs DHFR protein expression measured by Western analysis

● =UCOE, ● =non-UCOE cell lines.

Correlation coefficients and statistical significance are indicated on the top right corner of the scatter plots

Figure 3.23: Comparison of protein production against mRNA expression.



3.2.5. Effect of Sodium Butyrate (NaB) on eGFP expression

As discussed in Section 1.4.1.2, histone acetylation is mainly associated with an open chromatin structure, which is linked with transcriptionally active genes and it can be reversed by histone deacetylase (HDAC) activity resulting in a more condensed chromatin structure. Sodium butyrate (NaB) is a sodium salt of butyric acid. NaB has been shown to enhance the expression of heterologous genes controlled by major promoters including CMV (Laubach et al., 1996) and SV40 (Palermo et al., 1991). NaB was shown to increase global acetylation of histones, especially H3/H4, through inactivation of histone deacetylases (Lee et al., 1993), which results in reactivated epigenetically silenced genes.

In an effort to clarify if the decrease in eGFP expression observed in the U2 and U5 cell lines, following removal of MTX, was due to the deacetylation of histones, the cells were exposed to 2.5mM NaB. Treatment of cells with NaB should give a rapid increase in eGFP fluorescence if the genes are silenced as a result of histone deacetylation (Hunt et al., 2002, Jiang and Sharfstein, 2008). To investigate whether NaB treatment resulted in a full recovery of eGFP fluorescence, frozen stocks of the U2 and U5 cell lines, at early generation growing in MTX and at late generation in the absence of MTX, were revived together and treated with NaB, as defined in the legend to Figure 3.24.

Figure 3.24A shows cell growth profiles of the cultures with and without NaB addition. Inhibition of cell growth was observed 24 hours after NaB treatment, which resulted in significantly lower viable cell densities throughout batch culture. This was consistent in all cell lines tested.









eGFP expression was determined by Flow Cytometry 24 and 48 hours after treatment. The presence of NaB caused an increase in eGFP fluorescence (by approximately 8.7 fold) in the late generation U2 cell line relative to the untreated control cells after 24 hours. The increase reached to 14.5 fold after 48 hours of NaB exposure (Figure 3.24B). Furthermore, NaB addition also caused an increase in eGFP expression in the early generation U2 cell lines. This increase was 3.8 and 6 fold after 24 and 48 hours of treatment respectively

(Figure 3.24B). A smaller increase was observed in the late generation U5 cell line in response to NaB with a 5.5 and 7 fold increases after 24 and 48 hours of treatment respectively. The increase was smaller for the early generation cells being only 2.9 and 3 fold after 24 and 48 hours respectively (Figure 3.24B).


To assess whether the increase in eGFP fluorescence was due to an increase in eGFP mRNA expression, cells were harvested at 24 hours after NaB treatment. The eGFP mRNA levels in the treated and control cells were determined by using q-RT PCR (Figure 24C). The enhancement in eGFP mRNA mirrored the enhancement in eGFP fluorescence in both the U2 and U5 early generation cell lines. The late generation U2 cell line showed a 6.7 fold increase in mRNA expression which was lower than the increase in eGFP fluorescence (8.7-fold). The late generation U5 cell line did not show any change in eGFP mRNA in response to NaB treatment, which suggests that the increase in eGFP fluorescence was not as a result of up-regulation of eGFP gene transcription.

Liquid nitrogen stocks were revived in early and late generation and cultured for a further 7 days either with or without MTX following revival. Batch growth cultures were created at an initial density of 1×10^5 in 6-well plates. After 24 hours, cells were treated with a final concentration of 2.5mM Sodium Butyrate (NaB). Control cells had no treatment. (A) Samples were taken every 24-48 hours to assess cell viability (Section 2.4.2) (B) GFP fluorescence was measured 24 and 48 hours after NaB addition by using Flow Cytometry (Section 2.5.7). (C) mRNA samples were taken after 24 hours of NaB treatment and analysed by using q-RT PCR (Section 2.6). Values are presented as \pm SD ($n=3$). * indicates $p < 0.05$, using independent samples t-test to compare control and NaB treated cells at the same time of culture (Section 2.10).

Annotations for Figure 3.24A

-  U2 early generation Control
-  U5 early generation Control
-  U2 late generation Control
-  U5 late generation Control
-  U2 early generation with NaB
-  U5 early generation with NaB
-  U2 late generation with NaB
-  U5 late generation with NaB

Annotations for Figure 3.24B

-  48h - Control
-  72h - Control
-  48h - NaB (24h after NaB addition)
-  72h - NaB (48h after NaB addition)

Annotations for Figure 3.24C



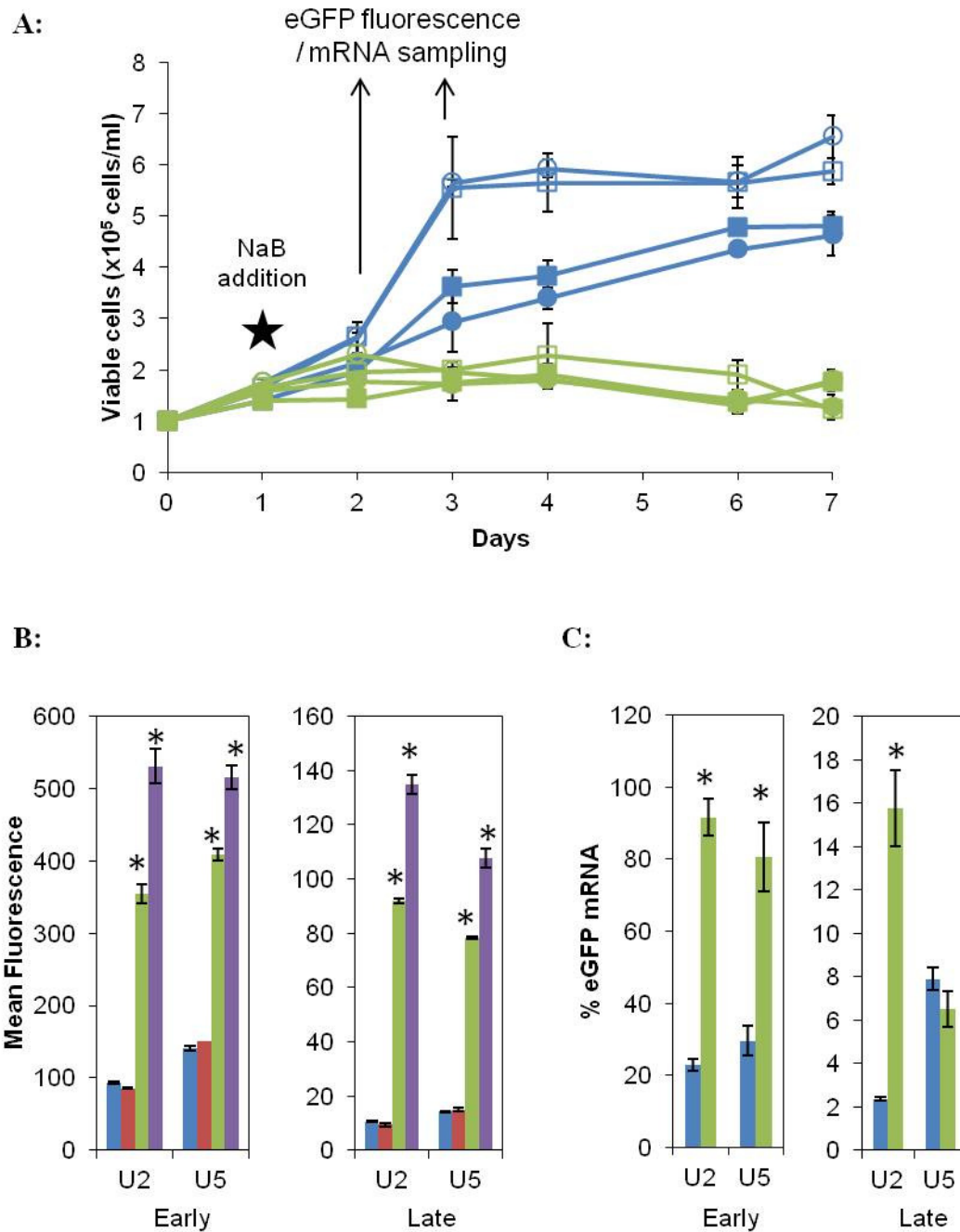
-  Control (without NaB)
-  With NaB

Figure 3.24: Effect of Sodium Butyrate on growth, eGFP fluorescence and mRNA.



3.3. Discussion

MTX-mediated amplification is widely used in recombinant protein production to achieve high-level protein production. However, generating stable and high-producing cell lines has been the major challenge for the biopharmaceutical industry as the molecular mechanism of instability is not yet fully understood (Section 1.3). This issue has been addressed in several studies which suggested a loss in transgene copy numbers (Fann et al., 2000, Hammill et al., 2000, Kim et al., 1998b, Pallavicini et al., 1990), a decrease in transcriptional efficiency (Chusainow et al., 2009, Kim et al., 1998a) or a change in the chromosomal integration site of the plasmid (Yoshikawa et al., 2000b, Yoshikawa et al., 2000a, Kim and Lee, 1999) could be reasons for the decline in productivity (Section 1.3). Different approaches have been made to overcome instability caused by transgene silencing, such as flanking the transgenes with chromosomal elements including S/MARs and LCRs (Kim et al., 2004, May et al., 2000, Zahn-Zabal et al., 2001). More recently, UCOE has been suggested to prevent gene silencing and give stable and high-levels of recombinant protein production (Section 1.5.2.3). Moreover, a previous study in our laboratory showed that UCOEs can be used in combination with MTX-mediated gene amplification (Croxford, 2008). However, the mechanism that underlies the stability and change in protein expression in amplified CHO cells with the utilisation of UCOEs has not yet been reported. Therefore, a comparative analysis of CHO-DG44 cells that expressed eGFP, with or without the inclusion of UCOE in their vector construct, was performed in the current study.

The growth analysis of initial cell lines showed that there was no difference between UCOE and non-UCOE cell lines in terms of viable cell densities and CCT values (Section 3.1.1). Moreover, growth characteristics did not change over 80 days of continuous culture. eGFP expression measured by flow cytometry and western blotting showed that UCOE cell lines displayed significantly higher levels of eGFP fluorescence compared to non-UCOE cell lines (Section 3.1.2). These results are in agreement with the previous studies, where vectors combining the UCOE with the CMV promoter have given an increased level of eGFP and EPO production compared to the control cells (Benton et al., 2002, Williams

et al., 2005). Furthermore, eGFP expression was stable up to 80 days in the UCOE cell lines. eGFP expression in the non-UCOE cell lines approached to UCOE cell lines when long-term culture progressed. UCOE cell lines were more homogenous in the beginning of long-term culture as shown by their low CV values. However, the CV value increased over time, whereas no significant change was observed in the non-UCOE cell lines.

The top 10 highest producing cell lines from each group were pooled and amplified to 250 nM MTX (Section 3.2). The results showed that despite containing significantly lower eGFP gene copy numbers, the UCOE cell lines displayed a higher amount of eGFP mRNA compared to the non-UCOE cell lines. These results strongly suggest that UCOEs provide higher transcriptional activity for the heterologous transgene. However, the high level of eGFP mRNA did not correlate with the eGFP expression as it was found that the eGFP expression was lower in the UCOE cell lines following amplification. This may indicate that the high amount of eGFP mRNA content saturates the translational capacity of the UCOE cell lines.

To assess the recombinant eGFP expression, flow cytometry and western blotting experiments have been conducted (Section 3.2.2). Flow cytometry is a commonly used method to measure the fluorescence of a cell population. It also provides valuable information on population characteristics and statistical parameters such as the mean, median, CV and SD. Western blotting is a useful approach to identify, determine if protein is the correct size and quantitate total protein expression and assess changes in protein expression. Despite the good correlation that exists between eGFP fluorescence and protein expression, the results showed that some cell lines displayed a higher total eGFP expression than eGFP fluorescence detected by flow cytometry. It should be noted that the expression level and fluorescence properties of GFP can be affected by many factors. Among these, the requirement for fluorophore formation and the sensitivity to cellular pH may result in lower fluorescence intensities than the actual GFP concentration (George, 1997, Tsien, 1998, Patterson et al., 1997).

The eGFP and DHFR gene copy numbers ranged from 50 to 262 and 185 to 1400 in the UCOE and non-UCOE cell lines respectively following MTX amplification (Section 3.2.3). It was observed that the higher gene copy number did not necessarily result in higher protein expression either in the UCOE or in the non-UCOE cell lines (Lattenmayer et al., 2007a, Lattenmayer et al., 2007b, Chusainow et al., 2009). For example, among the UCOE cell lines, the U1 cell line had the highest eGFP gene copy number, however, the protein expression was similar to the others, whereas the U5 cell line displayed the lowest eGFP gene copy numbers with a relatively high level of protein expression. Similarly, the N2 cell line contained the highest number of eGFP gene copies among the non-UCOE cell lines and the lowest protein expression. Conversely, the N3 cell line had a similar number of eGFP gene copies that had a higher level of protein expression following MTX amplification. This was also reflected in the relationship between the eGFP gene copy numbers and the eGFP mRNA expression. The lowest eGFP gene copy number resulted in a similar level of eGFP mRNA in the N1 cell line compared to the other non-UCOE cell lines as well as in the U5 cell line compared to the remaining UCOE cell lines. The MTX-mediated gene amplification is a complex mechanism and induces chromosomal rearrangements (Section 1.2.3.2.2). Therefore, the different locations of the inserted transgene may result in different transcription rates, a phenomenon which is known as the 'position effect' (Section 1.4.1.1). Further observations showed a good correlation between eGFP mRNA and protein expression levels (Section 3.2.4). However, as explained in the beginning of this section, despite having significantly higher eGFP mRNA content, the UCOE cell lines displayed lower levels of eGFP expression compared to the non-UCOE cell lines. This suggests that along with the gene copy number and mRNA expression, other factors such as translation efficiency also play a role in recombinant protein production. DHFR protein expression was analysed by western blotting which showed no significant difference between the UCOE and non-UCOE groups (Section 3.2.2.2).

It was found that, although eGFP and mRNAs are a part of bi-cistronic transcription units, they did not respond to the MTX amplification in the same manner (Section 3.2.4). This remains unexplained but could be due to rearrangements of the integrated DNA sequence during the complex process of MTX amplification and failure of the IRES containing

vector to maintain a linkage between the two recombinant genes (Heller-Harrison et al., 2009). It would be informative to carry out southern and northern blot experiments to assess the integrity of the inserted plasmid DNA and RNA. It was shown in Section 3.2.2.2 that DHFR and eGFP protein expression was moderately correlated; however, the pattern of expression was not parallel to each other. IRESs are complex RNA structures, mainly found within the mRNAs of proteins involved in cell growth and apoptosis (Bonnal et al., 2003). It has been shown that IRES frequently becomes activated under stress conditions, when cap-dependent translation is compromised (Holcik et al., 2000, Spriggs et al., 2005, Spriggs et al., 2010). A recent study conducted by Yang et al. (2010a) showed that IRES mediated translation was activated and increased the expression of an endogenous protein involved in cell death in specific diseases when the lymphoid cancer cells were treated with the chemotherapeutic drug vincristine. Therefore, it may be suggested that the IRES usage is limited and an expression of a gene of interest from an IRES-containing vector might be unpredictable.

In order to assess the stability of protein expression, the cell lines were cultured continuously for up to 80 days in the presence and absence of MTX selection. The results showed that eGFP expression remained relatively stable over time in the presence of MTX, whereas both UCOE and non-UCOE cell lines displayed a decrease in eGFP expression by >80% during long-term culture when MTX had been removed (Section 3.2.2). The cell lines were shown to respond to MTX removal in different ways (Section 3.2.2, 3.2.3, 3.2.4). For example, the loss of eGFP expression was as a result of a decrease in eGFP gene copies in the N2 cell line which also lost its eGFP mRNA and protein expression accordingly. In contrast, despite stable retention of eGFP gene copies over the long-term culture, the N4 and N5 cell lines lost more than 83% of their eGFP expression over prolonged culture in the absence of MTX. The proportionate decline in the eGFP mRNA levels in these cell lines when cultured without MTX suggested that the decreased protein expression upon long-term culture in the absence of MTX selection was as a result of a decrease in transcriptional efficiency rather than a loss of gene copies. Gene silencing or the position effect, induced by chromosomal rearrangements may result in transcription inhibition, or a decrease in mRNA content may also be as a result of reduced mRNA

stability. The N3 cell line displayed an initial loss of eGFP gene copies after the removal of MTX and this remained constant for up to 80 days. However, this cell line showed a decrease in eGFP expression of 86% along with eGFP mRNA during long-term culture in the absence of MTX. This may suggest that the reduced transcription rates of the remaining gene copies result from a preferential loss of transcriptionally-active genes or a decline in transcriptional efficiency of the remaining genes.

Similar observations were made for the UCOE cell lines (Section 3.2.2, 3.2.3, 3.2.4). In the U1 and U3 cell lines the decrease in eGFP gene copies, mRNA and protein expression occurred concurrently at the end of long-term culture in the absence of MTX. Despite having similar numbers of eGFP gene copies, protein and mRNA, expression profiles were distinct in the U2 and U4 cell lines over the extended culture in the absence of MTX. The U2 cell line lost its eGFP expression accompanied by eGFP mRNA; however the eGFP gene copy loss was not proportional suggesting a decrease in the transcriptional efficiency of the remaining eGFP genes, whereas the U4 cell line displayed an initial loss of eGFP gene copies after removal of MTX, which was constant up to 80 days. However, the U4 cell line lost eGFP expression along with eGFP mRNA, which suggested that some of the eGFP genes may not be transcriptionally active at the end of long-term culture in the absence of MTX. The U5 cell line showed a similar pattern to the N4 cell line, where eGFP gene copies did not change over long-term culture in the absence of MTX. However, the eGFP expression decreased by 92% with a corresponding 86% loss of eGFP mRNA at the end of long-term culture without MTX selection. The DHFR protein expression was relatively stable in the presence of MTX, whereas a significant decrease was observed after removal of MTX (Section 3.2.2.2). These findings suggest that UCOEs do not provide any advantages in terms of stability of protein production when MTX is absent.

The growth analysis showed that the UCOE cell lines achieved higher cell densities compared to the non-UCOE cell lines in the presence of MTX, which was also reflected in the CCT values (Section 3.2.1). Cell growth is an important parameter when screening for a suitable cell line for therapeutic protein production as maximum volumetric productivity can be achieved by a combination of a maximum amount of cells and a high cell specific

productivity. There are conflicting reports as to the effect of over-expression of recombinant protein on the growth of CHO cells. Several studies reported that the level of recombinant protein production was inversely correlated with cell specific growth rate (Gu et al., 1996, Page and Sydenham, 1991, Pendse et al., 1992, Jiang et al., 2006), whereas others suggested no clear correlation between recombinant protein production and cell growth (Chusainow et al., 2009, Fann et al., 2000, Kim et al., 1998a). Provided that there was no significant difference in DHFR protein expression between the UCOE and non-UCOE cell lines, the better growth characteristics observed in the UCOE cell lines may suggest that UCOEs provide higher tolerance to MTX.

Both the UCOE and non-UCOE cell lines showed an increase in CCTs and maximal cell densities at the end of long-term culture in the presence of MTX. This increase in cell growth may be as a result of the development of MTX resistance. In addition to an increased expression of DHFR by gene amplification (Section 1.2.3.2.2), CHO cells can acquire resistance to continuous exposure to MTX by other mechanisms. Among these, the most common mechanisms are an altered affinity of DHFR enzyme to MTX (Flintoff and Essani, 1980, Haber and Schimke, 1981) and reduced transport of MTX by reducing the folate receptor expression (Assaraf and Schimke, 1987, Cavalcanti et al., 1992, Saikawa et al., 1993). MTX resistance may occur as a result of one or more mechanisms together in individual cells (Haber et al., 1981).

As explained in Section 3.2.2, the U2 and U5 cell lines showed a decrease in eGFP expression during long-term culture in the absence of MTX. The U2 cell line displayed a decrease in eGFP gene copies by 32% whereas the decrease in eGFP expression was 94% after 80 days of culture without MTX selection. In contrast, the U5 cell line did not show any change in eGFP gene copy numbers. However, 92% of the eGFP expression was lost at the end of long-term culture in the MTX-free medium. Both cell lines displayed a proportionate loss of eGFP mRNA and protein expression during long-term culture. Therefore, the effect of NaB, a histone deacetylase inhibitor (Riggs et al., 1977), on these cell lines was investigated to examine if the decrease in eGFP expression observed following the removal of MTX was due to deacetylation of histones associated with eGFP

gene (Section 3.2.5). Cell lines in both early generation in the presence of MTX and late generation without MTX selection were used in this study to investigate whether cell lines fully recovered the eGFP fluorescence. The results showed that both the U2 and U5 cell lines were influenced by NaB addition and displayed enhanced eGFP fluorescence in early and late generations. The increased eGFP fluorescence in the late generation U2 cell line without MTX selection was partly due to an increase in the eGFP mRNA level. However, the observed increase in eGFP fluorescence cannot be fully attributed to the increase in mRNA levels as increase in mRNA was lower than increase in eGFP fluorescence. Furthermore, no change in eGFP mRNA content was observed in the late generation U5 cell line, which was cultured in MTX-free medium, even though this cell line also showed an increase in eGFP fluorescence after the addition of NaB to the medium. Taken together, these findings indicate that the increase in eGFP expression cannot be solely attributed to a direct transcription effect of the transgene. NaB has been reported to affect the expression of a wide range of genes in cultured mammalian cells, including the genes responsible for cell cycle, apoptosis, protein processing and secretion (Yee et al., 2008, De Leon Gatti et al., 2007). Therefore, the ability of NaB to influence different cellular processes suggests that the observed effects of NaB may not necessarily be due to deacetylation of histones associated with the integrated transgene. However, it would be worthwhile conducting experiments using ChIP technology to confirm this result.

3.3.1. Summary

The results in this chapter showed that although recombinant protein expression was relatively stable in the presence of MTX for both the UCOE and non-UCOE group, the UCOEs did not confer any advantages in terms of stability of recombinant protein production in the absence of MTX. However, it was observed that the UCOE cell lines displayed better growth characteristics following MTX amplification which may provide an advantage in recombinant protein production. Furthermore, transcriptional activity per gene copy was greater when UCOE was present in the expression construct both in the presence and absence of MTX.

CHAPTER 4:

Results-2

The results presented in Chapter 3 showed that the intracellular eGFP production remained stable over long-term culture in the presence of MTX. Removal of MTX resulted in a decrease in eGFP expression in both UCOE and non-UCOE cell lines. Furthermore, it was demonstrated that the inclusion of UCOE elements with vector constructs promotes better growth in the presence of MTX. The main priority in recombinant protein production by the biopharmaceutical industry is to achieve the maximum amount of recombinant protein per litre of medium. This is known as volumetric productivity. In order to achieve a high volumetric productivity, cells need to grow to high maximum cell densities, whilst, hopefully, showing high specific productivity. Consequently, the use of UCOEs to produce cell lines with a secreted recombinant protein may improve volumetric protein production following MTX amplification. This section details the establishment of DG44-CHO cell lines expressing a model secreted protein (Erythropoietin, EPO) containing the hCMV-EPO-IRES-DHFR expression cassette with or without the inclusion of UCOE and the Chapter also addresses how such cell lines perform following MTX amplification of the inserted transgenes. The work presented in this chapter extends that from Chapter 3 and the aim of the work is to answer the following questions. Firstly, do cell lines constructed using UCOE-containing vectors achieve higher volumetric productivity than cell lines generated using equivalent constructs lacking UCOE elements (non-UCOE) under conditions of MTX amplification? Secondly, is EPO expression at protein level more stable over long-term culture in cell lines generated with UCOE-containing vectors than with non-UCOE-containing vectors?

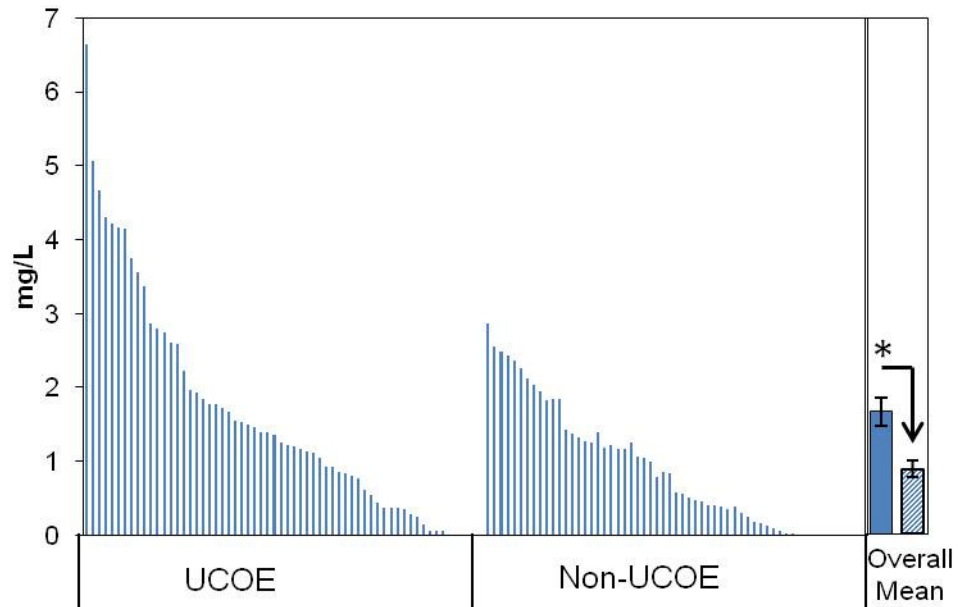
4.1. Establishment of CHO-EPO initial cell lines

The strategy used to create CHO-EPO cell lines was summarized in Figure 2.1. The initial cell lines were obtained by transfection of the DG44-CHO cell lines with either the linearised p1010-EPO (UCOE-containing) or p901-EPO (non-UCOE) vectors (Appendix 3). The cells acquiring DHFR along with the EPO transgene were selected by the exclusion of hypoxanthine and thymine from the medium. After the limiting dilution cloning (Section 2.4.6), more than 60 single colonies (these are referred to as CHO-EPO cell lines)

from each group were scaled up to 6-well plates and the expression of EPO protein was determined by ELISA (Section 2.5.8).

In accordance with the results obtained from Chapter 3, UCOE cell lines showed significantly higher EPO production than non-UCOE cell lines (Figure 4.1). The top 10 high producing cell lines were selected from each group and scaled up to T-75 flasks and were cryopreserved (Section 2.4.3). From the cell lines, the three highest producing cell lines (in terms of volumetric EPO expression, Figure 4.1) were grown continuously for up to 77 days in adherent culture. Viable cell densities, volumetric EPO production and specific productivity were analysed over long-term cultivation (Section 4.1.1).

Figure 4.1: EPO production in initial CHO-EPO cell lines.



*CHO-EPO cell lines were created by transfection with either linearised p1010-EPO-DHFR (UCOE) or p901-EPO-DHFR (non-UCOE, See Section 2.4.5). Transfected cells were cloned by limiting dilution cloning (Section 2.4.6), and scaled-up into 6-well plates. Cells were grown in RPMI medium plus 4mM L-Glutamine and 10% (v/v) FBS till approximately 90% confluent, when a medium sample was taken and frozen at -80°C. Samples were analysed by EPO ELISA to determine volumetric EPO production (Section 2.5.8). ■ = UCOE cell lines, ▨ = non-UCOE cell lines. Overall mean values are shown ± SEM for each group (n≥60). * indicates p<0.05, using independent samples t-test to compare UCOE and non-UCOE cell lines (Section 2.10).*

4.1.1. Analysis of growth characteristics and productivity of initial CHO-EPO cell lines during long-term culture

Batch growth cultures were created for the three selected cell lines from each group (Section 4.1) at the start (day 0) and the end (day 77) of long-term culture (Section 2.4.9). Cells were seeded at an initial density of 1×10^5 cells/ml. Samples were taken every 24-48 hours to assess viable cell densities (Section 2.4.2) and recombinant EPO production (Section 2.5.8). The average viable cell densities of three cell lines from each group are represented in Figure 4.2A. In agreement with the results obtained from Chapter 3, the maximal viable cell densities for UCOE and non-UCOE cell lines were similar in early and late generations. This was also reflected in CCT values, where UCOE and non-UCOE cell lines showed similar total cell numbers (Figure 4.2B). An increase in CCT values was observed in both the UCOE and non-UCOE groups when long-term culture progressed. However, this was not statistically significant ($p > 0.05$, using paired samples t-test to compare early and late generations at the same time of the batch culture [Section 2.10]). Furthermore, a difference was observed in the growth profile of the cultures generated at the start and end of long-term culture with late generation cell lines exhibiting a more prolonged stationary phase. In addition, the viability of the late generation cultures declined more suddenly at day-9, presumably as a result of nutrient depletion (Figure 4.2B).

Specific growth rates (μ) were calculated as described in Section 2.11 for individual cell lines in both early and late generations (Figure 4.2C). The cell growth rates were in the range of 0.016 - 0.025 h^{-1} , which is consistent with previous studies (Chusainow et al., 2009, Fann et al., 2000, Jiang et al., 2006). Overall, no significant difference in the growth rates was observed between the UCOE and non-UCOE cell lines ($p > 0.05$ using independent samples t-test to compare the UCOE and non-UCOE cell lines in the same generation [Section 2.10]). Furthermore, the UCOE cell lines showed an increase in growth rate over long-term culture. The cell specific growth rate remained relatively constant during prolonged culture in non-UCOE cell lines.









The volumetric production of EPO was examined over the long-term culture by ELISA (Section 2.5.8). In agreement with the results observed for GFP in Chapter 3, the expression of EPO from UCOE cell lines was shown to be significantly higher than that of non-UCOE cell lines for all cells (Figure 4.3A). A decrease in EPO volumetric production was observed in two of the non-UCOE cell lines over the long-term culture, whereas volumetric production of EPO increased in the N0E2 cell line. In contrast, all UCOE cell lines showed relatively stable and high levels of EPO production compared to non-UCOE cell lines. Although non-UCOE cell lines showed a trend towards a loss in production, no significant difference was observed between the group mean values for volumetric production at day 0 and day 77 for either UCOE or non-UCOE cell lines ($p > 0.05$, using paired samples t-test to compare the early and late generation for the same group of cell lines [Section 2.10]).

Specific productivity was calculated during the exponential phase (48 to 96 hours), Figure 4.3B). UCOE cell lines showed consistently higher specific productivity than the non-UCOE group and this was reflected in the group mean values. A decrease in specific productivity was observed in the N0E1 and N0E3 cell lines, whereas the N0E2 cell line showed an increase over long-term culture. Although the U0E1 and U0E2 cell lines showed a decrease in EPO production, this was not statistically significant ($p > 0.05$, using paired samples t-test to compare early and late generations of the same cell line [Section 2.10]). The group mean values showed that specific productivity remained constant over the long-term culture in UCOE cell lines, whereas a decrease was observed in non-UCOE, although this was not statistically significant ($p > 0.05$, using paired samples t-test to compare early and late generations of the same cell line [Section 2.10]). The behaviour of cell line N0E2 contrasts markedly from that of cell lines N0E1 and N0E3.

Figure 4.3C and 4.3D show comparisons of cell growth rate, total EPO production and the specific productivity. No clear correlation was observed between the cell growth and the specific productivity in either UCOE or non-UCOE cell lines (when early generation N0E1 cell line omitted) (Figure 4.3C). Volumetric production was strongly correlated with specific productivity in both UCOE and non-UCOE cell lines (Figure 4.3D).

*CHO-EPO cell lines were cultured in T-75 flasks using RPMI medium plus 4mM L-Glutamine and 10% (v/v) FBS. Cells were cultured every 2-3 days up to 77 days (Section 2.4.1). Batch growth cultures were created at an initial density of 1×10^5 cells/ml in 6-well plates, at early (day 0), and late (day 77) generations. Samples were taken throughout batch culture for determining cell number. (A) Viable cell numbers were measured using light microscopy and trypan blue exclusion (Section 2.4.2). Values are presented as average of each group \pm SEM (n=3). (B) Cumulative cell time (CCT) was calculated during batch growth culture created in early and late generations (Section 2.11) Values are presented as average of each group \pm SEM (n=3). (C) Cell growth rates were calculated for individual cell lines during exponential phase of batch culture using cell counts from 48-96 hours (Section 2.11). Prefix U0E- and N0E- stand for initial UCOE and non-UCOE cell lines respectively. Overall mean values are shown \pm SEM for each group (n=3). An independent samples t-test performed to compare CCTs of early and late generation cell lines of the same group and also UCOE vs non-UCOE cell lines at the same generation, $p > 0.05$ (Section 2.10). * indicates $p < 0.05$, using paired samples t-test to compare early and late generation cultures (for the same group of cell lines) (Section 2.10)*

Annotations for Figure 4.2A and 4.2B

-   UCOE cell lines early generation
-   non-UCOE cell lines early generation
-   UCOE cell lines late generation
-   non-UCOE cell lines late generation

Annotations for Figure 4.2C



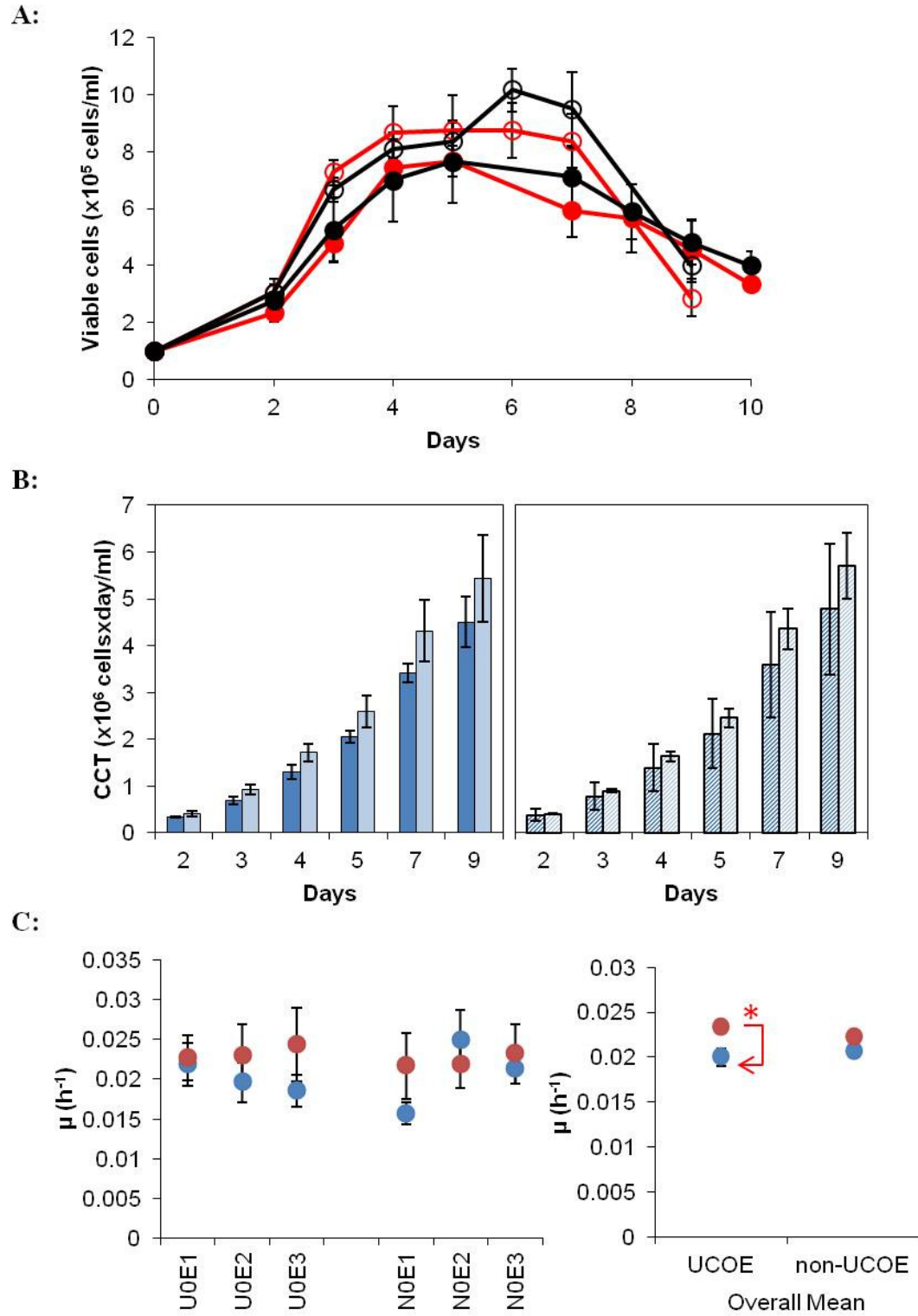




-  Early generation
-  Late generation

Figure 4.2: Analysis of growth characteristics of initial CHO-EPO cell lines during batch growth.



*Cell lines were grown in attached culture for a total of 77 days and subcultured every 2-3 days (Section 2.4.1). EPO production was assessed in batch cultures, performed at the start and end of long-term culture (Sections 2.4.9 and 2.5.8). Samples were taken every 24-48 hours to assess recombinant EPO expression by ELISA (Section 2.5.8). (A) Maximum recombinant EPO production, obtained at the end of batch cultures, is shown. (B) Specific productivity (Section 2.11) was calculated during the exponential phase, using samples and cell counts from 48-96 hours. Two biological replicates were set up and errors bars represent the range. Overall mean values are presented as \pm SEM (n=3). * indicates $p < 0.05$, using independent samples t-test to compare UCOE and non-UCOE cell lines (at the same time of long-term culture).*

 =UCOE cell lines early generation,  =UCOE cell lines late generation

 = non-UCOE cell lines early generation,  = non-UCOE cell lines late generation.

(C) Cell growth rate is plotted against the specific productivity for individual cell lines at all times. (D) Volumetric EPO production is plotted against the specific productivity for individual cell lines at all times. Correlation coefficients and p values are shown with the scatter plots. UCOE statistics are shown in red and non-UCOE statistics are written in black.


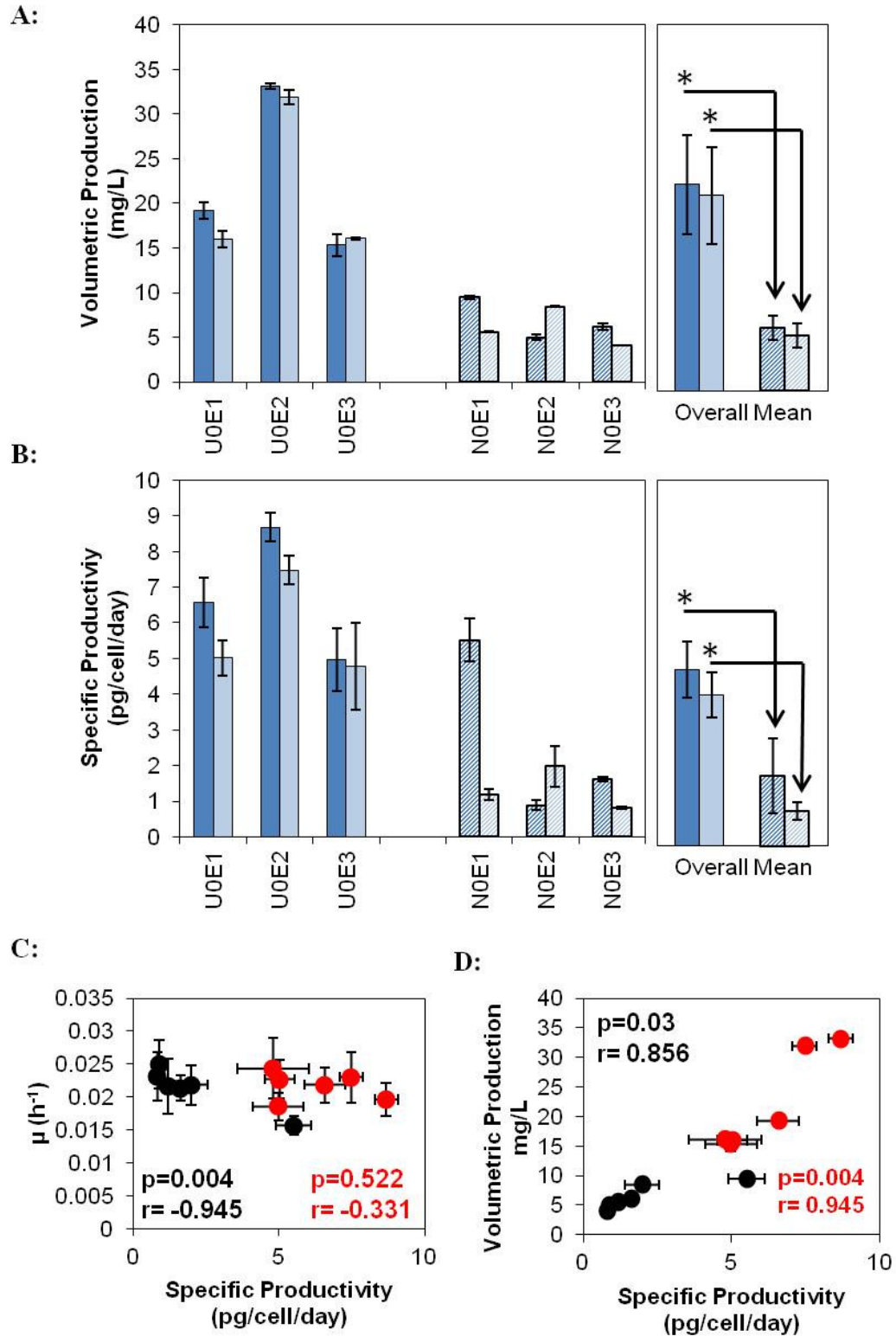
 = UCOE cell lines,  = non-UCOE cell lines

Figure 4.3: Analysis of total EPO production and specific productivity in initial CHO-EPO cell lines over long-term culture.

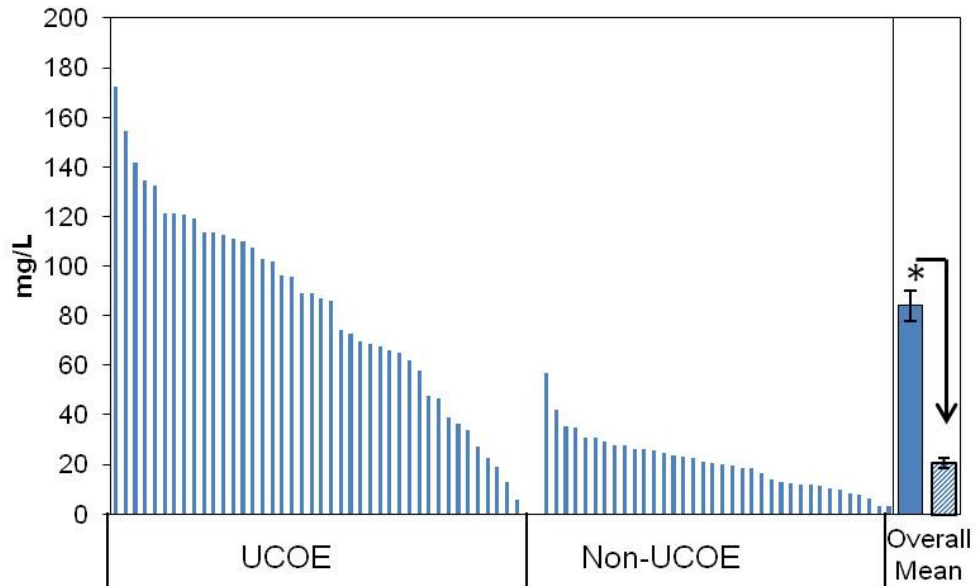


4.2. Establishment of amplified CHO-EPO cell lines

The strategy for amplification of CHO-EPO cell lines is detailed in Figure 2.1. In short, the top-ten EPO producing cell lines were selected from both UCOE and non-UCOE groups. Each group of selected cell lines was pooled and treated with 250nM MTX and this was followed by limiting dilution cloning. Following similar processes, more than 60 single colonies were observed for the UCOE cell lines following limiting dilution cloning, whereas only 38 single colonies were recovered from non-UCOE cell lines. All the single colonies observed in non-UCOE cell lines and a total of 40 single colonies from the UCOE group were scaled up into 6-well plates.

Volumetric production of EPO for the selected cell lines over a period of 72 hours was determined by ELISA (Section 2.5.8) and shown in Figure 4.4. Following MTX amplification, the EPO production was ~49 and ~23 times higher than non-amplified pools in UCOE and non-UCOE group respectively compared to non-amplified pools. The mean level of volumetric EPO production was 84 ± 6.2 mg/L for the UCOE group, as opposed to 20.7 ± 1.9 mg/L for the non-UCOE group. The group mean value of EPO expression for the UCOE cell lines was significantly higher than the non-UCOE group (Figure 4.4). This was in contrast to the results obtained from Chapter 3, where eGFP expression was lower in the UCOE cell lines compared to the non-UCOE group after MTX amplification.

Figure 4.4: EPO production in amplified CHO-EPO cell lines.



The top ten highest producing initial cell lines were pooled and treated with 250nM MTX (Section 2.4.7). Cells were cloned by limiting dilution cloning (Section 2.4.6), and single colonies were selected and scaled-up into 6-well plates. Selected clones were grown in RPMI medium plus 4mM L-Glutamine and 10% (v/v) FBS with 250nM MTX till approximately 90% confluent, then a medium sample was taken and frozen at -80°C. Volumetric EPO production was assessed by ELISA (Section 2.5.8).

■ = UCOE cell lines, ▨ = non-UCOE cell lines. Overall mean values are shown ± SEM for each group (n≥38). * indicates $p < 0.05$, using independent samples *t*-test to compare UCOE and non-UCOE cell lines (Section 2.10).

4.2.1. Long-term culture in amplified CHO-EPO cell lines

As described in Section 4.1.1, the three highest producers cell lines (in terms of EPO production) from both UCOE and non-UCOE group were selected for further long-term culture studies. Cells were subcultured every 2-3 days continuously for 77 days either with or without MTX selection. Samples were taken at the beginning (day 0) and at the end of long-term culture (day 77). Growth characteristics (Section 4.2.1.1), volumetric protein production and specific productivity (Section 4.2.1.2) of amplified CHO-EPO cell lines were examined over long-term culture. Furthermore, plasmid copy number and mRNA expression were analysed with the intention of understanding the effects of amplification and long-term culture on recombinant EPO production (Section 4.2.1.3 and 4.2.1.4 respectively).

4.2.1.1. Analysis of batch growth of amplified CHO-EPO cell lines

Batch growth cultures were created from cell lines at early generation (day 0), late generation with MTX selection (day 77) and late generation in the absence of MTX (day 77). Figure 4.5 shows the average viable cell densities and CCTs for each group in the presence and absence of MTX over prolonged culture.

UCOE cell lines at early generation showed similar viable cell densities and CCTs as the non-amplified UCOE cell lines suggesting that growth was not affected by MTX pressure (Figure 4.2 and 4.5). However, the late generation amplified UCOE cell lines showed higher maximum cell densities both in the presence and absence of MTX compared to the non-amplified UCOE cell lines, which was reflected by CCT values on days 4 and 5 of batch culture. In contrast, the maximum cell densities were lower in the amplified non-UCOE group compared to the non-amplified cell lines in early generation. Although this was also reflected in CCT values, the difference was not statistically significant. This was most probably due to the high standard deviation observed in non-amplified cell lines ($p > 0.05$, using independent samples t-test to compare the amplified and non-amplified cell lines on the same day of batch culture for the same generations [Section 2.10]). Moreover,

the peak viable cell densities and CCT values increased over time and reached to a similar level as the non-amplified non-UCOE cell lines (Figure 4.2 and 4.5).

In agreement with the results from Section 3.2.1, the UCOE cell lines were found to have higher maximum viable cell densities compared to the non-UCOE cell lines in the early and late generations in the presence of MTX (Figures 4.5A). A difference in viable cell densities was also observed on days 4 and 5 of batch culture created at late generation in the absence of MTX between the UCOE and non-UCOE cell lines. Moreover, an increase in the viable cell densities was observed in both the UCOE and non-UCOE cell lines at late generations in the presence and absence of MTX. The alterations to viable cell densities can also be observed with changes to CCT (Figure 4.5B and 4.5C). CCT values were significantly higher in UCOE cell lines throughout batch culture in the presence of MTX and on days 4 and 5 of late generation batch culture without MTX selection compared to the non-UCOE group. Furthermore, an increase in CCT values was observed over long-term culture in the presence and absence of MTX for both the UCOE and non-UCOE cell lines. These results confirm the results obtained in Section 3.2.1 and indicate that the growth of UCOE cell lines is not affected by MTX. As a consequence, UCOE cell lines achieved higher maximum cell densities than non-UCOE cell lines.

Figure 4.6 shows the specific growth rates of individual cell lines and group mean values. It was observed that the non-UCOE cell lines showed lower growth rates after MTX amplification at the start and end of long-term culture in the presence of MTX compared to non-amplified cell lines ($p < 0.05$, using independent samples t-test to compare amplified and non-amplified cell lines at the same generation [Section 2.10]). Although the amplified UCOE cell lines displayed lower cell growth rates than the non-amplified UCOE group at the beginning of prolonged culture, this was not statistically significant ($p = 0.091$, using independent samples t-test to compare amplified and non-amplified cell lines at early generation [Section 2.10]). Moreover, the UCOE cell lines showed significantly higher specific cell growth rates compared to the non-UCOE cell lines at all times following MTX amplification. The cell growth rate increased over prolonged culture in both UCOE and non-UCOE cell lines in the presence and absence of MTX. No significant difference was

observed between amplified and non-amplified UCOE cell lines at the end of long-term culture ($p > 0.1$, using independent samples t-test to compare amplified and non-amplified cell lines at the same generation [Section 2.10]). The cell growth rate of amplified non-UCOE cell lines achieved that of their non-amplified counterparts at the end of prolonged culture after MTX removal.

Cell lines were cultured every 2-3 days up to 77 days in T-75 flasks using RPMI medium plus 4mM L-Glutamine and 10% (v/v) FBS either with or without MTX selection (Section 2.4.1). Batch growth cultures were created as described in Figure 4.2 (Section 2.4.9). (A) The viable cell numbers are presented as average of each group \pm SEM ($n=3$) (Section 2.10). (B) CCTs were calculated (Section 2.11) during batch growth culture created in early and late generations for the cell lines growing in the presence of MTX selection. (C) CCT values were calculated for the cell lines growing without MTX selection. All CCT values are presented as average of each group \pm SEM ($n=3$).

• indicates $p < 0.05$, using independent samples t-test to compare UCOE and non-UCOE cell lines (on the same day of batch culture). * indicates $p < 0.05$, using paired samples t-test to compare early and late generation cultures (for the same group of cell lines on the same day of batch culture.) (Section 2.10).

Annotations for Figure 4.5

- UCOE cell lines early generation
- non-UCOE cell lines early generation
- UCOE cell lines late generation with MTX selection
- non-UCOE cell lines late generation with MTX selection
- ✖ UCOE cell lines late generation in the absence of MTX
- ✖ non-UCOE cell lines late generation in the absence of MTX

Figure 4.5: Analysis of batch culture growth and cumulative cell time in amplified CHO-EPO cell lines.

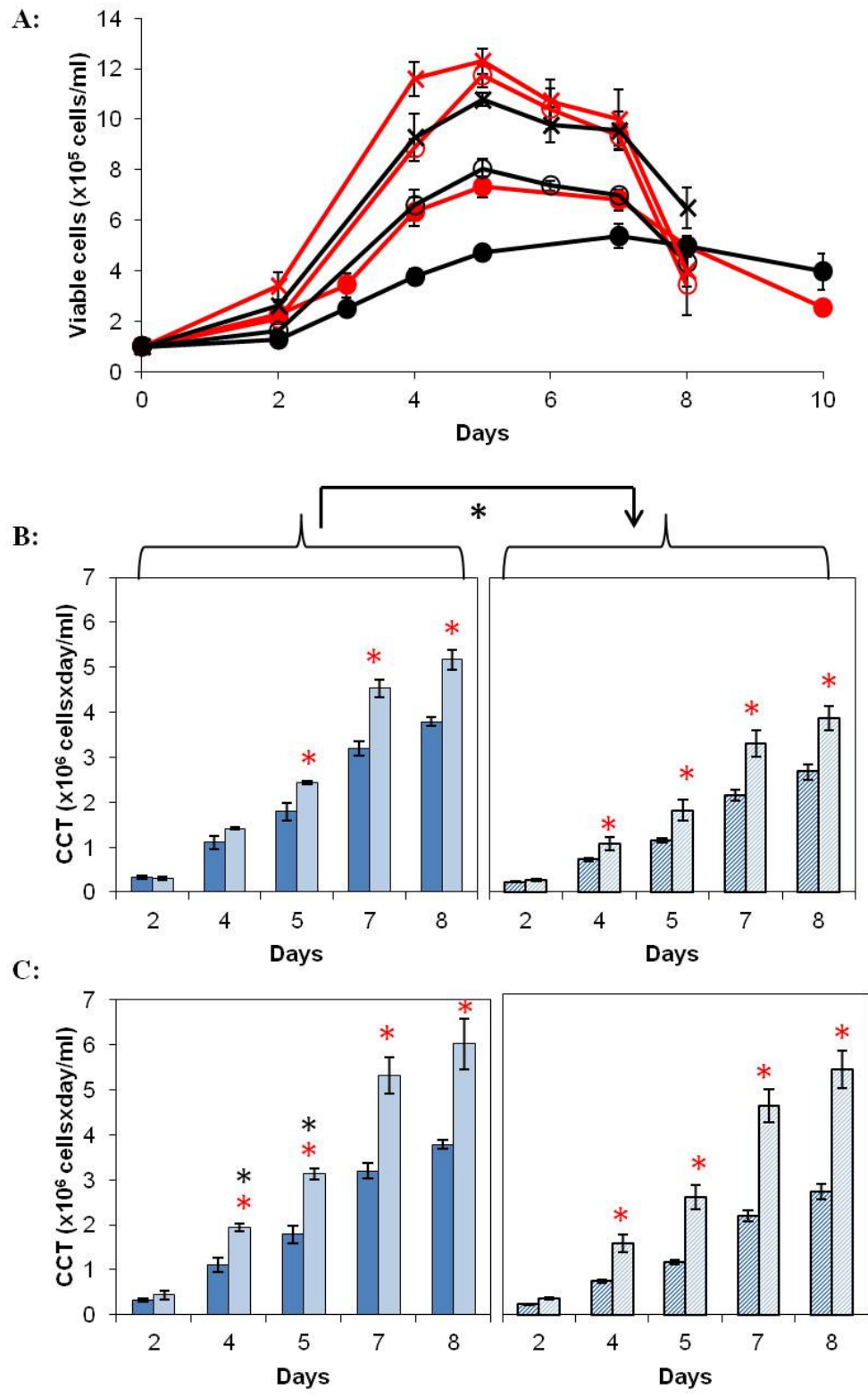
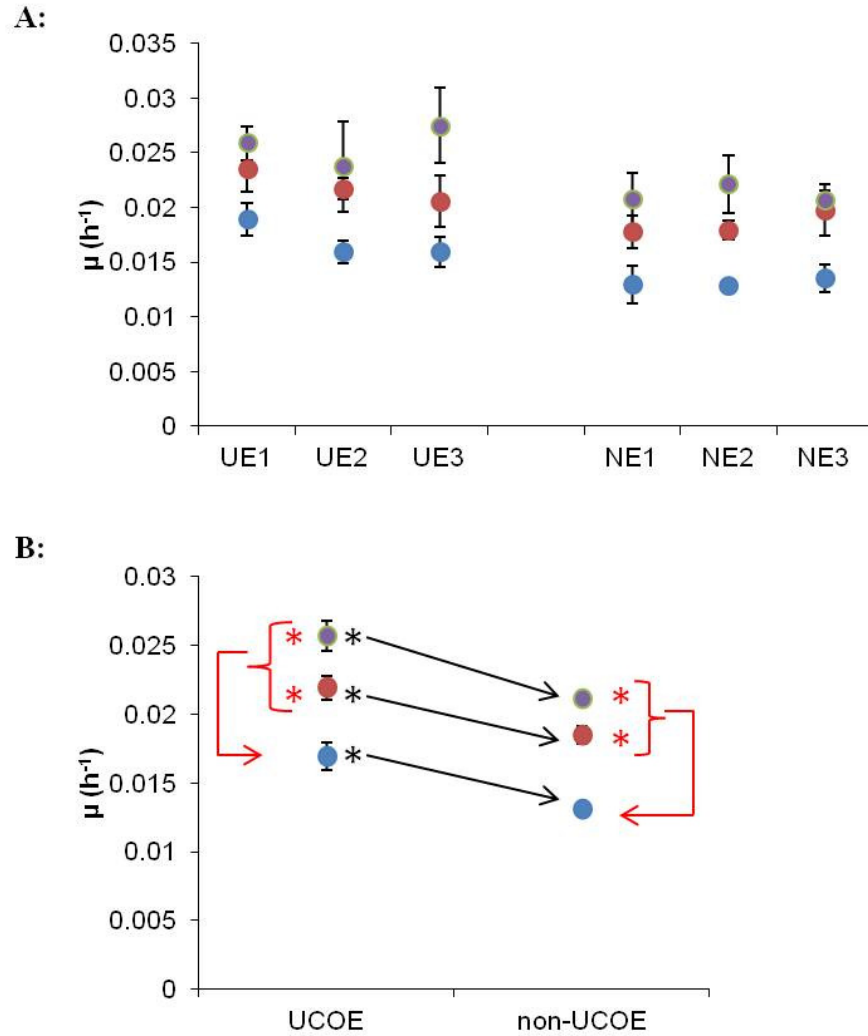


Figure 4.6: Growth kinetics of amplified CHO-EPO cell lines over long-term culture.



The cell growth rates of individual cell lines were calculated during exponential phase of batch culture (48-96 hours) as described in Section 2.11 Prefix UE- and NE- stand for EPO producing amplified UCOE and non-UCOE cell lines respectively. (A) Growth rates of individual cell lines are shown. Values presented as \pm range. (B) Average growth rates of each group are presented as mean values \pm SEM ($n=3$). * indicates $p<0.05$, using independent samples t -test to compare UCOE and non-UCOE cell lines, * indicates $p<0.05$, using paired samples t -test to compare early and late generation cultures (for the same group of cell lines) (Section 2.10). ●= Early generation, ●=Late generation with MTX selection, ●= Late generation without MTX selection

4.2.1.2. Effect of amplification on recombinant EPO production during long-term culture

EPO production was assessed by ELISA at the beginning and end of long-term culture. In agreement with the results obtained from the initial cell lines, total EPO production was lower in the non-UCOE cell lines both in the presence and absence of MTX (Figure 4.7). This was in contrast to the results of the amplified eGFP cell lines (Section 3.2.2), where non-UCOE cell lines showed higher eGFP expression compared to UCOE cell lines after MTX amplification. I surmise that this discrepancy is a consequence of intracellular processing of eGFP at high concentration (this will be discussed in Section 4.3).

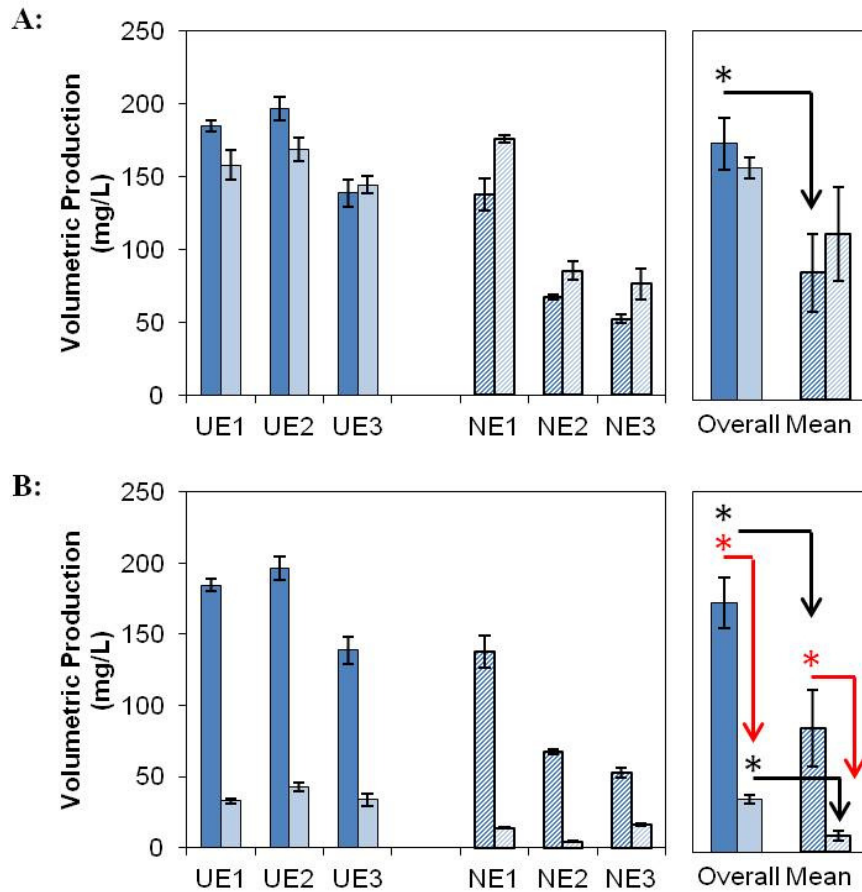
In parallel with the results in Section 3.2.2, the volumetric EPO production was relatively stable in all UCOE cell lines in the presence of MTX for 77 days (Figure 4.7A). This was reflected by the group mean value. An increase in the total EPO production was observed in the non-UCOE cell lines in the presence of MTX over long-term culture. This can be seen in the group mean value. However, the increase was not statistically significant ($p > 0.05$, using paired samples t-test to compare early and late generation cell lines for the same group, Figure 4.7A). All cell lines showed a decrease in total EPO production over prolonged culture in the absence of MTX (Figure 4.7B). The decrease was 78% and 87% in UCOE and non-UCOE cell lines respectively. However, the UCOE cell lines still showed significantly higher EPO production compared to the non-UCOE cell lines (group mean values; $36.5 \pm 3 \text{ mg/L}$, $11 \pm 3.7 \text{ mg/L}$ in UCOE and non-UCOE group respectively).

The UCOE cell lines showed higher specific productivity compared to non-UCOE cell lines at early generation. However this was not statistically significant. In addition, no significant difference was observed between the late generation UCOE and non-UCOE cell lines in the presence of MTX ($p > 0.05$, using independent samples t-test to compare UCOE and non-UCOE cell lines at same generation [Section 2.10], Figure 4.8A). However, the specific productivity was significantly higher in the UCOE cell lines compared to the non-UCOE group at the end of long-term culture in the absence of MTX (Figure 4.8B).

A decrease in specific productivity was observed in all UCOE cell lines over long-term culture in the presence of MTX, which was reflected in the mean value (Figure 4.8A). Among the non-UCOE cell lines, NE1 and NE3 cell lines showed an increased specific productivity over long-term culture in the presence of MTX, whereas specific productivity remained constant in the NE2 cell line. All cell lines displayed a decrease in specific productivity over long-term culture in the absence of MTX (Figure 4.8B).

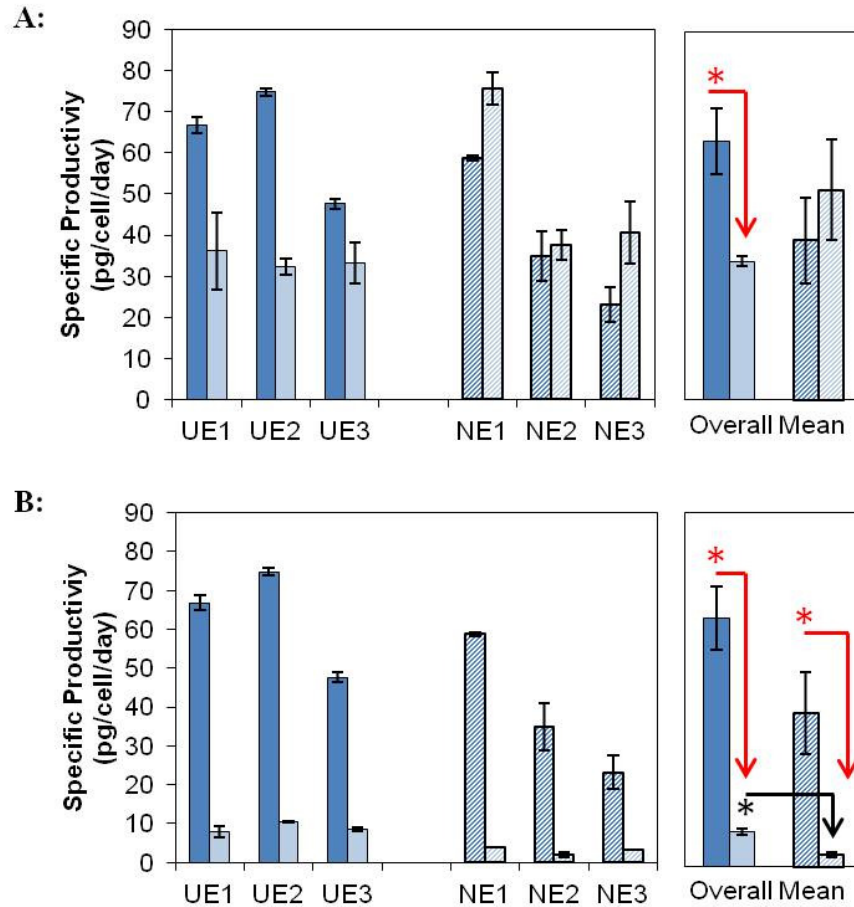
Figure 4.9A shows scatter plots for individual UCOE and non-UCOE cell lines comparing the specific productivity and the cell growth rate (μ). A relatively strong negative correlation between the growth rate and the specific productivity was observed in the UCOE cell lines. There was no consistent correlation between the cell growth and the specific productivity in the non-UCOE cell lines. Furthermore, it was observed that the volumetric EPO production and specific productivity increased proportionally in both UCOE and non-UCOE cell lines (Figure 4.9B).

Figure 4.7: Production of recombinant EPO during long-term culture in amplified CHO-EPO cell lines.



Cells were grown in attached culture either with or without MTX selection. EPO production was assessed in batch cultures, performed at the start and end of long-term culture (Sections 2.4.9). Samples were taken every 24-48 hours to assess recombinant EPO expression by ELISA (Section 2.5.8). Maximum recombinant EPO production, obtained on day 8 of batch cultures, is shown. (A) Volumetric EPO production in the presence of MTX (B) Volumetric EPO production in the absence of MTX. * indicates $p < 0.05$, using independent samples *t*-test to compare UCOE and non-UCOE cell lines at same generation, * indicates $p < 0.05$, using paired samples *t*-test to compare early and late generation cultures (for the same group of cell lines [Section 2.10]). ■ = UCOE cell lines early generation, □ = UCOE cell lines late generation, ▨ = non-UCOE cell lines early generation, ▩ = non-UCOE cell lines late generation. Error bars represent the range. Overall mean values are quoted \pm SEM ($n=3$).

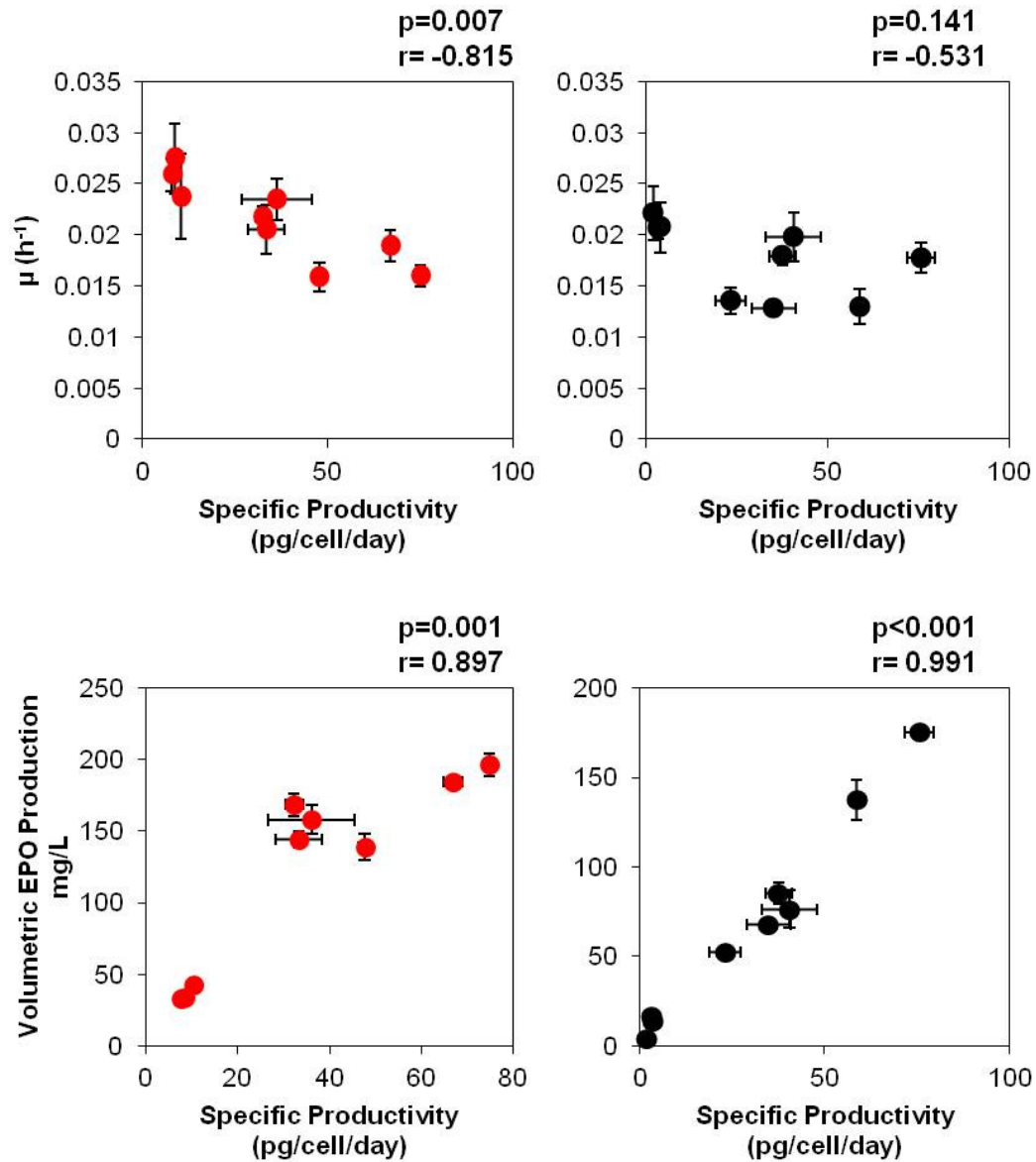
Figure 4.8: Effect of amplification and long-term culture on specific productivity in CHO-EPO cell lines.



Experimental details are described in legend to Figure 4.7. Specific productivity (Section 2.11) was assessed during the exponential phase using samples and cell counts from 48-96 hours. (A) Specific productivity for the cell lines in the presence of MTX (B) Specific productivity for the cell lines in the absence of MTX. * indicates $p < 0.05$, using independent samples *t*-test to compare UCOE and non-UCOE cell lines at same generation, * indicates $p < 0.05$, using paired samples *t*-test to compare early and late generation cultures (for the same group of cell lines [Section 2.10]).

■ =UCOE cell lines early generation, □=UCOE cell lines late generation, ▨ = non-UCOE cell lines early generation, ▩ = non-UCOE cell lines late generation. Two biological replicates were set up and errors bars represent the range. Samples were analysed in triplicate. Overall mean values quoted \pm SEM ($n=3$).

Figure 4.9: Comparison of growth rate and volumetric EPO production against the specific productivity.



Cell specific growth rate (Figure 4.6), volumetric EPO production (Figure 4.7) and specific productivity (Figure 4.8) for individual cell lines were compared in scatter diagrams. (A) Growth rate is plotted against the specific productivity, (B) Volumetric EPO production is plotted against the specific productivity. Correlation coefficients and statistical significance are noted above the scatter diagrams.

● = UCOE cell lines, ● = non-UCOE cell lines

4.2.1.3. Copy number analysis over long-term culture in amplified CHO-EPO cell lines

The number of copies of recombinant vector integrated within the host cell genome was assessed by qPCR to determine if variations in recombinant EPO production were as a result of the change in gene copy number per cell (Figure 4.10). Samples were taken at the start and end of long-term culture from the cell lines growing in the presence and absence of MTX selection.

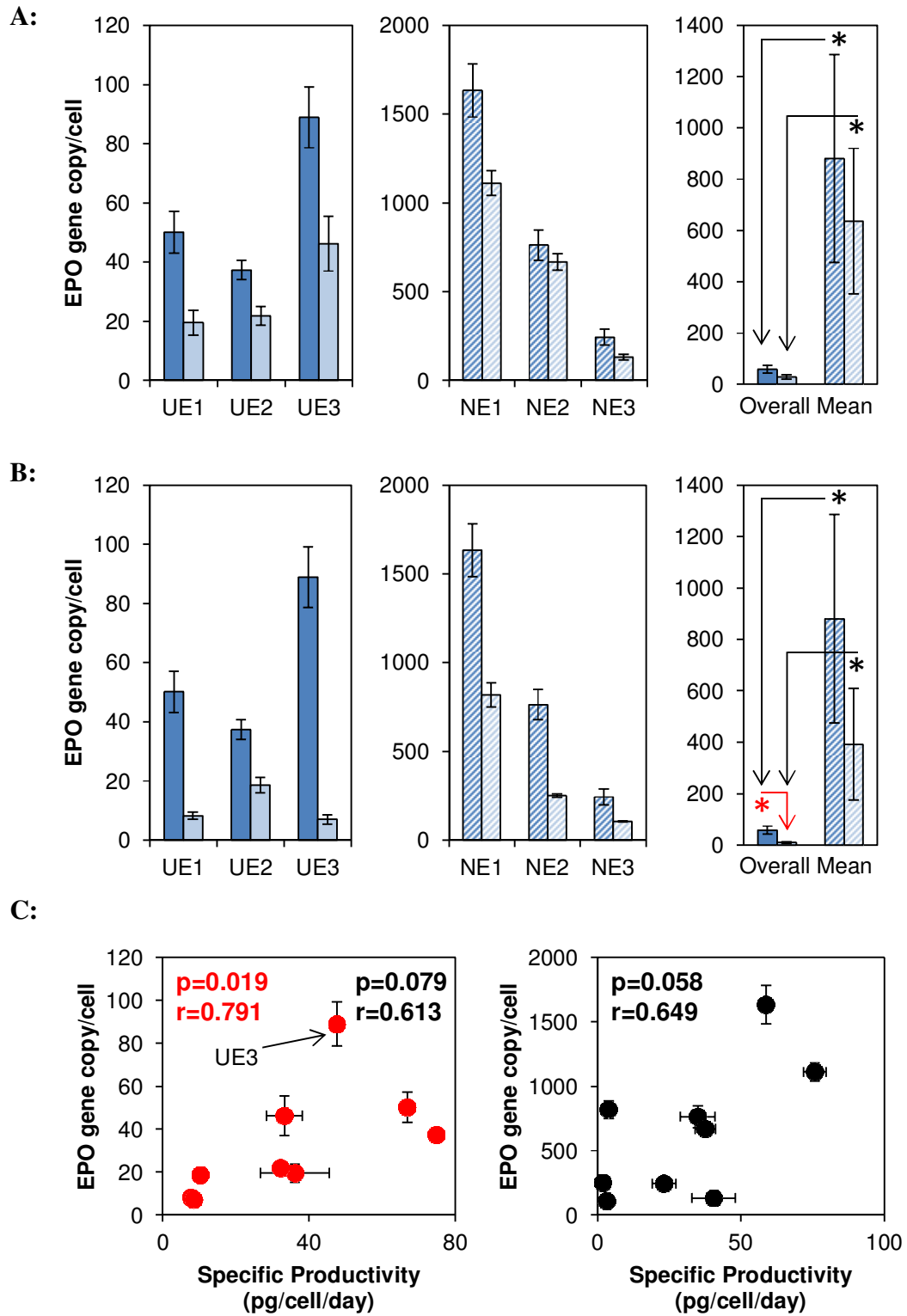
In accordance with the results depicted in Section 3.2.3, all UCOE cell lines showed lower EPO gene copy numbers compared to the non-UCOE cell lines at both early and late generations, which was also reflected in group mean values (Figure 4.10). Furthermore, a decrease in the plasmid copy number was observed in all UCOE cell lines both in the presence and absence of MTX. The decrease was more pronounced in the absence of MTX, which was also reflected in the group mean values (Figure 4.10B). The NE2 cell line showed no change in plasmid copy numbers over time, whereas a decrease was observed in NE1 and NE3 cell lines in the presence of MTX (Figure 4.10A). All non-UCOE cell lines displayed a decrease in gene copy numbers during prolonged culture in the absence of MTX. This can also be seen in group mean values. However this was not statistically significant, presumably due to large standard deviation (Figure 4.10B).

Cell lines were cultured as described in Figure 4.5. Genomic DNA were extracted from early and late generations during exponential growth (approximately 72 hours after subculture, Section 2.7.1) and EPO gene copy number was assessed by q-PCR (Section 2.7.2). Genomic DNA content was normalised using β -Actin primers specific for DNA. (A) EPO gene copy number in the presence of MTX, (B) EPO gene copy number in the absence of MTX. Error bars represent SD of three technical replicates. Overall mean values quoted \pm SEM ($n=3$). * indicates $p<0.05$, using paired samples t -test to compare early and late generation cultures (for the same group of cell lines, Section 2.10). ■=UCOE cell lines early generation, □=UCOE cell lines late generation, ▨=non-UCOE cell lines early generation, ▩=non-UCOE cell lines late generation.

(C) Specific productivity was determined as described in Figure 4.8. EPO gene copy number is plotted against the specific productivity. Correlation coefficients and statistical significance are noted above the scatter diagrams. Correlation coefficient after omitting early generation UE3 cell line is shown in red.

●=UCOE cell lines, ●=non-UCOE cell lines.

Figure 4.10: Analysis of EPO gene copy number over long-term culture in amplified CHO-EPO cell lines.



The result of the gene copy number and specific productivity is summarised in Table 4.1. The results obtained from cell lines in early generation were compared to the results of the late generation cell lines in the presence and absence of MTX. According to these results, the decrease in specific productivity in UE1 and UE3 cell lines was accompanied by a decrease in plasmid copy number, during long-term culture in the presence and absence of MTX selection. However, the UE2 cell line showed 86% loss of specific productivity, whereas the gene copy loss was only 50% at the end of long-term culture in the absence of MTX, suggesting that gene transcription or post-translational events might be accountable for loss of protein production.

Although a decrease was observed in the gene copy numbers in the NE1 and NE3 cell lines at the end of long-term culture in the presence of MTX this was not reflected in specific productivity. All non-UCOE cell lines lost their EPO production in the absence of MTX. However, as plasmid copy numbers in these cell lines remained at a reasonably high level (more than 100 copies per cell), the very low specific productivity observed in these cell lines could not be only due to gene copy loss.

Furthermore, no general correlation was observed between the gene copy number and specific productivity in either the UCOE or non-UCOE group (Figure 4.10C). Nevertheless, after omitting the early generation UE3 cell line a correlation of 0.791 was achieved in the UCOE cell lines.

Table 4.1: Effect of amplification and long-term culture on EPO gene copy number and specific productivity.

Cell Lines	Generations (+ / - MTX)	Gene copy/cell \pmSD	% Decrease in gene copy	Specific Productivity (pg/cell/day) \pmSD	% Decrease in specific productivity
UE1	Early	50.1 \pm 4.2		66.9 \pm 1.9	
	Late+MTX	19.5 \pm 4.3	61.0	36.1 \pm 9.4	46.0
	Late-MTX	8.2 \pm 1.2	83.6	7.8 \pm 1.4	88.3
UE2	Early	37.4 \pm 3.3		74.8 \pm 1	
	Late+MTX	21.8 \pm 3.2	41.5	32.3 \pm 2	56.8
	Late-MTX	18.7 \pm 2.7	50.0	10.3 \pm 0.1	86.2
UE3	Early	88.9 \pm 10.3		47.7 \pm 1.3	
	Late+MTX	46.2 \pm 9.3	48.0	33.3 \pm 4.9	30.2
	Late-MTX	7 \pm 1.5	93.0	8.5 \pm 0.6	82.1
NE1	Early	1633.1 \pm 148.6		58.7 \pm 0.6	
	Late+MTX	1111.5 \pm 71	31.9	75.7 \pm 3.9	-28.9
	Late-MTX	817.4 \pm 68.7	49.9	3.8 \pm 0.01	93.5
NE2	Early	763.2 \pm 85.2		35 \pm 6.1	
	Late+MTX	668.2 \pm 39.2	12.4	37.6 \pm 3.6	-7.4
	Late-MTX	252.4 \pm 9.7	66.9	1.9 \pm 0.5	94.6
NE3	Early	244.3 \pm 45.3		23.2 \pm 4.2	
	Late+MTX	131.6 \pm 15.7	46.0	40.5 \pm 7.6	-74.6
	Late-MTX	106.2 \pm 3.4	56.5	3.2 \pm 0.01	86.0

Summary of EPO gene copy number (Figure 4.10) and specific productivity (Figure 4.8) for individual cell lines. The % decrease values were calculated by comparing the results obtained from cell lines at late generation either with or without MTX selection to the results of early generation cell lines.

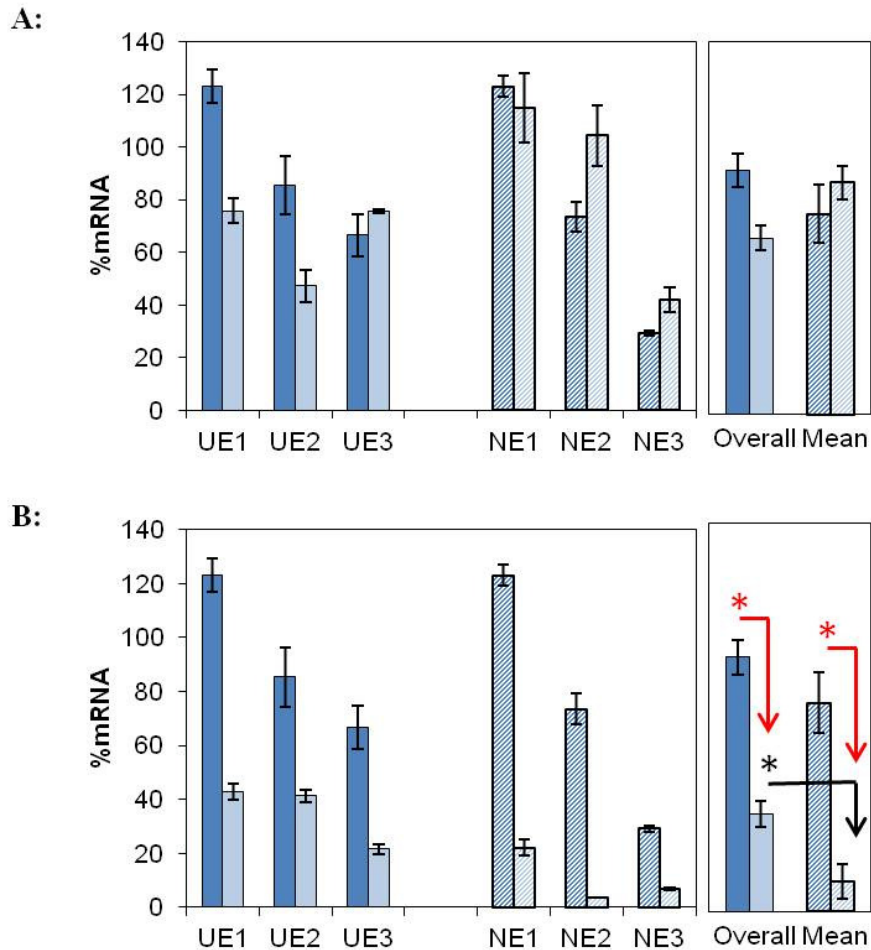
4.2.1.4. Analysis of EPO mRNA over long-term culture in amplified CHO-EPO cell lines

EPO mRNA expression was assessed by q-RT PCR to examine if the differing levels of protein production were due to changes in EPO gene transcription or if post-translational events were responsible (Figure 4.11).

The UCOE and non-UCOE cell lines showed a similar amount of EPO mRNA expression in the presence of MTX (Figure 4.11A, Table 4.2). The relative mRNA expression was significantly higher in the UCOE cell lines compared to the non-UCOE group after 77 days in the absence of MTX (Figure 4.11B, Table 4.2). However, despite having similar or higher level of mRNA expression, the UCOE cell lines had lower gene copies per cell compared to the non-UCOE cell lines, suggesting that UCOE provides higher transcriptional activity, in agreement with the results presented in Section 3.2.4 (Table 4.2).

The UE1 and UE2 cell lines showed a decrease in EPO mRNA expression over prolonged culture in the presence of MTX, whereas mRNA expression remained constant in the UE3 and NE1 cell lines (Figure 4.11A). In contrast, an increase in mRNA expression was observed in the NE2 and NE3 cell lines over long-term culture in the presence of MTX (Figure 4.11A). All cell lines displayed a decrease in EPO mRNA expression when MTX selection was removed. However, the UCOE cell lines still had higher mRNA expression than the non-UCOE cell lines at the end of long-term culture.

Figure 4.11: Analysis of EPO mRNA expression over long-term culture in amplified CHO-EPO cell lines.



Cell lines were cultured as described in Figure 4.5. RNA samples were isolated at early and late generations during exponential growth (approximately 72 hours after subculture, Section 2.6.1) and EPO mRNA expression was assessed by q-PCR (Section 2.6.5). Samples were normalised using mRNA β -Actin primers (A) EPO mRNA in the presence of MTX, (B) EPO mRNA in the absence of MTX. ■ =UCOE cell lines early generation, □ =UCOE cell lines late generation, ▨ = non-UCOE cell lines early generation, ▩ = non-UCOE cell lines late generation. Error bars represent SD of three technical replicates. Overall mean values quoted \pm SEM ($n=3$). * indicates $p<0.05$, using independent samples t-test to compare UCOE and non-UCOE cell lines at same generation, * indicates $p<0.05$, using paired samples t-test to compare early and late generation cultures (for the same group of cell lines [Section 2.10]).

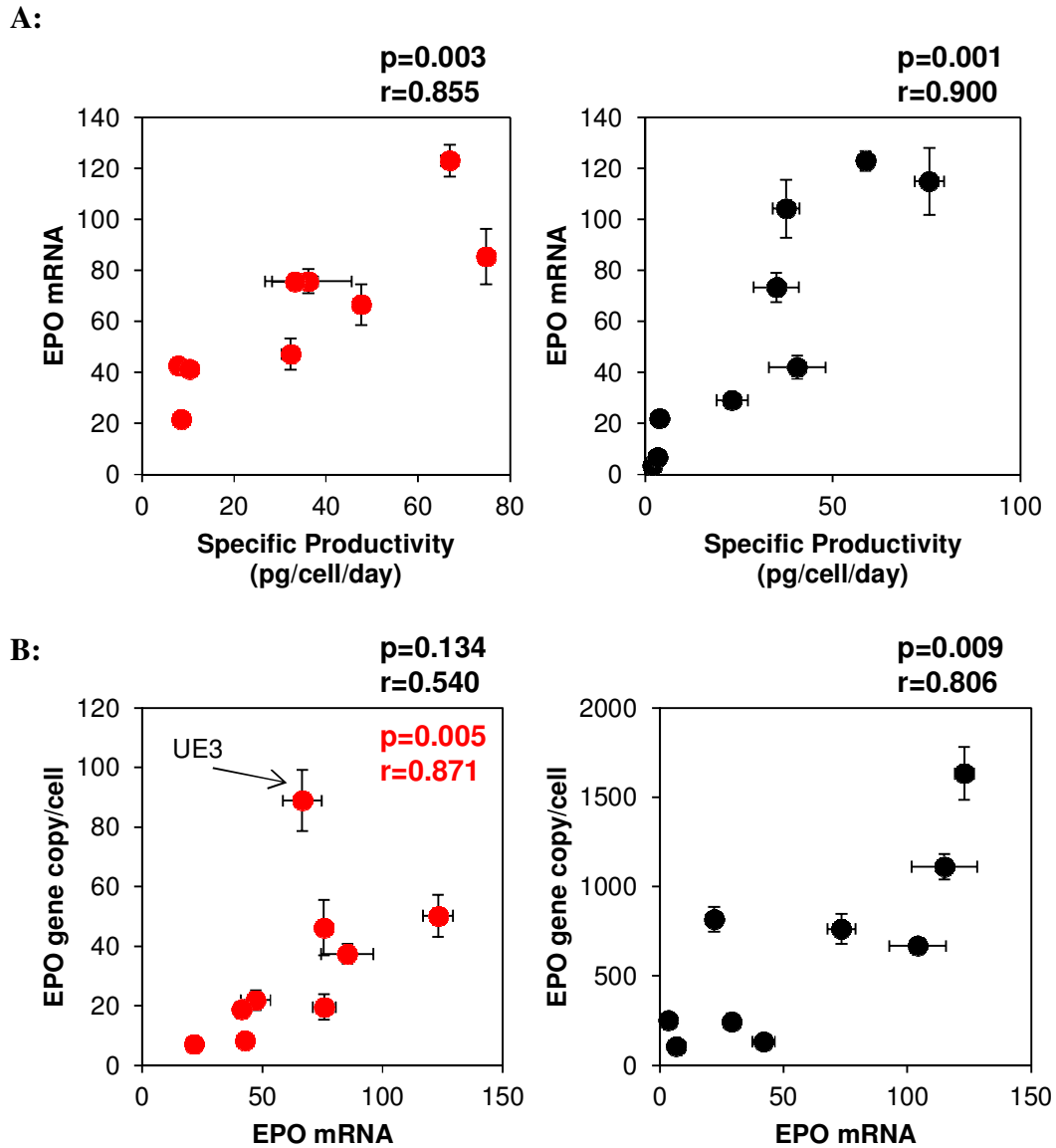
Table 4.2: Summary of EPO gene copy number per cell and relative amount of EPO mRNA.

Cell Lines	Generations (+ / - MTX)	Gene copy/cell \pmSD	% EPO mRNA \pmSD
UE1	Early	50.1 \pm 4.2	123.1 \pm 6.3
	Late+MTX	19.5 \pm 4.3	75.7 \pm 4.7
	Late-MTX	8.2 \pm 1.2	42.7 \pm 3
UE2	Early	37.4 \pm 3.3	85.4 \pm 10.9
	Late+MTX	21.8 \pm 3.2	47.2 \pm 6.2
	Late-MTX	18.7 \pm 2.7	41.4 \pm 2.2
UE3	Early	88.9 \pm 10.3	66.6 \pm 8
	Late+MTX	46.2 \pm 9.3	75.6 \pm 0.6
	Late-MTX	7 \pm 1.5	21.59 \pm 1.8
NE1	Early	1633.1 \pm 148.6	123 \pm 3.9
	Late+MTX	1111.5 \pm 71	114 \pm 13.1
	Late-MTX	817.4 \pm 68.7	21.9 \pm 3
NE2	Early	763.2 \pm 85.2	73 \pm 5.8
	Late+MTX	668.2 \pm 39.2	104.3 \pm 11.4
	Late-MTX	252.4 \pm 9.7	3.5 \pm 0.1
NE3	Early	244.3 \pm 45.3	29.1 \pm 1
	Late+MTX	131.6 \pm 15.7	41.9 \pm 4.6
	Late-MTX	106.2 \pm 3.4	6.73 \pm 0.3

Summary of EPO gene copy number (Figure 4.10) and EPO mRNA content (Figure 4.11) for individual cell lines.

mRNA expression was strongly correlated with specific productivity in both UCOE and non-UCOE cell lines (Figure 4.12A). However, no general correlation was observed between the gene copy number and mRNA expression in the UCOE cell lines (Figure 4.12B). A strong positive correlation was achieved by omitting the early generation UE3 cell line. The non-UCOE cell lines showed a relatively strong correlation between the gene copy number and mRNA expression.

Figure 4.12: Comparison of specific productivity and EPO gene copy number against mRNA expression.



Specific productivity (Figure 4.8) and EPO gene copy number (Figure 4.10) is compared against EPO mRNA expression (Figure 4.11) for individual cell lines. (A) Scatter diagram comparing EPO mRNA and specific productivity, (B) Scatter diagram comparing EPO mRNA and EPO gene copy number. Correlation coefficients and statistical significance are noted above the scatter diagrams. The red note indicates the correlation after omitting UE3 cell line. ● = UCOE cell lines, ● = non-UCOE cell lines.

Figure 4.13 summarizes the effect of long-term culture on protein productivities and genetic parameters in both UCOE and non-UCOE cell lines. The results suggest that in the UE1 cell line the loss of productivity was mainly due to the loss of gene copies in the presence of MTX, which was mirrored by a decrease in EPO mRNA expression (Figure 4.13A). This cell line showed further loss of productivity together with EPO gene copies and mRNA expression in the absence of MTX. The decrease in mRNA expression was less pronounced than the productivity and gene copy loss. The UE2 cell line also showed a decrease in specific productivity over long-term culture in the presence of MTX, which was reflected in EPO mRNA and the gene copy number. Moreover, although this cell line showed similar mRNA expression and gene copy numbers at the end of prolonged culture in the presence and absence of MTX, the specific productivity was lower in the late generation cell line without MTX selection. The UE3 cell line showed a loss of protein production over time in the presence of MTX, which was reflected in the gene copy numbers, but the mRNA expression did not change. Therefore, these observations may suggest that translation and secretion of the correctly folded protein is a further obstacle in case of complicated products like EPO. Furthermore, the loss of productivity observed in the UE3 cell line occurred in unison with a loss of gene copy and mRNA expression in the absence of MTX.

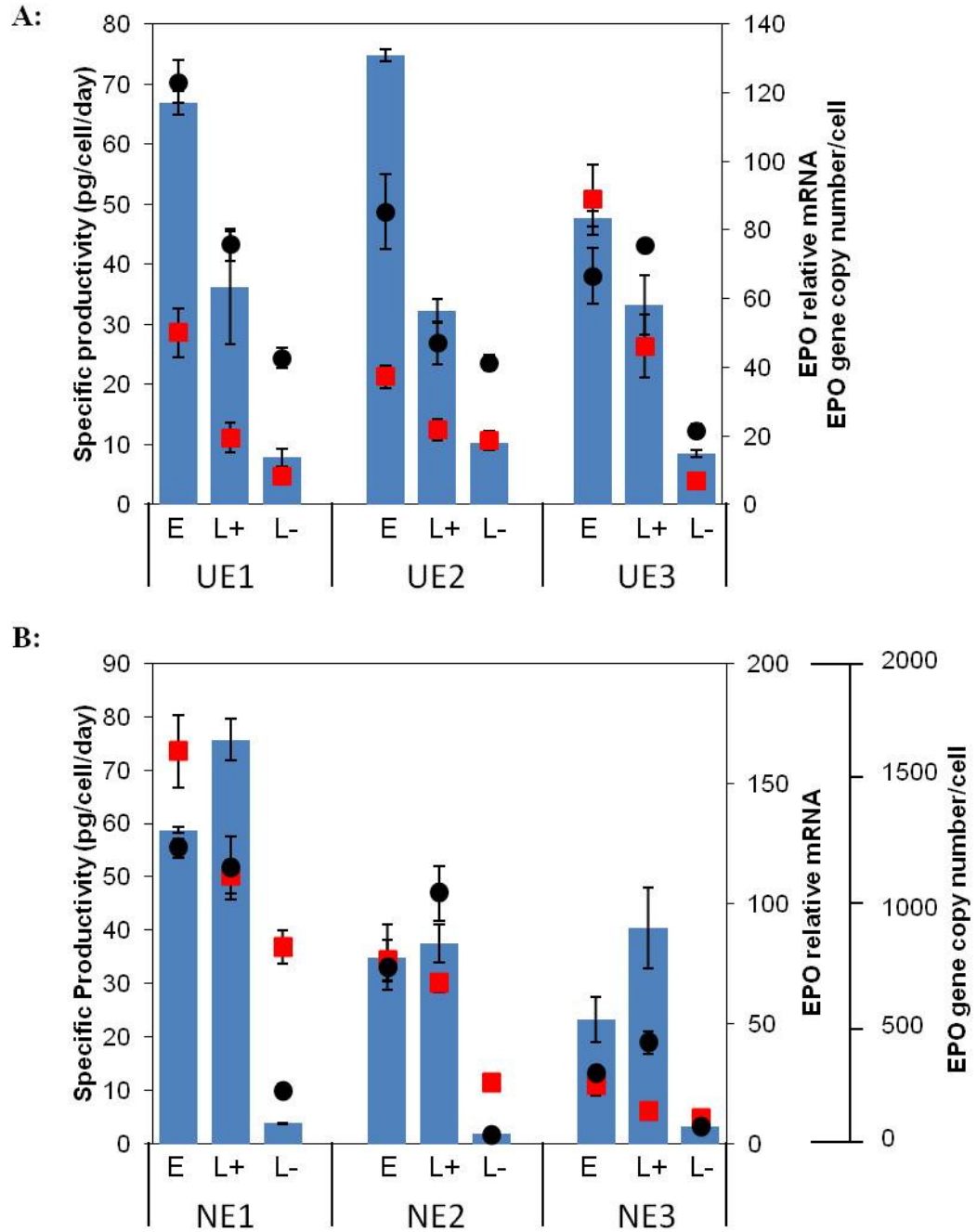
Among the non-UCOE cell lines, the NE1 cell line showed a decrease in gene copy number while mRNA expression remained constant and specific productivity increased over time in the presence of MTX (Figure 4.13B). This may suggest that the loss of gene copy occurred in transcriptionally passive sites. Further decrease in protein production was observed in the absence of MTX, which was reflected in loss of mRNA expression. However, the gene copy number was still relatively high suggesting that some epigenetic silencing might be taking place in the absence of MTX. The NE2 cell line showed stable productivity and relatively constant gene copy numbers over long-term culture in the presence of MTX, whereas an increase in mRNA expression was observed. This may suggest that the EPO genes are in a transcriptionally more active state at the end of long-term culture; however the cell line is experiencing a problem during translation. The specific productivity decreased significantly over time in the absence of MTX, which was

accompanied by a decrease in mRNA expression. A further loss of EPO gene copy was also observed in the absence of MTX but gene copy loss was not proportional to the change in protein production and mRNA expression, suggesting that the NE2 cell line also might be experiencing some gene silencing in the absence of MTX. Although the NE3 cell line showed a decrease in gene copy number over time in the presence of MTX, mRNA expression and protein production increased over long-term culture, suggesting that the remaining EPO genes are in a more active state. This cell line showed significant loss of specific productivity during prolonged culture in the absence of MTX together with EPO mRNA expression and gene copy numbers. These findings will be discussed in Section 4.3.

The specific productivity was assessed as described in Figure 4.8. EPO gene copy number (Figure 4.10) and mRNA expression (Figure 4.11) were determined as described in Sections 2.7 and 2.6 respectively. The specific productivity is plotted against relative EPO mRNA and gene copy number. Results obtained from cell lines at early generation (E), late generation with MTX (L+) and late generation in the absence of MTX selection (L-) compared to each other in (A) UCOE cell lines and (B) non-UCOE cell lines.

■ = Protein, ● = mRNA, ■ = Gene copy number

Figure 4.13: Changes to the molecular characteristics during long-term culture in amplified CHO-EPO cell lines.



4.3. Discussion

It was shown in Chapter 3 that the inclusion of UCOE in expression constructs provide better growth characteristics in the presence of MTX selection. The main priority in recombinant protein production is to obtain the maximum volumetric production. To achieve high volumetric production it is desirable to develop cells that can grow to high maximum cell densities and hopefully show high specific productivity. The results presented here demonstrate that volumetric production can be improved by using UCOEs in combination with MTX-mediated gene amplification.

In accordance with the results denoted in Chapter 3, the UCOE cell lines displayed significantly higher levels of EPO expression than the non-UCOE cell lines (Section 4.1). In order to address the stability of recombinant protein production, cell lines were subcultured continuously for up to 77 days (Section 4.1.1). The results showed that the UCOE cell lines maintained a stable and high volumetric production over long-term culture, whereas two of the non-UCOE cell lines displayed a decrease in volumetric EPO production at the end of prolonged culture. Furthermore, cell lines containing the UCOE element showed significantly higher cell specific productivity than the non-UCOE cell lines. Specific productivity was stable for up to 77 days in the UCOE cell lines. In contrast, a decrease in the cell specific productivity was observed in two of the non-UCOE cell lines. The cell growth rates were found to be similar in both the UCOE and non-UCOE cell lines at the beginning of long-term culture. As the cells aged over time, the growth profile of these cultures changed in both the UCOE and non-UCOE cell lines. It was shown that cells in late generation exhibited a longer stationary phase and a sudden decrease in viable cell densities was observed at day 9. This was presumably as a result of depletion of key nutrients. No clear correlation was found between the cell specific productivity and the cell growth rate in either the UCOE or non-UCOE cell lines. The proportional increase in the specific productivity and volumetric production suggested that the growth rate did not affect the volumetric productivity.

The top 10 cell lines that displayed the highest volumetric EPO production from each group were pooled and treated with 250nM MTX. In contrast to the results depicted in Chapter 3, where the UCOE cell lines displayed lower eGFP fluorescence than the non-UCOE cell lines, the results here showed that the volumetric EPO production was significantly higher in the UCOE group (Section 4.2). It has been reported that GFP can be toxic to cells that constantly express this protein (Liu et al., 1999). In fact, a previous study conducted in our laboratory showed that cells expressing very high levels of eGFP displayed crystals of eGFP protein when observed using immunofluorescent microscopy (Croxford, 2008). This may suggest that the UCOE cell lines that express high levels of eGFP did not survive during the amplification process, as such high levels of intracellular protein may be detrimental to the cell line. Although this discrepancy still remains unexplained, it is also plausible that this is a consequence of intracellular processing of eGFP at high concentrations. These findings indicate that it can be misleading to use an intracellular protein such as GFP to assess a process that is in the end going to be used to produce a secreted protein. This was a major reason to extend the current study to examine the manner in which EPO expression reflected that of GFP.

The results presented in this chapter demonstrate that despite the lower number of gene copies per cell (Section 4.2.1.3), the UCOE cell lines displayed significantly higher volumetric EPO production than the non-UCOE cell lines following MTX amplification (Section 4.2.1.2). It was also shown that the transcriptional activity per gene copy was greater in the UCOE cell lines compared to the non-UCOE group (Section 4.2.1.4). This is consistent with the results obtained in Chapter 3.

As demonstrated in Chapter 3, the growth analysis showed that the UCOE cell lines reached higher maximum cell densities than the non-UCOE cell lines when MTX was present (Section 4.2.1.1). This was also observed in the CCT values, where the UCOE cell lines displayed higher CCTs. The cell specific growth rates were also found to be significantly higher in the UCOE cell lines. These findings support the suggestion made in Chapter 3 that the UCOE cell lines have a higher tolerance to MTX than the non-UCOE group. The growth characteristics of individual cell lines were evaluated at the beginning

and end of long-term culture in the presence and absence of MTX. The results demonstrated that both the UCOE and non-UCOE cell lines displayed an increase in viable cell densities and CCTs at the end of long-term culture in the presence and absence of MTX, which further corroborates the results presented in Chapter 3. Furthermore, an increase in the growth rate was observed over prolonged culture in both the UCOE and non-UCOE groups in the presence and absence of MTX. However, the growth rate of UCOE cell lines was still significantly higher than that of non-UCOE cell lines at the end of long-term culture in both conditions (+/- MTX). As explained in Chapter 3, cells that are exposed to continuous MTX pressure may develop alternative resistance to MTX (Section 1.2.3.2.2) (Kim et al., 2001). It has also been reported that despite clonally derivation using limiting dilution cloning, cell populations can become quite heterogenous in terms of growth rate and productivity following MTX amplification (Kim et al., 1998a, Kim and Lee, 1999, Kim et al., 2001). Therefore, it is likely that a cell population that was growing more quickly became dominant during long-term culture, which may result in the higher growth rate and viable cell densities that were observed at the end of long-term culture.

A relatively strong negative correlation between the growth rate and the cell specific productivity was observed in the UCOE cell lines. Conversely, no consistent correlation existed between the growth rate and the cell specific productivity in the non-UCOE group.

The UCOE cell lines displayed higher specific productivities than the non-UCOE cell lines at early generation. Although the UCOE cell lines showed a decrease in cell-specific productivity over prolonged culture in the presence of MTX, this did not outweigh its beneficial effect on the overall productivity. The UCOE cell lines showed stable and high levels of volumetric EPO production for up to 77 days in the presence of MTX. This was due to the better growth characteristics they displayed when MTX selection was present. A strong positive correlation was observed between the specific productivity and volumetric production in both the UCOE and non-UCOE groups. The cell-specific and volumetric productivity decreased in both the UCOE and non-UCOE cell lines in the absence of MTX. However, the specific productivity and volumetric EPO production was still significantly higher in the UCOE cell lines compared to the non-UCOE group.

In order to understand the changes in the cell specific productivity over long-term culture, the EPO gene copy number and the mRNA content were analysed at the beginning and end of prolonged culture. According to the results, the loss of specific productivity in the UE1 and UE2 cell lines in the presence of MTX was as a result of a decline in the EPO gene copies which was also mirrored by a decrease in EPO mRNA expression. The UE3 cell line had a smaller decrease in cell specific productivity in the presence of MTX. This cell line displayed similar amounts of EPO mRNA content at the beginning and end of long-term culture when MTX was present. Therefore, it is possible that the decrease in specific productivity is as a consequence of problems in other areas of protein production such as translation and post-translational events (Pendse et al., 1992, Schröder and Friedl, 1997, Lattenmayer et al., 2007b). The UE1 and UE2 cell lines showed more than an 86% loss of productivity after 77 days of culture in MTX-free medium. These cell lines also showed a decrease in EPO gene copies per cell in the absence of MTX (83%, 50%, UE1 and UE2 respectively). However, both the UE1 and UE2 cell lines still had relatively high mRNA contents, suggesting that translation and secretion of a complicated product like EPO is a further impediment in the production of recombinant protein production (Schröder and Friedl, 1997, Pendse et al., 1992, Lattenmayer et al., 2007b). The loss of productivity was as a result of gene copy loss in the UE3 cell line in the absence of MTX, as productivity, EPO gene copy number and mRNA content decreased concurrently (Fann et al., 2000, Hammill et al., 2000, Kim et al., 1998b, Pallavicini et al., 1990, Weidle et al., 1988). These results suggest that even though UCOE provides resistance to gene-silencing mechanisms, UCOE-containing cell lines are still prone to instability due to gene copy loss or other mechanisms involved in protein production such as translation, folding or secretion of recombinant protein. Therefore, when using UCOE in combination with MTX amplification for the creation of recombinant cell lines, screening over long-term culture may still be required.

The non-UCOE cell lines were more heterogeneous in terms of their response to long-term culture in the presence of MTX. All three cell lines showed different levels of productivity, gene copy number and mRNA content. Previous studies have also reported that despite

being derived from a single clone, cell lines can become quite heterogeneous following MTX amplification (Kim et al., 2001, Kim et al., 1998a, Kim and Lee, 1999, Yoshikawa et al., 2000b, Yoshikawa et al., 2000a). All non-UCOE cell lines had reduced productivity over long-term culture in the absence of MTX, with a~90% decrease in productivity, which contrasted with a ~50% loss of gene copy that was observed in the absence of MTX. This suggests that it is not possible to attribute gene copy loss to the very low level of productivity in these cell lines, as they still contained more than 100 gene copies per cell. Therefore, it can be suggested that these cell lines are experiencing some gene silencing after removal of MTX selection.

4.3.1. Summary

These findings confirm that UCOEs within the expression construct provide a high level of cell-specific productivity and volumetric production of secreted recombinant protein following MTX-mediated gene amplification. However, instability of protein production was observed during long-term culture in the absence of MTX. Volumetric EPO production was stable for up 77 days in the presence of MTX. It has also been demonstrated that UCOEs confer higher transcriptional activity per gene copy, as shown by the mRNA and gene copy number analysis.

CHAPTER 5:

Results-3

In Chapter 3, eGFP expression in amplified CHO-GFP cell lines was investigated over long-term culture in the presence and absence of MTX selection. eGFP expression and the stability of expression during long-term culture was found to be variable between UCOE and non-UCOE cell lines. Furthermore, protein expression and stability of the cell lines was not simply correlated with recombinant gene copy number. As an extension from these findings, chromosome painting (to define molecular karyotype) and FISH (to define chromosomal localisation of recombinant genes) were performed. These approaches were developed to provide a molecular analysis of the manner in which the location of amplified genes might relate to the differential productivity and stability of amplified cell lines. As the UCOE cell lines showed higher mRNA expression, even though they contained fewer plasmid copies than non-UCOE cell lines, it was hypothesised that the studies would also provide an insight into the chromosomal positions that might be potential hotspots. The studies described below focused on 3 UCOE (U1, U2 and U3) and 3 non-UCOE (N1, N2 and N4) cell lines and defined their chromosomal profile at the start and end of long-term culture, both in the presence and absence of MTX. These cell lines were fully characterised in Chapter 3 in terms of recombinant protein production and stability of expression over long-term culture.

5.1. Effect of amplification and long-term culture on chromosome number

In order to analyse the chromosome number distribution in amplified CHO-GFP cell lines, metaphase spreads were prepared for each cell line at early and late generations with cells cultured in the presence and absence of MTX. The chromosome numbers were counted in 20 metaphase spreads for each cell line and the frequency of chromosome number distribution is shown in Figure 5.1. The majority of the non-transfected parental DG44 cells contained 20 chromosomes (Figure 5.1A). Although some of the UCOE cell lines contained 18, 19 or 21 chromosomes, the majority of them contained the median number of chromosomes (20) observed in the parental cell population (Figure 5.1B). However, the chromosome number distribution was more diverse in the non-UCOE cell lines (particularly N2 and N4, Figure 5.1C). Moreover, all non-UCOE cell lines contained some

abnormal chromosomes (>30 chromosomes). In the N2 cell line, the frequency of cells containing more than 30 chromosomes decreased over long-term culture in both the presence and absence of MTX. Metaphase spreads containing 34 and 35 chromosomes were observed on a number of occasions in the late generation N4 cell lines growing in the presence of MTX, whereas these were not observed when cells had been cultured in the absence of MTX. The frequency of cells containing 20 chromosomes increased over time both in the presence and absence of MTX in all non-UCOE cell lines. UCOE cell lines retained the same profile of chromosomes over long-term culture both in the presence and absence of MTX.

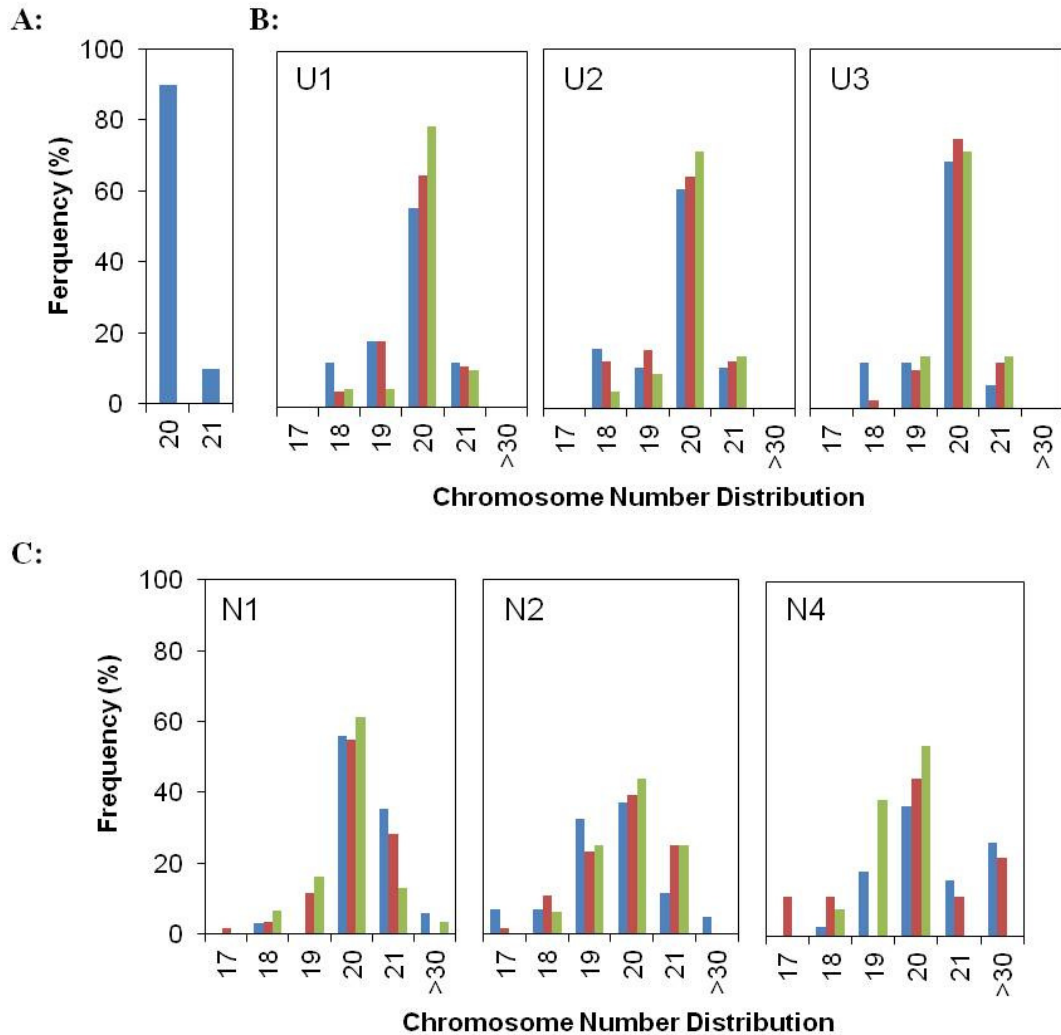
5.2. Analysing plasmid localization using dual colour FISH

In order to investigate the chromosome-specific localization of plasmid integration sites, dual colour FISH with Chinese hamster chromosome painting probes and plasmid probes were performed (Section 2.9). Metaphase spreads of early generation U2 and N2 cell lines were used as examples of each cell group.

Chinese hamster (*Cricetulus griseus*) chromosome-specific paints were provided by Dr. Willem Rens (University of Cambridge) (Rens et al., 2006). Briefly, chromosomes of Chinese hamster were prepared from a fibroblast cell line. Chinese hamster chromosomes were flow-sorted and chromosome-specific paints were generated from flow-sorted chromosomes by using DOP-PCR (Rens et al., 2006, Yang et al., 2000).

Although derived from *C. griseus*, the genome of DG44 cells is highly rearranged, resulting in an altered karyotype compared to Chinese hamster cells (Derouazi et al., 2006). Therefore, it was not possible to construct a karyotype for the cell lines used in this study. Instead, metaphase spreads of the parental DG44 cells were prepared and stained with DAPI and chromosomes of a typical spread of the parental DG44 cells were organised into groups in terms of size and centromere position to classify the hybridization of paint probes and plasmid integration types observed in the amplified cell lines (Figure 5.2).

Figure 5.1: Investigating chromosome number distribution over long-term culture in amplified CHO-GFP cell lines

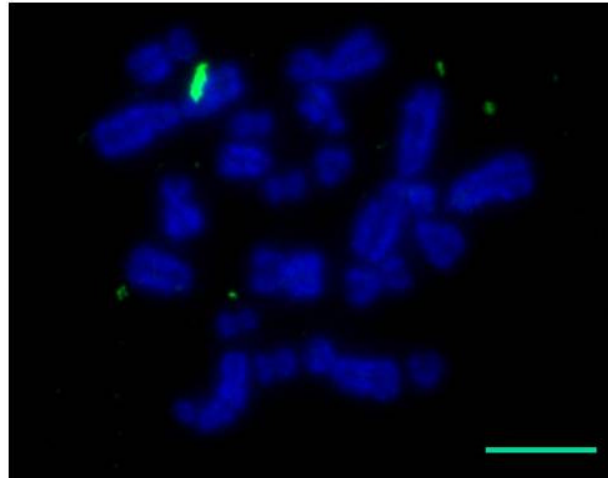


Metaphase spreads were prepared for 3 UCOE and 3 non-UCOE cell lines (Section 2.8.1), and slides were stained with 20ng/ml DAPI (Section 2.8.5). Slides were viewed using an Olympus Widefield fluorescent microscope, using the 100x oil immersion objective and images were captured using MetaVue software (Section 2.9.5). 20 images were taken for each cell line. Frequency of chromosome number distribution in individual (A) DG44, (B) UCOE and (C) non-UCOE cell lines are shown.

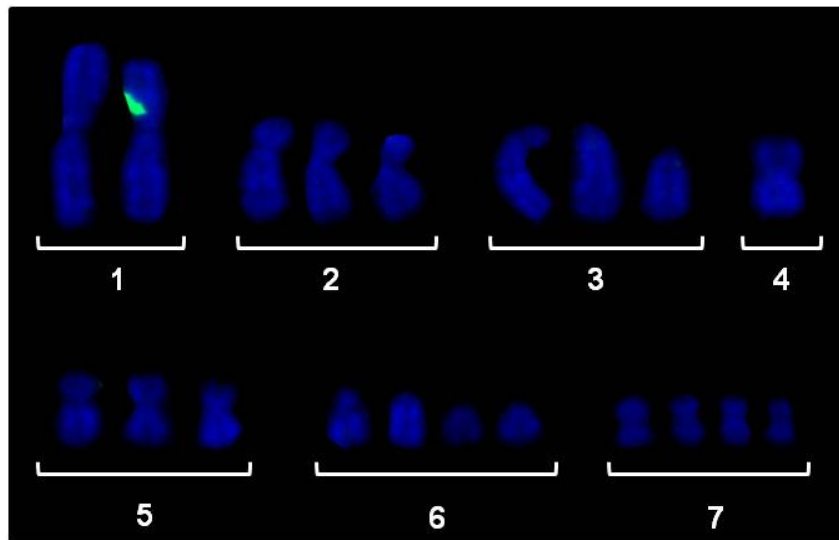
■ = Early generation in the presence of MTX, ■ = Late generation in the presence of MTX, ■ = Late generation in the absence of MTX.

Figure 5.2: Karyotype of CHO-DG44 parental cell line

A:



B:



Chromosome spreads of DG44 cells were prepared (Section 2.8.1), and slides were stained with 20ng/ml DAPI (Section 2.8.5). Slides were viewed using an Olympus Widefield fluorescent microscope, using the 100x oil immersion objective and images were captured using MetaVue software (Section 2.9.5) (A) Metaphase spread of DG44 cell line. (B) Chromosomes in (A) have been arranged into identifiable groups: 1- Long; 2- Medium size, centromere off centre; 3- Medium size, centromere top; 4- Medium size, centromere centre; 5- Small, centromere centre/off-centre; 6- Small, centromere top; 7- Very Small. White scale bar (bottom right) = 10 μ m.

10 to 20 metaphase spreads were observed for each cell line. When Chinese hamster chromosome-specific paints were hybridized onto the chromosomes of U2 and N2 cell lines, paints 4 and 6 (generated from DNA of chromosome 4 or 6 of Chinese hamster, respectively) painted a single region in a group-3 chromosome (Figures 5.3A, 5.3B, 5.4-7). Furthermore, chromosome paint 7 hybridized to two of the group-3 chromosomes (Figures 5.3C, 5.8 and 5.9), chromosome paint x and y painted three group-7 chromosomes. Hybridization to a single region in a group-5 and a group-6 chromosome was also observed with paint x and y probe (Figures 5.3D, 5.10 and 5.11).

For the N2 cell line, one metaphase spread showed co-localization of paint-7 and the inserted plasmid (Figure 5.3C and 5.7A). The majority of the remaining metaphase spreads contained integration into a group-1 chromosome, which is analysed in more detail in Section 5.3. In cell line U2, plasmid integration sites were localized mainly on a group-2 chromosome (Section 5.3). On a number of occasions, inserted plasmid was localized on chromosomes painted with chromosome 6, 7 and xy probes (Figures 5.7B, 5.9C and 5.11C).

Metaphase spreads were prepared for U2 (UCOE containing) and N2 (non-UCOE) cell lines (Section 2.8.1). Dual color FISH was performed using chromosome-specific paints generated from Chinese hamster (C. griseus) cells labeled with Biotin-16-dUTP and p1010-GFP plasmid labeled with digoxigenin as probes. (Section 2.9.1, 2.9.2). Slides were counterstained with DAPI (Section 2.9.4). Slides were viewed using an Olympus Widefield fluorescent microscope, using the 100x oil immersion objective, and images were captured using MetaVue Software (Section 2.9.5). 10-20 images were taken for each cell line. Yellow signal shows the plasmid integration site and regions in red are those hybridized with a chromosome paint prepared from Chinese hamster cells. Chromosomes for N2 (i) and U2 (ii) cell line have been hybridized with;

(A) Chromosome 4 paint in Figure 5.4A (N2) and 5.5A (U2) ;

(B) Chromosome 6 paint in Figure 5.6A (N2) and 5.7A (U2) ;

(C) Chromosome 7 paint in Figure 5.8A (N2) and 5.9A (U2) ;

(D) Chromosome x and y paint in Figure 5.10A (N2) and 5.11A (U2) have been arranged into identifiable groups

Yellow arrows indicate plasmid integration sites, red arrows indicate hybridization with chromosome paint probes. White scale bar (bottom right) equals 10 μ m.

Figure 5.3: Plasmid localization in amplified CHO-GFP cell lines

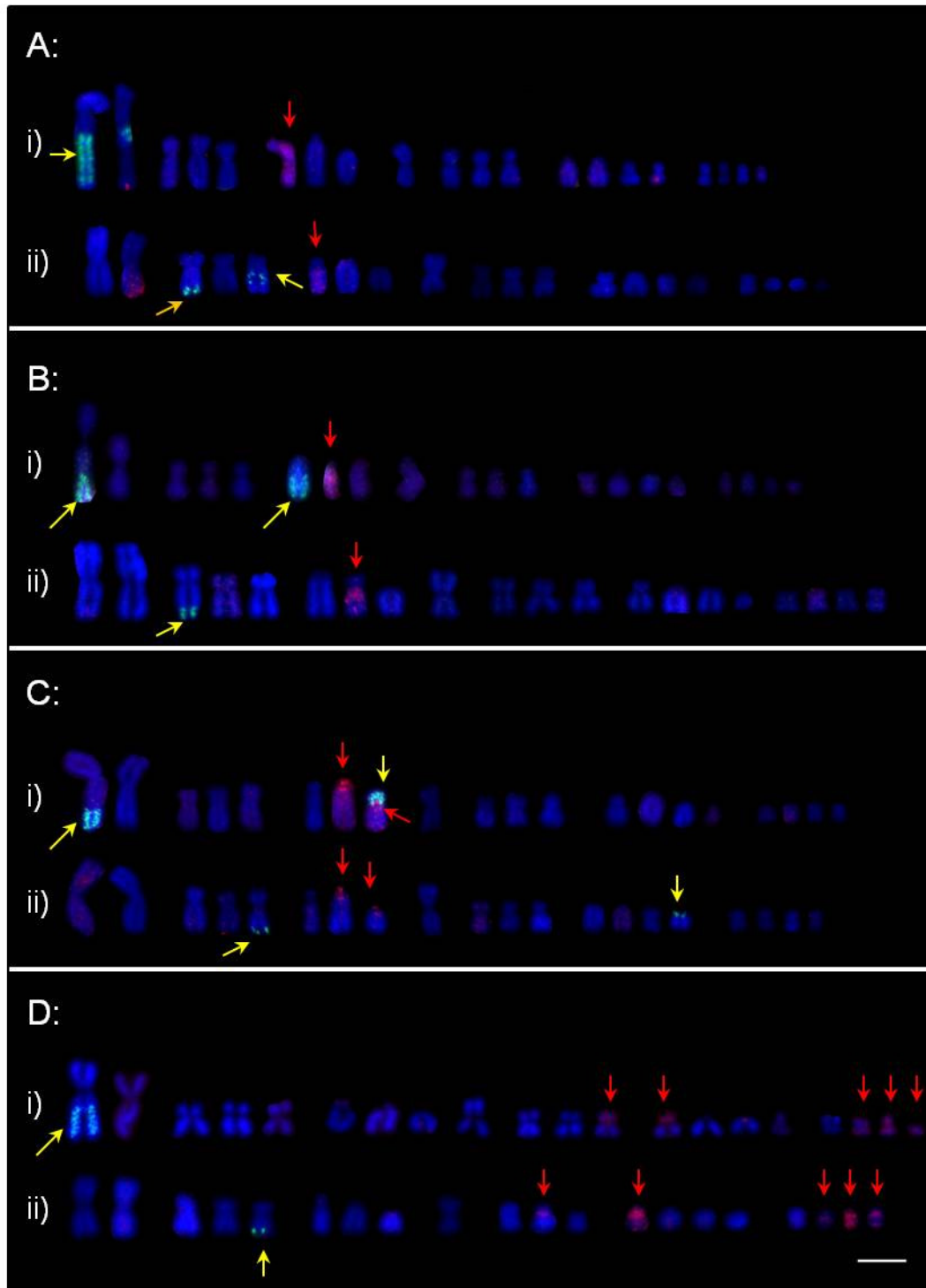
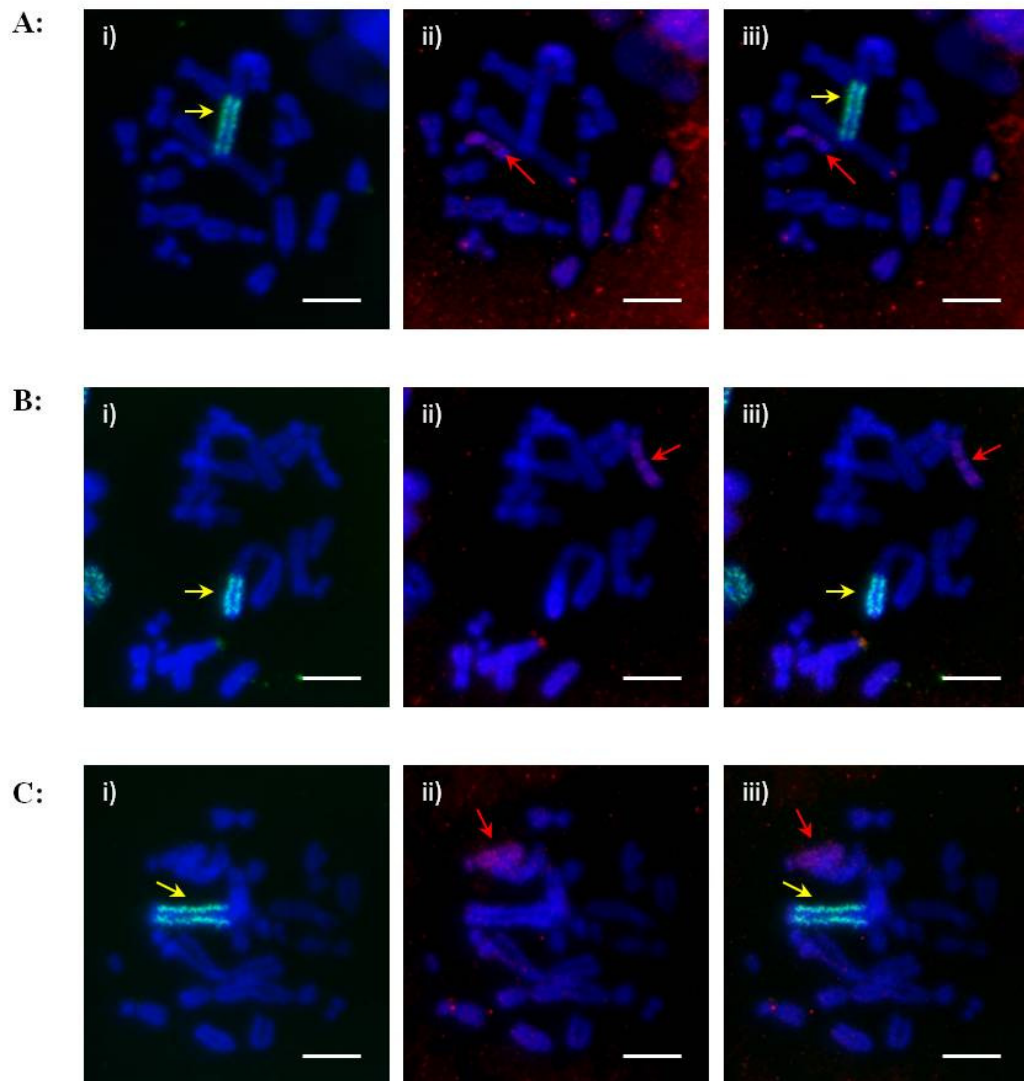
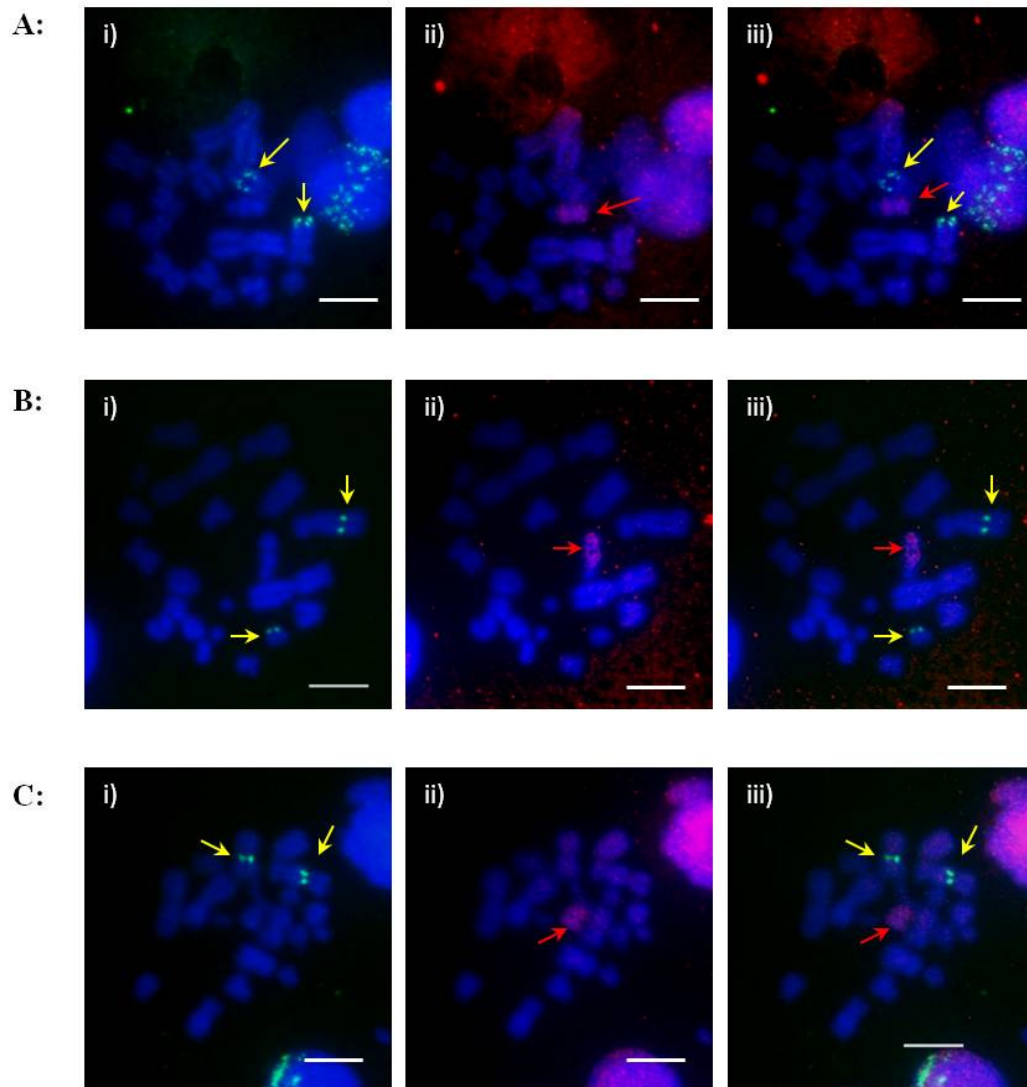


Figure 5.4: Plasmid localization and chromosome 4 hybridization observed for N2 cell line



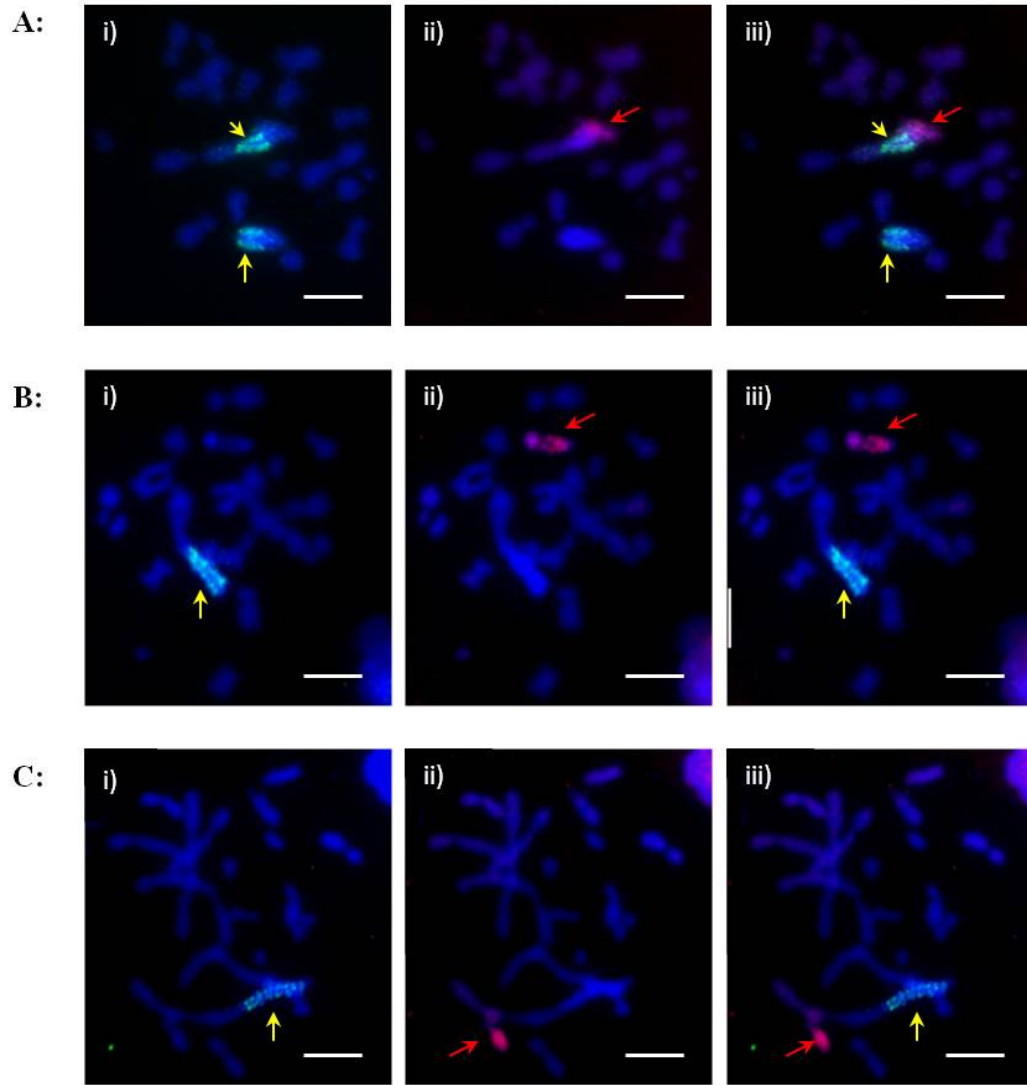
Experimental details are described in the legend to Figure 5.3. (A), (B), (C) FISH images of three different metaphase spreads of N2 cell line hybridized with chromosome 4 paint and plasmid probes are shown. Yellow signal shows the plasmid integration site (indicated by yellow arrows) and regions in red are those hybridized with a painting probe prepared from Chinese hamster cells chromosome 4 (indicated by red arrows). White scale bar (bottom right) equals 10 μ m. (i) Hybridization with plasmid probe only; (ii) hybridization with chromosome paint probe only; (iii) Dual color FISH (merged) image

Figure 5.5: Plasmid localization and chromosome 4 hybridization observed for U2 cell line



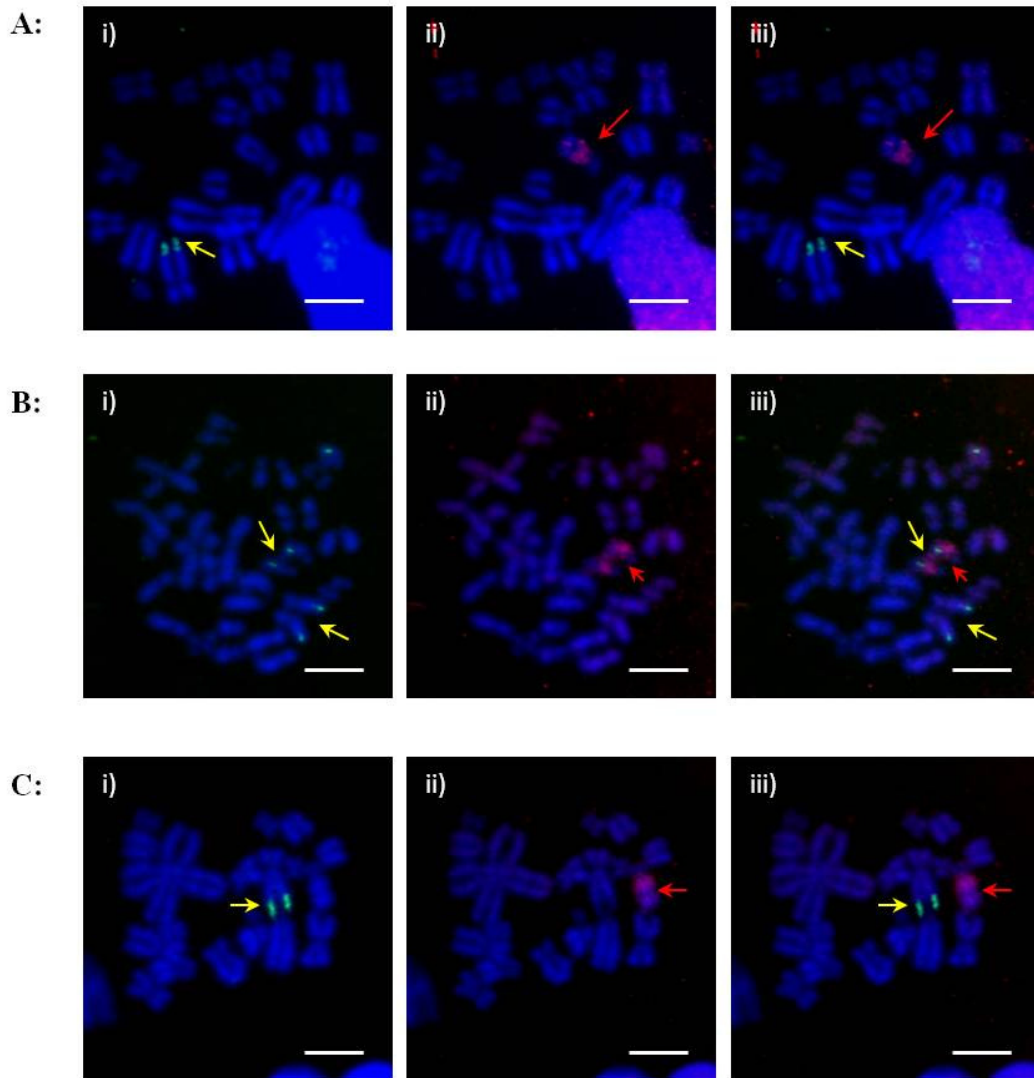
Experimental details are described in the legend to Figure 5.3. (A), (B), (C) FISH images of three different metaphase spreads of U2 cell line hybridized with chromosome 4 paint and plasmid probes are shown. Yellow signal shows the plasmid integration site (indicated by yellow arrows) and regions in red are those hybridized with a painting probe prepared from Chinese hamster cells chromosome 4 (indicated by red arrows). White scale bar (bottom right) equals 10 μ m. (i) Hybridization with plasmid probe only; (ii) hybridization with chromosome paint probe only; (iii) Dual color FISH (merged) image

Figure 5.6: Plasmid localization and chromosome 6 hybridization observed for N2 cell line



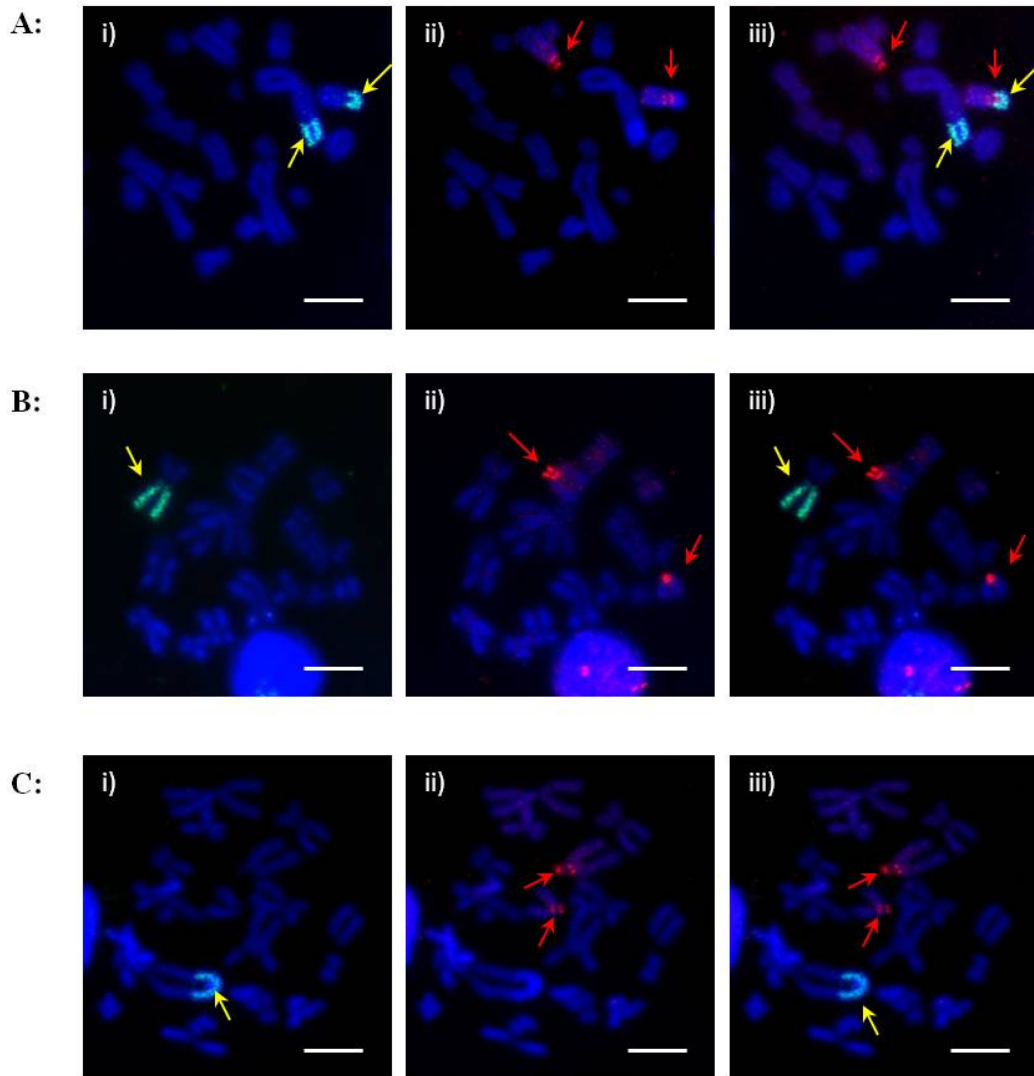
Experimental details are described in the legend to Figure 5.3. (A), (B), (C) FISH images of three different metaphase spreads of N2 cell line hybridized with chromosome 6 paint and plasmid probes are shown. Yellow signal shows the plasmid integration site (indicated by yellow arrows) and regions in red are those hybridized with a painting probe prepared from Chinese hamster cells chromosome 6 (indicated by red arrows). White scale bar (bottom right) equals 10 μm. (i) Hybridization with plasmid probe only; (ii) hybridization with chromosome paint probe only; (iii) Dual color FISH (merged) image

Figure 5.7: Plasmid localization and chromosome 6 hybridization observed for U2 cell line



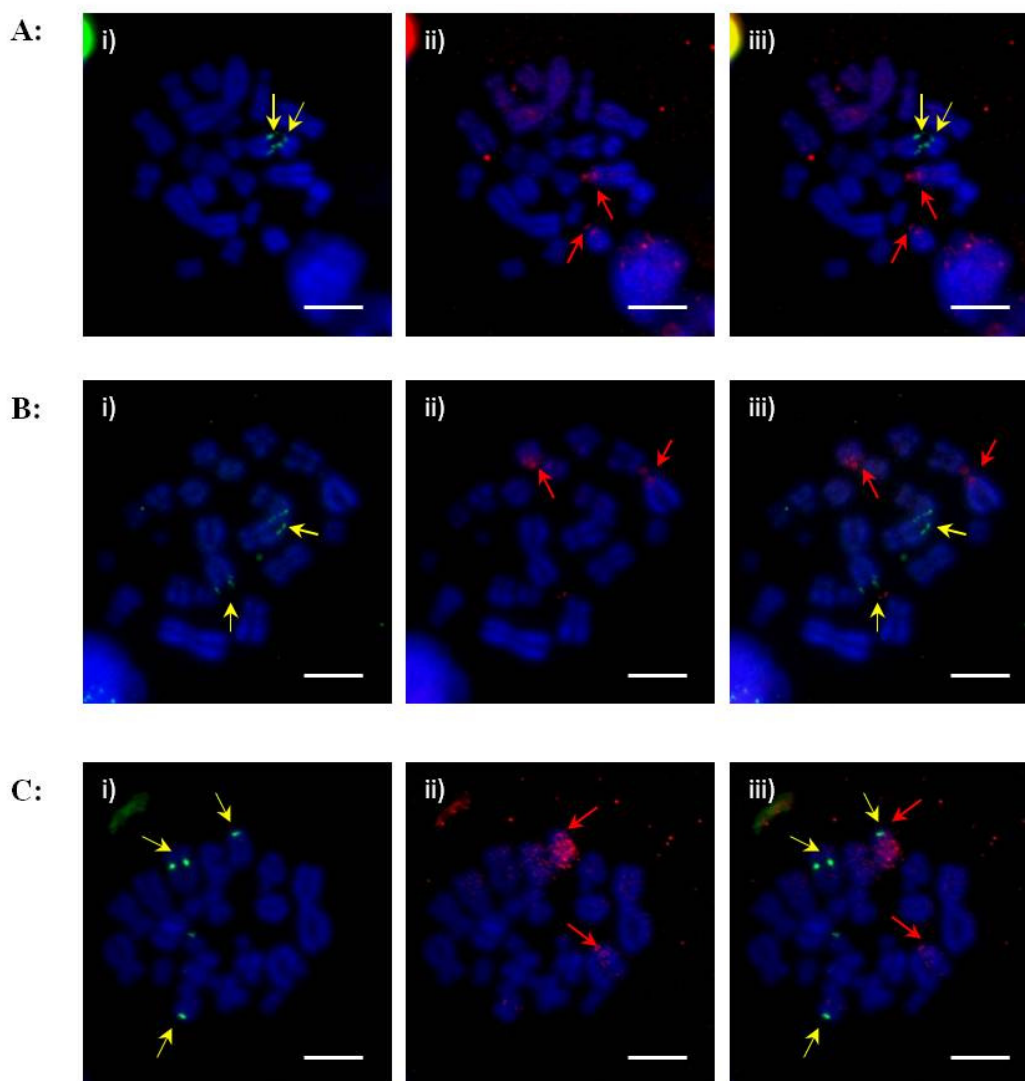
Experimental details are described in the legend to Figure 5.3. (A), (B), (C) FISH images of three different metaphase spreads of U2 cell line hybridized with chromosome 6 paint and plasmid probes are shown. Yellow signal shows the plasmid integration site (indicated by yellow arrows) and regions in red are those hybridized with a painting probe prepared from Chinese hamster cells chromosome 6 (indicated by red arrows). White scale bar (bottom right) equals 10 μ m. (i) Hybridization with plasmid probe only; (ii) hybridization with chromosome paint probe only; (iii) Dual color FISH (merged) image

Figure 5.8: Plasmid localization and chromosome 7 hybridization observed for N2 cell line



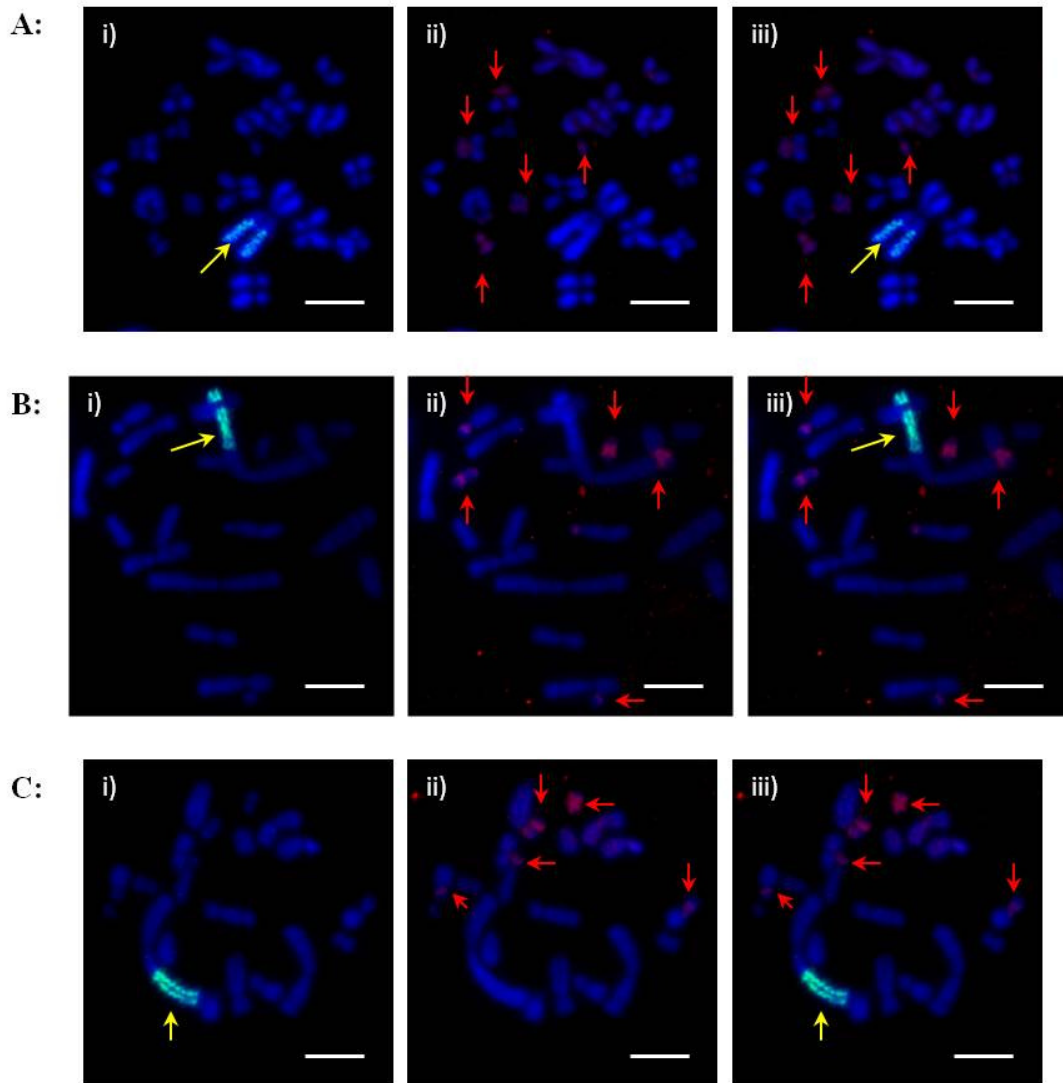
Experimental details are described in the legend to Figure 5.3. (A), (B), (C) FISH images of three different metaphase spreads of N2 cell line hybridized with chromosome 7 paint and plasmid probes are shown. Yellow signal shows the plasmid integration site (indicated by yellow arrows) and regions in red are those hybridized with a painting probe prepared from Chinese hamster cells chromosome 6 (indicated by red arrows). White scale bar (bottom right) equals 10 μ m. (i) Hybridization with plasmid probe only; (ii) hybridization with chromosome paint probe only; (iii) Dual color FISH (merged) image

Figure 5.9: Plasmid localization and chromosome 7 hybridization observed for U2 cell line



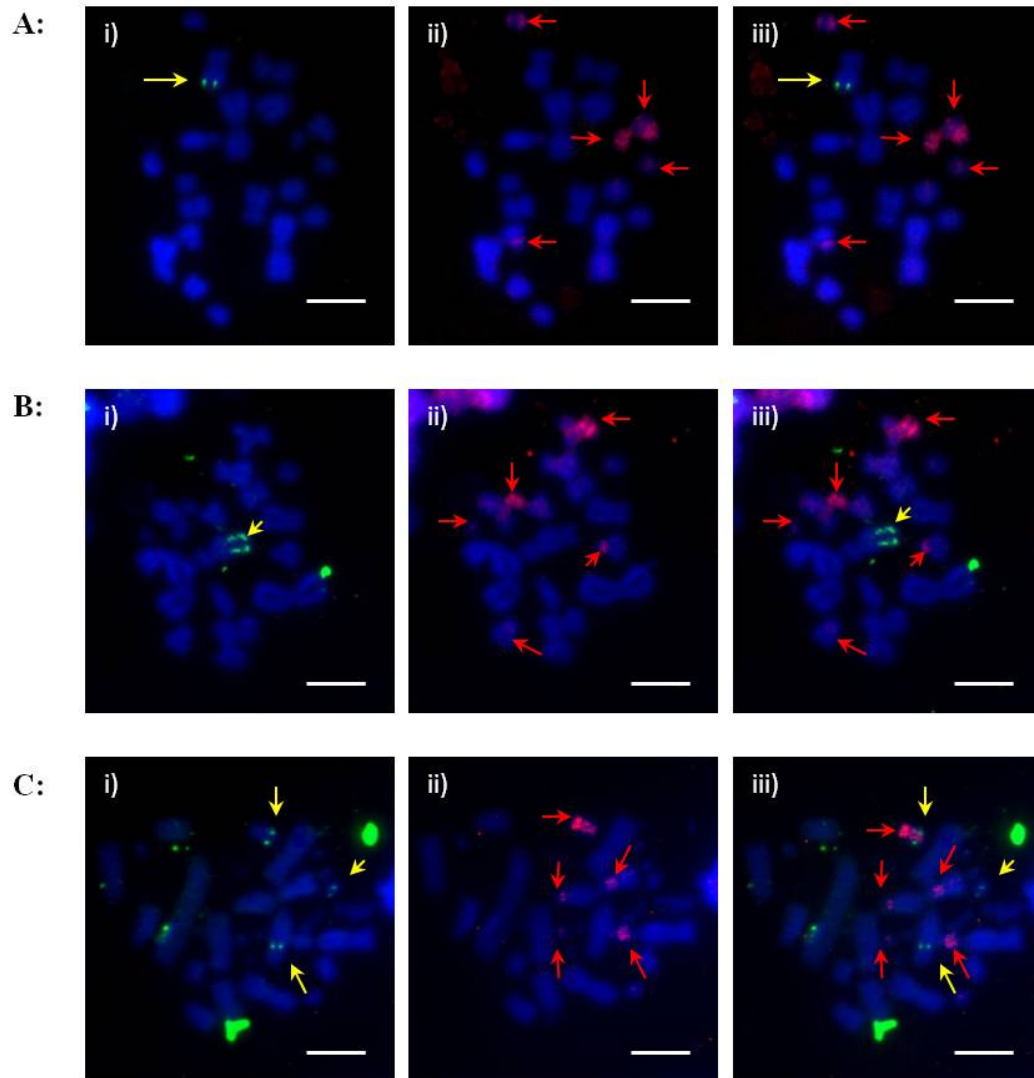
Experimental details are described in the legend to Figure 5.3. (A), (B), (C) FISH images of three different metaphase spreads of U2 cell line hybridized with chromosome 7 paint and plasmid probes are shown. Yellow signal shows the plasmid integration site (indicated by yellow arrows) and regions in red are those hybridized with a painting probe prepared from Chinese hamster cells chromosome 6 (indicated by red arrows). White scale bar (bottom right) equals 10 μ m. (i) Hybridization with plasmid probe only; (ii) hybridization with chromosome paint probe only; (iii) Dual color FISH (merged) image

Figure 5.10: Plasmid localization and chromosome X and Y hybridization observed for N2 cell line



Experimental details are described in the legend to Figure 5.3. (A), (B), (C) FISH images of three different metaphase spreads of N2 cell line hybridized with chromosome X and Y paint and plasmid probes are shown. Yellow signal shows the plasmid integration site (indicated by yellow arrows) and regions in red are those hybridized with a painting probe prepared from Chinese hamster cells chromosome 6 (indicated by red arrows). White scale bar (bottom right) equals 10 μ m. (i) Hybridization with plasmid probe only; (ii) hybridization with chromosome paint probe only; (iii) Dual color FISH (merged) image

Figure 5.11: Plasmid localization and chromosome X and Y hybridization observed for U2 cell line



Experimental details are described in the legend to Figure 5.3. (A), (B), (C) FISH images of three different metaphase spreads of U2 cell line hybridized with chromosome X and Y paint and plasmid probes are shown. Yellow signal shows the plasmid integration site (indicated by yellow arrows) and regions in red are those hybridized with a painting probe prepared from Chinese hamster cells chromosome 6 (indicated by red arrows). White scale bar (bottom right) equals 10 μ m. (i) Hybridization with plasmid probe only; (ii) hybridization with chromosome paint probe only; (iii) Dual color FISH (merged) image

5.3. Effect of long-term culture on plasmid localization

3 UCOE (U1, U2 and U3) and 3 non-UCOE (N1, N2 and N4) cell lines were selected for analysis of the genomic localisations of the inserted genes. To localize the transfected plasmid sequence on metaphase chromosomes, FISH was performed with DIG-labeled probes for the whole plasmid sequence (Section 2.8.2). To investigate the changes in integration patterns during long-term culture in the presence and absence of MTX, the metaphase chromosomes prepared from the cells at the start and end of the prolonged culture in the presence and absence of MTX were analyzed. Different integration patterns observed are summarized in Figure 5.12.

Figure 5.13 and 5.14 shows the results of FISH analysis of non-UCOE and UCOE cell lines, respectively, at early stages of culture. In the N2 and N4 cell lines, amplified arrays were longer whereas the N1 and all UCOE cell lines had less extended regions of inserted plasmid DNA. Five different integration types were observed in non-UCOE cell lines. In the first type of integration pattern, the site of insertion was on the end of a group-1 chromosome containing variable length of amplified array (1A and 1A^V). In 1B, the insertion is still on the group-1 chromosome but within the long arm of the chromosome instead of being at the end. Some of the cells contained 2A and 2B^V types of integration where the insertion site was on a group-2 chromosome either at the end or within the long arm of the chromosome respectively. Finally, dicentric chromosomes containing a very large region of insertion and integration into both ends of group-1 chromosomes were observed and are classified as U-type integration.

In the UCOE cell lines, the insertion site was mainly on a group-2 chromosome either on the end or within the long arm of the chromosome (2A, 2A^V and 2B^V). On some occasions there was also a FISH signal on group-5 and 6 chromosomes (5A and 6A respectively, Figure 5.14).

40 to 50 metaphase spreads from each cell line were analysed and the frequency of occurrence of the different integration types in UCOE and non-UCOE cell lines at early

generation are summarized in Figure 5.15 and 5.16. In the N2 cell line, 90% of the metaphase spreads contained the 1A integration pattern and 10% contained U-type integration at early stages of long-term culture (Figure 5.15B). The N4 cell line showed approximately 43% of 1A and 25% of 2A type of insertion, whereas 10% of the metaphases contained both 1A and 2A integration. U-type integration was found in 22% of the metaphases in the N4 cell line at early generation (Figure 5.15C). In the N1 cell line, the length of amplified array was shorter than the rest of non-UCOE cell lines. Therefore, 42% of the cells contained a variant of 1A (1A^V) and 49% of the metaphases contained 1B type of integration. Moreover, a small number of N1 spreads showed an integration of 2B^V (9%) (Figure 5.15A).

The frequency of different integration types in the metaphases of UCOE cell lines in early generation are shown in Figure 5.16. In the U1 cell line the majority of the metaphase spreads contained 2A and 2A^V variants of the insertion types (79%), whereas on a number of occasions plasmid was inserted in group-5 chromosome (3.5%, Figure 5.16A). Moreover, 17% of the cells contained both 2A^V and 5A types of insertion. The U2 cell line contained all 4 types of integration patterns with different frequencies where 2A and 2A^V dominated (~54%, Figure 5.16B). In addition, the 2B^V type of integration was also observed in 36% of the metaphase spreads. The remaining cells contained a combination of two different sites of integration in consisting of 2A^V, 2B^V, 5A and 6A patterns. 88% of the metaphase spreads of the U3 cell line contained 2A and 2A^V types of integration, whereas 7% contained 2B^V (Figure 5.16C). Furthermore, a small number of cells contained 2A^V, 5A and 6A types of integration together (5%).

After 80 days of culture in the presence of MTX, the frequency of the 1A^V type of integration increased to 66% from 42% in the N1 cell line, whereas the remaining metaphase spreads contained 1B type of insertion (Figure 5.17A, 5.19A). 74% of the metaphase spreads of the N2 cell line also contained the 1A type of integration. In addition, a small number of spreads contained the 2A and 2B insertion types (Figure 5.17B, 5.19B). 9% of the cells contained two different sites of integration (1A+2A) and the frequency of the U-type insertion decreased to 4%. The different integration patterns in the

early generation N4 cell line diminished or evolved to the 1A type of insertion at the end of prolonged culture in the presence of MTX (Figure 5.17C, 5.19C).

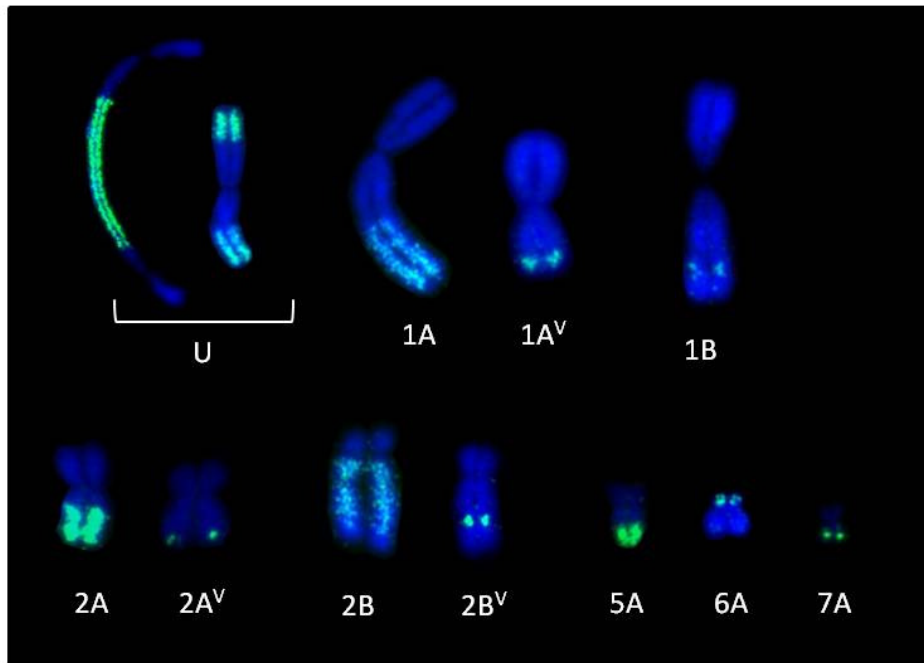
The majority of spreads from the U1 cell line contained a combination of different integration types at the end of long-term culture in the presence of MTX (Figure 5.18A, 5.20A). Among these, the dominant pattern was 2B^V and 6A together, which occurred with a frequency of 45%. The main differences between the early and late generation U1 cell line was the disappearance of 2A and occurrence of 2B^V and 6A types of insertion at the end of extended culture in the presence of MTX. The frequency of the 2A^V type of integration was increased to 76% in the U2 cell line after 80 days in the presence of MTX (Figure 5.18B, 5.20B). Moreover, the 2B^V type of insertion was not observed in late generation in contrast to the profile observed for early generation cell lines. There were also a number of cells containing 2A^V with 5A or 6A together with a slight increase in frequency of occurrence. In the presence of MTX, the U3 cell line retained the profile of the integration patterns observed at the beginning of culture (2A, 2A^V, 2B^V and 5A). In addition, a number of cells contained a new insertion type in the late generation cell line, where the plasmid sequence was observed to be on a group-7 chromosome (7A). This was seen together with 2A^V type of insertion, which occurred with a frequency of 5% (Figure 5.18C, 5.20C).

In the absence of MTX, the frequency of 1A^V integration decreased from 42% to 16% for the N1 cell line during long term culture. This loss in 1A^V integration was accompanied by an increase in 1B integration, from 49% to 84% compared to the early generation cell line (Figure 5.21A, 5.23A). For the N2 cell line, the U-type integration disappeared or evolved to 1A and 1B. However, the dominant type of insertion was still 1A (88%, Figure 5.21B, 5.23B). All the metaphase spreads observed in the N4 cell line contained only the 1A type of integration (Figure 5.21C, 5.23C).

In all UCOE cell lines, the majority of the metaphase spreads contained the 2A^V type of insertion after 80 days in the absence of MTX (U1=78%, U2=59%, U3=70%, Figure 5.22, 5.24). No 2A type of integration was observed in these cells instead of this 2A^V, a variant

of 2A with a decreased amplified array, became dominant in late generation in the absence of MTX. In addition, a number of spreads contained the 6A type of integration together with 2A^V, which was observed in 12% of the metaphase spreads in the U1 cell line. Moreover, the occurrence of 5A with 2A^V decreased to 10% from 17% (Figure 5.24A). For the U2 cell line, the frequency of occurrence of 2B^V decreased from 36% to 8% in the absence of MTX. Although no 2A was observed in metaphase spreads at late generation, the frequency of 2A^V became 59%. Furthermore, an increase in the frequency of the 2A^V+5A integration pattern was observed (12%) whilst the combination of 2A^V+6A and 2B^V+6A frequencies remained relatively similar (Figure 5.24B). After 80 days without MTX, the variability of types of integration patterns had decreased, predominantly changing into the 2A^V type, which showed a frequency of 70% in U3 cell line. There was no detectable signal in 30% of the metaphase spreads in the absence of MTX, which might be due to low plasmid copies observed in the U3 cell line in the absence of MTX (<20, Figure 5.24C).

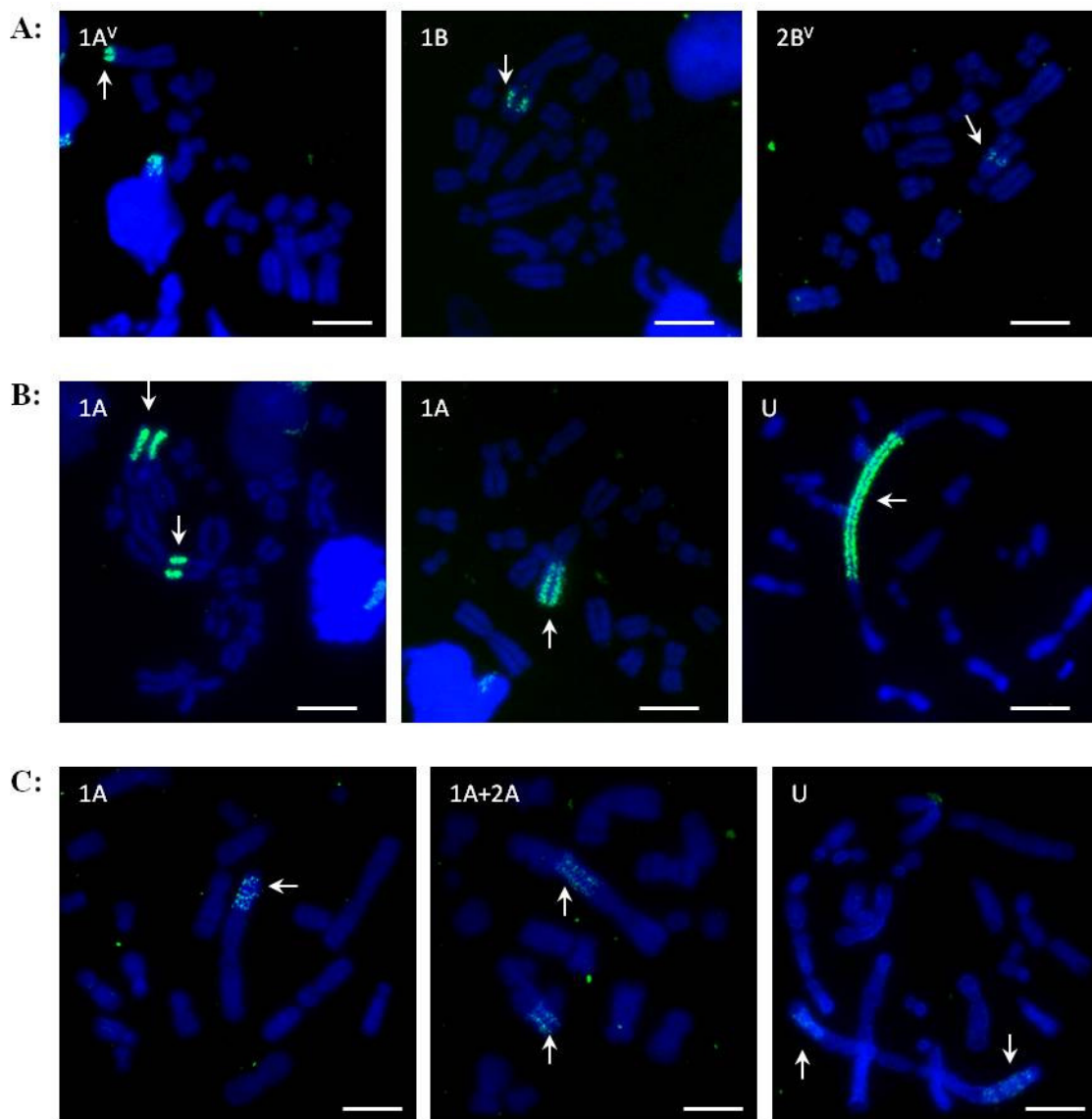
Figure 5.12: Different plasmid integration patterns observed in amplified CHO-GFP cell lines



Metaphase spreads were made for three different amplified UCOE and non-UCOE cell-lines (Section 2.8.1). FISH was performed using p1010-GFP plasmid, labelled with digoxigenin, as a probe (Section 2.8.2). Slides were counterstained with DAPI. Slides were viewed using an Olympus Widefield fluorescent microscope, using the 100x oil immersion objective, and images were captured using MetaVue Software (Section 2.9.5). 40-50 images were taken for each cell line. Plasmid integration events into different chromosomal locations are summarised above (See Figures 5.13-24). Chromosomes were identified by numbered groups outlined in Figure 5.2. Different locations in the same chromosome group is denoted by A, B etc. Variants of same location are denoted by (^V). U = unclassified.

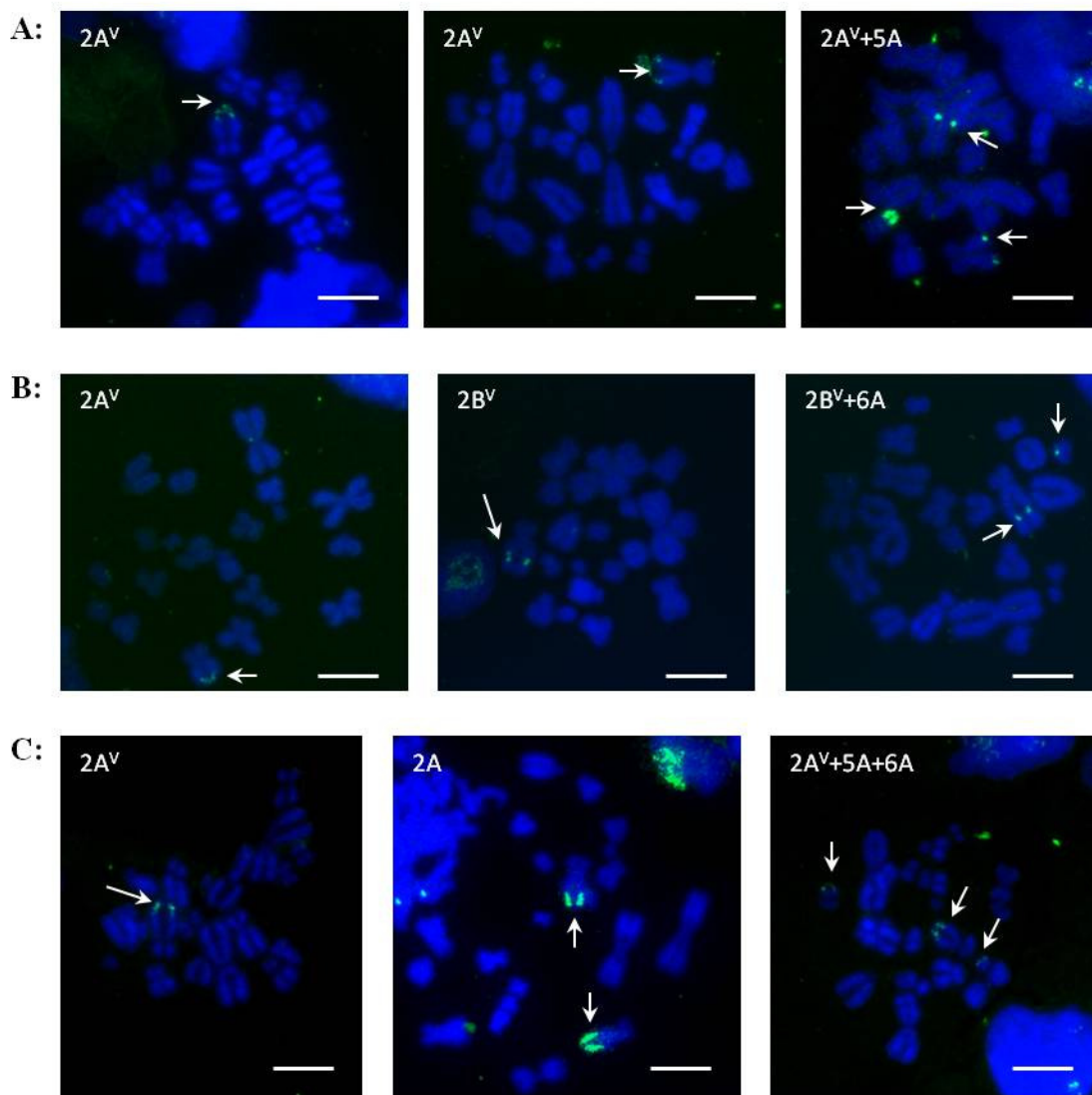
NB: Chromosomes shown are examples of the integration location, but do not necessarily represent the size of the inserted plasmid region for all cell lines listed.

Figure 5.13: Plasmid integration patterns observed in non-UCOE cell lines at the start of long-term culture in the presence of MTX



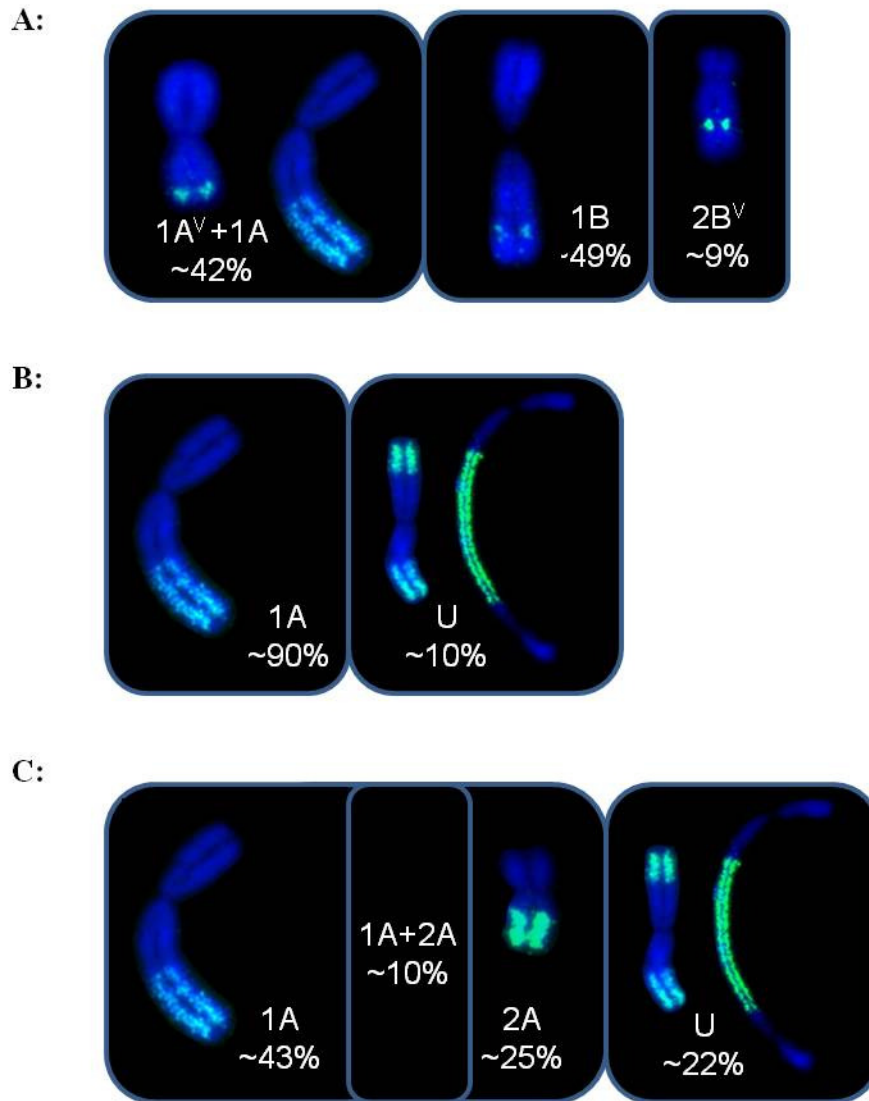
Experimental details are described in the legend to Figure 5.12. FISH images for (A) N1 (B) N2 (C) N4 cell lines. Different integration patterns observed is indicated in the top left of the image. White arrows indicate plasmid integration sites White scale bar (bottom right) equals 10 μ m.

Figure 5.14: Plasmid integration patterns observed in UCOE cell lines at the start of long-term culture in the presence of MTX



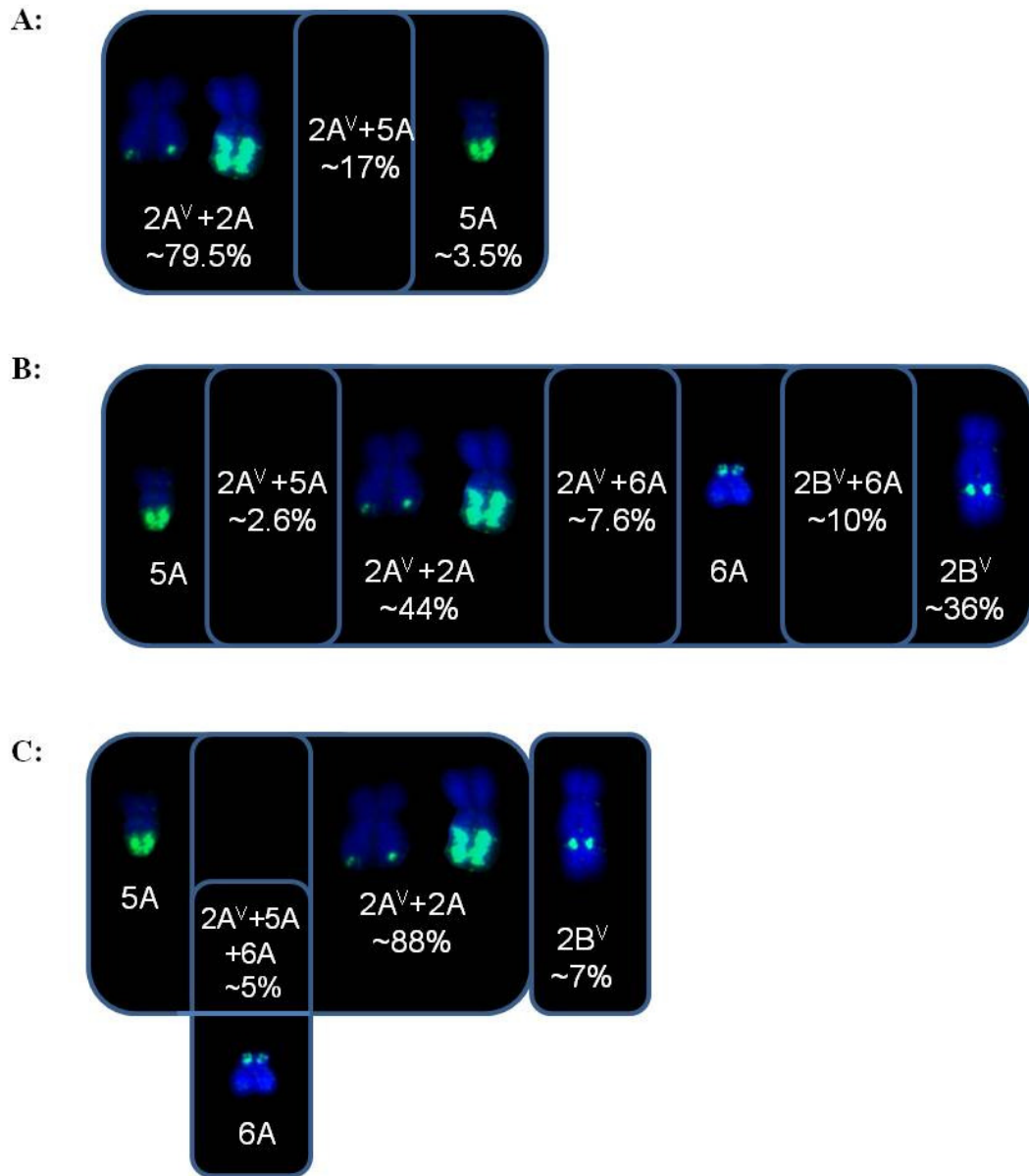
Experimental details are described in the legend to Figure 5.12. FISH images for (A) U1 (B) U2 (C) U3 cell lines. Different integration patterns observed is indicated in the top left of the image. White arrows indicate plasmid integration sites White scale bar (bottom right) equals 10 μ m.

Figure 5.15: Frequency of occurrence of plasmid integration patterns in non-UCOE cell lines at the start of long-term culture in the presence of MTX



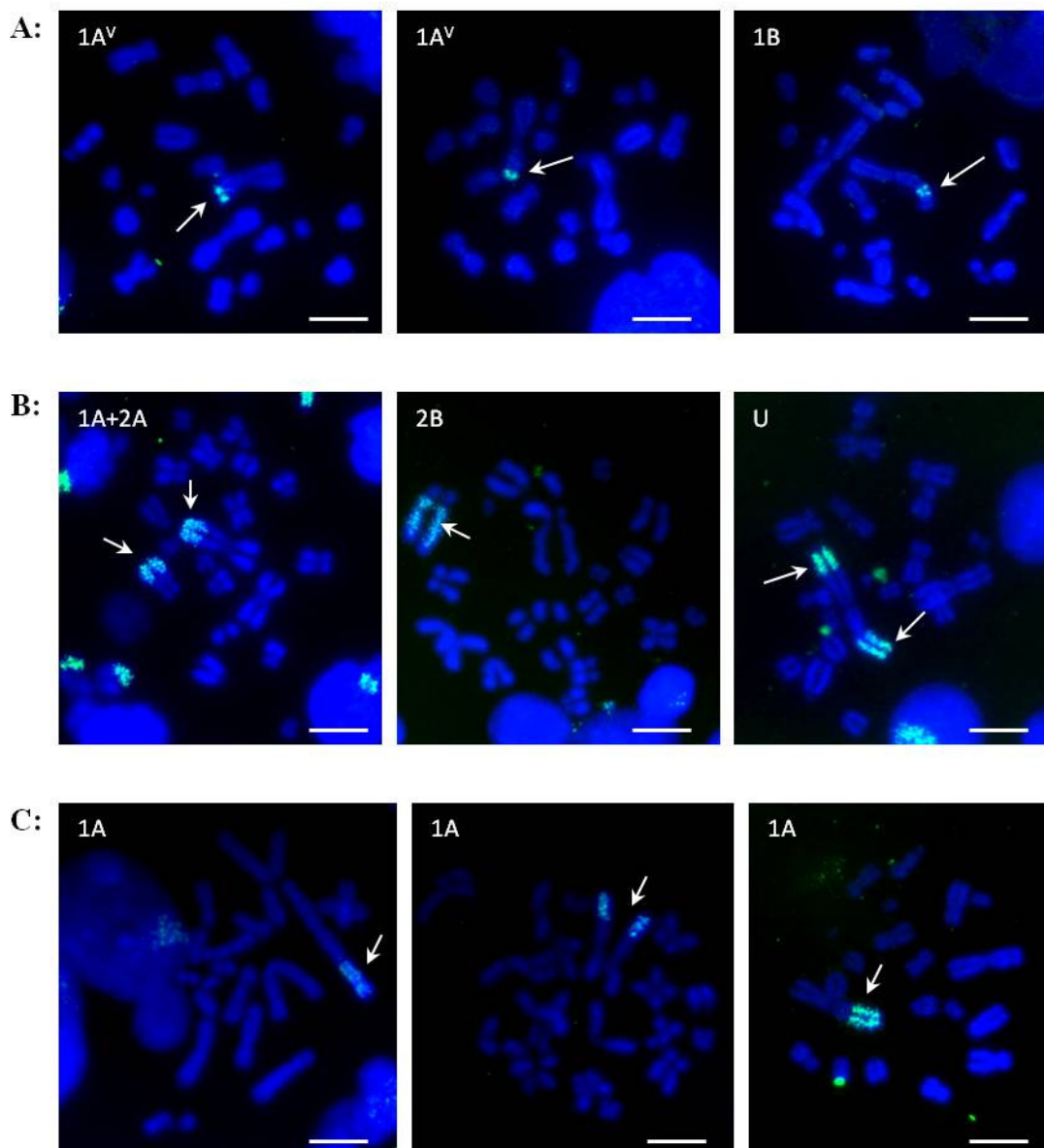
Experimental details are described in the legend to Figure 5.12. Frequency of occurrence of different plasmid integration types for (A) N1 cell line, (B) N2 cell line, (C) N4 cell line are shown. Each number represents percent metaphases containing corresponding integration pattern among total metaphases examined (40-50).

Figure 5.16: Frequency of occurrence of plasmid integration patterns in UCOE cell lines at the start of long-term culture in the presence of MTX



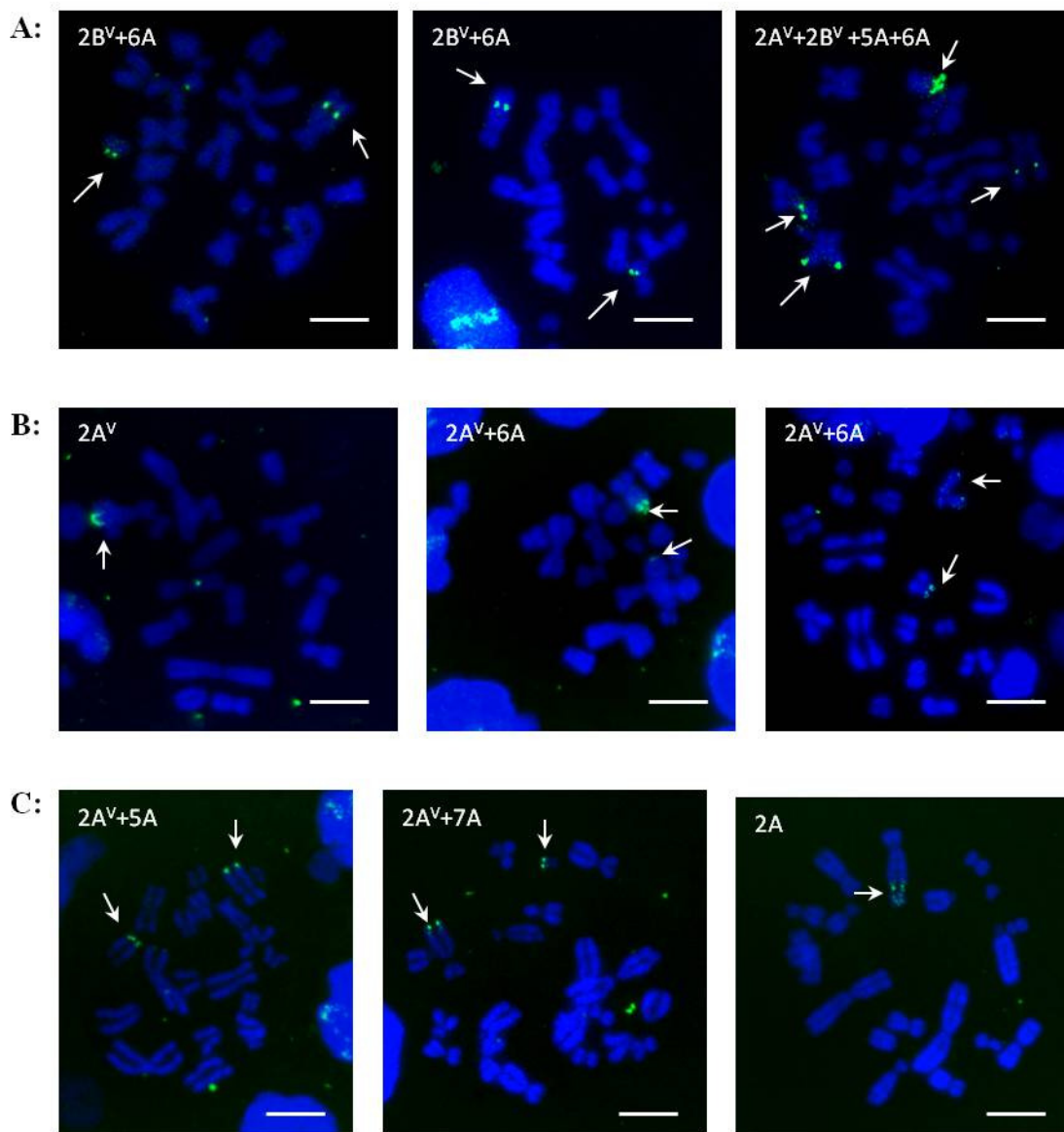
Experimental details are described in the legend to Figure 5.12. Frequency of occurrence of different plasmid integration types for (A) U1 cell line, (B) U2 cell line, (C) U3 cell line are shown. Each number represents percent metaphases containing corresponding integration pattern among total metaphases examined (40-50).

Figure 5.17: Plasmid integration patterns observed in non-UCOE cell lines at the end of long-term culture in the presence of MTX



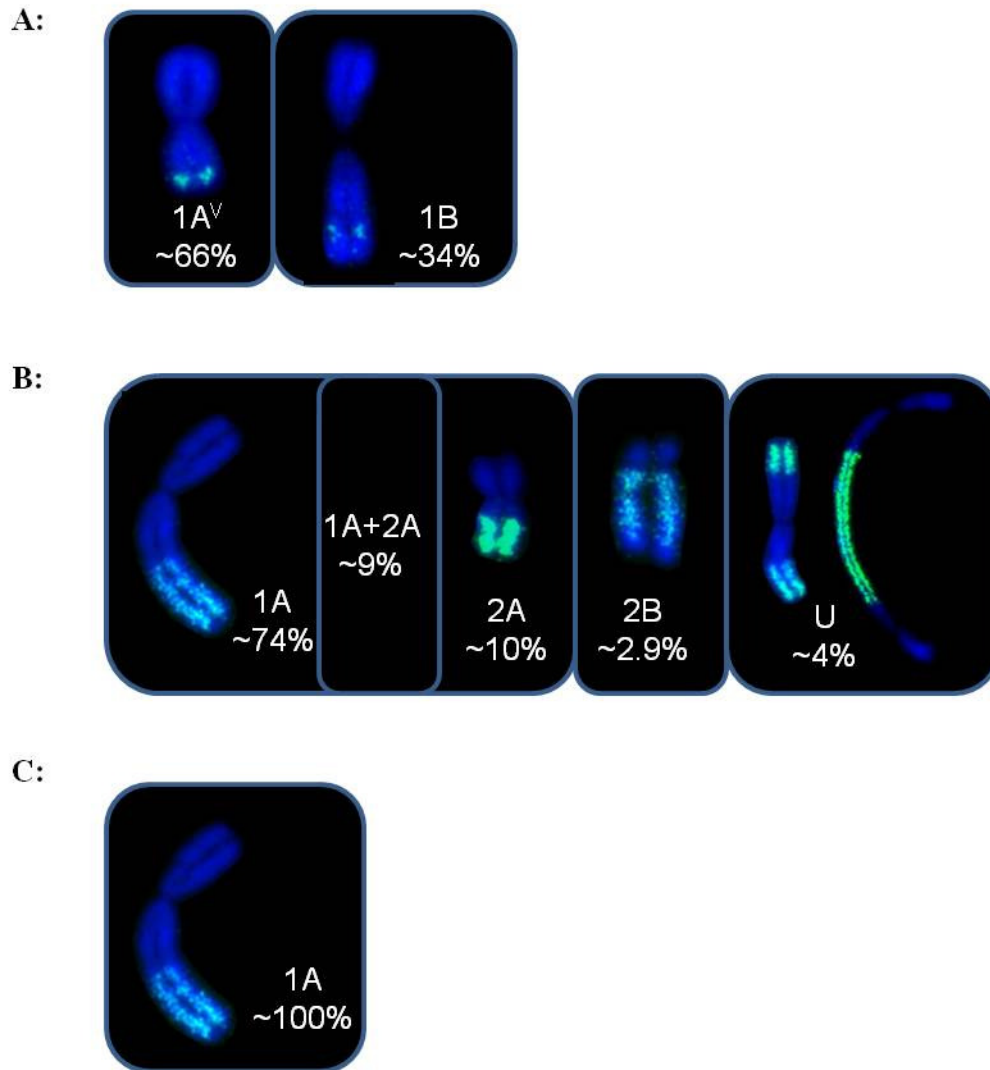
Experimental details are described in the legend to Figure 5.12. FISH images for (A) N1 (B) N2 (C) N4 cell lines. Different integration patterns observed is indicated in the top left of the image. White arrows indicate plasmid integration sites White scale bar (bottom right) equals 10μm.

Figure 5.18: Plasmid integration patterns observed in UCOE cell lines at the end of long-term culture in the presence of MTX



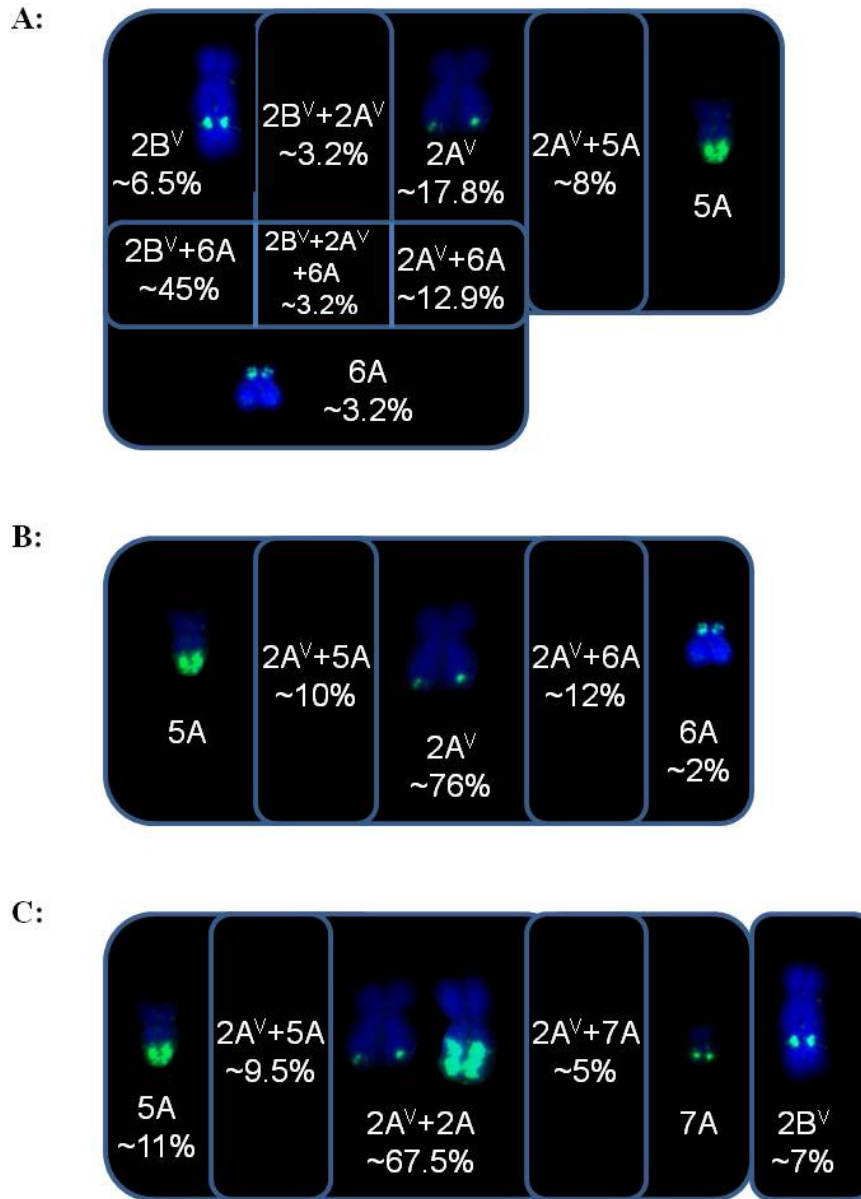
Experimental details are described in the legend to Figure 5.12. FISH images for (A) U1 (B) U2 (C) U3 cell lines. Different integration patterns observed is indicated in the top left of the image. White arrows indicate plasmid integration sites White scale bar (bottom right) equals 10 μm.

Figure 5.19: Frequency of occurrence of plasmid integration patterns in non-UCOE cell lines at the end of long-term culture in the presence of MTX



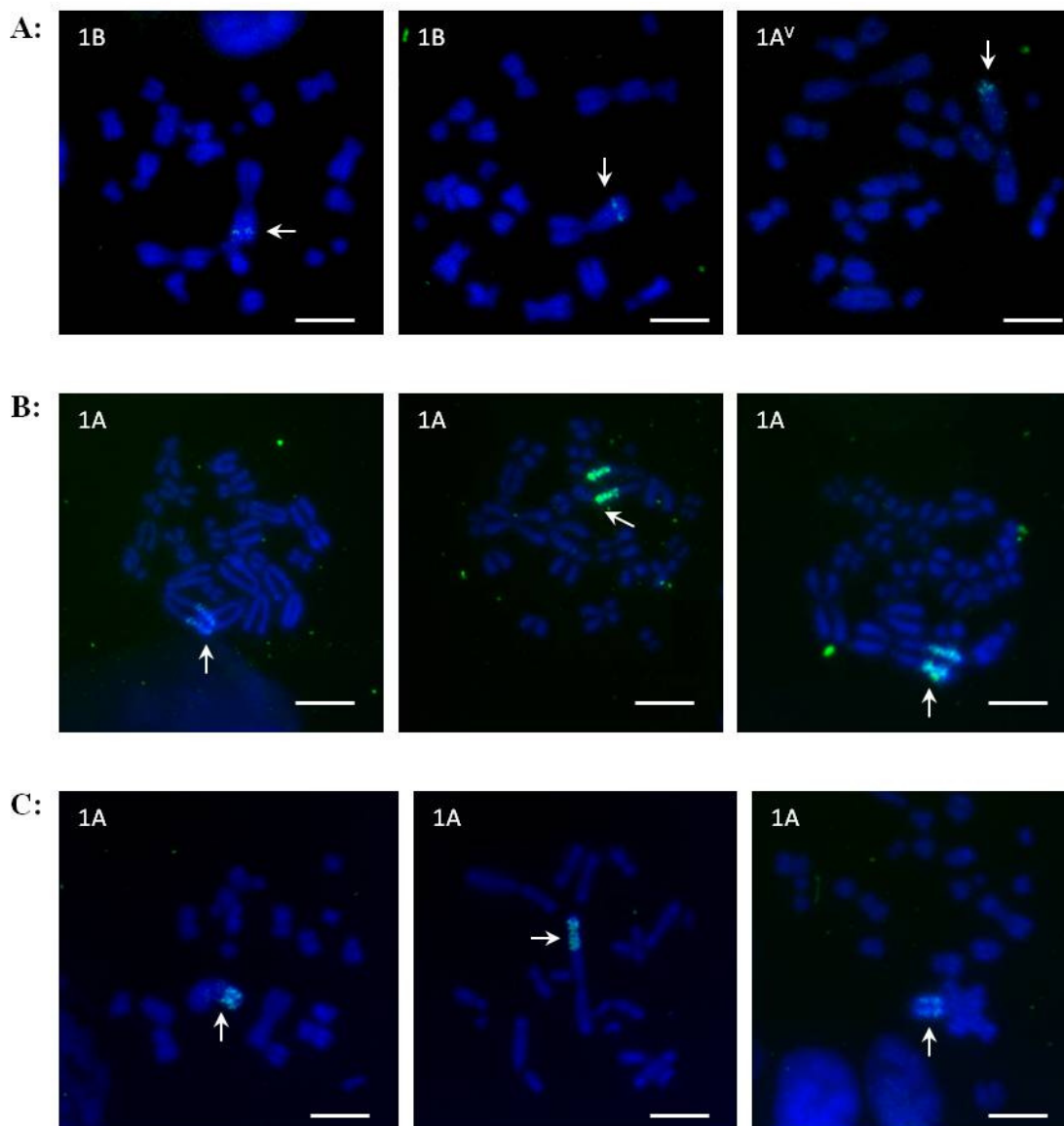
Experimental details are described in the legend to Figure 5.12. Frequency of occurrence of different plasmid integration types for (A) N1 cell line, (B) N2 cell line, (C) N4 cell line are shown. Each number represents percent metaphases containing corresponding integration pattern among total metaphases examined (40-50).

Figure 5.20: Frequency of occurrence of plasmid integration patterns in UCOE cell lines at the end of long-term culture in the presence of MTX



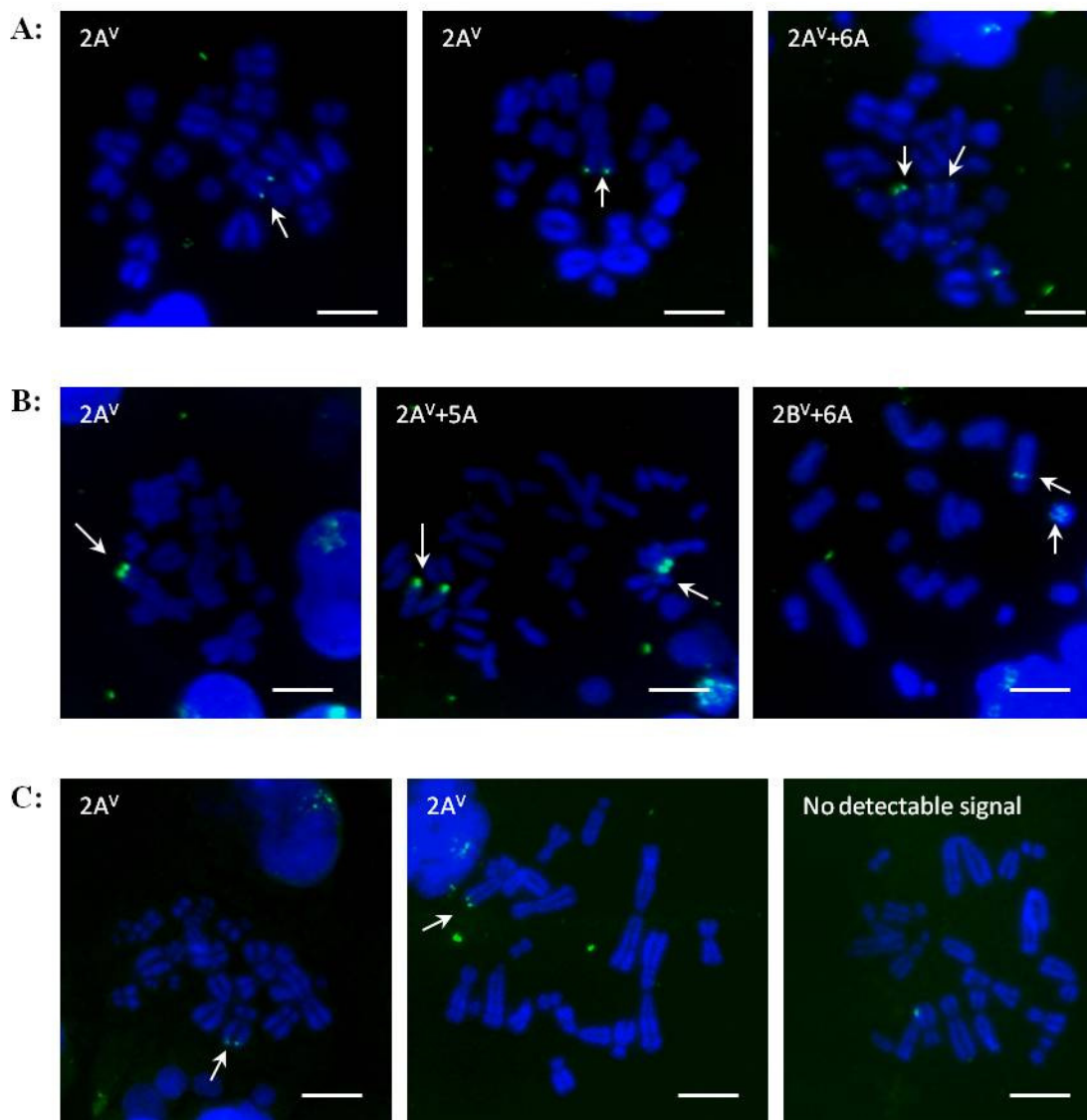
Experimental details are described in the legend to Figure 5.12. Frequency of occurrence of different plasmid integration types for (A) U1 cell line, (B) U2 cell line, (C) U3 cell line are shown. Each number represents percent metaphases containing corresponding integration pattern among total metaphases examined (40-50).

Figure 5.21: Plasmid integration patterns observed in non-UCOE cell lines at the end of long-term culture in the absence of MTX



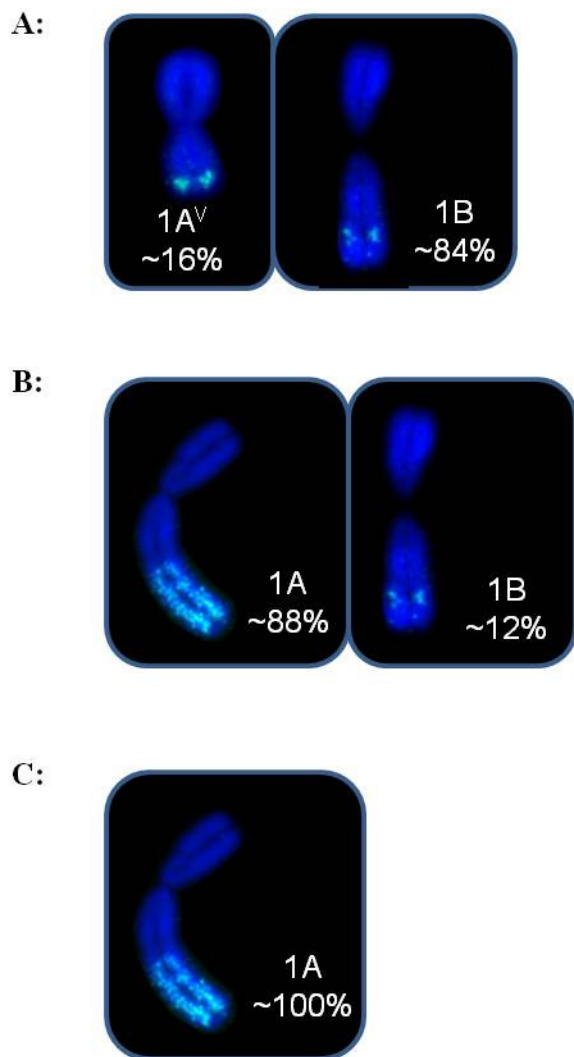
Experimental details are described in the legend to Figure 5.12. FISH images for (A) N1 (B) N2 (C) N4 cell lines. Different integration patterns observed is indicated in the top left of the image. White arrows indicate plasmid integration sites White scale bar (bottom right) equals 10 μ m.

Figure 5.22: Plasmid integration patterns observed in UCOE cell lines at the end of long-term culture in the absence of MTX



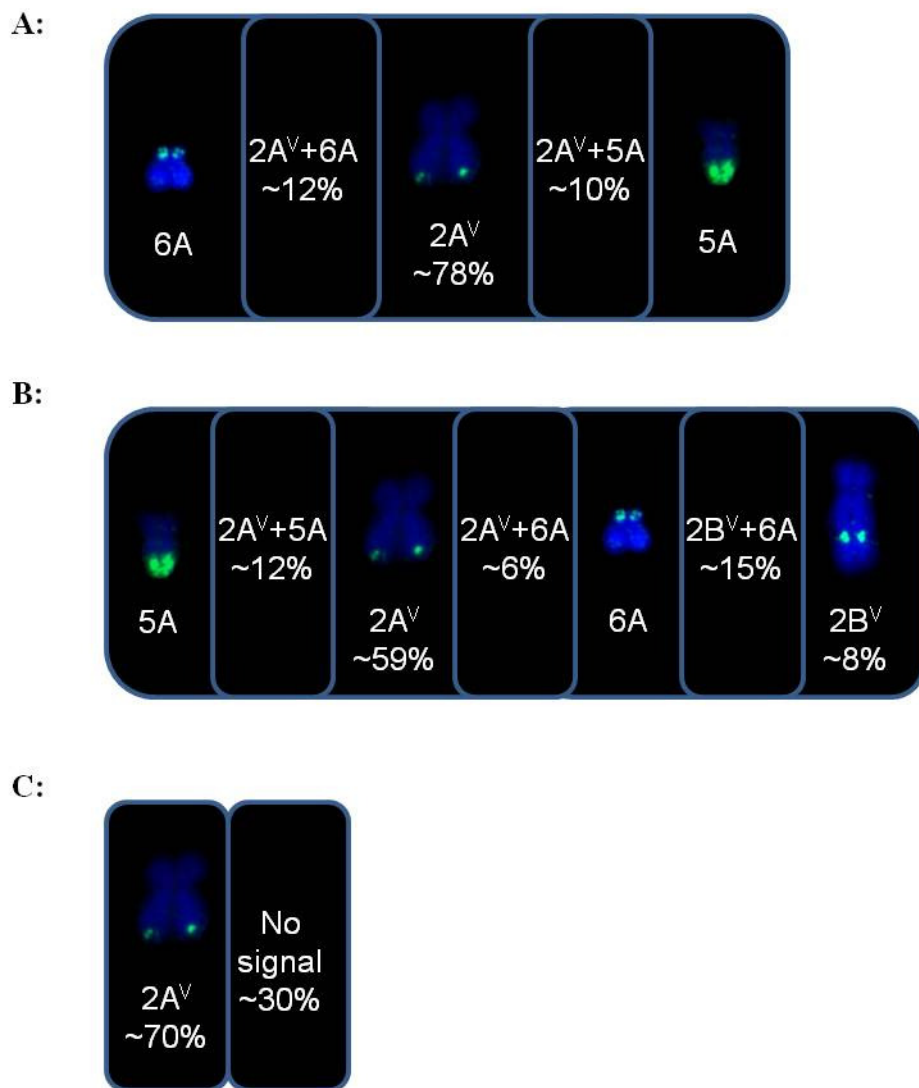
Experimental details are described in the legend to Figure 5.12. FISH images for (A) U1 (B) U2 (C) U3 cell lines. Different integration patterns observed is indicated in the top left of the image. White arrows indicate plasmid integration sites White scale bar (bottom right) equals 10 μm.

Figure 5.23: Frequency of occurrence of plasmid integration patterns in non-UCOE cell lines at the end of long-term culture in the absence of MTX



Experimental details are described in the legend to Figure 5.12. Frequency of occurrence of different plasmid integration types for (A) N1 cell line, (B) N2 cell line, (C) N4 cell line are shown. Each number represents percent metaphases containing corresponding integration pattern among total metaphases examined (40-50).

Figure 5.24: Frequency of occurrence of plasmid integration patterns in UCOE cell lines at the end of long-term culture in the absence of MTX



Experimental details are described in the legend to Figure 5.12. Frequency of occurrence of different plasmid integration types for (A) U1 cell line, (B) U2 cell line, (C) U3 cell line are shown. Each number represents percent metaphases containing corresponding integration pattern among total metaphases examined (40-50).

Table 5.1 summarizes the eGFP gene copy number, mRNA expression, protein production, CV values and the predominant plasmid integration patterns observed for individual cell lines. The relationship between CV values and integration profile will be discussed in Section 5.3. The results from Chapter 3 and 4 showed that UCOE cell lines displayed a greater mRNA/gene copy number ratio compared to non-UCOE cell lines. The FISH analysis revealed that plasmid was predominantly located on the end of a group-2 chromosome in UCOE cell lines, whereas in non-UCOE cell lines plasmid integration was on the end of a group-1 chromosome. These results might suggest that the locus of insertion is associated with high transcription in UCOE cell lines.

Among the UCOE cell lines, the mRNA/gene copy ratio was higher in the U3 cell line (Table 5.1). However, the plasmid integration patterns were not different when compared to other UCOE cell lines. Moreover, although the gene copy numbers in the U1 and U2 cell lines were higher than the U3 cell line, they showed similar amounts of mRNA expression as well as the similar type of predominant plasmid integration pattern at the end of long-term culture in the absence of MTX. It should be noted here that the profiling I have done is very large-scale; therefore the localisation to the same area may have different precise localisation. Among the non-UCOE cell lines, the N1 cell line displayed the highest mRNA/gene copy ratio (Table 5.1). The predominant integration pattern for the N1 cell line was a variant of 1A, which contained a smaller amplified array. Therefore, it is possible that not all the amplified genes are in an active state in the N2 and N4 cell lines.

Table 5.1: Summary of genomic parameters and plasmid integration patterns for eGFP expression

Cell Line	Culture time (days +/- MTX)	eGFP gene copy no/cell (\pm range)	% eGFP mRNA (\pm SD)	eGFP expression (\pm range)	CV (\pm SD)	Integration type
U1	+10	262 \pm 48	159 \pm 16	54 \pm 8	174 \pm 5.3	80%2A+2A ^V 17%2A ^V +5A
	+80	153 \pm 46	208 \pm 3	48 \pm 9	111 \pm 2.2	45%2B ^V +6A 18%2A ^V 13%2A ^V +6A
	-80	70 \pm 10	34 \pm 0.4	5 \pm 1	231 \pm 0.7	78% 2A ^V
U2	+10	141 \pm 13	112 \pm 4	66 \pm 12	146 \pm 4.4	44%2A+2A ^V 36% 2B ^V
	+80	280 \pm 22	73 \pm 9	34 \pm 13	176 \pm 3.3	76% 2A ^V
	-80	95 \pm 10	24 \pm 0.3	4 \pm 2	247 \pm 1.4	59%2A ^V
U3	+10	101 \pm 5	108 \pm 7	58 \pm 4	105 \pm 1.4	88%2A+2A ^V
	+80	83 \pm 12	160 \pm 15	40 \pm 7	87 \pm 0.5	68%2A+2A ^V 11%5A
	-80	19 \pm 3	28 \pm 3	6 \pm 2	156 \pm 1	70%2A ^V
N1	+10	185 \pm 6	39 \pm 7	95 \pm 9	94 \pm 1.4	42%1A+1A ^V 49% 1B
	+80	94 \pm 9	58 \pm 4	72 \pm 12	54 \pm 1	66% 1A ^V 34% 1B
	-80	65 \pm 2	5 \pm 0.4	20 \pm 3	161 \pm 1	84%1B
N2	+10	1377 \pm 85	41 \pm 6	35 \pm 9	172 \pm 13	90% 1A
	+80	1128 \pm 54	46 \pm 5	34 \pm 6	114 \pm 1.1	74% 1A
	-80	560 \pm 28	2.7 \pm 0.2	15 \pm 0.1	151 \pm 1	88%1A
N4	+10	502 \pm 84	55 \pm 4	177 \pm 39	93 \pm 5	43%1A 25%2A 22% U
	+80	389 \pm 53	24 \pm 0.8	198 \pm 24	58 \pm 3.4	100% 1A
	-80	690 \pm 67	6 \pm 0.1	25 \pm 4	232 \pm 31	100%1A

Summary of eGFP gene copy number per cell (Figure 3.16, 3.17), mRNA expression normalized to β -actin (Figure 3.20), protein expression detected by western blotting and normalized to total ERK protein (Figure 3.10, 3.11), CV values of eGFP fluorescence detected by flow cytometry (Figure 3.9) and predominant plasmid integration patterns (Figure 5.14, 5.15, 5.18, 5.19, 5.22, 5.23) are shown.

5.4. Discussion

It was shown in Chapter 3 that the non-UCOE cell lines displayed greater plasmid copies per cell after MTX amplification with the exception of the N1 cell line. Furthermore, the UCOE and non-UCOE cell lines showed varied levels of eGFP mRNA and protein expression. There is significant evidence and expectation that the locus of integration influences expression and may determine differences observed with specific cell lines (Section 1.3). Plasmid integration into a chromosomal region of clusters of highly transcribed endogenous genes may well result in high transcription rate for the recombinant gene, whereas lower transcription rates may be expected if the DNA is inserted into a cluster of repetitive, non-coding sequence elements. Therefore, FISH analysis was performed to investigate the gross chromosomal location of the inserted plasmids in UCOE and non-UCOE cell lines and to address if correlations were observed with stability or instability of eGFP expression over long-term culture. This study was undertaken with acknowledgement of the caveats of multiple integration sites in amplified CHO cell lines and the difficulty in assignment of transcriptional activity across different sites (and the potential for single site integration events at the level of detection of FISH analyses). Despite these caveats the study has generated novel information on CHO cell chromosomal structures and changes during long-term culture.

CHO-DG44 cells have been shown to contain 20 chromosomes (Derouazi et al., 2006). Chromosome number distribution of the amplified CHO-GFP cell lines showed that the majority of the metaphase spreads of the UCOE cell lines also contained a total of 20 chromosomes. Among the non-UCOE cell lines, the frequency of cells containing 20 chromosomes was higher in the N1 cell line, whereas the cell population in the N2 and N4 cell lines was more heterogeneous with wider distributions of chromosome numbers. Moreover, unlike non-UCOE, the UCOE cell lines did not show any metaphase spreads with more than 21 chromosomes. This might be as a result of lower transgene expression of non-UCOE cell lines which resulted in slower growth rate in the presence of MTX. Therefore, this may indicate that these cell lines are more prone to chromosomal

abnormalities or only the cells with gross rearrangements may survive to the particular concentration of MTX selection.

The CHO-DG44 cell line has an altered karyotype compared to Chinese hamster cells (Ray and Mohandas, 1976). A recent comprehensive study showed that DG44 cells contained a total of 20 chromosomes rather than 22 observed in the Chinese hamster cells (Section 1.2.3.2.1). Furthermore, only 7 of the Chinese hamster chromosomes appeared to be normal in the majority of the DG44 cells including two copies of chromosome 1 and one copy of chromosomes 2, 4, 5, 8 and 9 (Derouazi et al., 2006). The remaining DG44 chromosomes included 4 Z group chromosomes (Deaven and Petersen, 1973), 7 structurally-altered chromosomes (derivatives) and 2 structurally abnormal marker chromosomes (Derouazi et al., 2006). Moreover, recombinant cell lines showed an altered karyotype compared to the parental DG44 cells, as it was reported that only 37% of the recombinant cell lines tested had the same karyotype as DG44 strain (Derouazi et al., 2006). Therefore, it was not possible to detect all DG44 chromosomes with chromosome painting probes as the probes used in this study were generated from Chinese hamster cells. Despite the limitations, significant amounts of information were obtained from the chromosome painting experiments. Dual colour FISH with chromosome painting probes specific to Chinese hamster chromosomes and plasmid probes revealed that plasmid integration sites were localized into chromosome 6, 7 and xy as well as other group-2 chromosomes in the U2 cell line. For the N2 cell line, one metaphase spread showed integration in chromosome 7, the remaining spreads displayed plasmid localization in a group-1 chromosome.

The FISH data showed that following MTX amplification, the N2 and N4 cell lines contained gross chromosomal rearrangements such as highly extended amplified regions and dicentric chromosomes. Such chromosomal structures are characteristics of MTX amplification mediated by a breakage-fusion-bridge cycle mechanism, as reported by Kim *et al.* (1999). In contrast, the UCOE cell lines and N1 cell line did not show such chromosomal rearrangements. This difference between the N2 and N4 cell lines and the N1 and UCOE cell lines was also observed in chromosome number distributions, where the

distribution of the number of chromosomes observed in N2 and N4 cell lines were broader than the UCOE and N1 cell lines. Based on these results, N2 and N4 cell lines seem to be more prone to gross chromosomal rearrangements following MTX amplification, showing characteristics of amplified cell lines. Hence, N2 and N4 cell lines had a diverse range of chromosome numbers and greater number of plasmid copies per cell as a result.

The location of amplified sequences was mainly within a group-1 chromosome in the non-UCOE cell lines, whereas the majority of the UCOE cell lines displayed plasmid integration within a group-2 chromosome. It was observed that the N2 cell line had a very homogenous population in terms of plasmid integration at the start of long-term culture. However, this was not reflected in the CV values as the N2 cell line had the highest CV value among all the other non-UCOE cell lines, suggesting that some other factors such as the presence of non-active genes in some cells might play a role in the population heterogeneity of eGFP expression (Table 5.1).

It is likely that chromosomes that have undergone gross rearrangements may be more prone to instability and will be subjected to further chromosome rearrangements (Wurm et al., 1996, Wurm et al., 2003). Therefore, FISH analysis was performed with metaphase spreads prepared from cell lines at late generation in the presence and absence of MTX. After 80 days of continuous culture in the presence of MTX, chromosomal location of the amplified gene did not change in the N1 and N4 cell lines. However, the frequency of different integration patterns changed over time leading to a more homogenous cell population. This was also mirrored in CV values as a decrease was observed over long-term culture in the presence of MTX (Table 5.1). The N2 cell line was more heterogeneous in terms of plasmid integration patterns at the end of prolonged culture in the presence of MTX compared to the N1 and N4 cell lines, which was also reflected in the CV values where the N2 cell line displayed the highest CV. A possible explanation to the genotypic heterogeneity observed in the N2 cell line is that in the presence of MTX, only diverse cells with sufficient MTX resistance would survive. To achieve this, MTX might induce genetic rearrangements in the chromosomes of cells with low MTX resistance. Therefore, cells with new plasmid location that have sufficient MTX resistance can emerge during

culture in the presence of MTX (Kim and Lee, 1999, Pallavicini et al., 1990). This was also observed in the U1 and U3 cell lines as CV values decreased over time in the presence of MTX whereas cell populations displayed genotypic heterogeneity at the end of prolonged culture in the presence of MTX. In contrast, despite an increase in the CV value, the genotypic heterogeneity was not increased in the U2 cell line in the presence of MTX; instead the cell population became more homogenous.

In the absence of MTX, the more homogenous population showing unique hybridization patterns was predominant in the N1 and N4 cell lines after long-term culture. However, CV values increased after MTX removal in these cell lines, suggesting that despite possessing the plasmid copies, eGFP fluorescence was not the same in individual cells. In the N2 cell line, the same type of integration was still predominant within the population at the end of long-term culture in the absence of MTX. This was consistent with the CV value of the N2 cell line, which was constant over long-term culture after removal of MTX. Moreover, chromosomes that underwent gross morphological changes disappeared in non-UCOE cell lines in the absence of MTX.

Some chromosomal integration patterns (i.e. 2A) were decreased in abundance or disappeared from the cell population in the UCOE cell lines during long-term culture in the absence of MTX. Instead a variant of 2A with a shortened amplified sequence became predominant, possibly due to a loss of plasmid copies observed in the UCOE cell lines in the absence of MTX. This was more visible in the U3 cell line as 30% of the cells did not contain a detectable FISH signal at the end of prolonged culture in the absence of MTX. Therefore, the low-producing population of cells might be responsible for the increase in CV value. The U1 and U2 cell lines also displayed more varied eGFP fluorescence between cells after MTX removal, suggesting that although cells reached a stable genotype, eGFP expression was not the same for individual cells.

These findings suggest that the varied response of non-UCOE cell lines to long-term culture in the presence of MTX may be attributed to the changes in integration profile as more homogeneous profile resulted in less variation in eGFP fluorescence (i.e. N1, N4),

whereas heterogeneous genotype at the end of long-term culture was reflected in high CV values in N2 cell line. The reaction to removal of MTX was also found to be variable between non-UCOE cell lines as shown by CV values. However, cell lines displayed a more homogeneous integration profile after 80 days culture in MTX-free medium, suggesting that although non-UCOE cell lines are containing a more stable genotype, the rate of gene copy loss and transcriptional activity may not be the same between all cells at the end of prolonged culture in the absence of MTX. It may also be concluded that, the unstable, extended region of integrations contribute to overall productivity when MTX is present. Therefore, it is plausible that removal of MTX may result in decline in productivity due to elimination of the unstable integration types. In contrast, UCOE cell lines were found to be less prone to genomic rearrangements following MTX amplification. UCOE cell lines displayed more consistent integration profile over long-term culture in the presence and absence of MTX.

Previous studies have described the stability of recombinant protein expression based on plasmid integration near a telomere site (Yoshikawa et al., 2000a, Yoshikawa et al., 2000b). However, no obvious correlation between the stability of eGFP expression and the plasmid integration sites was observed in this study, as all cell lines showed predominant integration near the end of a chromosome and, yet, displayed different amounts of mRNA and protein. In their study, Yoshikawa et al. (2000b) transfected the parental DG44 cells with a vector containing DHFR and hGM-CSF genes, where both genes are driven by SV40 promoter. The transfected cell pools then treated with increasing levels of MTX concentration from 10nM to 1000nM. The probe they used for FISH analysis was prepared from DHFR sequence. Therefore, considering that the amplification unit might be disrupted by possible genetic rearrangements during stepwise MTX amplification, the data that have been achieved are limited. Nevertheless, it would be beneficial to perform dual-color FISH with telomere and plasmid probes to obtain more accurate results on the relationship between stability of recombinant protein productivity and localization of inserted transgene. In addition, other factors may also play a role in transgene expression, such as chromatin structure surrounding the transgene and repeated arrangement of transgene (Section 1.3) (Dorer and Henikoff, 1994).

5.4.1. Summary

These findings suggest that non-UCOE cell lines are more prone to gross genomic rearrangements that are characteristics of amplified cell lines. In contrast, no such chromosomal aberrations were observed in UCOE cell lines. Cell lines generated using UCOE construct displayed more stable chromosomal structure, which resulted in consistent integration profile over long-term culture in the presence and absence of MTX.

CHAPTER 6:
Concluding Remarks
&
Future Work

6.1. Concluding Remarks

Due to an increasing demand for increased production of clinical grade proteins, which can often only be produced in mammalian cells, improvements in protein yields from mammalian cells and a reduced time for production are key objectives. Productivity has been improved over the last 20 years due to identification and selection of specific host cells, vector developments, cell culture conditions and downstream processing (Matasci et al., 2008). However, clonal heterogeneity and expression instability remain as the key obstacles to "predictable" recombinant protein production in mammalian cell lines, particularly when focused on the various CHO cell platforms. As a consequence, it can be an arduous and costly process to isolate a stable high producing clone. Therefore, more recently, studies have focussed on improving cell line stability and decreasing the laborious process of screening a large number of clones (Chusainow et al., 2009, Pilbrough et al., 2009). In this regard, UCOE vectors were used in combination with MTX amplification to improve the frequency of positive clones and to achieve a high and stable expression of recombinant protein production in the current study. The following discussion will focus on whether the specific objectives outlined in the Introduction have been met.

The first objective stated at the start of this thesis was to determine if the UCOE vectors provided more stable recombinant protein production over long-term culture. The results obtained from non-amplified CHO-GFP and CHO-EPO cell lines showed that UCOEs provide higher levels of recombinant protein production compared to non-UCOE vectors (Section 3.1.2, Section 4.1.1). Moreover, recombinant protein production was found to be stable during prolonged culture in non-amplified cell lines.

The second objective was to determine whether the use of UCOE elements within expression construct increased the proportion of high-producing clones that produce an industrially relevant recombinant protein (i.e. EPO) following MTX amplification. In this regard, the top ten high producer initial CHO-EPO cell lines were pooled and amplified with 250nM MTX. A large number of colonies, producing a higher amount of recombinant

EPO protein, were achieved with pools generated using cells with the UCOE expression vector compared to non-UCOE control vectors (Section 4.2). Amplification studies showed that the time required for cell line development could be greatly decreased by using UCOEs, which was due to the superior growth of UCOE-containing cell lines in the presence of MTX selection. It was also shown that through the use of UCOE elements in combination with MTX amplification, the yield of secreted recombinant protein was dramatically improved as compared to the non-UCOE control group.

The third objective stated at the beginning of the current study was to determine whether protein production was more stable during prolonged culture in cell lines with UCOE vector constructs that have undergone MTX amplification. In this regard, the CHO-GFP and CHO-EPO cell lines which were amplified to 250nM MTX were cultured continuously up to ~80 days in the presence and absence of MTX selection (Section 3.2.2, Section 4.2.1.2). Recombinant protein production remained constant when MTX selection was present in both the UCOE and the non-UCOE cell lines. MTX removal resulted in a decrease in recombinant protein production over long-term culture in all cell lines (whether constructed with or without UCOE inclusion). Again UCOEs appear to offer no preferential advantage in terms of stability. Nevertheless, the use of UCOE elements increased the industrially relevant recombinant protein expression and therefore could potentially shorten the time needed for the selection of cell lines by increasing the proportion of high-producer clones and decreasing the time required for the amplification process.

To address the fourth objective, I have examined genetic parameters including the plasmid copy numbers and mRNA content of the amplified CHO-GFP and CHO-EPO cell lines at the beginning and end of prolonged culture (Section 3.2.3, 3.2.4, 4.2.1.3, 4.2.1.4). It was shown that, despite having significantly higher numbers of plasmid copies per cell, mRNA expression was lower in the non-UCOE cell lines, suggesting that some integrated genes may be transcriptionally inactive or in a location where the expression is more sporadic (Section 3.2.4, Section 4.2.1.4). The higher mRNA content in the UCOE cell lines was also reflected in the higher total production of EPO protein compared to the non-UCOE group.

However, in contrast, eGFP expression was found to be lower in the UCOE cell lines. This remains unexplained but it may be surmised that the intracellular processing of eGFP may result in this discrepancy. It has been shown that the intracellular GFP can be toxic to the cells that constantly express this protein (Liu et al., 1999). In fact, crystals of eGFP were observed in cells that are expressing high amount of eGFP (Croxford, 2008). This may suggest that the UCOE cell lines that express high levels of eGFP did not survive during the amplification process, as such high levels of intracellular protein may be detrimental to the cell line. These observations may indicate that the use of eGFP has some limitations due to the intracellular nature of the eGFP and it can be misleading to use such an intracellular protein to evaluate a process that is eventually going to be used to produce a secreted protein.

Both plasmid copies per cell and mRNA content were relatively stable during prolonged culture irrespective of whether UCOE was present within the expression construct in the presence of MTX selection. However, removal of MTX caused a significant decrease in mRNA expression in both the UCOE and non-UCOE cell lines. Most of the UCOE and non-UCOE cell lines also displayed a loss of transgene copies in the absence of MTX. However, the transgene copies were still significantly higher in the non-UCOE cell lines than the UCOE group. Therefore, it may be suggested that the use of UCOE elements in expression construct resulted in greater mRNA recovery per transgene copy.

In most of the UCOE cell lines the instability of protein production was partly due to a loss of transgene copies. However in some cases (i.e. U2 and U5), the cell lines experienced instability of eGFP expression with little or no change in plasmid copies per cell during long-term culture in the absence of MTX. Treatment with sodium butyrate caused an increase in eGFP fluorescence in both the U2 and U5 cell lines. An increase in eGFP mRNA was also observed in the U2 cell line following sodium butyrate treatment, however the increase in mRNA content was lower than the increase in eGFP fluorescence. Moreover, no change in eGFP mRNA content was observed in the U5 cell line following sodium butyrate addition. Sodium butyrate treatment can influence different cellular processes (Yee et al., 2008). It cannot be concluded from the experimental data in the

current study whether the enhancement in eGFP fluorescence was caused by acetylation of the histones or improved gene accessibility associated with the integrated plasmid or up-regulation of proteins involved in other cellular processes or biological events. It would be worthwhile to conduct further experiments using ChIP technology and DNase I footprinting to have a better understanding as to how the transgene expression was improved by treatment with sodium butyrate. These findings suggest that the use of UCOEs may still require the screening of clones over prolonged culture for desirable properties when used in combination with MTX amplification. The instability of protein production observed in the non-UCOE cell lines was also partly due to a loss of transgene copies over long-term culture in the absence of MTX. However it should be noted that the non-UCOE cell lines still contained over 100 transgene copies per cell (>500 in most cases) at the end of prolonged culture in the absence of MTX. Therefore, the very low level of protein expression in non-UCOE cell lines in the absence of MTX selection cannot solely be attributed to the loss of plasmid copies. Some of the non-UCOE cell lines did not show any loss in transgene copies, although they displayed a profound loss of protein production and mRNA expression during prolonged culture in the absence of MTX.

It has been reported that CHO-DG44 derived recombinant cell lines lost their protein expression during long-term culture in the absence of selective pressure through gene silencing by DNA methylation, with no change in plasmid copies (Yang et al., 2010b, Heller-Harrison et al., 2009, Chusainow et al., 2009). In addition, Heller-Harrison et al. (2009) have also reported that loss of transgene expression may occur by genetic re-arrangement of transgenes resulting in uncoupling of bi-cistronic transcript and subsequent loss of monoclonal antibody production. Therefore, it may be suggested that in the current study, cell lines which showed instability of protein production despite having stable numbers of transgene copies over long-term culture may be experiencing gene silencing in the absence of MTX. Moreover, the greater loss of mRNA and protein expression whilst containing relatively high number of transgene copies observed in non-UCOE cell lines in the absence of MTX may indicate that remaining gene copies are low expressers or are undergoing strong epigenetic silencing.

The fifth objective of the current study was to investigate the effect of integration site on transgene expression following MTX amplification. To address this, chromosome painting and FISH analysis were performed (Chapter 5). The results showed that the non-UCOE cell lines tested contained an abnormal number of chromosomes and gross chromosomal structures. This could be a consequence of a lower expression of transgene from the non-UCOE vectors, which may have resulted in selection of cells with gross amplification of plasmid inserts and the surrounding areas to express enough DHFR to survive a particular concentration of MTX selection. This may have resulted in a greater number of integrated plasmid copies in the non-UCOE cell lines (Section 3.2.3, Section 4.2.1.3). The fact that non-UCOE cell lines displayed slow growth in the presence of MTX may indicate that the site of integration was not favourable for transgene expression and that, as a result, these cell lines required more transgene copies to express sufficient DHFR to survive. In fact, the results showed that non-UCOE cell lines displayed similar amount of DHFR protein compared to UCOE cell lines despite possessing significantly higher numbers of DHFR gene copies. However, further measurements of DHFR enzyme activity would be beneficial to prove this. The cell lines generated with the UCOE vector construct displayed a more consistent karyotype and no abnormal genomic rearrangements were observed (Chapter 5).

The final objective of this study was to determine how the transgene integration sites changed over long-term culture as one indicator of instability. In this regard, FISH analysis was performed at the start and end of prolonged culture in the presence and absence of MTX selection (Section 5.3). It was shown that the non-UCOE cell lines displayed a varied response to long-term culture in terms of integration profile in the presence of MTX. In the absence of MTX, the unstable integration types (i.e. chromosomes with extended amplified arrays and dicentric chromosomes) seemed to be eliminated after the period of long-term culture, which may be one of the reasons that cell lines displayed a loss of protein production. In contrast, the UCOE cell lines displayed a more consistent integration profile over long-term culture in the presence and absence of MTX (i.e. similar integration patterns were observed during long-term culture, with similar numbers of chromosomes within and between cell lines).

Taken all together, my results confirmed that the cell lines with UCOE construct displayed better growth characteristics in the presence of MTX selection which resulted in an improved proportion of high-producing cell lines after single step MTX amplification. The higher level of protein production was paralleled by increased recombinant gene mRNA expression in the UCOE cell lines compared to the non-UCOE group. Protein production remained stable when MTX selection was present. However, all cell lines displayed instability during long-term culture after the removal of MTX. In addition, cell lines with a UCOE construct showed more consistent and stable chromosomal structure as opposed to the non-UCOE cell lines, which displayed gross chromosomal rearrangements and an abnormal number of chromosomes following MTX amplification.

The mechanism(s) by which UCOEs may promote an open chromatin structure is largely unknown and no direct work to elucidate these mechanisms was undertaken in this study. However, there are some similarities that exist between the results obtained from the current study and those observed from other well known DNA regulatory elements such as S/MARs. Several published works have shown that the use of S/MAR elements in vector constructs resulted in an increased proportion of clones that have detectable levels of transgene expression as well as improved levels of protein production (Girod et al., 2005, Girod et al., 2007, Kim et al., 2004, Kim et al., 2005, Zahn-Zabal et al., 2001, Harraghy et al., 2011). These results are similar to the effect of UCOE on transgene expression observed in the current study (Section 4.2). Another similarity is that transfection with S/MAR containing vectors resulted in enhanced growth characteristics in the presence of MTX selection, which was also observed in the current study with UCOE containing cell lines (Section 3.2.1, 4.2.1.1). Therefore, these combined observations may suggest that the overall effect of S/MARs and UCOEs on transgene expression in mammalian cell lines is similar.

However, contradictory results have been reported in a study conducted by Otte et al., where the effect of different DNA elements, including UCOEs, S/MARs, cHS4 insulator and anti-repressor elements, on protein expression levels was compared (Otte et al., 2007).

They reported that the inclusion of UCOE in expression vectors did not result in an increase in reporter gene expression compared to the controls. In their study, CHO-K1 cells were transfected with vector constructs including shortened 2.6kb UCOE element upstream of hCMV-d2eGFP. The neomycin selection marker was located on a different plasmid that was cotransfected with the UCOE-d2eGFP expression constructs. In the current study, an 8kb UCOE element has been used with a DHFR selection marker on the same plasmid. Previous studies have shown that the truncated 1.5kb UCOE element, which is included within the 2.6kb sequence used by Otte et al., was fully functional. Therefore, a reason for the difference in transgene expression may be attributed to the selectable markers being on the same or separate plasmids. It is likely that UCOE may improve the expression of linked transgene if the selectable marker is located on the same plasmid.

No direct study has been published so far in relation to hypotheses that UCOEs open the chromatin environment of linked transgenes. It has been reported that the UCOE contains an extensive region of unmethylated DNA, which has been suggested to ease the binding of transcription factors (Allen and Antoniou, 2007). Based on the similarities observed between S/MARs and UCOEs in terms of their overall effect on transgene expression, it may be suggested that similar to S/MARs, UCOEs could potentially promote enhanced transgene expression by recruiting transcription factors and chromatin remodelling proteins, which may be allowed by the methylation-free region, and may create an open chromatin environment. However, further experimental work needs to be undertaken to provide evidence to the mechanism that underlies the UCOE function.

The data from Section 4.2.1.3 showed a significant correlation between the specific EPO productivity and EPO gene copy numbers in UCOE cell lines, suggesting that the expression of the transgene may be copy number dependent. It was also observed that the UCOE cell lines showed a loss of EPO gene copies over long-term culture both in the presence and absence of MTX selection, which resulted in the loss of specific productivity. Earlier studies have shown that S/MAR elements may comprise targets of DNA recombination or rearrangement events. Examples of this may include the many deletions and translocations observed in leukaemia and breast cancer that were related with S/MAR

elements (Iarovaia et al., 2004, Welch and King, 2001). It was also shown that S/MAR elements may be targets for retroviral integration which often occurs within or close to S/MARs (Johnson and Levy, 2005). Taken together, these data could reflect an enhanced recombigenicity in these genomic loci. A more recent study proposed that S/MARs promote homologous recombination (Grandjean et al., 2011). This mode of action might result from their ability to maintain chromatin in an accessible state therefore providing an access to DNA binding proteins i.e. DNA topoisomerase II, an enzyme that catalyzes double-strand breaks (Blasquez et al., 1989, Grandjean et al., 2011). Assuming that UCOEs and S/MARs have a similar mechanism of action, it is suggested that UCOEs may increase the recombigenic events, hence the use of UCOE in expression construct may result in the loss of the inserted plasmid copies.

6.2. Future Work

There are several lines of research arising from this project. First of all, future work could be performed to address the question arising from Chapter 3 and 4. Is UCOE maintaining an open chromatin environment following MTX amplification? ChIP-on-chip technology could be utilized to investigate potential histone modifications associated with the linked transgene which would provide further information on the effect of UCOE on the local chromatin structure when used in combination with MTX amplification.

In view of the results from Chapters 3 and 4, another line of research would be to investigate the mechanism by which UCOE improves the transgene expression. Using ChIP methodology will provide significant information concerning the association with transcription factors and other DNA binding proteins. This may provide additional information on the UCOE mechanism.

In addition, future experiments may be undertaken to investigate the spatial arrangements of the integrated transgene and association with specific nuclear domains such as transcriptional factories (Section 1.5.1). There are several methods that can be used for this purpose including, 3D-FISH and chromosome conformation capture approaches (such as

3C and 4C). The principal of the 3D-FISH method is similar to the FISH used in this study (Section 2.8). However, instead of metaphase spreads, fixed interphase nuclei on slides are used in 3D-FISH. This technique can be used to analyse spatial positioning of the integrated transgene. Furthermore, this technique can be used in combination with immunofluorescence techniques to determine the association with particular nuclear structures (Chaumeil et al., 2008). 3C can also be used to investigate the three-dimensional nuclear space to determine whether certain genomic regions are in close proximity (Dekker, 2006). In this method, chromatin regions that are in close proximity are cross-linked with formaldehyde and digested with a restriction enzyme followed by intramolecular ligation of DNA fragments. qPCR can be used to identify the DNA sequences that are closely associated in the nucleus which ligated into the same strand. 3C-on-ChIP (4C) allows screening of the whole genome in an unbiased manner for DNA loci closely associated with a given sequence (Simonis et al., 2006). This methodology involves restriction digestion of ligation products from 3C with a frequent cutter. These trimmed fragments are then circularized. An inverse PCR from the 'bait' sequence will amplify the small unknown captured fragment and its interacting partners. This can be labeled and hybridized to a tailored microarray or identified by large-scale sequencing.

In light of the results described in Chapter 5, it would be beneficial to gain a better understanding of the relationships between chromosome profiling and the location of the inserted plasmid. Therefore, future work focusing on chromosome specific painting with multi-colour FISH analysis, using chromosome paint probes prepared from CHO-DG44 chromosomes could be undertaken.

Another aspect for the future work could be the determination of the exact location of transgene insertion within the host genome, which may have implications on transgene stability. In this regard, the genomic regions flanking the transgene can be determined by sequence alignment with published sequence data (Section 1.2.3.2.1) and Expressed Sequence Tag (EST) using DNA walking methodology.

In summary, it is concluded that the inclusion of UCOEs within the expression construct offer significant benefits for consistency of cell line generation and that UCOEs can be successfully used in combination with MTX amplification. My results indicate that UCOEs facilitate increased cell line recovery by transcriptional enhancement of selection markers, such as DHFR.

REFERENCES

- ALLEN, M. L. & ANTONIOU, M. (2007) Correlation of DNA Methylation with Histone Modifications Across the HNRPA2B1-CBX3 Ubiquitously-Acting Chromatin Open Element (UCOE). *Epigenetics*, 2, 227-236.
- ALTMANN, F., STAUDACHER, E., WILSON, I. B. H. & MÄRZ, L. (1999) Insect cells as hosts for the expression of recombinant glycoproteins. *Glycoconjugate Journal*, 16, 109-123.
- ANDERSEN, D. C. & KRUMMEN, L. (2002) Recombinant protein expression for therapeutic applications. *Current Opinion in Biotechnology*, 13, 117-123.
- ANTEQUERA, F. & BIRD, A. (1993) Number of CpG islands and genes in human and mouse. *Proc Natl Acad Sci*, 90, 11995-11999.
- ANTONIOU, M. & CROMBIE, R. (2000) Polynucleotide comprising a ubiquitous chromatin opening element that is not derived from a locus control region, useful in gene therapy. United States.
- ANTONIOU, M., HARLAND, L., MUSTOE, T., WILLIAMS, S., HOLDSTOCK, J., YAGUE, E., MULCAHY, T., GRIFFITHS, M., EDWARDS, S., IOANNOU, P. A., MOUNTAIN, A. & CROMBIE, R. (2003) Transgenes encompassing dual-promoter CpG islands from the human TBP and HNRPA2B1 loci are resistant to heterochromatin-mediated silencing. *Genomics*, 82, 269-279.
- AROLAS, J. L., AVILES, F. X., CHANG, J.-Y. & VENTURA, S. (2006) Folding of small disulfide-rich proteins: clarifying the puzzle. *Trends in Biochemical Sciences*, 31, 292-301.
- ASSARAF, Y. G. & SCHIMKE, R. T. (1987) Identification of methotrexate transport deficiency in mammalian cells using fluoresceinated methotrexate and flow cytometry. *Proc Natl Acad Sci*, 84, 7154-7158.
- BALAJEE, A. S., OH, H. J. & NATARAJAN, A. T. (1994) Analysis of restriction enzyme-induced chromosome aberrations in the interstitial telomeric repeat sequences of CHO and CHE cells by FISH. *Mutation Research/Fundamental and Molecular Mechanisms of Mutagenesis*, 307, 307-313.
- BARNES, L. M., BENTLEY, C. M. & DICKSON, A. J. (2000) Advances in animal cell recombinant protein production: GS-NS0 expression system. *Cytotechnology*, 32, 109-123.
- BARNES, L. M., BENTLEY, C. M. & DICKSON, A. J. (2001) Characterization of the stability of recombinant protein production in the GS-NS0 expression system. *Biotechnology and Bioengineering*, 73, 261-270.
- BARNES, L. M., BENTLEY, C. M. & DICKSON, A. J. (2003) Stability of protein production from recombinant mammalian cells. *Biotechnology and Bioengineering*, 81, 631-639.
- BARNES, L. M., MOY, N. & DICKSON, A. J. (2006) Phenotypic variation during cloning procedures: Analysis of the growth behavior of clonal cell lines. *Biotechnology and Bioengineering*, 94, 530-537.
- BARTOS, J. D., GAILE, D. P., MCQUAID, D. E., CONROY, J. M., DARBARY, H., NOWAK, N. J., BLOCK, A., PETRELLI, N. J., MITTELMAN, A., STOLER, D. L. & ANDERSON, G. R. (2007) aCGH local copy number aberrations associated

- with overall copy number genomic instability in colorectal cancer: Coordinate involvement of the regions including BCR and ABL. *Mutation Research/Fundamental and Molecular Mechanisms of Mutagenesis*, 615, 1-11.
- BEBBINGTON, C. R., RENNER, G., THOMSON, S., KING, D., ABRAMS, D. & YARRANTON, G. T. (1992) High-Level Expression of a Recombinant Antibody from Myeloma Cells Using a Glutamine Synthetase Gene as an Amplifiable Selectable Marker. *Nat Biotech*, 10, 169-175.
- BECK, A., WURCH, T., BAILLY, C. & CORVAIA, N. (2010) Strategies and challenges for the next generation of therapeutic antibodies. *Nat Rev Immunol*, 10, 345-352.
- BECSKEI, A., KAUFMANN, B. B. & VAN-OUDENAARDEN, A. (2005) Contributions of low molecule number and chromosomal positioning to stochastic gene expression. *Nat Genet*, 37, 937-944.
- BENTON, T., CHEN, T., MCENTEE, M., FOX, B., KING, D., CROMBIE, R., THOMAS, T. C. & BEBBINGTON, C. (2002) The use of UCOE vectors in combination with a preadapted serum free, suspension cell line allows for rapid production of large quantities of protein. *Cytotechnology*, 38, 43-46.
- BESTOR, T. H. (2000) Gene silencing as a threat to the success of gene therapy. *J Clin Invest*, 105, 409.
- BIRD, A. P. & WOLFFE, A. P. (1999) Methylation-induced repression--belts, braces, and chromatin. *Cell*, 99, 451-4.
- BLACKWOOD, E. M. & KADONAGA, J. T. (1998) Going the Distance: A Current View of Enhancer Action. *Science*, 281, 60-63.
- BLASQUEZ, V. C., SPERRY, A. O., COCKERILL, P. N. & GARRARD, W. T. (1989) Protein:DNA interactions at chromosomal loop attachment sites. *Genome*, 31, 503-509.
- BODE, J., BENHAM, C., KNOPP, A. & MIELKE, C. (2000) Transcriptional augmentation: modulation of gene expression by scaffold/matrix-attached regions (S/MAR elements). *Crit Rev Eukaryot Gene Expr*, 10, 73-90.
- BOLZAN, A. D. (2011) Chromosomal aberrations involving telomeres and interstitial telomeric sequences. *Mutagenesis*, 27, 1-15.
- BONNAL, S., BOUTONNET, C., PRADO-LOURENÇO, L. & VAGNER, S. (2003) IRES: the Internal Ribosome Entry Site database. *Nucleic Acids Research*, 31, 427-428.
- BROWN, J. M., LEACH, J., REITTIE, J. E., ATZBERGER, A., LEE-PRUDHOE, J., WOOD, W. G., HIGGS, D. R., IBORRA, F. J. & BUCKLE, V. J. (2006) Coregulated human globin genes are frequently in spatial proximity when active. *The Journal of Cell Biology*, 172, 177-187.
- BUCETA, M., GALBETE, J. L., KOSTIC, C., ARSENIJEVIC, Y. & MERMOD, N. (2011) Use of human MAR elements to improve retroviral vector production. *Gene Ther*, 18, 7-13.
- BULGER, M. (2005) Hyperacetylated Chromatin Domains: Lessons from Heterochromatin. *Journal of Biological Chemistry*, 280, 21689-21692.
- BUTLER, M. (2005) Animal cell cultures: recent achievements and perspectives in the production of biopharmaceuticals. *Applied Microbiology and Biotechnology*, 68, 283-291.

- CARTER, D., CHAKALOVA, L., OSBORNE, C. S., DAI, Y. F. & FRASER, P. (2002) Long-range chromatin regulatory interactions in vivo. *Nature Genetics*, 32, 623-626.
- CAVALCANTI, F., CALVO, N., GRAU-OLIETE, M. & RIVERA-FILLAT, M. (1992) Simultaneous changes in various mechanisms that mediate the cell incorporation of folate compounds account for low levels of resistance to methotrexate. *Cell Biochemistry and Function*, 10, 1-7.
- CHAMBEYRON, S. V. & BICKMORE, W. A. (2004) Chromatin decondensation and nuclear reorganization of the HoxB locus upon induction of transcription. *Genes & Development*, 18, 1119-1130.
- CHAUDHURI, T. K., HORII, K., YODA, T., ARAI, M., NAGATA, S., TERADA, T. P., UCHIYAMA, H., IKURA, T., TSUMOTO, K., KATAOKA, H., MATSUSHIMA, M., KUWAJIMA, K. & KUMAGAI, I. (1999) Effect of the Extra N-terminal Methionine Residue on the Stability and Folding of Recombinant Î±-Lactalbumin Expressed in Escherichia coli. *Journal of Molecular Biology*, 285, 1179-1194.
- CHAUMEIL, J., AUGUI, S., CHOW, J. C., HEARD, E. & HANCOCK, R. (2008) Combined Immunofluorescence, RNA Fluorescent In Situ Hybridization, and DNA Fluorescent In Situ Hybridization to Study Chromatin Changes, Transcriptional Activity, Nuclear Organization, and X-Chromosome Inactivation The Nucleus. IN WALKER, J. M. (Ed.). Humana Press.
- CHEN, D., MA, H., HONG, H., KOH, S. S., HUANG, S.-M., SCHURTER, B. T., ASWAD, D. W. & STALLCUP, M. R. (1999) Regulation of Transcription by a Protein Methyltransferase. *Science*, 284, 2174-2177.
- CHOI, J. H. & LEE, S. Y. (2004) Secretory and extracellular production of recombinant proteins using Escherichia coli. *Applied Microbiology and Biotechnology*, 64, 625-635.
- CHUANG, C.-H., CARPENTER, A. E., FUCHSOVA, B., JOHNSON, T., DE LANEROLLE, P. & BELMONT, A. S. (2006) Long-Range Directional Movement of an Interphase Chromosome Site. *Current Biology*, 16, 825-831.
- CHUSAINOW, J., YANG, Y. S., YEO, Y. H. M., TOH, P. C., ASVADI, P., WONG, N. S. C. & YAP, M. G. S. (2009) A Study of Monoclonal Antibody-Producing CHO Cell Lines: What Makes a Stable High Producer? *Biotechnology and Bioengineering*, 102, 1182-1196.
- COCKERILL, P. N. (2011) Structure and function of active chromatin and DNase I hypersensitive sites. *Febs Journal*, 278, 2182-2210.
- COGONI, C. & MACINO, G. (2000) Post-transcriptional gene silencing across kingdoms. *Current Opinion in Genetics & Development*, 10, 638-643.
- COQUELLE, A., PIPIRAS, E., TOLEDO, F., BUTTIN, G. & DEBATISSE, M. (1997) Expression of Fragile Sites Triggers Intrachromosomal Mammalian Gene Amplification and Sets Boundaries to Early Amplicons. *Cell*, 89, 215-225.
- CREMER, T., CREMER, M., DIETZEL, S., MULLER, S., SOLOVEI, I. & FAKAN, S. (2006) Chromosome territories - a functional nuclear landscape. *Current Opinion in Cell Biology*, 18, 307-316.
- CROXFORD, A. S. (2008) Optimisation of Recombinant Protein Production in Chinese Hamster Ovary Cells using Ubiquitous Chromatin Opening Elements. *The Faculty of Life Sciences*. Manchester, The University of Manchester.

- DE LEON GATTI, M., WLASCHIN, K. F., NISSOM, P. M., YAP, M. & HU, W.-S. (2007) Comparative transcriptional analysis of mouse hybridoma and recombinant Chinese hamster ovary cells undergoing butyrate treatment. *Journal of Bioscience and Bioengineering*, 103, 82-91.
- DE POORTER, J. J., LIPINSKI, K. S., NELISSEN, R. G. H. H., HUIZINGA, T. W. J. & HOEBEN, R. C. (2007) Optimization of short-term transgene expression by sodium butyrate and ubiquitous chromatin opening elements (UCOEs). *The Journal of Gene Medicine*, 9, 639-648.
- DEAN, A. (2006) On a chromosome far, far away: LCRs and gene expression. *Trends in genetics : TIG*, 22, 38-45.
- DEAVEN, L. L. & PETERSEN, D. F. (1973) The chromosomes of CHO, an aneuploid Chinese hamster cell line: G-band, C-band, and autoradiographic analyses. *Chromosoma*, 41, 129-144.
- DEKKER, J. (2006) The three 'C' s of chromosome conformation capture: controls, controls, controls. *Nat Meth*, 3, 17-21.
- DELORME, E., LORENZINI, T., GIFFIN, J., MARTIN, F., JACOBSEN, F., BOONE, T. & ELLIOTT, S. (1992) Role of glycosylation on the secretion and biological activity of erythropoietin. *Biochemistry*, 31, 9871-9876.
- DEMAIN, A. L. & VAISHNAV, P. (2009) Production of recombinant proteins by microbes and higher organisms. *Biotechnology Advances*, 27, 297-306.
- DEROUAZI, M., MARTINET, D., BESUCHET SCHMUTZ, N., FLACTIONS, R., WICHT, M., BERTSCHINGER, M., HACKER, D. L., BECKMANN, J. S. & WURM, F. M. (2006) Genetic characterization of CHO production host DG44 and derivative recombinant cell lines. *Biochemical and Biophysical Research Communications*, 340, 1069-1077.
- DOBIE, K. W., LEE, M., FANTES, J. A., GRAHAM, E., CLARK, A. J., SPRINGBETT, A., LATHE, R. & MCCLENAGHAN, M. (1996) Variegated transgene expression in mouse mammary gland is determined by the transgene integration locus. *Proc Natl Acad Sci*, 25, 6659-6664.
- DORAI, H., CORISDEO, S., ELLIS, D., KINNEY, C., CHOMO, M., HAWLEY-NELSON, P., MOORE, G., BETENBAUGH, M. J. & GANGULY, S. (2011) Early prediction of instability of chinese hamster ovary cell lines expressing recombinant antibodies and antibody-fusion proteins. *Biotechnology and Bioengineering*, n/a-n/a.
- DORER, D. R. & HENIKOFF, S. (1994) Expansions of transgene repeats cause heterochromatin formation and gene silencing in Drosophila. *Cell*, 77, 993-1002.
- DRISSEN, R., PALSTRA, R.-J., GILLEMANS, N., SPLINTER, E., GROSVELD, F., PHILIPSEN, S. & DE LAAT, W. (2004) The active spatial organization of the β -globin locus requires the transcription factor EKLF. *Genes & Development*, 18, 2485-2490.
- DUROCHER, Y. & BUTLER, M. (2009) Expression systems for therapeutic glycoprotein production. *Current Opinion in Biotechnology*, 20, 700-707.
- ELLIOTT, S., LORENZINI, T., ASHER, S., AOKI, K., BRANKOW, D., BUCK, L., BUSSE, L., CHANG, D., FULLER, J., GRANT, J., HERNDAY, N., HOKUM, M., HU, S., KNUDTEN, A., LEVIN, N., KOMOROWSKI, R., MARTIN, F., NAVARRO, R., OSSLUND, T., ROGERS, G., ROGERS, N., TRAIL, G. &

- EGRIE, J. (2003) Enhancement of therapeutic protein in vivo activities through glycoengineering. *Nat Biotech*, 21, 414-421.
- FANN, C. H., GUIRGIS, F., CHEN, G., LAO, M. S. & PIRET, J. M. (2000) Limitations to the amplification and stability of human tissue-type plasminogen activator expression by Chinese hamster ovary cells. *Biotechnology and Bioengineering*, 69, 204-212.
- FANTI, L. & PIMPINELLI, S. (2008) HP1: a functionally multifaceted protein. *Current Opinion in Genetics & Development*, 18, 169-174.
- FERRER-MIRALLES, N., DOMINGO-ESPIN, J., CORCHERO, J. L., VAZQUEZ, E. & VILLAVERDE, A. (2009) Microbial factories for recombinant pharmaceuticals. *BioMed Central*, 8.
- FESTENSTEIN, R., TOLAINI, M., CORBELLA, P., MAMALAKI, C., PARRINGTON, J., FOX, M., MILIOU, A., JONES, M. & KIOUSSIS, D. (1996) Locus Control Region Function and Heterochromatin-Induced Position Effect Variegation. *Science*, 271, 1123-1125.
- FLINTOFF, W., DAVIDSON, S. & SIMINOVITCH, L. (1976) Isolation and partial characterization of three methotrexate-resistant phenotypes from Chinese hamster ovary cells. *Somatic Cell Genetics*, 2, 245-261.
- FLINTOFF, W. F. & ESSANI, K. (1980) Methotrexate-resistant Chinese hamster ovary cells contain a dihydrofolate reductase with an altered affinity for methotrexate. *Biochemistry*, 19, 4321-4327.
- FRASER, H. B., HIRSH, A. E., GIAEVER, G., KUMM, J. & EISEN, M. B. (2004) Noise Minimization in Eukaryotic Gene Expression. *PLoS Biol*, 2, e137.
- FRASER, P. & BICKMORE, W. (2007) Nuclear organization of the genome and the potential for gene regulation. *Nature*, 447, 413-417.
- GAJDUSKOVA, P., SNIJDERS, A., KWEK, S., ROYDASGUPTA, R., FRIDLAND, J., TOKUYASU, T., PINKEL, D. & ALBERTSON, D. (2007) Genome position and gene amplification. *Genome Biology*, 8, R120.
- GALBETE, J. L., BUCETA, M. & MERMOD, N. (2009) MAR elements regulate the probability of epigenetic switching between active and inactive gene expression. *Mol. BioSyst*, 5, 143-150.
- GARRICK, D., FIERING, S., MARTIN, D. I. K. & WHITELAW, E. (1998) Repeat-induced gene silencing in mammals. *Nature Genetics*, 18, 56-59.
- GELATO, K. A. & FISCHLE, W. (2008) Role of histone modifications in defining chromatin structure and function. *Biological Chemistry*, 389, 353-63.
- GEORGE, N., PHILLIPS, JR. (1997) Structure and dynamics of green fluorescent protein. *Current Opinion in Structural Biology*, 7, 821-827.
- GEORGIU, G. & SEGATORI, L. (2005) Preparative expression of secreted proteins in bacteria: status report and future prospects. *Current Opinion in Biotechnology*, 16, 538-545.
- GIROD, P.-A., NGUYEN, D.-Q., CALABRESE, D., PUTTINI, S., GRANDJEAN, M., MARTINET, D., REGAMEY, A., SAUGY, D., BECKMANN, J. S., BUCHER, P. & MERMOD, N. (2007) Genome-wide prediction of matrix attachment regions that increase gene expression in mammalian cells. *Nat Meth*, 4, 747-753.

- GIROD, P.-A., ZAHN-ZABAL, M. & MERMED, N. (2005) Use of the chicken lysozyme 5' matrix attachment region to generate high producer CHO cell lines. *Biotechnology and Bioengineering*, 91, 1-11.
- GOODSELL, D. S. (1999) The Molecular Perspective: p53 Tumor Suppressor. *The Oncologist*, 4, 138-139.
- GOULIAN, M., BLEILE, B. & TSENG, B. Y. (1980) Methotrexate-induced misincorporation of uracil into DNA. *Proceedings of the National Academy of Sciences*, 77, 1956-1960.
- GRANDJEAN, M., GIROD, P. A., CALABRESE, D., KOSTYRKO, K., WICHT, M., YERLY, F., MAZZA, C., BECKMANN, J. S., MARTINET, D. & MERMED, N. (2011) High-level transgene expression by homologous recombination-mediated gene transfer. *Nucleic Acids Research*, 39, 15.
- GROSVELD, F., VAN ASSENDELFT, G. B., GREAVES, D. R. & KOLLIAS, G. (1987) Position-independent, high-level expression of the human β -globin gene in transgenic mice. *Cell*, 51, 975-985.
- GU, M. B., TODD, P. & KOMPALA, D. S. (1996) Metabolic burden in recombinant CHO cells: effect of *dhfr* gene amplification and *lacZ* expression. *Cytotechnology*, 18, 159-166.
- GUARINO, C. & DELISA, M. P. (2011) A prokaryote-based cell-free translation system that efficiently synthesizes glycoproteins. *Glycobiology*.
- GUPTA, R. G., BEG, Q. B., KHAN, S. K. & CHAUHAN, B. C. (2002) An overview on fermentation, downstream processing and properties of microbial alkaline proteases. *Applied Microbiology and Biotechnology*, 60, 381-395.
- HABER, D. A., BEVERLEY, S., KIELY, M. L. & SCHIMKE, R. T. (1981) Properties of an Altered Dihydrofolate Reductase Encoded by Amplified Genes in Cultured Mouse Fibroblasts. *Journal of Biological Chemistry*, 256, 9501-9510.
- HABER, D. A. & SCHIMKE, R. T. (1981) Unstable amplification of an altered dihydrofolate reductase gene associated with double-minute chromosomes. *Cell*, 26, 355-362.
- HAMILTON, S. R., BOBROWICZ, P., BOBROWICZ, B., DAVIDSON, R. C., LI, H., MITCHELL, T., NETT, J. H., RAUSCH, S., STADHEIM, T. A., WISCHNEWSKI, H., WILDT, S. & GERNGROSS, T. U. (2003) Production of Complex Human Glycoproteins in Yeast. *Science*, 301, 1244-1246.
- HAMILTON, S. R., DAVIDSON, R. C., SETHURAMAN, N., NETT, J. H., JIANG, Y., RIOS, S., BOBROWICZ, P., STADHEIM, T. A., LI, H., CHOI, B.-K., HOPKINS, D., WISCHNEWSKI, H., ROSER, J., MITCHELL, T., STRAWBRIDGE, R. R., HOOPEES, J., WILDT, S. & GERNGROSS, T. U. (2006) Humanization of Yeast to Produce Complex Terminally Sialylated Glycoproteins. *Science*, 313, 1441-1443.
- HAMILTON, S. R. & GERNGROSS, T. U. (2007) Glycosylation engineering in yeast: the advent of fully humanized yeast. *Current Opinion in Biotechnology*, 18, 387-392.
- HAMMILL, L., WELLES, J. & CARSON, G. R. (2000) The gel microdrop secretion assay: Identification of a low productivity subpopulation arising during the production of human antibody in CHO cells. *Cytotechnology*, 34, 27-37.
- HAMMOND, S., SWANBERG, J., KAPLAREVIC, M. & LEE, K. (2011) Genomic sequencing and analysis of a Chinese hamster ovary cell line using Illumina sequencing technology. *BMC Genomics*, 12, 67.

- HAMMOND, S. M., BERNSTEIN, E., BEACH, D. & HANNON, G. J. (2000) An RNA-directed nuclease mediates post-transcriptional gene silencing in *Drosophila* cells. *Nature*, 404, 293-296.
- HANSEN, J. C., AUSIO, J., STANIK, V. H. & VAN HOLDE, K. E. (1989) Homogeneous reconstituted oligonucleosomes, evidence for salt-dependent folding in the absence of histone H1. *Biochemistry*, 28, 9129-9136.
- HARD, K., BITTER, W., KAMERLING, J. P. & VLIEGENTHART, J. F. G. (1989) O-Mannosylation of recombinant human insulin-like growth factor I (IGF-I) produced in *Saccharomyces cerevisiae*. *FEBS Letters*, 248, 111-114.
- HARIKRISHNAN, K. N., CHOW, M. Z., BAKER, E. K., PAL, S., BASSAL, S., BRASACCHIO, D., WANG, L., CRAIG, J. M., JONES, P. L., SIF, S. & EL-OSTA, A. (2005) Brahma links the SWI/SNF chromatin-remodeling complex with MeCP2-dependent transcriptional silencing. *Nat Genet*, 37, 254-264.
- HARLAND, L., CROMBIE, R., ANSON, S., DEBOER, J., IOANNOU, P. A. & ANTONIOU, M. (2002) Transcriptional Regulation of the Human TATA Binding Protein Gene. *Genomics*, 79, 479-482.
- HARRAGHY, N., REGAMEY, A., GIROD, P.-A. & MERMOD, N. (2011) Identification of a potent MAR element from the mouse genome and assessment of its activity in stable and transient transfections. *Journal of Biotechnology*, 154, 11-20.
- HEITZ, E. (1929) Heterochromatin, chromocentren, chromomeren [Heterochromatin, chromocentres, chromomeres]. *Ber Deutsch Bot Ges*, 47, 274-284.
- HELLER-HARRISON, R., CROWE, K., COOLEY, C., HONE, M., MCCARTHY, K. & LEONARD, M. (2009) Managing cell line instability and its impact during cell line development. *BioPharm Int Suppl*.
- HENDZEL, M. J., WEI, Y., MANCINI, M. A., VAN HOOSER, A., RANALLI, T., BRINKLEY, B. R., BAZETT-JONES, D. P. & ALLIS, C. D. (1997) Mitosis-specific phosphorylation of histone H3 initiates primarily within pericentromeric heterochromatin during G2 and spreads in an ordered fashion coincident with mitotic chromosome condensation. *Chromosoma*, 106, 348-360.
- HENG, H. H. Q., GOETZE, S., YE, C. J., LIU, G., STEVENS, J. B., BREMER, S. W., WYKES, S. M., BODE, J. & KRAWETZ, S. A. (2004) Chromatin loops are selectively anchored using scaffold/matrix-attachment regions. *Journal of Cell Science*, 117, 999-1008.
- HENIKOFF, S. (2008) Nucleosome destabilization in the epigenetic regulation of gene expression. *Nat Rev Genet*, 9, 15-26.
- HILLER, A. (2009) Fast Growth Foreseen for Protein Therapeutics. *GEN-BioMarket Trends*, 29, 153-155.
- HITZEMAN, R. A., HAGIE, F. E., LEVINE, H. L., GOEDDEL, D. V., AMMERER, G. & HALL, B. D. (1981) Expression of a human gene for interferon in yeast. *Nature*, 293, 717-722.
- HOLCIK, M., SONENBERG, N. & KORNELUK, R. G. (2000) Internal ribosome initiation of translation and the control of cell death. *Trends in Genetics*, 16, 469-473.
- HUNT, L., BATARD, P., JORDAN, M. & WURM, F. M. (2002) Fluorescent proteins in animal cells for process development: Optimization of sodium butyrate treatment as an example. *Biotechnology and Bioengineering*, 77, 528-537.

- IAROVAIA, O. V., SHKUMATOV, P. & RAZIN, S. V. (2004) Breakpoint cluster regions of the AML-1 and ETO genes contain MAR elements and are preferentially associated with the nuclear matrix in proliferating HEL cells. *Journal of Cell Science*, 117, 4583-4590.
- IZUMI, M. & GILBERT, D. M. (2000) Homogeneous tetracycline-regulatable gene expression in mammalian fibroblasts. *Journal of Cellular Biochemistry*, 76, 280-289.
- JAYAPAL, K. P., WLASCHIN, K. F., HU, W. S. & YAP, M. G. S. (2007) Recombinant protein therapeutics from cho cells 20 years and counting. *Chemical Engineering Progress*, 103, 40-47.
- JEFFERIS, R. (2009) Glycosylation as a strategy to improve antibody-based therapeutics. *Nat Rev Drug Discov*, 8, 226-234.
- JIANG, Z., HUANG, Y. & SHARFSTEIN, S. T. (2006) Regulation of recombinant monoclonal antibody production in Chinese hamster ovary cells: A comparative study of gene copy number, mRNA level, and protein expression. *Biotechnology Progress*, 22, 313-318.
- JIANG, Z. & SHARFSTEIN, S. T. (2008) Sodium Butyrate Stimulates Monoclonal Antibody Over-expression in CHO Cells by Improving Gene Accessibility. *Biotechnology and Bioengineering*, 100, 189-194.
- JOHNSON, C. & LEVY, L. (2005) Matrix attachment regions as targets for retroviral integration. *Virology Journal*, 2, 68.
- JONES, L., HAMILTON, A. J., VOINET, O., THOMAS, C. L., MAULE, A. J. & BAULCOMBE, D. C. (1999) RNA-DNA Interactions and DNA Methylation in Post-Transcriptional Gene Silencing. *The Plant Cell Online*, 11, 2291-2302.
- JONES, P., TAYLOR, S., - & WILSON, V. (1983) Inhibition of DNA methylation by 5-azacytidine. *Recent Results in Cancer Research*, 84, 202-211.
- JUN, S. C., KIM, M. S., HONG, H. J. & LEE, G. M. (2006) Limitations to the Development of Humanized Antibody Producing Chinese Hamster Ovary Cells Using Glutamine Synthetase-Mediated Gene Amplification. *Biotechnology Progress*, 22, 770-780.
- KAO, F.-T. & PUCK, T. T. (1967) Genetics of Somatic Mammalian Cells. IV. Properties of Chinese Hamster Cell Mutants with Respect to the Requirement for Proline. *Genetics*, 55, 513-524.
- KAO, F.-T. & PUCK, T. T. (1968) Genetics of somatic mammalian cells, VII. Induction and isolation of nutritional mutants in Chinese hamster cells. *Proc Natl Acad Sci*, 60, 1275-1281.
- KAO, F.-T. & PUCK, T. T. (1969) Genetics of somatic mammalian cells. IX. Quantitation of mutagenesis by physical and chemical agents. *Journal of Cellular Physiology*, 74, 245-257.
- KAO, F.-T. & PUCK, T. T. (1970) Genetics of Somatic Mammalian Cells: Linkage Studies with Human-Chinese Hamster Cell Hybrids. *Nature*, 228, 329-332.
- KARG, S. R. & KALLIO, P. T. (2009) The production of biopharmaceuticals in plant systems. *Biotechnology Advances*, 27, 879-894.
- KARPUSAS, M., WHITTY, A., RUNKEL, L. & HOCHMAN, P. (1998) The structure of human interferon- β : implications for activity. *Cellular and Molecular Life Sciences*, 54, 1203-1216.

- KATSANTONI, E., ANGHELESCU, N., ROTTIER, R., MOERLAND, M., ANTONIOU, M., DE CROM, R., GROSVELD, F. & STROUBOULIS, J. (2007) Ubiquitous expression of the rtTA2S-M2 inducible system in transgenic mice driven by the human hnRNPA2B1/CBX3 CpG island. *BMC Developmental Biology*, 7, 108.
- KAUFMAN, R. J. (1998) Post-translational Modifications Required for Coagulation Factor Secretion and Function. *Thrombosis and Haemostasis*, 79, 1068-1220.
- KAUFMAN, R. J., BROWN, P. C. & SCHIMKE, R. T. (1979) Amplified dihydrofolate reductase genes in unstably methotrexate-resistant cells are associated with double minute chromosomes. *Proc Natl Acad Sci*, 76, 5669-5673.
- KAUFMAN, R. J. & GOEDEL, D. V. (1990) [42] Selection and coamplification of heterologous genes in mammalian cells. *Methods in Enzymology*. Academic Press.
- KAUFMAN, R. J. & SCHIMKE, R. T. (1981) Amplification and loss of dihydrofolate reductase genes in a Chinese hamster ovary cell line. *Molecular and Cellular Biology*, 1, 1069-1076.
- KAUFMAN, R. J., SHARP, P. A. & LATT, S. A. (1983) Evolution of chromosomal regions containing transfected and amplified dihydrofolate reductase sequences. *Molecular and Cellular Biology*, 3, 699-711.
- KAUFMANN, B. B. & VAN OUDENAARDEN, A. (2007) Stochastic gene expression: from single molecules to the proteome. *Current Opinion in Genetics & Development*, 17, 107-112.
- KIM, A., SONG, S.-H., BRAND, M. & DEAN, A. (2007) Nucleosome and transcription activator antagonism at human β -globin locus control region DNase I hypersensitive sites. *Nucleic Acids Research*, 35, 5831-5838.
- KIM, J.-M., KIM, J.-S., PARK, D.-H., KANG, H. S., YOON, J., BAEK, K. & YOON, Y. (2004) Improved recombinant gene expression in CHO cells using matrix attachment regions. *Journal of Biotechnology*, 107, 95-105.
- KIM, J. D., YOON, Y., HWANG, H.-Y., PARK, J. S., YU, S., LEE, J., BAEK, K. & YOON, J. (2005) Efficient Selection of Stable Chinese Hamster Ovary (CHO) Cell Lines for Expression of Recombinant Proteins by Using Human Interferon β SAR Element. *Biotechnology Progress*, 21, 933-937.
- KIM, M., O'CALLAGHAN, P. M., DROMS, K. A. & JAMES, D. C. (2011) A Mechanistic Understanding of Production Instability in CHO Cell Lines Expressing Recombinant Monoclonal Antibodies. *Biotechnology and Bioengineering*, 108, 2434-2446.
- KIM, N. S., BYUN, T. H. & LEE, G. M. (2001) Key determinants in the occurrence of clonal variation in humanized antibody expression of CHO cells during dihydrofolate reductase mediated gene amplification. *Biotechnology Progress*, 17, 69-75.
- KIM, N. S., KIM, S. J. & LEE, G. M. (1998a) Clonal variability within dihydrofolate reductase-mediated gene amplified Chinese hamster ovary cells: Stability in the absence of selective pressure. *Biotechnology and Bioengineering*, 60, 679-688.
- KIM, S. J., KIM, N. S., RYU, C. J., HONG, H. J. & LEE, G. M. (1998b) Characterization of chimeric antibody producing CHO cells in the course of dihydrofolate reductase-mediated gene amplification and their stability in the absence of selective pressure. *Biotechnology and Bioengineering*, 58, 73-84.

- KIM, S. J. & LEE, G. M. (1999) Cytogenetic analysis of chimeric antibody-producing CHO cells in the course of dihydrofolate reductase-mediated gene amplification and their stability in the absence of selective pressure. *Biotechnology and Bioengineering*, 64, 741-749.
- KIMURA, H. & SHIOTA, K. (2003) Methyl-CpG-binding Protein, MeCP2, Is a Target Molecule for Maintenance DNA Methyltransferase, Dnmt1. *Journal of Biological Chemistry*, 278, 4806-4812.
- KOUZARIDES, T. (2007) Chromatin Modifications and Their Function. *Cell*, 128, 693-705.
- KÜPPER, K., KÖLBL, A., BIENER, D., DITTRICH, S., VON HASE, J., THORMEYER, T., FIEGLER, H., CARTER, N., SPEICHER, M., CREMER, T. & CREMER, M. (2007) Radial chromatin positioning is shaped by local gene density, not by gene expression. *Chromosoma*, 116, 285-306.
- KWAKS, T. H. J. & OTTE, A. P. (2006) Employing epigenetics to augment the expression of therapeutic proteins in mammalian cells. *Trends in Biotechnology*, 24, 137-142.
- LATTENMAYER, C., LOESCHEL, M., SCHRIEBL, K., TRUMMER, E., VORAUER-UHL, K., MUELLER, D., KATINGER, H., KUNERT, R. & SMITH, R. (2007a) Analysis of Genetic Parameters in Order to Get More Information on High Producing Recombinant CHO Cell Lines
Cell Technology for Cell Products. Springer Netherlands.
- LATTENMAYER, C., TRUMMER, E., SCHRIEBL, K., VORAUER-UHL, K., MUELLER, D., KATINGER, H. & KUNERT, R. (2007b) Characterisation of recombinant CHO cell lines by investigation of protein productivities and genetic parameters. *Journal of Biotechnology*, 128, 716-725.
- LAUBACH, V. E., GARVEY, E. P. & SHERMAN, P. A. (1996) High-Level Expression of Human Inducible Nitric Oxide Synthase in Chinese Hamster Ovary Cells and Characterization of the Purified Enzyme. *Biochemical and Biophysical Research Communications*, 218, 802-807.
- LEE, D. Y., HAYES, J. J., PRUSS, D. & WOLFFE, A. P. (1993) A positive role for histone acetylation in transcription factor access to nucleosomal DNA. *Cell*, 72, 73-84.
- LI, J. C. & KAMINSKAS, E. (1984) Accumulation of DNA strand breaks and methotrexate cytotoxicity. *Proceedings of the National Academy of Sciences*, 81, 5694-5698.
- LIN, K. W. & YAN, J. (2008) Endings in the middle: Current knowledge of interstitial telomeric sequences. *Mutation Research/Reviews in Mutation Research*, 658, 95-110.
- LISOWSKI, L. & SADELAIN, M. (2008) Current status of globin gene therapy for the treatment of β -thalassaemia. *British Journal of Haematology*, 141, 335-345.
- LITT, M. D., SIMPSON, M., RECILLAS-TARGA, F., PRIOLEAU, M.-N. & FELSENFELD, G. (2001) Transitions in histone acetylation reveal boundaries of three separately regulated neighboring loci. *EMBO J*, 20, 2224-2235.
- LIU, H.-S., JAN, M.-S., CHOU, C.-K., CHEN, P.-H. & KE, N.-J. (1999) Is Green Fluorescent Protein Toxic to the Living Cells? *Biochemical and Biophysical Research Communications*, 260, 712-717.

- LIU, W., XIONG, Y. & GOSSSEN, M. (2006) Stability and homogeneity of transgene expression in isogenic cells. *Journal of Molecular Medicine*, 84, 57-64.
- LIVINGSTONE, L. R., WHITE, A., SPROUSE, J., LIVANOS, E., JACKS, T. & TLSTY, T. D. (1992) Altered cell cycle arrest and gene amplification potential accompany loss of wild-type p53. *Cell*, 70, 923-935.
- LOUIS-MARIE, H. (2009) Production of pharmaceutical proteins by transgenic animals. *Comparative Immunology, Microbiology and Infectious Diseases*, 32, 107-121.
- MA, C., MARTIN, S., TRASK, B. & HAMLIN, J. L. (1993) Sister chromatid fusion initiates amplification of the dihydrofolate reductase gene in Chinese hamster cells. *Genes & Development*, 7, 605-620.
- MARCHAL, I., JARVIS, D. L., CACAN, R. & VERBERT, A. (2001) Glycoproteins from Insect Cells: Sialylated or Not? *Biological Chemistry*, 382, 151-159.
- MATASCI, M., HACKER, D. L., BALDI, L. & WURM, F. M. (2008) Recombinant therapeutic protein production in cultivated mammalian cells: current status and future prospects. *Drug Discovery Today: Technologies*, 5, e37-e42.
- MAY, C., RIVELLA, S., CALLEGARI, J., HELLER, G., GAENSLER, K. M. L., LUZZATTO, L. & SADELAIN, M. (2000) Therapeutic haemoglobin synthesis in [beta]-thalassaemic mice expressing lentivirus-encoded human [beta]-globin. *Nature*, 406, 82-86.
- MEISTER, G. & TUSCHL, T. (2004) Mechanisms of gene silencing by double-stranded RNA. *Nature*, 431, 343-349.
- MERGULHAO, F. J. M., SUMMERS, D. K. & MONTEIRO, G. A. (2005) Recombinant protein secretion in *Escherichia coli*. *Biotechnology Advances*, 23, 177-202.
- MICHNICK, D. A., PITTMAN, D. D., WISE, R. J. & KAUFMAN, R. J. (1994) Identification of individual tyrosine sulfation sites within factor VIII required for optimal activity and efficient thrombin cleavage. *Journal of Biological Chemistry*, 269, 20095-102.
- MIRANDA, T. B. & JONES, P. A. (2007) DNA methylation: The nuts and bolts of repression. *Journal of Cellular Physiology*, 213, 384-390.
- MIRKOVITCH, J., MIRAULT, M.-E. & LAEMMLI, U. K. (1984) Organization of the higher-order chromatin loop: specific DNA attachment sites on nuclear scaffold. *Cell*, 39, 223-232.
- NAIR, A., JINGER, X. & HERMISTON, T. (2011) Effect of different UCOE-promoter combinations in creation of engineered cell lines for the production of Factor VIII. *BMC Research Notes*, 4, 178.
- NAKAO, M. (2001) Epigenetics: interaction of DNA methylation and chromatin. *Gene*, 278, 25-31.
- NAN, X., NG, H.-H., JOHNSON, C. A., LAHERTY, C. D., TURNER, B. M., EISENMAN, R. N. & BIRD, A. (1998) Transcriptional repression by the methyl-CpG-binding protein MeCP2 involves a histone deacetylase complex. *Nature*, 393, 386-389.
- NEEDHAM, M., BARRATT, D., CERILLO, G., GREEN, I., WARBURTON, H., ANDERSON, M., STURGESS, N., ROLLINS, B., REILLY, C. & HOLLIS, M. (1996) High Level Expression of Human MCP-1 Using the LCR/MEL Expression System. *Protein Expression and Purification*, 7, 173-182.

- NEEDHAM, M., EGERTON, M., MILLEST, A., EVANS, S., POPPLEWELL, M., CERILLO, G., MCPHEAT, J., MONK, A., JACK, A., JOHNSTONE, D. & HOLLIS, M. (1995) Further Development of the Locus Control Region/Murine Erythroleukemia Expression System: High Level Expression and Characterization of Recombinant Human Calcitonin Receptor. *Protein Expression and Purification*, 6, 124-131.
- NEILDEZ-NGUYEN, T. M. A., PARISOT, A., VIGNAL, C., RAMEAU, P., STOCKHOLM, D., PICOT, J., ALLO, V., LE BEC, C., LAPLACE, C. & PALDI, A. (2008) Epigenetic gene expression noise and phenotypic diversification of clonal cell populations. *Differentiation*, 76, 33-40.
- NEVALAINEN, K. M. H., TE'O, V. S. J. & BERGQUIST, P. L. (2005) Heterologous protein expression in filamentous fungi. *Trends in Biotechnology*, 23, 468-474.
- NOORDERMEER, D., BRANCO, M. R., SPLINTER, E., KLOUS, P., VAN IJCKEN, W., SWAGEMAKERS, S., KOUTSOURAKIS, M., VAN DER SPEK, P., POMBO, A. & DE LAAT, W. (2008) Transcription and Chromatin Organization of a Housekeeping Gene Cluster Containing an Integrated β -Globin Locus Control Region. *PLoS Genet*, 4, e1000016.
- NOWAK, S. J. & CORCES, V. G. (2004) Phosphorylation of histone H3: a balancing act between chromosome condensation and transcriptional activation. *Trends in Genetics*, 20, 214-220.
- NUNBERG, J. H., KAUFMAN, R. J., SCHIMKE, R. T., URLAUB, G. & CHASIN, L. A. (1978) Amplified dihydrofolate reductase genes are localized to a homogeneously staining region of a single chromosome in a methotrexate-resistant Chinese hamster ovary cell line. *Proc Natl Acad Sci*, 75, 5553-5556.
- OKANO, M., BELL, D. W., HABER, D. A. & LI, E. (1999) DNA Methyltransferases Dnmt3a and Dnmt3b Are Essential for De Novo Methylation and Mammalian Development. *Cell*, 99, 247-257.
- OMASA, T. (2002) Gene amplification and its application in cell and tissue engineering. *Journal of Bioscience and Bioengineering*, 94, 600-605.
- OMASA, T., CAO, Y., PARK, J. Y., TAKAGI, Y., KIMURA, S., YANO, H., HONDA, K., ASAKAWA, S., SHIMIZU, N. & OHTAKE, H. (2009) Bacterial artificial chromosome library for genome-wide analysis of Chinese hamster ovary cells. *Biotechnology and Bioengineering*, 104, 986-994.
- ORTIZ, B. D., CADDO, D., CHEN, V., DIAZ, P. W. & WINOTO, A. (1997) Adjacent DNA elements dominantly restrict the ubiquitous activity of a novel chromatin-opening region to specific tissues. *EMBO J*, 16, 5037-5045.
- OSBORNE, C. S., CHAKALOVA, L., BROWN, K. E., CARTER, D., HORTON, A., DEBRAND, E., GOYENECHEA, B., MITCHELL, J. A., LOPES, S., REIK, W. & FRASER, P. (2004) Active genes dynamically colocalize to shared sites of ongoing transcription. *Nat Genet*, 36, 1065-1071.
- OSTERMEIER, G. C., LIU, Z., MARTINS, R. P., BHARADWAJ, R. R., ELLIS, J., DRAGHICI, S. & KRAWETZ, S. A. (2003) Nuclear matrix association of the human β globin locus utilizing a novel approach to quantitative real-time PCR. *Nucleic Acids Research*, 31, 3257-3266.
- OTTAGGIO, L., BOZZO, S., MORO, F., SPARKS, A., CAMPOMENOSI, P., MIELE, M., BONATTI, S., FRONZA, G., LANE, D. P. & ABBONDANDOLO, A. (2000)

- Defective nuclear localization of p53 protein in a Chinese hamster cell line is associated with the formation of stable cytoplasmic protein multimers in cells with gene amplification. *Carcinogenesis*, 21, 1631-1638.
- OTTAGGIO, L., CAMPOMENOSI, P., FRONZA, G., MENICHINI, P., MIELE, M., MORO, F., VIAGGI, S., ZUNINO, A. & ABBONDANDOLO, A. (2006) Stable formation of mutated p53 multimers in a Chinese hamster cell line causes defective p53 nuclear localization and abrogates its residual function. *Journal of Cellular Biochemistry*, 98, 1689-1700.
- OTTE, A. P., KWAKS, T. H. J., VAN BLOKLAND, R. J. M., SEWALT, R. G. A. B., VERHEES, J., KLAREN, V. N. A., SIERSMA, T. K., KORSE, H. W. M., TEUNISSEN, N. C., BOTSCHUIJVER, S., VAN MER, C. & MAN, S. Y. (2007) Various Expression-Augmenting DNA Elements Benefit from STAR-Select, a Novel High Stringency Selection System for Protein Expression. *Biotechnology Progress*, 23, 801-807.
- PAGE, M. J. & SYDENHAM, M. A. (1991) High Level Expression of the Humanized Monoclonal Antibody CAMPATH-1H in Chinese Hamster Ovary Cells. *Nat Biotech*, 9, 64-68.
- PALERMO, D. P., DEGRAAF, M. E., MAROTTI, K. R., REHBERG, E. & POST, L. E. (1991) Production of analytical quantities of recombinant proteins in Chinese hamster ovary cells using sodium butyrate to elevate gene expression. *Journal of Biotechnology*, 19, 35-47.
- PALLAVICINI, M. G., DETERESA, P. S., ROSETTE, C., GRAY, J. W. & WURM, F. M. (1990) Effects of methotrexate on transfected DNA stability in mammalian cells. *Mol. Cell. Biol.*, 10, 401-404.
- PALSTRA, R. J., TOLHUIS, B., SPLINTER, E., NIJMEIJER, R., GROSVELD, F. & DE LAAT, W. (2003) The beta-globin nuclear compartment in development and erythroid differentiation. *Nature Genetics*, 35, 190-194.
- PANNING, B. & JAENISCH, R. (1998) RNA and the epigenetic regulation of X chromosome. *Cell*, 93, 305-308.
- PARK, J. Y., TAKAGI, Y., YAMATANI, M., HONDA, K., ASAKAWA, S., SHIMIZU, N., OMASA, T. & OHTAKE, H. (2010) Identification and analysis of specific chromosomal region adjacent to exogenous Dhfr-amplified region in Chinese hamster ovary cell genome. *Journal of Bioscience and Bioengineering*, 109, 504-511.
- PATTERSON, G. H., KNOBEL, S. M., SHARIF, S. R. & PISTON, D. W. (1997) Use of the Green Fluorescent Protein and Its Mutants in Quantitative Fluorescence Microscopy. *Biophysical Journal*, 73, 2782-2790.
- PAVAN, K. P., BISCHOF, O., PURBEY, P. K., NOTANI, D., URLAUB, H., DEJEAN, A. & GALANDE, S. (2007) Functional interaction between PML and SATB1 regulates chromatin-loop architecture and transcription of the MHC class I locus. *Nat Cell Biol*, 9, 45-56.
- PENDSE, G. J., KARKARE, S. & BAILEY, J. E. (1992) Effect of cloned gene dosage on cell growth and hepatitis B surface antigen synthesis and secretion in recombinant CHO cells. *Biotechnology and Bioengineering*, 40, 119-129.
- PILBROUGH, W., MUNRO, T. P. & GRAY, P. (2009) Intraclonal Protein Expression Heterogeneity in Recombinant CHO Cells. *PLoS ONE*, 4, e8432.

- POMBO, A., JACKSON, D. A., HOLLINSHEAD, M., WANG, Z., ROEDER, R. G. & COOK, P. R. (1999) Regional specialization in human nuclei: visualization of discrete sites of transcription by RNA polymerase III. *EMBO J*, 18, 2241-2253.
- PORRO, D., GASSER, B., FOSSATI, T., MAURER, M., BRANDUARDI, P., SAUER, M. & MATTANOVICH, D. (2011) Production of recombinant proteins and metabolites in yeasts. *Applied Microbiology and Biotechnology*, 89, 939-948.
- POTGIETER, T. I., CUKAN, M., DRUMMOND, J. E., HOUSTON-CUMMINGS, N. R., JIANG, Y., LI, F., LYNAUGH, H., MALLEM, M., MCKELVEY, T. W., MITCHELL, T., NYLEN, A., RITTENHOUR, A., STADHEIM, T. A., ZHA, D. & DÂ€™MANJOU, M. (2009) Production of monoclonal antibodies by glycoengineered *Pichia pastoris*. *Journal of Biotechnology*, 139, 318-325.
- PRADHAN, S., BACCOLLA, A., WELLS, R. D. & ROBERTS, R. J. (1999) Recombinant Human DNA (Cytosine-5) Methyltransferase. *Journal of Biological Chemistry*, 274, 33002-33010.
- QUINA, A. S., BUSCHBECK, M. & DI CROCE, L. (2006) Chromatin structure and epigenetics. *Biochemical Pharmacology*, 72, 1563-1569.
- R&D-PIPELINE-NEWS (2011) Special Edition. La Merie Business Intelligence, available at www.pipelinerreview.com.
- RAJ, A., PESKIN, C. S., TRANCHINA, D., VARGAS, D. Y. & TYAGI, S. (2006) Stochastic mRNA Synthesis in Mammalian Cells. *PLoS Biol*, 4, e309.
- RAJ, A. & VAN OUDENAARDEN, A. (2008) Nature, Nurture, or Chance: Stochastic Gene Expression and Its Consequences. *Cell*, 135, 216-226.
- RAY, M. & MOHANDAS, T. (1976) Proposed banding nomenclature for the Chinese hamster chromosomes (*Cricetulus griseus*). *Cytogenetics and Cell Genetics*, 16, 83-91.
- RAY, M. V. L., DUYNE, P. V., BERTESENT, A. H., JACKSON-MATTHEWS, D. E., STURMER, A. M., MERKLER, D. J., CONSALVO, A. P., YOUNG, S. D., GILLIGAN, J. P. & SHIELDS, P. P. (1993) Production of Recombinant Salmon Calcitonin by In Vitro Amidation of an *Escherichia coli* Produced Precursor Peptide. *Nat Biotech*, 11, 64-70.
- REN, X. W., LIANG, M., MENG, X., YE, X., MA, H., ZHAO, Y., GUO, J., CAI, N., CHEN, H. Z., YE, S. L. & HU, F. (2006) A tumor-specific conditionally replicative adenovirus vector expressing TRAIL for gene therapy of hepatocellular carcinoma. *Cancer Gene Ther*, 13, 159-168.
- RENS, W., FU, B., O'BRIEN, P. C. M. & FERGUSON-SMITH, M. (2006) Cross-species chromosome painting. *Nat. Protocols*, 1, 783-790.
- RIGGS, M. G., WHITTAKER, R. G., NEUMANN, J. R. & INGRAM, V. M. (1977) n-Butyrate causes histone modification in HeLa and Friend erythroleukaemia cells. *Nature*, 268, 462-464.
- RUIZ, J. C. & WAHL, G. M. (1990) Chromosomal destabilization during gene amplification. *Molecular and Cellular Biology*, 10, 3056-3066.
- RUNKEL, L., MEIER, W., PEPINSKY, R. B., KARPUSAS, M., WHITTY, A., KIMBALL, K., BRICKELMAIER, M., MULDOWNY, C., JONES, W. & GOELZ, S. E. (1998) Structural and Functional Differences Between Glycosylated and Non-glycosylated Forms of Human Interferon- β (IFN- β). *Pharmaceutical Research*, 15, 641-649.

- SAIKAWA, Y., KNIGHT, C. B., SAIKAWA, T., PAGE, S. T., CHABNER, B. A. & ELWOOD, P. C. (1993) Decreased expression of the human folate receptor mediates transport-defective methotrexate resistance in KB cells. *Journal of Biological Chemistry*, 268, 5293-5301.
- SCHALCH, T., DUDA, S., SARGENT, D. F. & RICHMOND, T. J. (2005) X-ray structure of a tetranucleosome and its implications for the chromatin fibre. *Nature*, 436, 138-141.
- SCHNEIDER, R. & GROSSCHEDL, R. (2007) Dynamics and interplay of nuclear architecture, genome organization, and gene expression. *Genes & Development*, 21, 3027-3043.
- SCHRÖDER, M. & FRIEDL, P. (1997) Overexpression of recombinant human antithrombin III in Chinese hamster ovary cells results in malformation and decreased secretion of recombinant protein. *Biotechnology and Bioengineering*, 53, 547-559.
- SELKER, E. U. (1997) Epigenetic phenomena in filamentous fungi: useful paradigms or repeat-induced confusion? *Trends in Genetics*, 13, 296-301.
- SIGAL, A., MILO, R., COHEN, A., GEVA-ZATORSKY, N., KLEIN, Y., LIRON, Y., ROSENFELD, N., DANON, T., PERZOV, N. & ALON, U. (2006) Variability and memory of protein levels in human cells. *Nature*, 444, 643-646.
- SIMONIS, M., KLOUS, P., SPLINTER, E., MOSHKIN, Y., WILLEMSSEN, R., DE WIT, E., VAN STEENSEL, B. & DE LAAT, W. (2006) Nuclear organization of active and inactive chromatin domains uncovered by chromosome conformation capture-on-chip (4C). *Nat Genet*, 38, 1348-1354.
- SINCLAIR, A. M. & ELLIOTT, S. (2005) Glycoengineering: The effect of glycosylation on the properties of therapeutic proteins. *Journal of Pharmaceutical Sciences*, 94, 1626-1635.
- SMALLWOOD, A., ESTÁˆVE, P.-O., PRADHAN, S. & CAREY, M. (2007) Functional cooperation between HP1 and DNMT1 mediates gene silencing. *Genes & Development*, 21, 1169-1178.
- SMITH, C. L. & PETERSON, C. L. (2004) ATP-Dependent Chromatin Remodeling. *Current Topics in Developmental Biology*. Academic Press.
- SOLÁ, R. J. & GRIEBENOW, K. (2009) Effects of glycosylation on the stability of protein pharmaceuticals. *Journal of Pharmaceutical Sciences*, 98, 1223-1245.
- SPRIGGS, K. A., BUSHELL, M., MITCHELL, S. A. & WILLIS, A. E. (2005) Internal ribosome entry segment-mediated translation during apoptosis: the role of IRES-trans-acting factors. *Cell Death Differ*, 12, 585-591.
- SPRIGGS, K. A., BUSHELL, M. & WILLIS, A. E. (2010) Translational Regulation of Gene Expression during Conditions of Cell Stress. *Molecular Cell*, 40, 228-237.
- STRAHL, B. D., OHBA, R., COOK, R. G. & ALLIS, C. D. (1999) Methylation of histone H3 at lysine 4 is highly conserved and correlates with transcriptionally active nuclei in Tetrahymena. *Proceedings of the National Academy of Sciences*, 96, 14967-14972.
- STRUTZENBERGER, K., BORTH, N., KUNERT, R., STEINFELLNER, W. & KATINGER, H. (1999) Changes during subclone development and ageing of human antibody-producing recombinant CHO cells. *Journal of Biotechnology*, 69, 215-226.

- SUTHERLAND, H. & BICKMORE, W. A. (2009) Transcription factories: gene expression in unions? *Nat Rev Genet*, 10, 457-466.
- SWARTZ, J. R. (2001) Advances in Escherichia coli production of therapeutic proteins. *Current Opinion in Biotechnology*, 12, 195-201.
- THOMSON, S., MAHADEVAN, L. C. & CLAYTON, A. L. (1999) MAP kinase-mediated signalling to nucleosomes and immediate-early gene induction. *Seminars in Cell & Developmental Biology*, 10, 205-214.
- TJIO, J. H. & PUCK, T. T. (1958) GENETICS OF SOMATIC MAMMALIAN CELLS II. CHROMOSOMAL CONSTITUTION OF CELLS IN TISSUE CULTURE. *Journal of Experimental Medicine*, 108, 259-268.
- TSIEN, R. Y. (1998) THE GREEN FLUORESCENT PROTEIN. *Annual Review of Biochemistry*, 67, 509-544.
- TUAN, D., SOLOMON, W., LI, Q. & LONDON, I. M. (1985) The "beta-like-globin" gene domain in human erythroid cells. *Proc Natl Acad Sci*, 82, 6384-6388.
- TUSCHL, T., ZAMORE, P. D., LEHMANN, R., BARTEL, D. P. & SHARP, P. A. (1999) Targeted mRNA degradation by double-stranded RNA in vitro. *Genes & Development*, 13, 3191-3197.
- URLAUB, G. & CHASIN, L. A. (1980) Isolation of Chinese hamster cell mutants deficient in dihydrofolate reductase activity. *Proc Natl Acad Sci*, 77, 4216-4220.
- URLAUB, G., KÄS, E., CAROTHERS, A. M. & CHASIN, L. A. (1983) Deletion of the diploid dihydrofolate reductase locus from cultured mammalian cells. *Cell*, 33, 405-412.
- VAISSIERE, T., SAWAN, C. & HERCEG, Z. (2008) Epigenetic interplay between histone modifications and DNA methylation in gene silencing. *Mutation Research/Reviews in Mutation Research*, 659, 40-48.
- VAKOC, C. R., LETTING, D. L., GHELDOLF, N., SAWADO, T., BENDER, M. A., GROUDINE, M., WEISS, M. J., DEKKER, J. & BLOBEL, G. A. (2005) Proximity among Distant Regulatory Elements at the β^2 -Globin Locus Requires GATA-1 and FOG-1. *Molecular Cell*, 17, 453-462.
- VALENZUELA, L. & KAMAKAKA, R. T. (2006) Chromatin Insulators*. *Annual Review of Genetics*, 40, 107-138.
- VERMAAK, D., AHMAD, K. & HENIKOFF, S. (2003) Maintenance of chromatin states: an open-and-shut case. *Current Opinion in Cell Biology*, 15, 266-274.
- VOLPE, T. A., KIDNER, C., HALL, I. M., TENG, G., GREWAL, S. I. S. & MARTIENSSEN, R. A. (2002) Regulation of Heterochromatic Silencing and Histone H3 Lysine-9 Methylation by RNAi. *Science*, 297, 1833-1837.
- WAHL, G. M., ROBERT DE SAINT VINCENT, B. & DEROSE, M. L. (1984) Effect of chromosomal position on amplification of transfected genes in animal cells. *Nature*, 307, 516-520.
- WALSH, G. (2005) Therapeutic insulins and their large-scale manufacture. *Applied Microbiology and Biotechnology*, 67, 151-159.
- WALSH, G. (2010a) Biopharmaceutical benchmarks 2010. *Nat Biotech*, 28, 917-924.
- WALSH, G. (2010b) Post-translational modifications of protein biopharmaceuticals. *Drug Discovery Today*, 15, 773-780.
- WALSH, G. & JEFFERIS, R. (2006) Post-translational modifications in the context of therapeutic proteins. *Nat Biotech*, 24, 1241-1252.

- WANG, T.-Y., YANG, R., QIN, C., WANG, L. & YANG, X.-J. (2008) Enhanced expression of transgene in CHO cells using matrix attachment region. *Cell Biology International*, 32, 1279-1283.
- WEAKE, V. M. & WORKMAN, J. L. (2008) Histone Ubiquitination: Triggering Gene Activity. *Molecular Cell*, 29, 653-663.
- WEIDLE, U. H., BUCKEL, P. & WIENBERG, J. (1988) Amplified expression constructs for human tissue-type plasminogen activator in Chinese hamster ovary cells: instability in the absence of selective pressure. *Gene*, 66, 193-203.
- WELCSH, P. L. & KING, M.-C. (2001) BRCA1 and BRCA2 and the genetics of breast and ovarian cancer. *Human Molecular Genetics*, 10, 705-713.
- WESTERS, L., WESTERS, H. & QUAX, W. J. (2004) Bacillus subtilis as cell factory for pharmaceutical proteins: a biotechnological approach to optimize the host organism. *Biochimica et Biophysica Acta (BBA) - Molecular Cell Research*, 1694, 299-310.
- WIGHTMAN, B., HA, I. & RUVKUN, G. (1993) Posttranscriptional regulation of the heterochronic gene lin-14 by lin-4 mediates temporal pattern formation in *C. elegans*. *Cell*, 75, 855-862.
- WILLIAMS, S., MUSTOE, T., MULCAHY, T., GRIFFITHS, M., SIMPSON, D., ANTONIOU, M., IRVINE, A., MOUNTAIN, A. & CROMBIE, R. (2005) CpG-island fragments from the HNRPA2B1/CBX3 genomic locus reduce silencing and enhance transgene expression from the hCMV promoter/enhancer in mammalian cells. *BMC Biotechnology*, 5.
- WOLFFE, A. P. (1998) *Chromatin Structure and Function*, San Diego, CA, Academic Press.
- WOLFFE, A. P. & MATZKE, M. A. (1999) Epigenetics: Regulation Through Repression. *Science*, 286, 481-486.
- WONG, C.-H. (2005) Protein Glycosylation: New Challenges and Opportunities. *The Journal of Organic Chemistry*, 70, 4219-4225.
- WONG, S. L., YE, R. & NATHOO, S. (1994) Engineering and production of streptokinase in a Bacillus subtilis expression-secretion system. *Appl. Environ. Microbiol.*, 60, 517-523.
- WOODCOCK, C. L. & GHOSH, R. P. (2010) Chromatin Higher-order Structure and Dynamics. *Cold Spring Harbor Perspectives in Biology*, 2.
- WRIGHT, A. & MORRISON, S. L. (1997) Effect of glycosylation on antibody function: implications for genetic engineering. *Trends in Biotechnology*, 15, 26-32.
- WU, X. C., LEE, W., TRAN, L. & WONG, S. L. (1991) Engineering a Bacillus subtilis expression-secretion system with a strain deficient in six extracellular proteases. *J. Bacteriol.*, 173, 4952-4958.
- WURM, F. M. (2004) Production of recombinant protein therapeutics in cultivated mammalian cells. *Nat Biotech*, 22, 1393-1398.
- WURM, F. M., GWINN, K. A. & KINGSTON, R. E. (1986) Inducible overproduction of the mouse c-myc protein in mammalian cells. *Proc. Natl. Acad. Sci.*, 83, 5414-5418.
- WURM, F. M., JOHNSON, A., RYLL, T., KÖHNE, C., SCHERTHAN, H., GLAAB, F., LIE, Y. S., PETROPOULOS, C. J. & ARATHOON, W. R. (1996) Gene Transfer

- and Amplification in CHO Cells. *Annals of the New York Academy of Sciences*, 782, 70-78.
- WURM, F. M., JORDAN, M. & MAKRIDES, S. C. (2003) Gene transfer and gene amplification in mammalian cells. *New Comprehensive Biochemistry*. Elsevier.
- WURM, F. M. & PETROPOULOS, C. J. (1994) Plasmid Integration, Amplification and Cytogenetics in CHO Cells: Questions and Comments. *Biologicals*, 22, 95-102.
- XU, X., NAGARAJAN, H., LEWIS, N. E., PAN, S., CAI, Z., LIU, X., CHEN, W., XIE, M., WANG, W., HAMMOND, S., ANDERSEN, M. R., NEFF, N., PASSARELLI, B., KOH, W., FAN, H. C., WANG, J., GUI, Y., LEE, K. H., BETENBAUGH, M. J., QUAKE, S. R., FAMILI, I., PALSSON, B. O. & WANG, J. (2011) The genomic sequence of the Chinese hamster ovary (CHO)-K1 cell line. *Nat Biotech*, 29, 735-741.
- YANG, F., O'BRIEN, P. & FERGUSON-SMITH, M. (2000) Comparative Chromosome Map of the Laboratory Mouse and Chinese Hamster Defined by Reciprocal Chromosome Painting. *Chromosome Research*, 8, 219-227.
- YANG, L., GU, L., LI, Z. & ZHOU, M. (2010a) Translation of TRAF1 is regulated by IRES-dependent mechanism and stimulated by vincristine. *Nucleic Acids Research*, 38, 4503-4513.
- YANG, Y., MARIATI, CHUSAINOW, J. & YAP, M. G. S. (2010b) DNA methylation contributes to loss in productivity of monoclonal antibody-producing CHO cell lines. *Journal of Biotechnology*, 147, 180-185.
- YASUI, D., MIYANO, M., CAI, S., VARGA-WEISZ, P. & KOHWI-SHIGEMATSU, T. (2002) SATB1 targets chromatin remodelling to regulate genes over long distances. *Nature*, 419, 641-645.
- YEE, J. C., DE LEON GATTI, M., PHILP, R. J., YAP, M. & HU, W.-S. (2008) Genomic and proteomic exploration of CHO and hybridoma cells under sodium butyrate treatment. *Biotechnology and Bioengineering*, 99, 1186-1204.
- YIN, J., LI, G., REN, X. & HERRLER, G. (2007) Select what you need: A comparative evaluation of the advantages and limitations of frequently used expression systems for foreign genes. *Journal of Biotechnology*, 127, 335-347.
- YOSHIKAWA, T., NAKANISHI, F., ITAMI, S., KAMEOKA, D., OMASA, T., KATAKURA, Y., KISHIMOTO, M. & SUGA, K.-I. (2000b) Evaluation of stable and highly productive gene amplified CHO cell line based on the location of amplified genes. *Cytotechnology*, 33, 37-46.
- YOSHIKAWA, T., NAKANISHI, F., OGURA, Y., OI, D., OMASA, T., KATAKURA, Y., KISHIMOTO, M. & SUGA, K.-I. (2000a) Amplified Gene Location in Chromosomal DNA Affected Recombinant Protein Production and Stability of Amplified Genes. *Biotechnology Progress*, 16, 710-715.
- YUSUFZAI, T. M. & FELSENFELD, G. (2004) The 5'-HS4 chicken beta-globin insulator is a CTCF-dependent nuclear matrix-associated element. *Proceedings of the National Academy of Sciences of the United States of America*, 101, 8620-8624.
- ZAHN-ZABAL, M., KOBR, M., GIROD, P.-A., IMHOF, M., CHATELLARD, P., DE JESUS, M., WURM, F. & MERMOD, N. (2001) Development of stable cell lines for production or regulated expression using matrix attachment regions. *Journal of Biotechnology*, 87, 29-42.

- ZHANG, F., FROST, A. R., BLUNDELL, M. P., BALES, O., ANTONIOU, M. N. & THRASHER, A. J. (2010) A Ubiquitous Chromatin Opening Element (UCOE) Confers Resistance to DNA Methylation-mediated Silencing of Lentiviral Vectors. *Molecular Therapy*, 18, 1640-1649.
- ZHANG, F., THORNHILL, S. I., HOWE, S. J., ULAGANATHAN, M., SCHAMBACH, A., SINCLAIR, J., KINNON, C., GASPAR, H. B., ANTONIOU, M. & THRASHER, A. J. (2007) Lentiviral vectors containing an enhancer-less ubiquitously acting chromatin opening element (UCOE) provide highly reproducible and stable transgene expression in hematopoietic cells. *Blood*, 110, 1448-1457.

APPENDICES

APPENDIX 1 – Materials, Chemicals and Special Equipment

MEDIA AND SUPPLEMENTS

Lonza

RPMI with L-Glutamine (Cat No BE12702R)
Trypsin
Fetal Bovine Serum
DPBS (w/o calcium, magnesium, and sodium bicarbonate)

Gibco,

HT supplement

CHEMICALS AND SOLVENTS

Abcam, U.K.

Rabbit Polyclonal GFP antibody (ab290)
Rabbit Polyclonal DHFR antibody (ab49881)

BD Transduction Laboratories., U.S.

ERK antibody

BDH Chemicals Ltd., U.K.

Acetaldehyde
Ammonium persulphate
Calcium chloride
Chloroform
Citric acid
Ethanol
Ethylenediaminetetra-acetic acid (sodium salt)
Formaldehyde
Glacial acetic acid
Glycerol
Glycine
Hydrochloric acid
Isopropyl alcohol
Methanol
Orthoboric acid
Orthophosphoric acid
Perchloric acid
Potassium acetate
Ponsceau-S
Sodium chloride

Sodium hydrogen orthophosphate
Tri-sodium citrate
Sodium dodecylsulphate
Sodium hydroxide
Sulphuric acid
Sodium fluoride
Tris(hydroxymethyl) methylamine

BioLabs, UK

Prestained Protein Marker Broad Range 175 kD

Bioline, U.K.

1kb DNA ladder (DNA marker)

Bio-Rad Labs, U.S.A.

Bromophenol blue

Precision Plus All Blue Standards 250 kD

Boehringer-Mannheim Ltd., U.K.

Agarose (multipurpose)

Proteinase K

Calbiochem

Erythropoietin, Human Recombinant, CHO cells

DakoCytomation, U.K.

Polyclonal rabbit Anti-Mouse immunoglobulins HRP

Difco Labs, U.S.A

Bacto-agar

Bacto-tryptone

Bacto-yeast extract

Eurofins MWG Operon, Germany

Custom made oligonucleotides

Eurogentec Ltd., U.K.

qPCR Mastermix sybrGreen 1

Fisher Scientific, U.K.

Sodium dodecylsulphate

Fluka, Switzerland

Leupeptin hemisulphate

Invitrogen, U.K.

Avidin, FITC conjugated
TRIzol® Reagent
ProLong® Gold Antifade DAPI

Melfords Laboratories Ltd, U.K.
Phenyl Methyl Sulphonyl Fluoride (PMSF)

National Diagnostics, U.K.
Protogel solution

R&D Systems
Monoclonal Anti-human EPO antibody
Anti-human EPO antibody

Sigma-aldrich, U.K.
2-mercaptoethanol
3,3',5,5'-tetramethylbensidine tablets
Ampicillin
Albumin bovine (BSA)
Aprotinin
Diethyl polycarbonate (DEPC)
Dimethyl sulfoxide (DMSO)
Ethidium Bromide
Hydrogen peroxide
Isoamyl alcohol
Methotrexate
N-lauroyl sarcosine
NP-40
Phosphate buffered saline
Pepsin
Phenol
Phenol red
Potassium
RNase A
Sodium azide
Sodium bicarbonate
Sodium butyrate
Sodium deoxycolate
Sodium ortovanadate (Na_3VO_4)
Sodium pyrophosphate
Triton-X-100
Trizma® base
Trypan blue
Tween 20
Anti-rabbit IgG peroxidase

Roche Applied Science, U.K.

Biotin nick translation mix
Biotin-16-dUTP
DIG-nick translation mix
dATP (Li Salt)
dCTP (Li Salt)
dGTP (Li Salt)
dTTP (Li Salt)
Restriction endonucleases
Rhodamine conjugated Fab fragments
Taq DNA polymerase

Defatted milk (Marvel™) can be bought from supermarkets

KITS

Amersham Pharmacia, U.K.

ECL™ Western blotting detection reagents

Bioline, U.K.

cDNA Synthesis Kit

Qiagen Ltd., U.K.

Plasmid midi kit (Cat No – 12143)

Sigma-aldrich, U.K.

DNase I kit (AMPD1-1KT)

APPARATUS

All general and disposable glassware and plasticware were obtained from standard suppliers, specialised equipment was purchased from the following companies

BDH Chemicals Ltd., U.K

Haemocytometer (Improved Neubauer)

Beckman Coulter Inc., U.S.A.

CYAN ADP flow cytometer

J2-21 Centrifuge with JA-20 rotors

Boeco, Germany

Centrifuge

Bio-Rad Labs. Ltd., U.K.

Electroporation curvettes

Gene pulser™ machine

Mini-gel II Slab system
PCR 96 well plates
PCR tube strips
Thick filter paper
Trans-blot Semi-dry transfer cell
Electrophoresis tank
Power Pac 300 power supplier

Denver Instruments, U.S.A.
pH meter
Precision balance

Kodak, U.S.A.
X-ray film (Biomax MR-1)
X-ray film cassettes & intensifying paper

Life Technologies, Ltd., U.K.
Nunc-immuno plates (maxisorp F96)

LTE Scientific Ltd., U.K.
Series 250 Autoclave

Medical Airtech Ltd., U.K.
BioMAT-2 class II microbiological safety cabinet

Molecular Devices
MetaVue Software

Millipore, U.K.
Elix™ water purification system

Nunc, U.S.A.
Internal thread cryogenic vials

Olympus Ltd., U.K.
Olympus BX51 upright microscope

Photometrics
Coolsnap HQ camera

Schleicher & Schell Bioscience, U.S.A.
Nitrocellulose transfer membrane

Techne, U.K.
Chromo 4 thermal cycler

Thermo Fisher Scientific, U.S.A
NanoDrop 1000, UV/Vis spectrophotometer

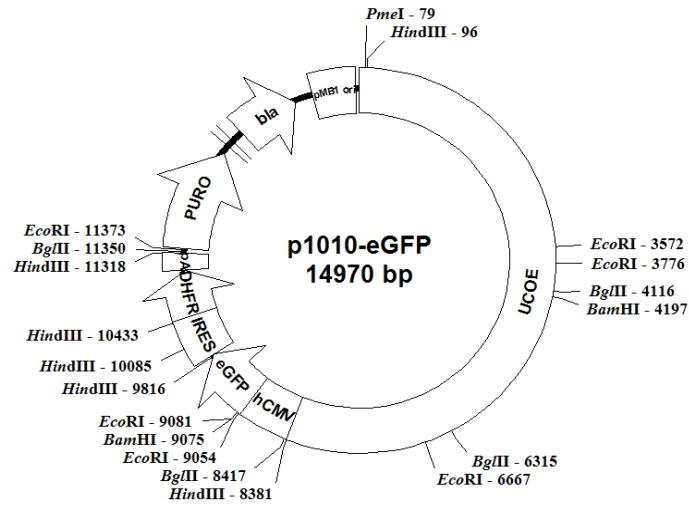
Wolf Laboratories, U.K.
Incubator

Web Scientific, U.K.
Glass plates (for SDS-PAGE)

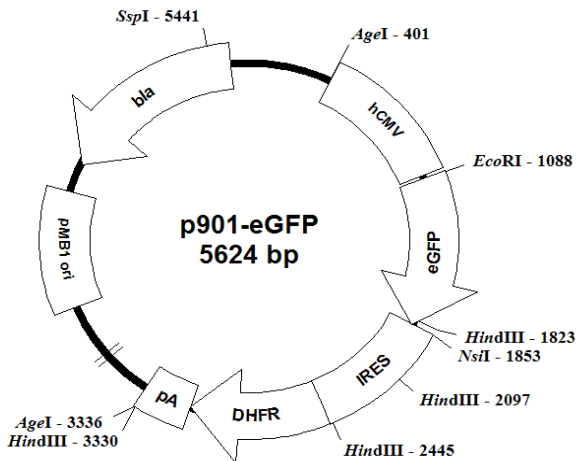
Vickers Instruments, U.K.
Light microscope

APPENDIX 2 – p1010-, p901-eGFP plasmid constructs

A:



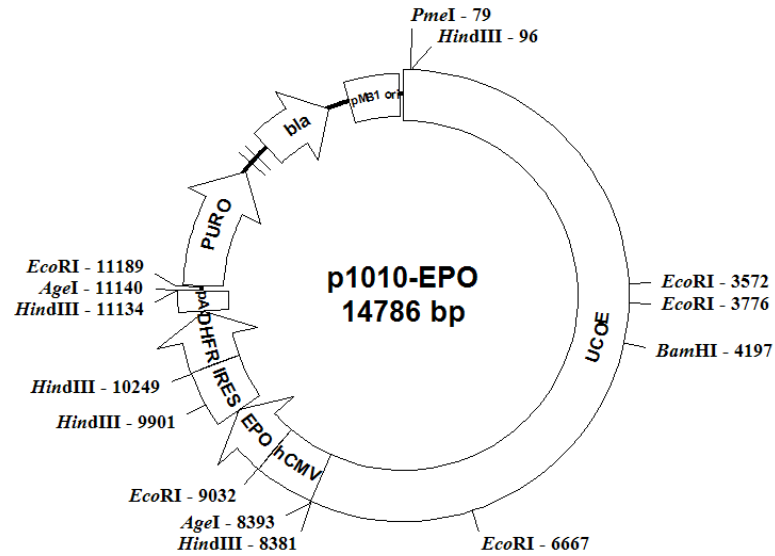
B:



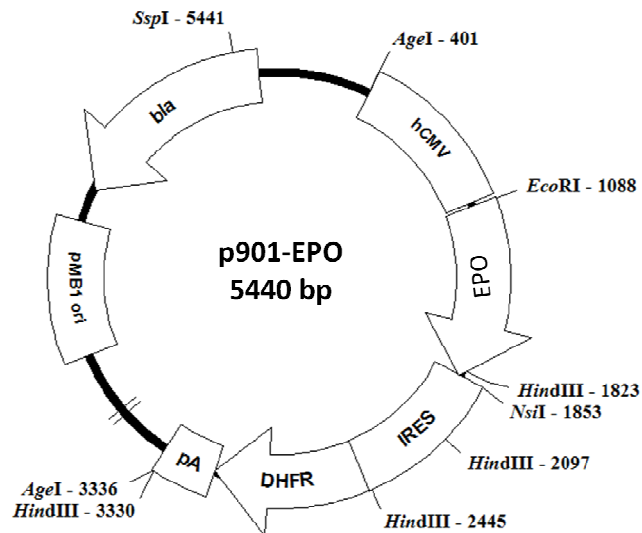
Plasmid constructs used to generate UCOE-containing (A) and non-UCOE-containing (B) CHO-GFP cell lines. Created by Croxford (2008).

APPENDIX 3 – p1010-, p901-EPO plasmid constructs

A:



B:



Plasmid constructs used to generate UCOE-containing (A) and non-UCOE-containing (B) CHO-EPO cell lines. Created by Croxford (2008).